Synthesis, Kinetics and Mechanisms of Designer and Natural Product Antioxidants: From Solution to Cells

By

Bo Li

Thesis submitted to the Department of Chemistry and Biomolecular Sciences

in conformity with the requirements for the

Degree of Doctor of Philosophy in Chemistry

University of Ottawa

Ottawa, Ontario, Canada

(March 2016)

Abstract

Lipid peroxidation has been implicated in the onset and progression of many degenerative diseases, including cardiovascular disease, Alzheimer's disease and cancer. Accordingly, for more than 50 years, considerable effort has been devoted to the design of synthetic compounds or the discovery of natural products that can slow lipid peroxidation. Despite the enormous investments made to date, no clear antioxidant strategies have emerged for the treatment and/or prevention of degenerative disease. We argue that this is because of a lack of fundamental understanding of the chemical reactivity of these compounds in relevant contexts.

Herein, we describe studies of our optimized synthetic radical-trapping antioxidant (RTA) – the tetrahydronaphthyridinols (THNs). We first present the synthesis of a series of THN analogs of α-tocopherol (Nature's premier lipid-soluble radical-trapping antioxidant) with varying sidechain substitution and then demonstrate how systematic changes in the lipophilicity of these potent antioxidants impact their peroxyl radical-trapping activities in lipid bilayers and mammalian cell culture. Their regenerability by water-soluble reductants in lipid bilayers, binding to human tocopherol transport protein (hTTP), and cytotoxicity were also evaluated to provide insight on whether this type of antioxidant can be potentially pushed toward animal studies.

We also describe analogous studies of natural products such as the garlic-derived thiosulfinate allicin and the grape-derived polyphenol resveratrol. These compounds have attracted significant attention in the past 20 years due to their purported health benefits, which are often ascribed to their purported radical-trapping activities. To date, systematic studies on their radical-trapping activities in solution, lipid bilayers and mammalian cells have been lacking. We have determined that allicin and petivericin, while effective RTAs in solution, are not so in lipid bilayers. Moreover, the compounds are not antioxidants in cell culture, but instead kill the cells. Similarly, resveratrol and its dimers pallidol and quadrangularin A, are found to be inefficient RTAs in lipid bilayers. Our studies to date rather suggest that they autoxidize readily to produce hydrogen peroxide, which may induce expression of phase 2 antioxidant enzymes, affording cytoprotection. Our insights underscore the need for systematic studies of antioxidant activity in multiple contexts.

Abstrait

La peroxydation des lipides a été impliquée au début et pendant la progression de plusieurs maladies dégénératives, incluant les maladies cardiovasculaires, l'Alzheimer et le cancer. Par conséquent, pendant plus de 50 ans, des efforts considérables ont été consacrés à la conception de produits synthétiques et à la découverte de produits naturels pouvant ralentir la peroxydation lipidique. Malgré les investissements considérables jusqu'à présent, il n'y a aucune stratégie impliquant des antioxydants pour le traitement des maladies dégénératives. Nous argumentons que cela est causé par un manque fondamental de compréhension sur la réactivité chimique de ces composés dans des contextes spécifiques.

Nous décrivons, ici, les études de nos antioxydants synthétiques optimisés pouvant piéger des radicaux, les tetrahydronaphthyridinols (THNs). Nous présentons, en premier, la synthèse d'une série de THN analogue à l'α-tocophérol (l'un des meilleurs antioxydant naturel solubles dans les lipides pouvant piéger des radicaux) avec différentes substitutions de chaine sur le côté de la molécule; par la suite, nous démontrons comment des changements systématiques de la lipophilicité de ces antioxydants ont un impact sur leurs réactivités avec les radicaux peroxyles dans les bicouches lipidiques et dans les cellules de mammifères. Leur régénération dans les bicouches lipidiques par des réducteurs solubles dans l'eau, leurs fixations à la protéine transporteuse de tocophérol (hTTP), ainsi que leurs cytotoxicité ont aussi été évalués afin de déterminer si ce type d'antioxydant pourrait mener à des études animales.

Nous décrivons aussi des études analogues de produits naturels telles que l'allicin, le thiolsulfinate retrouvé dans l'ail et le polyphénol resvératrol retrouvé dans les grappes. Ces composés ont attirés beaucoup d'attention au cours des dernières 20 années due à leurs bénéfices pour la santé, souvent attribué à leurs activités alléguées en tant qu'antioxydant capable de piéger des radicaux (APR). Jusqu'à présent, il y a très peu d'études systématiques sur leur capacité à piéger des radicaux en solutions, en bicouche lipidiques et dans des cellules de mammifères. Nous avons déterminé que les thiosulfinates allicin et petivericin, même s'ils sont efficaces en solution, ne le sont pas dans les bicouches lipidiques. De plus, ces composée ne sont pas des antioxydants dans les cultures cellulaires, tuant plutôt les cellules. De manière semblable, le resvératrol et ses dimères pallidol et quadrangularin A,

sont inefficacse comme APR dans les bicouches lipidiques. Jusqu'à date, nos études suggèrent plutôt qu'ils s'auto-oxydent rapidement pour produire du peroxyde d'hydrogène, ce qui pourrait induire l'expression d'enzyme antioxydante de phase 2, procurant ainsi une cytoprotection. Nos recherches et les connaissances approfondies que nous avons recueillies soulignent la nécessité d'études systématiques pour déterminer l'activé des antioxydants dans des contextes multiples.

Acknowledgements

First and foremost, I would like to thank my supervisor Professor Dr. Derek A. Pratt for accepting me as his student and introducing me into the amazing “free radicals and antioxidants” world. Huge thanks for giving me the opportunity to carry out research under his guidance over the past few years. It is his attitude, enthusiasm for chemistry and broad chemical knowledge which made me feel confident during challenging times. Without his support, it would not have been possible for me to progress to such a level.

I would also like to thank all the members in the Pratt group for their support, discussion, and advise on the project in the past few years. Thanks for their patience in answering all the questions I had. It has been a great time working with all you guys. I would like to thank all the collaborators that involved in these projects. Special thanks go to Dr. Eric Ye for the NMR spectroscopy and Peter Andrew Ochalski for flow cytometry assistance.

Huge thanks to my friends and my family members. Being with all of you helped me not feel alone in Canada and fight through the hardship in my research and hardtime in the past few years.

Statement of Originality

I hereby certify that all of the work described within this thesis is the original work of the author, with those exceptions noted in the thesis that are carried out by the collaborators listed in the preface in each chapter. Any published (or unpublished) ideas and/or techniques from the work of others are fully acknowledged in accordance with the references.

Bo Li

March 2016

Table of Contents

List of Schemes

List of Figures

List of Tables

List of Charts

List of Abbreviations

α-TOH α-tocopherol

AAPH 2,2’-azobis-(2-amidinopropane) monohydrochloride

AIBN 2,2’-azobis(2-methylpropionitrile)

AIPH 2,2'-azobis[2-(2-imidazolin-2-yl)propane]dihydrochloride

ApoE Apolipoprotein E

BDE bond dissociation enthalpy

BHT butylated hydroxytoluene (2,6-di-*tert*-butyl-4-methylphenol)

CAT catalase

CH_3CN acetonitrile

DCFH-DA 2’,7’-dichloro-dihydrofluorescein diacetate

DOPC dioleoylphosphatidylcholine

DMF *N*,*N*-dimethylformamide

DMSO dimethylsulfoxide

DTT Dithiothreitol

EDG electron-donating group

EWG electron-withdrawing group

GPX glutathione peroxidase

GR glutathione reductase

GSSG glutathione disulfide

HAT hydrogen-atom transfer

HB hydrogen bond

HBA hydrogen bond acceptor

HBD hydrogen bond donor

HDL high-density lipoprotein

HOMO highest occupied molecular orbital

HPLC high-pressure liquid chromatography

IP ionization potential

LDL low density lipoprotein

LOOH lipid peroxides

LOX lipoxygenase

LUMO lowest unoccupied molecular orbital

MeOAMVN 2,2’-azobis(4-methoxy-2,4-dimethylvaleronitrile)

MPO myeloperoxidase

NAC *N*-acetylcysteine

NADPH nicotinamide adenine dinucleotide phosphate

Nrf2 nuclear factor erythroid 2-related factor 2

PCET proton-coupled electron transfer

PLPC 1-palmitoyl-2-linoleoylphosphatidylcholine

PMC/PMHC 2,2,5,7,8-pentamethyl-6-chromanol

ROS reactive oxygen species

RTA radical-trapping antioxidant

SOD superoxide dismutase

SPLET sequential proton-loss electron transfer

THF tetrahydrofuran

THN tetrahydronaphthyridinol

Trolox 2-carboxy-2,5,7,8-tetramethyl-6-chromanol

TTP tocopherol transport protein

Chapter 1:

Background and Significance

1.1 Reactive Oxygen Species, Autoxidation and Its Inhibition by Radical-Trapping Antioxidants

1.1.1 Reactive Oxygen Species

"The paradox of aerobic life" is that "higher eukaryotic aerobic organisms cannot exist without oxygen, yet oxygen is inherently dangerous to their existence".[1] Although we cannot survive without oxygen, the free radical nature of oxygen can lead to oxidative stress. This is an unavoidable problem for all aerobic organisms, including humans. A free radical is any atom or molecule with one or more unpaired electrons in the outer valence shell, and molecular oxygen fits this definition, possessing two unpaired electrons in its outer valence shell (•O-O•). Molecular oxygen can be easily reduced under the reductive environment *in vivo*, producing the superoxide radical anion ($O_2^{\bullet-}$) with a redox potential $E°\sim$ -0.16V *vs*. NHE in water at pH 7.[2] In fact, although over 96% of the O_2 we used is reduced to water as a result of respiration,[1] about 4% receives a single electron from the ubiquinol-ubiquinone electron transport chain during the respiration process, generating superoxide (**Scheme 1.1**).[3]

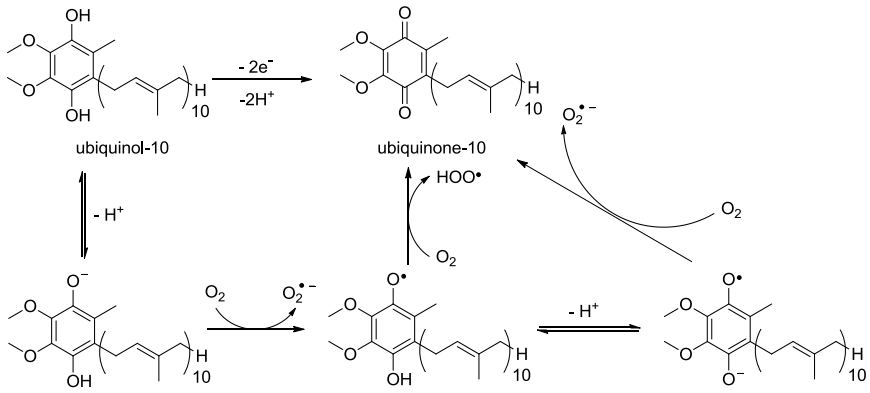

Scheme 1.1. The ubiquinol-10/ubiquinone redox couple and the reactions which may lead to superoxide production.

Superoxide is also produced by NADPH oxidase, a membrane bound enzyme that plays an essential role in the destruction of pathogens by neutrophils, the most abundant type of white blood cell in mammals, as an essential part of the innate immune system.[4] Although superoxide is nominally a reducing agent, its conjugate acid – the hydroperoxyl radical (HOO•, pK_a = 4.7)[2] – is a good oxidant, as are the other superoxide-derived oxidizing agents collectively referred to as reactive oxygen species (ROS), which include hydrogen peroxide (H_2O_2), hypochlorous acid (HOCl), peroxynitrite and its conjugate acid (ONOOH, pK_a = 6.8)[5] and the extremely reactive hydroxyl radical (HO•) (**Scheme 1.2**).

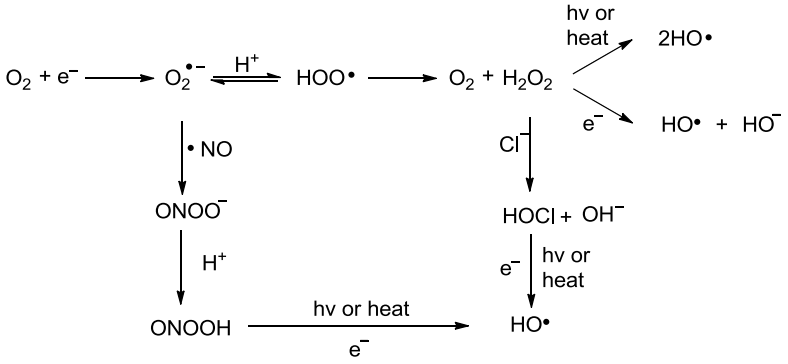

Scheme 1.2. The one electron reduction of O_2 can lead to a variety of oxidants collectively known as 'reactive oxygen species'.

Uncontrolled and/or excessive production of ROS gives rise to oxidative stress, which leads to damage of biomolecules such as DNA, proteins and lipids and their corresponding dysfunction or degradation. Biomolecule oxidation has been implicated in the onset and progression of degenerative diseases such as atherosclerosis, Alzheimer's, and cancer[6,7] Among the many types of DNA damage from ROS, 8-oxo-guanine is one of the most common DNA lesions that is associated with carcinogenesis.[8] It is formed from reactions of guanine with a variety of ROS, including the hydroxyl radical (**Scheme 1.3**), and leads to DNA replication errors from mismatched pairing of 8-oxo-guanine with adenine instead of cytosine.[9]

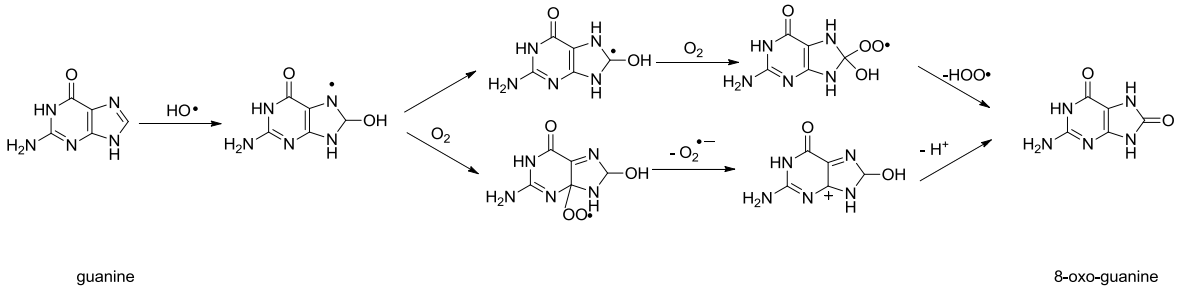

Scheme 1.3. Proposed mechanisms of the reaction of hydroxyl radical with guanine leads to 8-oxo-guanine.

The reactions of ROS with proteins is known to occur primarily on the amino acid sidechains, but can also take place on the protein backbone, leading to fragmentation.[10] The most easily oxidized amino acid sidechains are sulfur-containing cysteine and methionine residues, as well as electron-rich aromatic sidechains such as those found in tyrosine and tryptophan (**Scheme 1.4A**).[10] Oxidation of residues involved in the catalytic machinery of an enzyme may lead directly to enzyme dysfunction, while oxidation of residues further away from the catalytic site may still lead to enzyme dysfunction owing to changes in protein structure. Likewise, protein-protein interactions, or other interactions important in signal transduction can be directly or indirectly impacted by oxidative damage to amino acid sidechains. Under harsh oxidizing conditions (e.g. ionizing radiation), protein backbone cleavage can occur via H-atom transfer to reactive oxygen species such as hydroxyl radicals, followed by O_2 addition and the onset reactions (**Scheme 1.4B**).[10]

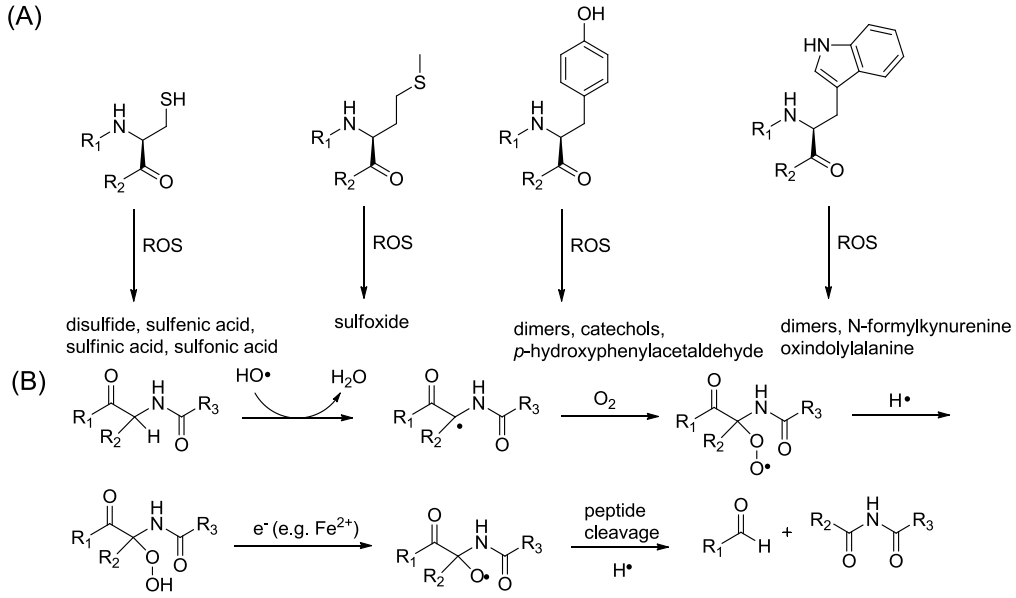

Scheme 1.4. Examples of ROS damage to proteins: (A) Oxidation of some amino acid sidechains; (B) Reactions of hydroxyl radicals can lead to protein backbone cleavage.

Although oxidative damage to DNA and proteins can lead to a loss of their normal function, it is widely acknowledged that reactions between ROS and lipids are even more problematic, as those reactions initiate an autocatalytic free radical chain reaction, referred to as "autoxidation" or "lipid peroxidation".[11] Moreover, many lipid peroxidation products decompose readily to cytotoxic electrophiles that react with proteins and DNA, which can alter their proper structure and function.[12,13]

1.1.2 (Lipid) Autoxidation

Autoxidation is a far-reaching problem; it is largely responsible for the oxidative degradation of all petroleum-derived materials in industry, including lubricating oils, fuels, rubbers and polymers, as well as the hydrocarbons that make up living matter, such as the polyunsaturated lipids and steroids that comprise biological membranes and lipoproteins (**Chart 1.1**).

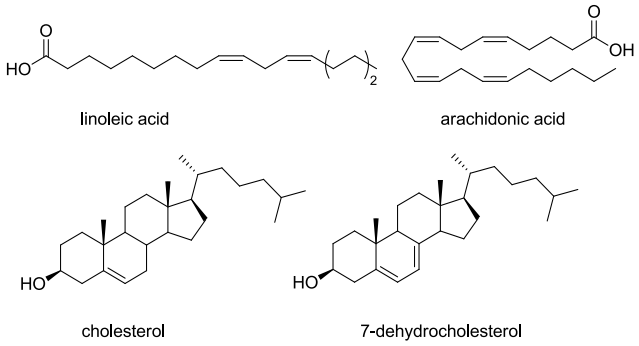

Chart 1.1. Highly oxidizable lipid substrates in biological settings.

Autoxidation is the archetype free radical chain reaction, and formally results in the insertion of O_2 into a C-H bond in the oxidizable substrate, by the mechanism shown in **Scheme 1.5** (Eq. 1.1-1.4).[14] The chain reaction can be initiated by any radical that can abstract a H-atom from an oxidizable substrate (R-H, Eq. 1.1). The resultant carbon-centered radical (R•) reacts with O_2 at (or near) the rate of diffusion to afford a peroxyl radical (ROO•, Eq. 1.2).[15] The peroxyl radical can then propagate the chain reaction by abstracting H atom from another molecule of oxidizable substrate to yield a hydroperoxide (ROOH) and a new alkyl radical (Eq. 1.3; this reaction is ascribed the key propagation rate constant k_p). Chain termination occurs by radical-radical reactions to give

non-radical products (Eq. 1.4), such as the reaction of two secondary peroxyl radicals, leading to an alcohol, a ketone and O_2.[16] The steady state concentration of ROO• is much higher than the steady state concentration of R• because the rate of reaction **1.3** is much slower than the rate of reaction **1.2**.

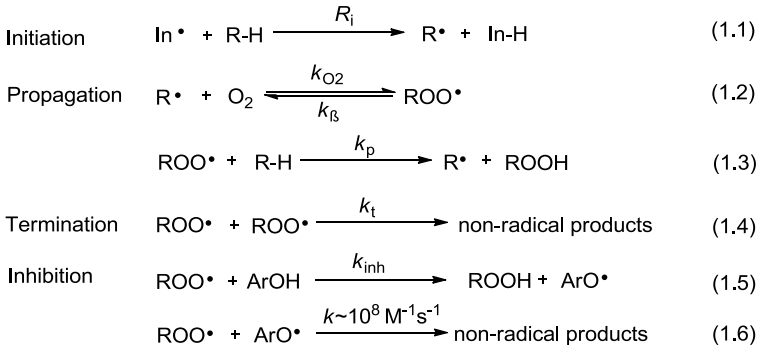

Scheme 1.5. The radical chain mechanism of hydrocarbon autoxidation.

Linoleic acid is the most abundant unsaturated lipid *in vivo* (k_p = 62 $M^{-1}s^{-1}$).[17] Its peroxidation produces as little as two and as many as five regioisomeric hydroperoxides depending on the reaction conditions, due to the reversibility of O_2 addition to the intermediate pentadienyl radical (**Scheme 1.6A**)[18,19] (A detailed reaction mechanism will be discussed later in this chapter.) Secondary products of linoleic acid autoxidation are mainly aldehydes such as 4-hydroxynonenal (4-HNE) (**Scheme 1.6B**), which is extremely toxic due to its reactivity toward nucleophilic sites on DNA and proteins.[20]

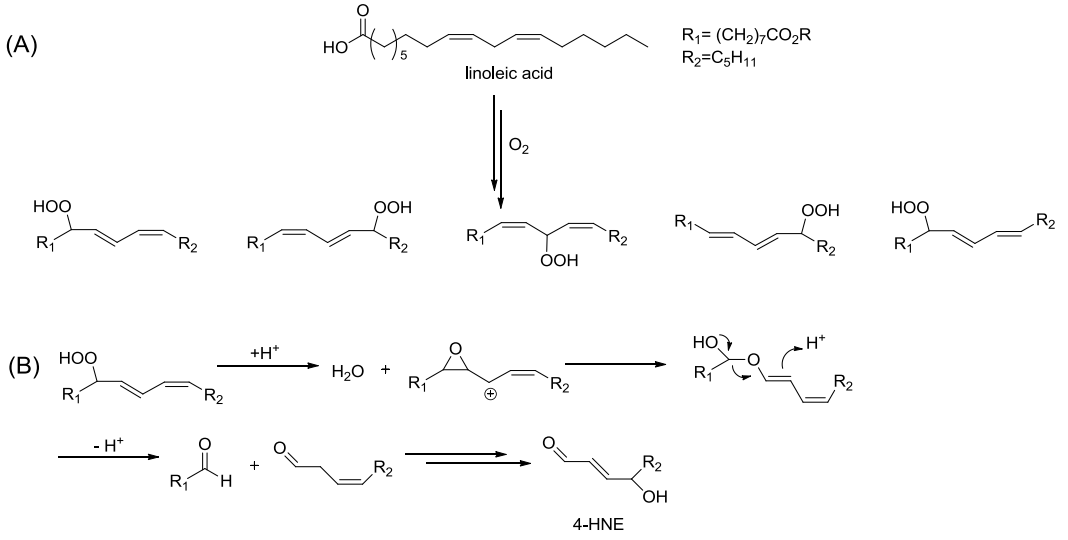

S**cheme 1.6.** (A) Lipid hydroperoxides that may arise from autoxidation of linoleic acid, depending on reaction conditions (see **Scheme 1.15**); (B) Formation of 4-HNE from 9-hydroperoxyoctadeca-10*E*,12*Z*-dienoic acid.

Oxidation of unsaturated lipids with higher levels of unsaturation, such as arachadonic acid (k_p = 197 $M^{-1}s^{-1}$),[21] leads to more complicated products including endoperoxides, isofurans and malondialdehyde as shown in **Scheme 1.7**.[11] Oxidation of cholesterol (k_p = 11 $M^{-1}s^{-1}$)[22] and 7-dehydrocholesterol (k_p = 2260 $M^{-1}s^{-1}$)[22] in low density lipoprotein is also problematic and oxidation products have been detected in atherosclerotic lesions and diseased liver tissue.[23,24]

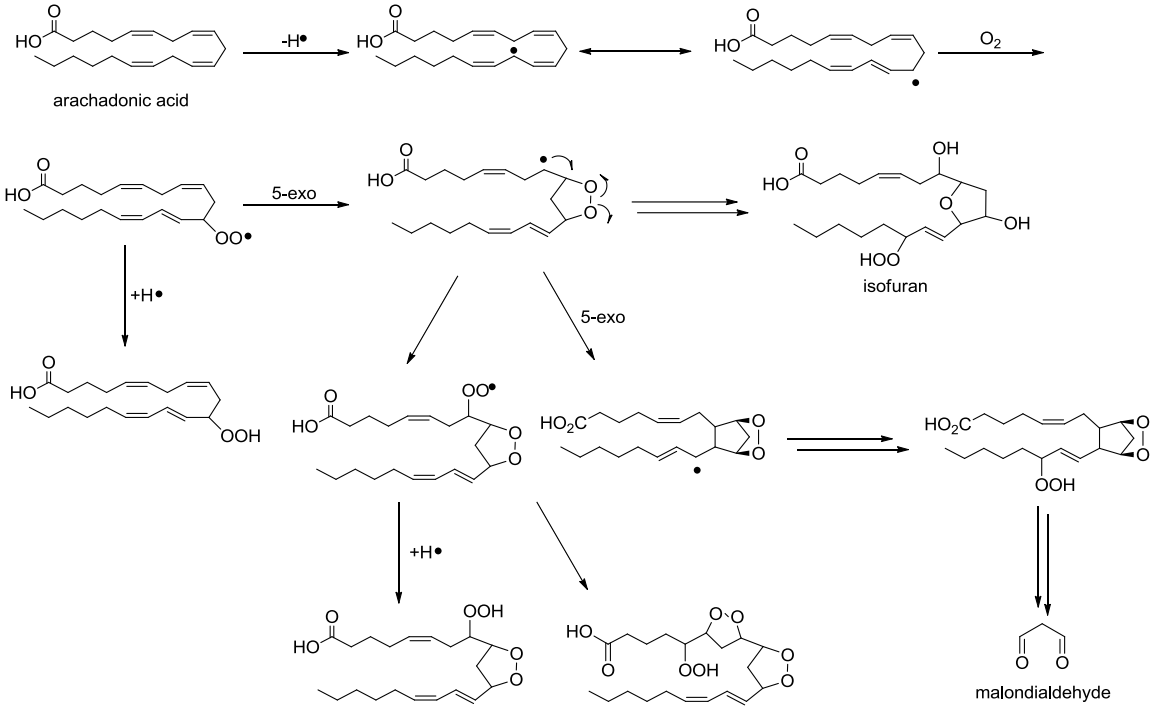

Scheme 1.7. Examples of products arising from the autoxidation of arachadonic acid.[11]

1.1.3 Antioxidants

Antioxidants are broadly defined as compounds which slow autoxidation. To survive the oxygenated environment *in vivo*, living organisms have a variety of antioxidants to slow the damage of ROS. In general, antioxidants are divided into two categories, based on their mechanism of action: preventive antioxidants and radical-trapping antioxidants (RTAs).[25,26]

1.1.3.1 Preventive Antioxidants

Preventive antioxidants decrease the rate at which new radical chains are started (the rate of initiation, R_i) by quenching the source of initiating radicals. The most important preventive antioxidants are those which decompose peroxides – either alkyl hydroperoxides or

hydrogen peroxide – precluding their ability to form chain-initiating hydroxyl radicals via Fenton-type (or photolytic) reactions (Eq. 1.7).[27]

$$Fe^{2+} + H_2O_2 \longrightarrow Fe^{3+} + HO\bullet + OH^- \qquad (1.7)$$

In biological settings, preventive antioxidants are often enzymes, such as superoxide dismutase (SOD), catalase (CAT), glutathione peroxidase (GPx), and glutathione reductase (GR). Superoxide dismutases are a series of enzymes existing in almost all living cells which catalyze dismutation of superoxide to oxygen and hydrogen peroxide at the rate of diffusion,[28] therefore, they act as the first antioxidant defense system against ROS (Eq 1.8).[29] There are three common isoforms of SODs, located in the cytoplasm, mitochondria, as well as extracellularly and contain either copper and zinc, manganese and iron, or nickel, to catalyze the reaction.[30]

$$2O_2^{\bullet -} + 2H^+ \xrightarrow{SOD} O_2 + H_2O_2 \qquad (1.8)$$

$$2H_2O_2 \xrightarrow{CAT} 2H_2O + O_2 \qquad (1.9)$$

Catalases are an important family of enzymes containing heme, non-heme iron or manganese groups which catalyze decomposition of millions of hydrogen peroxide molecules to water and oxygen every second (Eq 1.9).[31] Glutathione peroxidases (GPx's) are another series of enzymes that protect against oxidative stress. They catalyze the redox reaction between glutathione (GSH) and, hydrogen peroxide or lipid hydroperoxide to produce glutathione disulfide (GSSG) and water or the corresponding alcohol of the lipid hydroperoxide (**Scheme 1.8**).[32] Among the known isoforms of GPx, GPx4 is arguably most relevant since it is specifically responsible for reducing lipid hydroperoxides to the corresponding alcohols.[33,34]

$$\text{GPx-Se-H} + \text{or} \begin{matrix}\text{ROOH}\\ H_2O_2\end{matrix} \longrightarrow \text{GPx-Se-OH} + \text{or} \begin{matrix}\text{ROH}\\ H_2O\end{matrix}$$

$$\text{GPx-Se-OH} + \text{GSH} \longrightarrow \text{GPx-Se-SG} + H_2O$$

$$\text{GPx-Se-SG} + \text{GSH} \longrightarrow \text{GPx-Se-H} + \text{GSSG}$$

Scheme 1.8. Mechanism of glutathione peroxidase.

1.1.3.2 Radical-Trapping Antioxidants

Radical-trapping antioxidants (RTAs), also known as chain-breaking antioxidants, reacting with lipid peroxidation chain-carrying peroxyl radicals directly. The prototypical RTAs are

phenols (ArOH), which react with peroxyl radicals via transfer of the phenolic H-atom (Eq 1.10).[25,26] The resulting phenoxyl radicals (ArO•) are generally persistent, as they are slow to react with either the oxidizable substrate or O_2, and are eventually consumed by reaction with another peroxyl radical (Eq 1.11). The phenoxyl radical should be unreactive to abstract a H-atom from another lipid or lipid peroxide molecule, otherwise, the RTA is ineffective since it would act as a chain transfer agent (Eq 1.12, and Eq 1.13). It must be pointed out that a common misconception is that the biological activities of RTAs arise in part from their reactivity to hydroxyl radicals. This cannot be the case since hydroxyl radicals react with virtually all molecules at, or close to, diffusion-controlled rates.[35] Another misconception is that RTAs react with superoxide ($O_2^{\bullet -}$). Again, this is not the case, because both the RTA and superoxide are reducing agents.[36] Instead, the conjugate acid of superoxide, the hydroperoxyl radical ($pK_a = 4.7$),[2] reacts with RTAs.

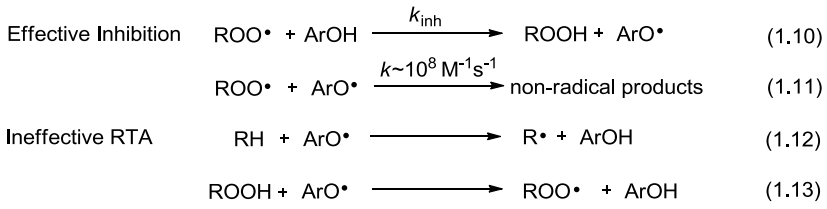

Much of what we know about RTAs stems from the longstanding need to inhibit hydrocarbon autoxidation in industrial contexts, which brought about the development of the phenol- and arylamine-containing compounds that are now almost universally added to petroleum-derived products. Among the most common additives are derivatives of 2,6-di-*tert*-butyl-4-methylphenol (BHT) and ring-alkylated diphenylamines (*cf.* **Chart 1.2**). The suggestion that nature makes use of phenolic compounds, such as α-tocopherol (α-TOH), the most biologically active form of Vitamin E,[37] to slow the autoxidation of polyunsaturated lipids and sterols in lipid bilayers and lipoproteins is almost recent.[38] Since then, a staggering number of naturally-occurring substituted phenols have been isolated and/or studied as RTAs of potential biological significance, but very few of them as rigorously as the compounds in **Chart 1.2**.[9,39,40] Aside from lipid peroxyl RTAs, of which α-TOH is the most active *in vivo*, water soluble radical-trapping antioxidants are also important to balance oxidative stress *in vivo*, among which ascorbate is the most important.[41,42] However, due to their poor lipid solubility, it is unlikely that their major

roles are to directly trap lipid peroxyl radicals.

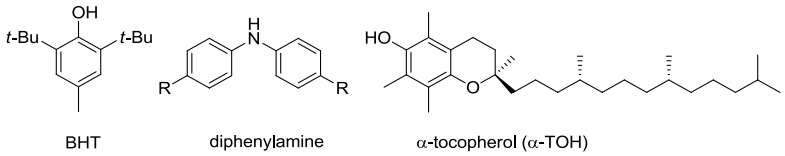

Chart 1.2. Well-studied RTAs.

The putative linkage between lipid peroxidation and the onset and progression of degenerative disease has prompted enormous interest in whether scavenging harmful free radicals by RTAs can reduce the risk of disease and/or increase longevity.[43] Huge research investments have been devoted to clinical trials to study the role of natural antioxidants, such as vitamin E (α-TOH), ascorbate and β-carotene as the preventive and/or therapeutic agents, but most have failed to identify a direct and clear role of the studied compounds in the progression of degenerative disease.[44] Several potential explanations for the failure of clear results in clinical trials have been suggested, including the notion that the types and dosage of antioxidants examined clinically, or the duration of the studies, have been inadequate.[45,46] It is also highly unlikely that RTAs function in a therapeutic way – precluding any positive outcome in trials wherein RTAs have been employed as treatments for degenerative conditions. It is far more likely that RTAs can be potent preventive agents, decreasing the rate at which mutations occur, or preventing protein dysfunction or aggregation driven by the reactions of lipid-derived electrophiles formed as a result of lipid peroxidation. Indeed, it has been shown in animal models that vitamin E was able to inhibit atherosclerosis when introduced at early stages but not late stage atherosclerosis in Apolipoprotein E (Apo-E) knockout mice.[47]

Another question is: are we studying the right compounds? Common compounds that are used in clinical trials such as α-TOH, ascorbate and β-carotene all have drawbacks as effective lipid soluble RTAs. α-TOH has a huge shortcoming because it promotes lipid peroxidation in low density lipoproteins due to the chain transfer reaction of α-TOH derived radical and unsaturated lipid.[48,49] Ascorbate can also be a prooxidant under certain conditions,[50] and β-carotene is only a good RTA under partial physiological oxygen pressure, otherwise it is a pro-oxidant.[51] Therefore, design and discovery of compounds that are better RTAs without those above-mentioned drawbacks under physiological

conditions may provide some insight into whether RTAs promote health, reduce progression of degenerative disease and/or prolong life.

Other natural compounds such as allicin extracted from garlic, resveratrol and oligomers in grape skin, quercetin and other flavonoids have also been heavily studied for their health promoting benefit, including inhibit atherosclerosis and cancers.[52,53] Although people have ascribed benefit of those compounds to their purported radical-trapping activities, their mechanism of action is far from clear.

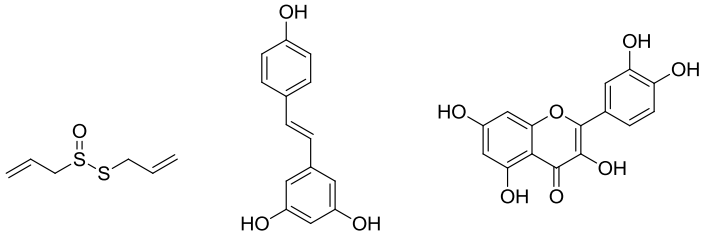

allicin resveratrol quercetin

1.2 Factors Affecting Radical-Trapping Activities of Phenolic and Aminic Antioxidants

The high reactivity of phenolic (and aminic) RTAs towards peroxyl radicals is due to both thermodynamic and kinetic factors. In 1963, Ingold and co-workers demonstrated that the inhibition of the autoxidation of a hydrocarbon (styrene) by para- and meta- substituted phenols followed an excellent Hammett correlation using the electrophilic substituent constants σ^+ (Eq. 1.14) with a reaction constant of ρ = -1.58; phenols bearing electron-donating groups (EDGs) were much better antioxidants than those bearing electron-withdrawing groups (EWGs).[54,55]

$$\log(k_{inh}^{X\text{-}C6H4OH}/k_{inh}^{PhOH}) = \rho\sigma^+ \qquad (1.14)$$

Since the effects of substituents on the phenolic O-H bond strength follow the same trends due to the inherent electron-poorness of the phenoxyl radical, it follows that the trends in the kinetics correlate very closely to the trends in the thermodynamics, in accord with the Bell-Evans-Polanyi principle.[56,57] Phenol itself has an O-H BDE of 87 kcal/mol,[58] which is roughly the same as the O-H BDE in a hydroperoxide (88 kcal/mol).[59] While this makes the overall driving force for the formal H-atom transfer reaction between phenol and a peroxyl radical roughly zero, the reaction proceeds with a rate constant of $k_{inh} \sim 10^3$

$M^{-1}s^{-1}$.[60] The low inherent energetic barrier to this reaction results in part from the formation of a H-bonded pre-reaction complex between the reactants, and in part from the interaction of the highest occupied molecular orbital (HOMO) of the electron-rich aromatic ring and the lowest unoccupied molecular orbital (LUMO) of the electron-poor peroxyl radical, which promote electron transfer with simultaneous proton transfer between the two oxygen atoms.[26] The O-H bond can be weakened, and k_{inh} correspondingly increased, by substitution of the phenolic ring with EDGs, which stabilize the electron-poor phenoxyl radical,[61] and reduce the energy gap between the phenol HOMO and peroxyl radical LUMO. For example, the substitution of the phenolic ring in α-TOH lowers the O-H BDE by 10 kcal/mol, and increases k_{inh} by over three orders of magnitude to 3×10^6 $M^{-1}s^{-1}$.[37] The reactivity of phenolic RTAs can also be affected by the steric environment around the reactive O-H moiety. For example, BHT is 6-times less reactive than 2,4,6-trimethylphenol despite having a weaker O-H bond by 1.7 kcal/mol.[62]

Stereoelectronic effects are another factor to reduce the BDE of phenolic antioxidants. One such example is that 4-methoxy-2,3,6-trimethylphenol is 3.3 times more reactive than 4-methoxy-2,3,5,6-tetramethylphenol, although the missing methyl group on the phenolic ring should decrease the electron density of the phenoxyl radical.[62] This is because of the increased overlap between the O-atom's lone pairs in the alkoxyl group and the aromatic ring in 4-methoxy-2,3,6-trimethylphenol compared to 4-methoxy-2,3,5,6-tetramethyl-phenol, which reduces the O-H BDE and increases the k_{inh}.[62]

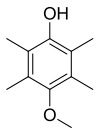

4-methoxy-2,3,5,6-tetramethylphenol

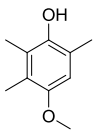

4-methoxy-2,3,6-trimethylphenol

Hydrogen bonding (HB) is another important factor affecting RTA activity. The intermolecular HB between a phenol and a hydrogen bond acceptor (HBA) molecule such as a hydrogen bond accepting solvent deactivates the radical trapping ability of RTAs, since only non-H-bonded phenols can react. This H-bonded pre-equilibrium figures directly into the kinetics of H-atom transfer to peroxyl radicals (**Scheme 1.9**).[63,64] Acids and bases in the system could also change the rate of H-atom abstraction due to different reaction mechanisms, which will be introduced in the next subsection.

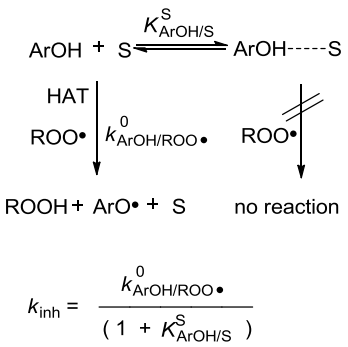

Scheme 1.9. Kinetic solvent effects on the reactions of phenols with peroxyl radicals.

1.3 Mechanism of H-atom Transfer

As shown above, the radical-trapping activity of antioxidants depends upon their ability to transfer a H-atom to peroxyl radicals. Although the strength of the labile bond to the H-atom of the RTA is often key to understanding the relative reactivities of compounds toward peroxyl radicals, it is not usually the sole determining factor. For example, H-atom transfer from PhO-H to peroxyl radicals ROO• is about 3000 times faster than for $PhCH_2$-H at 30°C.[54,61,65] Although the O-H BDE in phenol and the C-H BDE in toluene are almost identical, H-atom transfer between oxygen atoms has a lower barrier than H-atom transfer between oxygen and carbon. This is believed to be due to the lesser triplet repulsion between the oxygen atoms in the transition state of the former reaction than between oxygen and carbon in the latter (**Scheme 1.10**) due to the electronegativity difference between oxygen and carbon and the greater distance between the two oxygen atoms compared to the distance between carbon and oxygen atoms.[61,65,66]

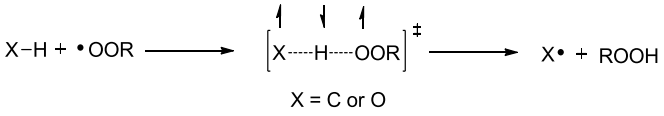

Scheme 1.10. H-atom transfer from phenol and toluene to peroxyl radicals.

However, it should also be pointed out that formal H-atom transfer from phenols can occur via three mechanisms: H-atom transfer (HAT), Sequential Proton Loss Electron Transfer (SPLET), and Proton-Coupled Electron Transfer (PCET), depending on the substitution, the hydrogen-bond accepting ability of the solvent, and the anion solvation

abilities of the solvent in which the reaction takes place.[63] These mechanisms are presented in **Scheme 1.11**. Phenolic RTAs trap peroxyl radicals via PCET (**Scheme 1.11A**). PCET was first proposed by Mayer and Borden to explain why the HAT between two oxygen atoms have higher rate constants and lower activation enthalpies than HAT between two carbon atoms when the O-H and C-H have the same BDE.[67,68] Subsequent theoretical calculations by DiLabio and Johnson on the *tert*-butylperoxyl/phenol reaction couple indicated that the formal H-atom transfer between a peroxyl and phenol also occurs by a PCET mechanism.[69] As shown in **Scheme 1.11A**, in the transition state for reactions between a phenol and a peroxyl radical, a hydrogen-bonded complex is formed between the peroxyl and OH group in the RTA. This occurs between the phenolic OH and O•, and the proton is transferred into the peroxyl radical's lone pair. The accompanying electron simultaneously moves from the π-HOMO of the phenol to the radical's π*-SOMO. In contrast, HAT from non-acidic hydrogen donors to peroxyl radicals, such as in the propagation step in autoxidation, is unaffected by reaction medium changes.[64] Ionizing solvents such as methanol and ethanol, which are commonly used in colourimetric assays of antioxidant activity, can promote H-atom transfer from phenolic antioxidants due to the presence of the more electron-rich phenoxide anion at equilibrium, which can react via electron transfer with radicals (especially those with high electron affinities, such as dpph• – more on this later).[63] This mechanism has been coined sequential proton loss electron transfer (SPLET, **Scheme 1.11B**).[70] This mechanism can be further promoted at basic pH, where the concentration of phenoxide is increased. In addition, reactions between phenols and peroxyl radicals can also be enhanced at acidic pH via the intervention of a different mechanism – one wherein protonation (or partial protonation) of the peroxyl radical increases its electron affinity such that electron transfer from the phenol to the hydroperoxide radical cation occurs (**Scheme 1.11C**).[71]

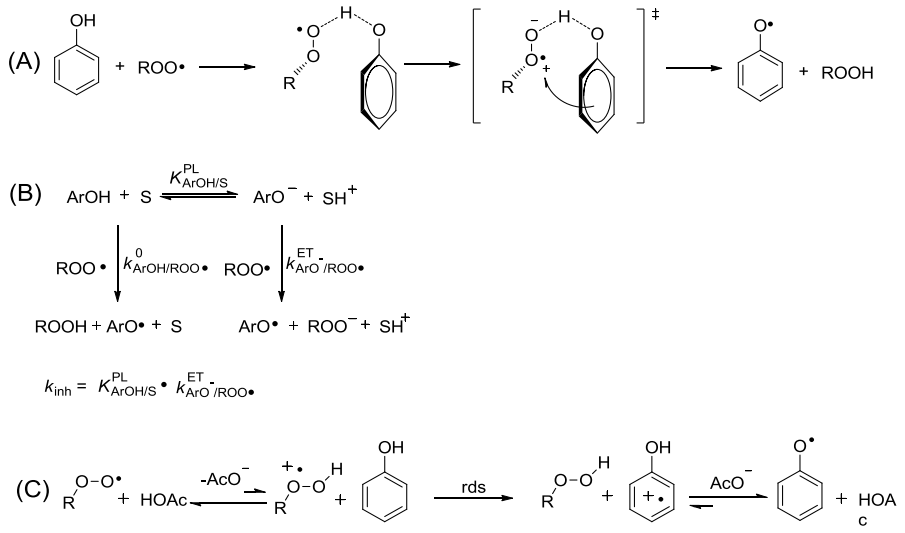

Scheme 1.11. Proton-coupled electron transfer (PCET) mechanism (A); mechanistic changes under basic (B) and acidic (C) conditions.

1.4 Methods to Determine the Efficacy of RTAs[i]

Historically, methods to determine the activities of RTAs were largely phenomenological observations (and continue to be so in many laboratories), but gave way to careful physical organic chemistry approaches from the 1950s to the 1980s, which enabled the elucidation of precise kinetic parameters and mechanistic information. More recently, comparatively simpler and correspondingly faster methods have been developed (some of which are available commercially as kits), but which often provide very limited (if any) information on the kinetics of the relevant reactions, and are often over-interpreted. In a biological context, consideration of RTA activity under each of these different conditions is vital to understand if it is likely to result from trapping of radicals. For instance, if a compound is a poor RTA in solution, but is highly reactive in cell culture, it is unlikely that its reactivity as an RTA is physiologically relevant and some other mechanism is more likely to be involved.[72]

[i] This section appears as in the published review: "Methods for determining the efficacy of radical-trapping antioxidants". See: Li, B.; Pratt, D. A. *Free Radical Biol. Med.*, **2015**, *82*, 187-202.

1.4.1 Measurements of RTA Activity in Solution

The most popular assays of radical-trapping antioxidant 'activity' share a simple principle and protocol: a measurement of the change in absorbance or fluorescence of a solution of an indicator upon addition of the test 'antioxidant'. The indicator is an oxidizing agent, which undergoes a redox reaction (generally a single electron transfer) with the 'antioxidant', a reducing agent, and the change in absorbance or fluorescence reflects the position of the equilibrium. The measurement is generally made after a sufficient amount of time in order to allow equilibrium to be established. These measurements effectively 'titrate' the reducing equivalents in the solution of the test 'antioxidant'. Examples of these popular assays are the 'total antioxidant capacity', TAC (employs a Cu^{2+} complex as the oxidant),[73] trolox equivalent antioxidant capacity, TEAC (employs the radical cation of 2,2'-azino-di-[3-ethylbenzthiazoline sulphonate] as the oxidant),[74] ferric reducing antioxidant capacity, FRAP (employs a Fe^{3+} complex as the oxidant),[75] and the dpph• scavenging activity (employs the 1,1-diphenyl-2-picrylhydrazyl radical as the oxidant).[76] The result is then given relative to a positive control, often Trolox, a water-soluble analog of α-TOH.[77,78]

The foregoing assays and variants thereof are popular for several reasons: commercial kits are readily available, they have well-defined protocols and they are easy and fast. Indeed, they are convenient for quick screens of the total reducing equivalents in biological samples or plant extracts. However, these assays suffer from two significant drawbacks. First, they generally report only on the position of the redox equilibrium, and not on the kinetics of the reaction of the 'antioxidant' with a peroxyl radical. Second, they are generally conducted in aqueous solution, or other highly ionizing media, which is not representative of the confines of lipid bilayers or lipoproteins – the major sites of peroxyl radical damage in the cell due to the ease of propagation of the radical chain reaction. Indeed, Ingold and co-workers have shown that not only are the kinetics of the reactions of RTAs with radicals strongly affected by the nature of the medium, but that the mechanism can also change, depending on the acidity or basicity of the solution.[63]

As such, translation of the results of simple colorimetric antioxidant assays to a physiological context is dubious at best. Rather than providing an extensive bibliography of

examples to illustrate this fact, and pointing the finger at those that may not have known better at the time, we will instead provide an overview of methods that enable a quantitation of the reactivity of an antioxidant toward a peroxyl radical – either directly or indirectly. This information is central to being able to determine whether a given compound can effectively inhibit peroxidation, which is only observed when the rate at which an antioxidant traps peroxyl radicals is much larger than the rate at which chain propagation occurs, i.e., $k_{inh}[ArOH] \geq k_p[R\text{-}H]$ (**Scheme 1.5**).

1.4.1.1 Indirect Methods

1.4.1.1 .1 Inhibited Autoxidation

Inhibited autoxidations are the best established among the methods to quantitatively measure the activities of RTAs. Examples are shown in **Figure 1.1**, where the reaction progress in each of a series of styrene autoxidations is monitored by O_2 consumption.

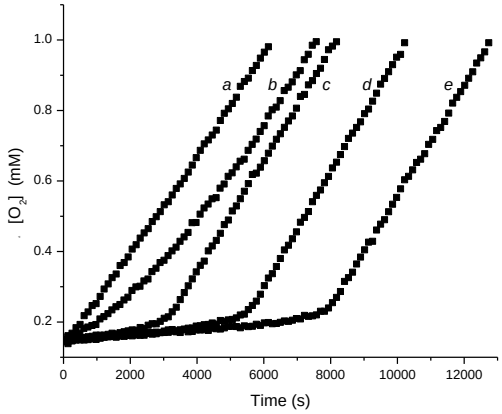

Figure 1.1 Oxygen consumption traces recorded during an inhibited autoxidation, in the absence of any antioxidant (*a*), in the presence of a mediocre RTA (*b*), in the presence of a good RTA at increasing concentrations (*c*, *d*, *e*).

Trace *a* corresponds to an uninhibited autoxidation, i.e., one wherein no RTA is present to inhibit the autoxidation. The rate of the oxidation is given by Eq. 1.15, which has been derived assuming a chain reaction (meaning the rate of oxidation, R_{ox}, is much larger than the rate of initiation, R_i), and therefore a steady state concentration of peroxyl radicals. Trace *b* corresponds to an autoxidation that is retarded by the addition of a mediocre RTA,

such that it competes with chain propagation and slows the rate of oxidation. Trace *c* corresponds to an autoxidation that is inhibited by a good RTA, which suppresses chain propagation sufficiently to give rise to an obvious 'inhibited period', commonly referred to as τ. The inhibited period is determined by the rate of initiation, the concentration of the RTA and the stoichiometry of its reaction with peroxyl radicals (hereafter referred to as *n*), as in Eq. 1.16. At the end of the inhibited period, the autoxidation continues at the same rate as the uninhibited autoxidation, just as in trace *a*. The rate of oxidation during the inhibited portion of the trace is given by Eq. 1.17, which enables determination of k_{inh} given the other terms are known. When no clear inhibited period is observed, as in trace *b*, k_{inh} can be determined by numerically fitting the experimental data to the relevant kinetic scheme with a kinetic simulation program such as Gepasi.[79] However, in order to do so, one must estimate a value for *n* (recall *n* is 2 for almost all phenolic RTAs due to Eq. 1.10 and Eq. 1.11). Phenolic RTAs first traps one peroxyl radical ROO•, and the so formed phenoxyl radical traps a second peroxyl radical to generate the non-radical product and terminate the radical chain reaction.

$$\frac{-d[\mathrm{O_2}]}{d\mathrm{t}} = \frac{-d[\mathrm{RH}]}{d\mathrm{t}} = \frac{d[\mathrm{ROOH}]}{d\mathrm{t}} = \frac{k_\mathrm{p}}{\sqrt{2k_\mathrm{t}}}[\mathrm{RH}]\sqrt{R_\mathrm{i}} \qquad \text{Eq. 1.15}$$

$$\tau = \frac{n[\mathrm{RTA}]}{R_i} \qquad \text{Eq. 1.16}$$

$$\frac{-d[\mathrm{O_2}]}{d\mathrm{t}} = \frac{-d[\mathrm{RH}]}{d\mathrm{t}} = \frac{d[\mathrm{ROOH}]}{d\mathrm{t}} = \frac{k_\mathrm{p}[\mathrm{RH}]}{\tau k_\mathrm{inh}} \qquad \text{Eq. 1.17}$$

The value of *n* for common RTAs, such as the phenols BHT and α-TOH, is generally 2, owing to the reactions in Eq. 1.10 and Eq. 1.11; the initial H-atom transfer from the phenol to a peroxyl radical, and subsequent reaction of the resultant phenoxyl radical with another peroxyl radical. Lower values of *n* reflect a different fate of the RTA-derived radical. For example, hydroquinones, such as reduced coenzyme Q_{10}, are often characterized by $n << 2$ because the semiquinone radical formed following H-atom transfer from the hydroquinone to a peroxyl radical undergoes a very fast reaction with O_2 to yield a hydroperoxyl radical that may propagate the autoxidation chain (e.g. the semiquinone radical derived from 2,5-di-*tert*-butyl-hydroquinone reacts with O_2 with a rate constant of 2.0×10^6 $M^{-1}s^{-1}$ in chlorobenzene at 298 K).[80] The non-integer values of *n* that are customarily observed in these systems reflect the partitioning of the semiquinone radical intermediate between

reactions with O_2 (which would result in $n = 0$ if all semiquinone radicals reacted this way) and reaction with another peroxyl radical ($n = 2$). It must be pointed out that the fate of the RTA-derived radicals does not affect the absolute rate constant at which antioxidant traps peroxyl radicals, k_{inh}.

Eq. 1.17 is only applicable if the inhibited autoxidation is a chain reaction, i.e. $R_{ox} >> R_i$, and therefore, it is often necessary to adjust the RTA concentration and the concentration and/or identity of RH to ensure that this condition is met. For very reactive antioxidants (k_{inh} = 10^6-10^7 $M^{-1}s^{-1}$), styrene (k_p = 41 $M^{-1}s^{-1}$) and methyl linoleate (k_p = 62 $M^{-1}s^{-1}$) are commonly used substrates, whereas for less reactive antioxidants (k_{inh} = 10^4-10^5 $M^{-1}s^{-1}$), cumene (k_p = 0.34 $M^{-1}s^{-1}$) and tetralin (k_p = 6.3 $M^{-1}s^{-1}$) are often used.[17] The radical chain reaction is usually initiated by the thermal decomposition of an azo compound, such as 2,2'-azobis(2-methylpropionitrile) (AIBN) (ek_d = 5.9 × 10^{-8} s^{-1} at 30 °C in chlorobenzene)[81] or 2,2'-azobis(4-methoxy-2,4-dimethylvaleronitrile) (MeOAMVN) (ek_d = 2.73 × 10^{-5} s^{-1} at 37 °C in benzene)[82]. While R_i can be calculated based on the known decomposition kinetics of these compounds and their concentrations, it is often more reliable to determine it using Eq. 1.16 and the inhibited period observed in an autoxidation inhibited by a good RTA for which n is known, such as α-TOH or its truncated analog, 2,2,5,7,8-pentamethyl-6-chromanol (PMC).

Reaction progress can be monitored by either consumption of O_2 or formation of products (usually ROOH). Oxygen consumption is usually monitored relative to a matched fully inhibited autoxidation using a differential pressure transducer,[62] but other methods have been developed. For example, the linewidth changes of the EPR signals of a persistent radical (e.g. TEMPO) as a function of O_2 can be monitored,[83] or the quenching of an O_2-sensistive fluorophore can be assayed by microplate reader.[84,85] Hydroperoxides were traditionally determined by iodometric analysis, which is based on the titration of sodium thiosulfate with the iodine produced upon incubation of the oxidized sample with potassium iodide (**Scheme 1.12**).[86]

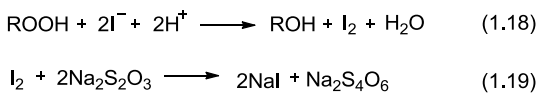

Scheme 1.12. Iodometric titration of hydroperoxides.

Alternatively, high-performance liquid chromatography (HPLC) with UV detection has been used when the product is a hydroperoxide that has a reasonable chromophore, such as the diene moiety of the linoleyl hydroperoxides, or the phenyl rings of cumene hydroperoxide or tetralin hydroperoxide.[56] GC/FID and/or GC/MS analyses are also possible, but must be preceded by reduction of the hydroperoxide to the corresponding alcohol using, e.g., sodium borohydride or triphenylphosphine,[87,88] and sometimes bolstered by silylation of the alcohols for better chromatographic separation.[89] Unfortunately, these methods are generally time-consuming. Unlike the continuous measurements involved in the oxygen consumption experiments, monitoring hydroperoxide production requires regular sampling of the reaction mixture, and subsequent analysis.

Hydroperoxide determination can be made slightly more high-throughput using (pro-)fluorescent probes, whose reactions with hydroperoxides can be followed by microplate reader. The probes are often fluorophores conjugated to phosphines, such as diphenyl-1-pyrenylphosphine[90,91] and Spy-LHP[92] (**Chart 1.3**); in the 'off-state' the fluorescence of the probe is quenched by photoinduced electron transfer from the phosphine, which no longer occurs upon oxidation of the phosphine to the 'on-state'. The majority of these probes were designed to report on hydroperoxide formation in real time in solution and/or cells, but can, in principle, be used in a quantitative manner. A single fluorescence reading is generally insufficient, since the rate of reaction between triarylphosphines and hydroperoxides are slow, making achieving the endpoint a lengthy process. Instead, it is best to carry out an initial rate measurement and, provided that the rate constant for the reaction of the probe with a hydroperoxide is known, the concentration of the hydroperoxide can be determined.

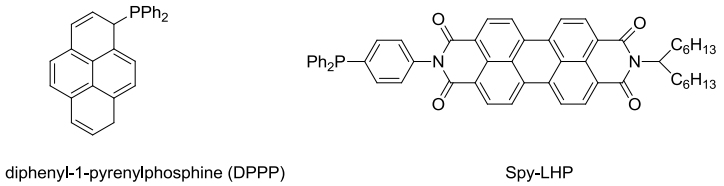

Chart 1.3. Commonly used fluorophores to quantify hydroperoxides.

Disappointed with the lack of commercial availability, solubility, and/or expense of many reported probes, our laboratory recently developed a trivially-prepared

coumarin-conjugated triarylphosphine fluorescent probe for hydroperoxide determination.[93] After a brief structure-activity optimization, we settled on the structure shown in **Scheme 1.13**, which reacts with secondary hydroperoxides with a rate constant of 9.1 $M^{-1}s^{-1}$ in methanol at 37°C. In practice, aliquots can be removed from an inhibited autoxidation and placed in the wells of a microplate, and the fluorescence of each well read over a short period of time (60 seconds) following addition of a solution of the dye to each well. The hydroperoxide concentration can then be calculated based upon the observed initial rate, concentration of the probe and the known rate constant. While far quicker than iodometric titrations or chromatographic analyses, these microplate assays are still slower than the continuous measurements in oxygen consumption experiments. However, they are more versatile, as they can be carried out under conditions where oxygen consumption cannot, such as autoxidations at elevated temperatures, where reactions must be continuously oxygenated in order to avoid rate-limiting mass transfer of O_2.[94]

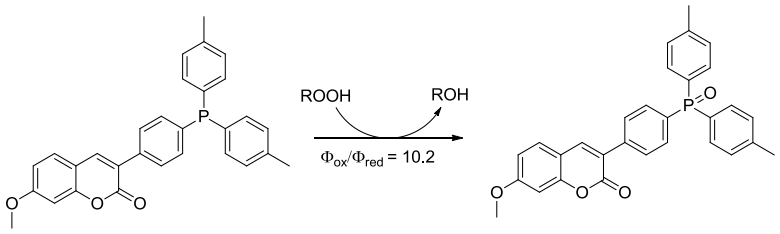

Scheme 1.13. Reaction of coumarin-triarylphosphine probe with hydroperoxide.

Inhibited autoxidation is suitable to measure the absolute k_{inh} values for reactions of RTAs with peroxyl radicals of 10^4 to 10^8 $M^{-1}s^{-1}$ (see some examples in **Table 1.1**).

Table 1.1. Examples of classical and next-generation RTAs whose inhibition rate constants have been measured by inhibited autoxidation.

classic RTAs

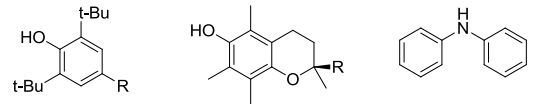

1 R = CH_3
2 R = OCH_3

3 R = $C_{16}H_{33}$
4 R = CH_3

5

next-generation RTAs

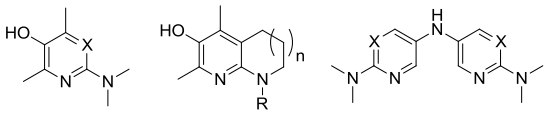

6 X = CH
7 X = N

8 n = 0
9 n = 1

10 X = CH
11 X = N

RTA	substrate/solvent	T	k_{inh} ($M^{-1}s^{-1}$)
1 (BHT)	styrene/PhCl[95]	30 °C	2.2×10^4
2	styrene/PhCl[96]	25 °C	1.2×10^5
3 (α-TOH)	styrene/PhCl[62]	30 °C	3.2×10^6
4 (PMC)	styrene/ PhCl[62]	30 °C	3.8×10^6
5	styrene/PhH[97]	65 °C	2.0×10^4
6	styrene/PhCl[98]	30 °C	1.4×10^7
7	styrene/PhCl[98,99]	30 °C	7.4×10^6
8	styrene/PhCl[95]	30 °C	2.8×10^8
9	styrene/PhCl[95]	30 °C	8.8×10^7
10	styrene/PhCl[100]	30 °C	1.0×10^7
11	styrene/PhCl[100]	30 °C	7.4×10^6

1.4.1.1.2 Peroxyl Radical Clocks

Peroxyl radical clocks are another indirect method to quantitatively measure the absolute inhibition rate constants corresponding to the reactions of RTAs and peroxyl radicals. The principle of radical clocks, in general, is based on the competition between a unimolecular radical reaction with a known rate constant, and a bimolecular reaction of the radical with an unknown rate constant.[101] Determination of the product distribution resulting from the two competing reactions as a function of the concentration of the reactant in the bimolecular reaction enables the determination of the unknown rate constant. The classic example is the determination of H-atom transfer kinetics to an alkyl radical in competition with its cyclization, the 5-hexenyl radical clock ($\log k_R/s^{-1} = (10.37 \pm 0.32) - (6.85 \pm 0.42)/\theta$, where $\theta = 2.3RT$ kcal/mol).[102]

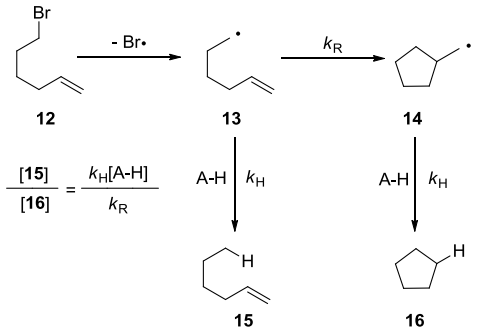

Scheme 1.14. The 5-hexenyl radical clock.

The unimolecular reaction upon which a peroxyl radical clock is based is the β-fragmentation of a peroxyl radical, the reverse of O_2 addition to an alkyl radical, which competes with its trapping in a bimolecular reaction with a H-atom donor (i.e. RTA).[103] The first-developed peroxyl radical clock was based on the autoxidation of methyl linoleate, whose mechanism is shown in **Scheme 1.15**.[19]

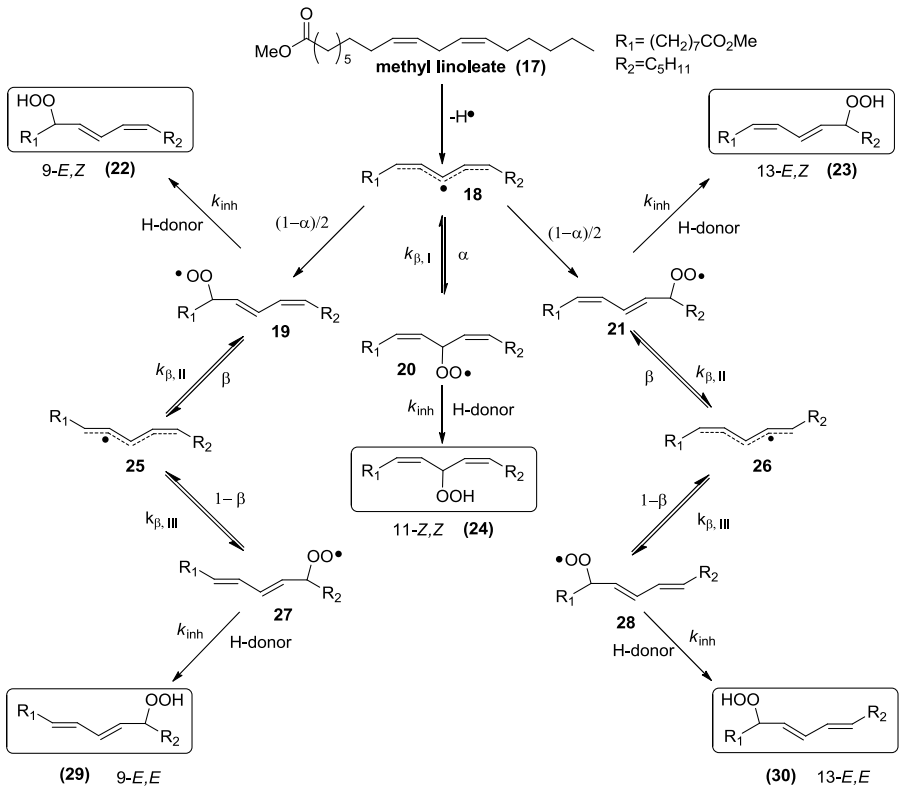

Scheme 1.15. Primary products of the autoxidation of methyl linoleate.

The mechanism of methyl linoleate autoxidation has been studied thoroughly – primarily by the Porter group – revealing that the product distribution is highly dependent

on the presence of H-atom donors (e.g. RTAs) in the medium due to the reversibility of O_2 addition to the intermediate pentadienyl radical.[18,19] In the presence of large concentrations of a very good H-donor such as α-TOH, three products are observed: the non-conjugated (bis-allylic) hydroperoxide **24** and the conjugated (*E*,*Z*)-diene hydroperoxides **22** and **23** (**Scheme 1.15**). The relative amounts of these products depend on the H-donor concentration because the β-fragmentation of the non-conjugated (bis-allylic) peroxyl radical ($k_{\beta,\,I}$ = 2.6 × 10^6 s^{-1}) competes with its reduction by the H-donor. The product distribution is related to the rate constants for β-fragmentation ($k_{\beta,\,I}$) and peroxyl radical trapping (k_{inh}) as in Eq. 1.20, and a plot of [**22**+**23**]/[**24**] as a function of 1/[H-donor] gives a line with a slope of ($k_{\beta,\,I}/k_{inh}$)[(1-α)/α)] from which k_{inh} can be calculated (α = 0.45, and reflects the partitioning of O_2 to the central position of the pentadienyl radical at the kinetic limit). As was the case for the inhibited autoxidations discussed above, these autoxidations are generally initiated by the decomposition of an azo compound, and the product ratio is most easily determined by HLPC with UV detection at 234 nm.

$$\frac{[\mathbf{22+23}]}{[\mathbf{24}]} = \frac{k_{\beta,\,I}}{[\mathrm{H-donor}]k_{inh}}\left(\frac{1-\alpha}{\alpha}\right) + \frac{1-\alpha}{\alpha} \qquad \text{Eq. 1.20}$$

When the autoxidation of methyl linoleate is carried out in the presence of H-donors that are too slow to compete with the β-fragmentation of the non-conjugated peroxyl, only conjugated diene hydroperoxides are observed, but now both (*E*,*Z*) and (*E*,*E*) stereoisomers are observed (**22**, **23**, **29**, and **30** in **Scheme 1.15**). The relative amounts of the (*E*,*Z*) and (*E*,*E*) products depend on the RTA concentration because the β-fragmentation of the (*E*,*Z*)-dienylperoxyl radicals ($k_{\beta,\,II}$ = 690 s^{-1}) competes with their reduction by an RTA. The product distribution is related to the rate constants for β-fragmentation ($k_{\beta,\,II}$) and peroxyl radical trapping (k_{inh}) as in Eq. 1.21, and a plot of ([**22**]+[**23**])/([**29**]+[**30**]) as a function of [H-donor] gives a line with a slope of $k_{inh}/k_{\beta,\,II}$(1-β) from which k_{inh} can be calculated (β = 0.69, and reflects the partitioning of O_2 to the *transoid* end of the asymmetric pentadienyl radical intermediate at the kinetic limit).

$$\frac{[\mathbf{22+23}]}{[\mathbf{29+30}]} = \frac{[\mathrm{H-donor}]k_{inh}}{k_{\beta,\,II}(1-\beta)} + \frac{k_{\beta,III}\beta}{k_{\beta,\,II}(1-\beta)} \qquad \text{Eq. 1.21}$$

Since the β-fragmentation of the non-conjugated peroxyl and (*E*,*Z*)-dienylperoxyl radicals proceed with $k_{\beta,\,I}$ = 2.6 × 10^6 s^{-1} and $k_{\beta,\,II}$ = 690 s^{-1}, respectively, these reactions are useful for determining rate constants for RTAs with k_{inh} of 10^6-10^7 and 10^3-10^4 $M^{-1}s^{-1}$,

respectively. Other hydrocarbon substrates can be used as precursors to peroxyl radical clocks, the requirement being the possibility to form (at least) two regioisomeric products, one of which is a thermodynamic product, the other of which is a kinetic product. An example is allylbenzene **31**, which autoxidizes to give α-vinylbenzyl hydroperoxide as the (non-conjugated) kinetic product and cinnamyl hydroperoxide as the (conjugated) thermodynamic product (**Scheme 1.16**).[104] The non-conjugated peroxyl radical undergoes β-fragmentation with $k_\beta = 2.6 \times 10^5$ s^{-1}, making it useful for clocking RTAs with k_{inh} values spanning those that can be determined using the two methyl linoleate clocks (i.e. 10^4-10^6 $M^{-1}s^{-1}$) using Eq. 1.22 (α = 0.74, and reflects the partitioning of O_2 to the benzylic position of the 1-phenylallyl radical at the kinetic limit). Instead of using HPLC, the allylbenzene-derived products are most easily determined (following reduction with PPh_3) by GC.

$$\frac{[\mathbf{36}]}{[\mathbf{35}]} = \frac{k_\beta}{[\mathrm{H-donor}]k_{inh}}\left(\frac{1-\alpha}{\alpha}\right) + \frac{1-\alpha}{\alpha} \qquad \text{Eq. 1.22}$$

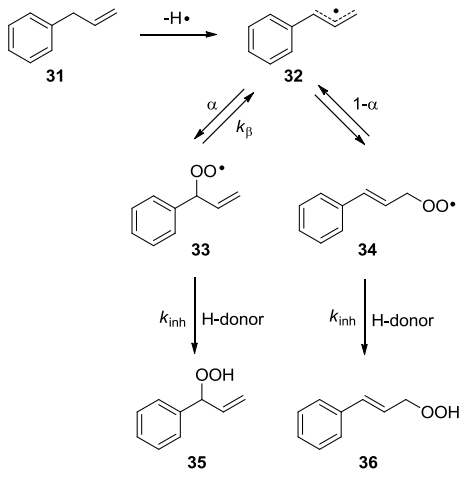

Scheme 1.16. General mechanism of allylbenzene oxidation.

A limitation to the applicability of the peroxyl radical clock approach is that it requires the antioxidant-derived radical to abstract an H-atom from the substrate to propagate the radical chain reaction, therefore requiring very high concentrations of substrate, and relatively reactive antioxidant-derived radicals. To overcome this limitation, our lab introduced the use of peroxyesters as sources of the key alkyl radical that sets up the clock.[105,106] For example, the β-naphthyl perbutenoate **37** undergoes O-O bond cleavage

under ambient conditions to generate a short-lived acyloxyl radical which decarboxylates to yield an 1-naphthylallyl radical analogous to the 1-phenylallyl radical intermediate in the allylbenzene autoxidation.[105] Since the formation of this radical does not require the very slow reaction of an antioxidant-derived radical with a hydrocarbon, and takes place quantitatively, only mM quantities of the peroxyester are required, enabling its use under a variety of conditions (i.e. in non-hydrocarbon solvents). Moreover, it is useful for the determination of kinetic isotope effects and thermokinetic parameters (i.e. $\Delta H^{\ddagger}$ and $\Delta S^{\ddagger}$), which provide mechanistic information.[100,105,107] It is important to point out that each of the peroxyl radical clock methods were calibrated using the k_{inh} value of α-TOH, i.e. the rate constant for β-fragmentation was determined by competition with trapping by α-TOH, so results should be directly comparable among the various methods.

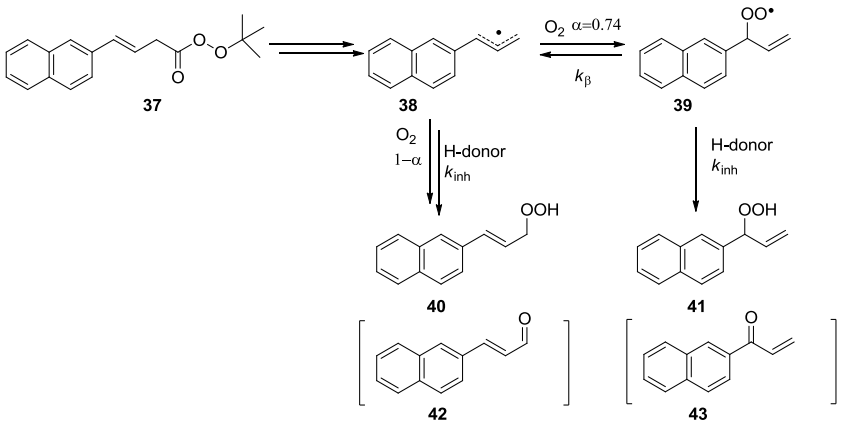

Scheme 1.17. Decomposition of *tert*-butyl β-naphthylperbut-3-enoate.

Overall, the methyl linoleate, allylbenzene and the β-naphthylperbut-3-enoate derived radical clocks developed since 2001 provide simple but reliable methods to measure the absolute k_{inh} for phenolic, aminic and organosulfur antioxidants in a number of different organic solutions.[104] Some examples are shown in **Table 1.2**.

Table 1.2. Examples of RTAs whose inhibition rate constants have been measured by the peroxyl radical clock method with the indicated substrate in chlorobenzene at 37°C.

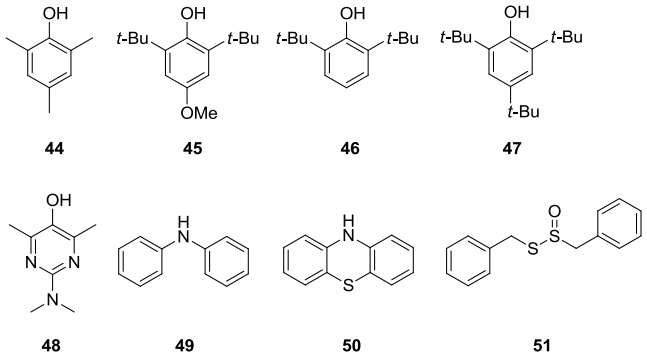

RTA	clock method	k_{inh} ($M^{-1}s^{-1}$)
PMC	methyl linoleate $_{Eq1.20}$[104]	2.7×10^6
BHT	allylbenzene **31**[104]	2.4×10^4
44	allylbenzene **31**[104]	2.3×10^5
44	naphthyl perbutenoate **37**[105]	2.3×10^5
45	naphthyl perbutenoate **37**[105]	5.6×10^5
46	methyl linoleate $_{Eq1.21}$[104]	3.2×10^4
47	methyl linoleate $_{Eq1.21}$[104]	1.7×10^4
48	methyl linoleate $_{Eq1.20}$[104]	9.4×10^6
49	naphthyl perbutenoate **37**[105]	4.6×10^4
50	naphthyl perbutenoate **37**[105]	8.5×10^6
51	methyl linoleate $_{Eq1.21}$[108]	2.0×10^5

1.4.1. 2 Direct Methods

1.4.1. 2.1 (Laser) Flash Photolysis

The kinetics of the reactions of RTAs with peroxyl radicals have been measured directly by flash photolysis. In a flash photolysis experiment, a pulsed light source (usually a nanosecond pulsed-laser) is used to generate peroxyl radicals which react with the RTA. The decay of the peroxyl radical or formation of the RTA-derived radical can be monitored

spectroscopically, and an observed rate constant obtained. The second order rate constant k_{inh} can then be determined by a series of experiments wherein the RTA concentration is varied under pseudo-first-order conditions. A common peroxyl radical precursor is dicumylketone, which yields cumylperoxyl radicals upon photolysis at ca. 300 nm of an aerated solution (**Scheme 1.18**).[109]

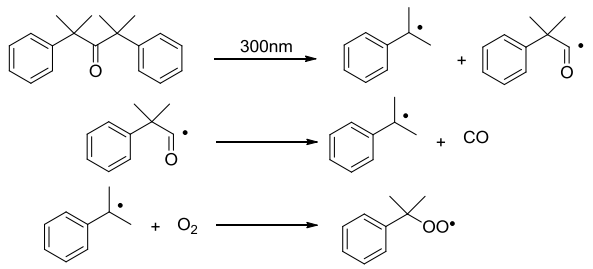

Scheme 1.18. Generation of cumylperoxyl radical by flash photolysis of dicumylketone at 300 nm.

Since cumylperoxyl radicals do not absorb above this wavelength of light, the appearance of the RTA-derived radical can be detected. For example, the reaction of α-tocopherol with cumylperoxyl radicals was monitored by monitoring the increase in absorbance at 420 nm due to the α-tocopheroxyl radical, yielding a k_{inh} value for α-tocopherol of 2.7×10^6 $M^{-1}s^{-1}$ at 25°C in chlorobenzene,[109] in excellent agreement with the value of 3.2×10^6 $M^{-1}s^{-1}$ obtained from the inhibited autoxidation of styrene in chlorobenzene at 30°C.[62]

Flash photolysis experiments are complicated by the need for specialized, expensive equipment, and the potential for photoionization of the RTA at the wavelength of the incident light. Moreover, it requires that the RTA-derived radical have a good absorbance at a lower energy wavelength than the excitation light. In order to overcome the latter issue, Lalevee's group developed a method to generate α-aminoalkylperoxyl radicals,[110] which have a strong absorbance from 350-450 nm due to charge transfer from the electron-rich nitrogen lone-pair to the electron-poor peroxyl. Photolysis of a mixture of tertiary amine and di-*tert*-butyl peroxide at 355 nm yields these radicals from the sequence of reactions in **Scheme 1.19.**[110] The decay of the α-aminoalkylperoxyl radicals can then be monitored in the presence of added RTA by UV-visible spectroscopy. For instance, α-TOH was determined to have k_{inh} = 1.1 × 10^6 $M^{-1}s^{-1}$ at 23 °C, which is comparable to the corresponding value measured at 30°C by the inhibited autoxidation of styrene of 3.2 × 10^6

$M^{-1}s^{-1}$.[62] The limitation of this method is that a large amount of tertiary amine (e.g. Et_3N) is necessary to ensure that all the alkoxyl radicals react with it but not with the RTA. Given the strong H-bonding interactions expected between the amine and H-bond-donating RTAs, it is likely that rate constants will be underestimated using this method when conducted in non-polar, non-H-bonding accepting solvents. Moreover, it is possible that the added tertiary amine can induce other reactions by acting as a nucleophile, and increasing the contribution of the SPLET mechanism to the overall rate of reaction.

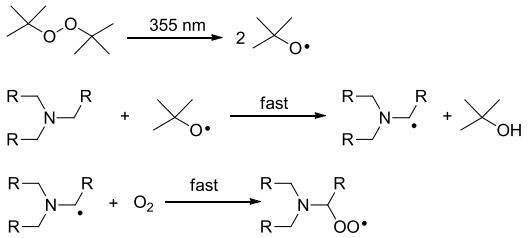

Scheme 1.19. Generation of α-aminoalkylperoxyl radical by laser flash photolysis at 355 nm.

1.4.1.2.2 Pulse Radiolysis

Pulse radiolysis is another method to directly monitor peroxyl radical reactions. It is similar to flash photolysis, but employs a pulse of ionizing radiation to generate radicals as opposed to UV light. Peroxyl radicals, hydroperoxyl radicals and superoxide can be instantaneously generated in aqueous media. The kinetics of the reactions of these radicals with antioxidants can be monitored by a variety of methods, but most common is UV-visible or EPR spectroscopy. This method is generally carried out in aqueous solution and, as a result, it provides a method to measure the k_{inh} of water-soluble antioxidants – fundamentally interesting, but arguably of less practical importance than determinations of k_{inh} in organic solutions, where chain reactions (i.e. lipid peroxidation) are much more efficient. The other major limitation of this approach is that the radiolytic generation of peroxyl radicals depends on reactions of much more highly oxidizing (and reducing) species, as are shown **Scheme 1.20**.

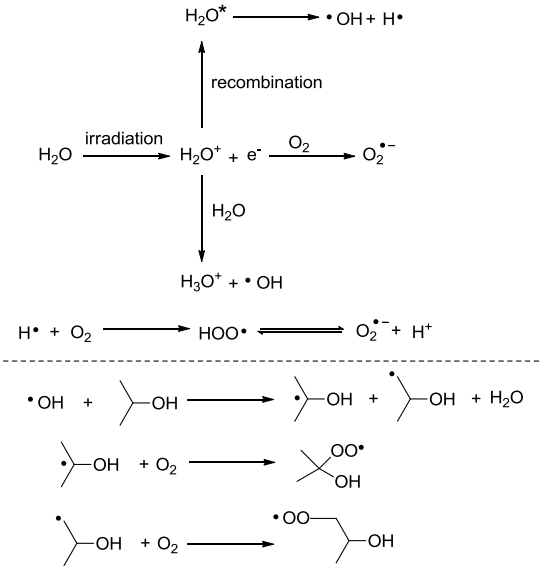

Scheme 1.20. Irradiation of water leads to hydroxyl radical formation (top), and hydroxyl radicals react with organic substrates (e.g. iso-propanol) to form peroxyl radicals (botttom).

Nevertheless, pulse radiolysis can be utilized to study RTA reactivity in aqueous solution provided that the reaction conditions are carefully manipulated to ensure that the desired reaction (RTA + peroxyl radical) is that which is being monitored.[53] For instance, k_{inh} of ascorbate was determined to be 1.7×10^6 $M^{-1}s^{-1}$ with $CH_3OO\bullet$ in aqueous solution containing 5% methanol.[111] Trichloromethylperoxyl, phenylperoxyl and pyridylperoxyl radicals are common examples of peroxyl radicals generated and studied using pulse radiolysis, but it must be pointed out that these are much more reactive species than most autoxidation chain-carrying alkylperoxyl radicals.[112]

1.4.2 Measurements of RTA Activity in Biphasic Media

To obtain a more physiologically relevant assessment of RTA activity, it is best to carry out investigations in biphasic media – a better model of the heterogeneity of cells and tissues – of which micelles and liposomes are most common. Micelles are self-assembled spherical particles composed of a monolayer of a surfactant, such as sodium dodecyl sulfate (SDS) or cetyl trimethylammonium bromide (CTAB), wherein the hydrophilic 'head' of the molecule faces outward towards the surrounding aqueous solution and the hydrophobic tail facing inward towards the center of the sphere. Liposomes are bilayer vesicles formed from the self-assembly of lipids in aqueous solution, often containing the phosphatidylcholine (PC)

backbone. They can be multilamellar or unilamellar depending on how they are assembled. Unilamellar liposomes are more homogenous, have narrower size distribution, and are better representations of biological membranes than multilamellar liposomes.[113]

Barclay, Niki and others have clearly shown that the efficacies of RTAs in biphasic media such as micelles and liposomes can be significantly different than what is predicted on the basis of their kinetics in homogenous solution – since RTA localization and mobility often trump inherent reactivity.[114] RTA localization and mobility are greatly impacted by the composition of the membrane (i.e. saturated *versus* unsaturated phospholipids and presence/absence of cholesterol), which affects its fluidity, as well as the surface charge at the lipid/aqueous interface.[115] Moreover, the identity and localization of the compound used to initiate autoxidation in model experiments is key. For instance, while the inherent chemical reactivities of PMC, 2-carboxy-2,5,7,8-tetramethyl-6-chromanol (Trolox) and α-TOH towards peroxyl radicals are essentially identical, α-TOH and PMC showed slower reactivities compared to Trolox in dimyristoyl or soybean phosphatidylcholine liposomes when using the hydrophilic 2,2'-azobis-(2-amidinopropane) monohydrochloride (AAPH) to initiate oxidation because water soluble Trolox has better accessibility to AAPH-derived peroxyl radicals.[114] The reactivity of α-TOH decreased as the radical went deeper into the interior of the membranes, but no such effect was observed for PMC presumably due to its greater mobility.[116]

Although quantitative measurements of the inhibition rate constants (k_{inh}) of antioxidants in liposomes and micelles are possible, the kinetics are more complex than in homogeneous solution.[117,118] In general, the values of k_{inh} measured for most antioxidants in heterogeneous systems can be 2 to 3 orders of magnitude lower than values measured in homogeneous solution, which can be understood as arising from two key factors.[119,120] First, the partitioning and rate of diffusion of peroxyl radicals and antioxidants between the aqueous phase and the lipid phase slows down the rate at which antioxidants encounter peroxyl radicals.[121,122] Second, hydrogen bonding of the reactive phenolic O-H group to water and/or other H-bond accepting moieties at the lipid-water interface, will slow H-atom transfer (vide supra).[114,119,122] As a result, measured values of k_{inh} reflect the overall chemical reactivity, lipophicility and mobility of the antioxidants as well as the lifetime of

the peroxyl radicals and antioxidant-derived radicals in the membranes.[114,123]

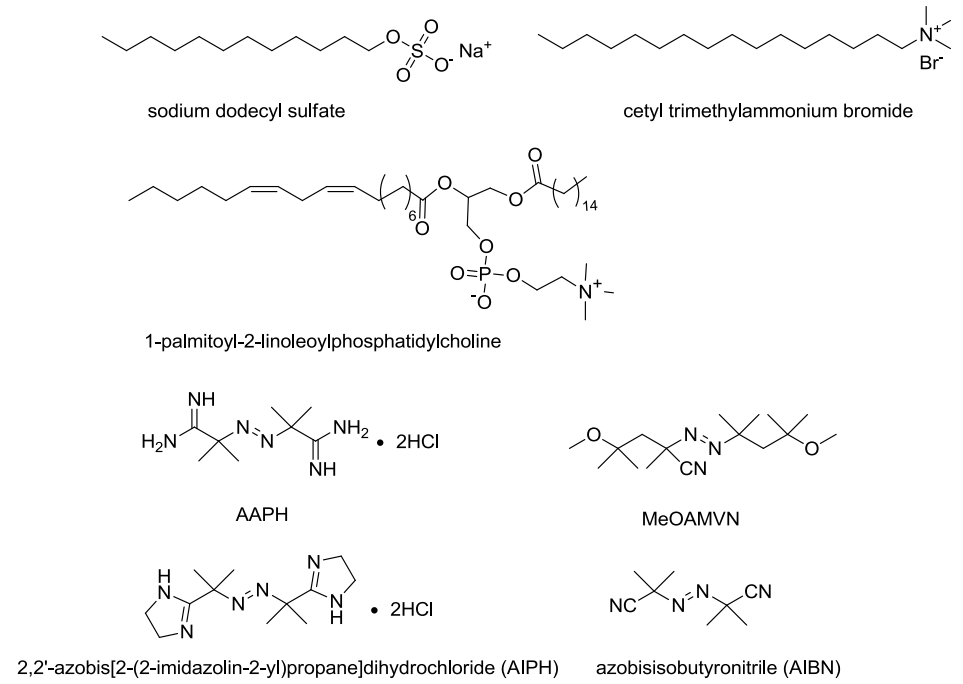

Chart 1.4. Examples of commonly used surfactants for micelle formation, phospholipids for liposomes formation and water- and lipid-soluble initiators.

1.4.2.1 Inhibited Autoxidation

Approaches to monitor the effects of RTAs on the rate of lipid hydroperoxide formation or the consumption of O_2 in the autoxidation of hydrocarbons in homogenous solution can also be applied in micellar and liposomal systems. While these processes still generally follow the same rate law and corresponding kinetic expressions (Eq. 1.1-1.3), values of k_p, k_t and R_i are generally different than in homogenous solution, and will vary with the composition of the mixture. First of all, in-cage recombination of initiator-derived radicals is generally much greater in heterogeneous mixtures,[116] leading to lower values of R_i with increasing viscosity of the microenvironment on moving from organic solution to micelles to liposomes.[117] For instance, ek_d of MeOAMVN is 2.7×10^{-5} s^{-1} in benzene, but decreases to 0.71×10^{-5} s^{-1} in SDS micelles and 0.33×10^{-5} s^{-1} in soybean PC liposomes.[82] While unsymmetrical amphiphilic azo initiators developed in the Porter laboratory increase efficiency of radical generation in micelles and liposomal membranes, they are neither commercially available nor trivial to synthesize.[124] This is obviously a bigger problem for hydrophobic initiators such as MeOAMVN than for hydrophilic initiators such as AAPH,

which concentrate in the aqueous phase of the mixture, which is little different from bulk aqueous solution. However, hydrophilic initiators must diffuse into the membrane, or rely on reactions with RTAs to initiate autoxidation,[125] also leading to diminished R_i relative to homogeneous solution. Fortunately, R_i can be measured easily by adding a known amount of a well-studied RTA (e.g. α-TOH), with known stoichiometry (n, usually 2) and determining the inhibited period (τ) (Eq.1.23).[122,126] Initiator efficiency e in biphasic media can be calculated using Eq. 1.24 in which k_d is the measured decomposition rate of the azo initiator (determined by HPLC, or other means) and [In] is the concentration of the initiator.

$$R_i = \frac{n[RTA]_0}{\tau} \qquad \text{Eq. 1.23}$$

$$R_i = 2ek_d[In] \qquad \text{Eq. 1.24}$$

Termination rate constants, k_t, have been determined in liposomes and micelles using the rotating sector method, as in homogenous solution.[127] Propagation rate constants (k_p) can then be derived from Eq. 1.15 using the data from an uninhibited autoxidation of the substrate in the system under investigation. Propagation rate constants generally drop by a factor of 2-3 in aqueous micelles and bilayers compared to homogeneous solution due to the diffusion of polar peroxyl radicals away from the non-polar oxidizable region of the biphasic system,[119,126] while termination rate constants k_t of lipid peroxyl radicals markedly decrease due to their stabilization by hydrogen bonding with water.[126]

From a practical perspective, antioxidants are usually introduced into a model membrane by first dissolving the antioxidants with the surfactants /phospholipids together in organic solution, forming a thin film by evaporation of organic solvent under reduced pressure followed by preparation of the liposomes or micelles in a buffer.[128,129] Following addition of the initiator, the progress of the autoxidation can be followed by any number of the different methods introduced above for measurements in homogenous solution. Oxygen consumption can be used to monitor reaction progress directly; alternatively, hydroperoxides can be determined following removal of aliquots from the solution at regular time intervals. Often, the samples are first reduced to the corresponding alcohol[122,130] in methanol and, if phospholipids are the oxidizable substrate, hydrolyzed to produce the free fatty acids. After extraction with organic solvent, the amount of carboxylic

acids generated from oxidized lipids can be analyzed by HPLC with either UV or MS detection, or even GC with either FID or MS detection. Direct identification of phospholipid hydroperoxides can be achieved by reverse-phase HPLC with UV[131,132] or chemiluminescence detection.[133] Fluorescent phosphines such as the coumarin-triarylphosphine conjugate shown in **Scheme 1.13** can also be used to quantify the amount of lipid hydroperoxides formed following disruption of the micelles or liposomes, and this can be greatly enabled by the use of a microplate reader.

In order to obtain the absolute k_{inh} value of RTAs from inhibited autoxidations using Eq. 1.15-1.17 given above, k_p and k_t of the substrate in heterogeneous media must be known for each experimental system. However, this involves both special equipment and can be quite laborious. As a result, investigators often report the rates of RTAs relative to a well-known RTA such as α-TOH, PMC or Trolox (i.e. k_{inh}= 5.8 × 10^3, 17.8 × 10^3, 5.8 × 10^3 $M^{-1}s^{-1}$, respectively, measured in dilinoleoylphosphatidylcholine liposomes)[119] instead of the absolute k_{inh} value to avoid issues associated with the *de novo* measurement of k_p and k_t.

1.4.2.2 Peroxyl Radical Clocks

The peroxyl radical clock method used to evaluate RTA activities in homogeneous solution was actually first applied in heterogeneous media.[120,122,134] As in solution, the ratio of kinetic (*Z*,*E*) to thermodynamic (*E*,*E*) dienyl hydroperoxides derived from oxidation of linoleate-containing phospholipids reflects the rate at which the precursor peroxyl radicals are trapped by an RTA. Thus, by determining the (*Z*,*E*) to (*E*,*E*) product ratio as a function of antioxidant concentration, a value of k_{inh} can be determined as in Eq. 1.20-1.21. For example, the inhibition rate constant of α-TOH in 1-palmitoyl-2-linoleoylphosphatidylcholine (PLPC) liposomes was determined to be two orders of magnitude slower compared to that determined in solution (k_{inh}= 4.7×10^4 M^{-1} s^{-1}).[134] However, it must be noted that the application of the peroxyl radical clock method in this context is based on the assumption that the rate constant for β-fragmentation of the key intermediate (*Z*,*E*)-dienylperoxyl radical (k_β = 690 s^{-1}) is the same as that in homogenous solution.[135] We have shown that the rates of β-fragmentation of peroxyl radicals decrease with increasing polarity of the medium,[106] which would lead to overestimates of k_{inh}. From

a practical perspective, one carries out the reaction as above, but rather than simply determining the total hydroperoxide concentration, it is necessary to determine the concentrations of the individual isomeric hydroperoxides. As such, aliquots of the reaction mixture must be analyzed by HPLC with either of UV, MS or chemiluminescence detection in order to separate and quantify the products.

1.4.2.3 Competition with Fluorogenic Substrates

Increasing in popularity with the near ubiquity of microplate readers in biochemical/chemical research laboratories is the use of substrates that undergo a fluorescence enhancement upon reaction with peroxyl radicals as a reporter for the relative efficacies with which RTAs react with peroxyl radicals. Thus, by determining the effect of the antioxidant on the rate at which the fluorescence of the sample increases, kinetic information on the RTAs capability to trap peroxyl radicals can, in principle, be obtained.

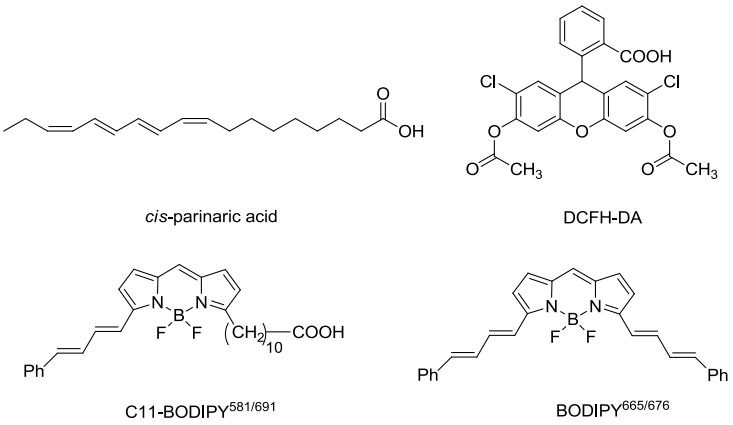

cis-parinaric acid | DCFH-DA | C11-BODIPY$^{581/691}$ | BODIPY$^{665/676}$

Chart 1.5. Examples of commonly used fluorescent probes to follow lipid peroxidation.

One of the earliest examples of the use of such a probe was with the naturally-occurring *cis*-parinaric acid (**Chart 1.5**), reported in 1975 by Hudson and co-workers.[136] This compound emits at 432 nm when excited at 320 nm; fluorescence which decreases substantially when oxidized. The application of *cis*-parinaric acid to study RTA efficacies is limited by its absorbance wavelength, since many RTAs absorb at this wavelength. Following on this seminal work, BODIPY$^{665/676}$ and C11-BODIPY$^{581/591}$ were developed (**Chart 1.5**).[137,138] These compounds have better stability and they absorb in the visible wavelength range. In fact, C11-BODIPY$^{581/591}$ is one of the most commonly used

probes for evaluating lipid peroxidation and antioxidant activities. For example, it has been applied to study the antioxidant activities of Trolox, α-carotene, β-carotene, lutein, and probucol in dioleoylphosphatidylcholine (DOPC) liposomes using a fluorescent microplate reader.[139] Antioxidant activities of some natural products such as astaxanthin and related carotenoids have been studied using C11-BODIPY$^{581/591}$ as the lipid peroxidation indicator as well.[140] Both the loss of fluorescence at longer wavelength (λ_{ex} = 580 nm, λ_{em} = 620 nm) or increase in fluorescence at shorter wavelength (λ_{ex} = 488 nm, λ_{em} = 520 nm) can be monitored to report on reactions with peroxyl radicals using C11-BODIPY$^{581/591}$ in liposomes (**Scheme 1.21**).[141]

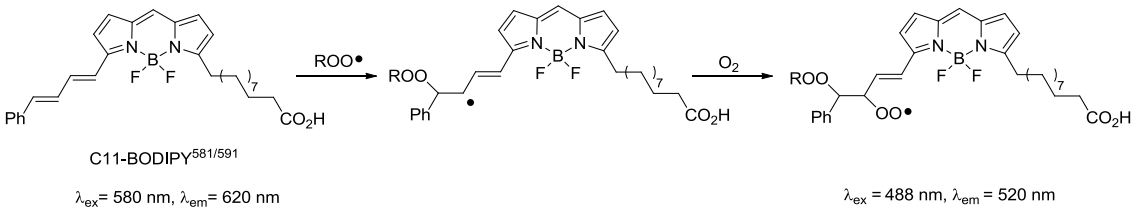

Scheme 1.21. The reaction of C11-BODIPY$^{581/591}$ towards peroxyl radicals.

In order to quantitatively measure the efficacy of RTAs, rates of C11-BODIPY$^{581/591}$ reaction towards peroxyl radicals in liposomes ($k_{inh} \approx 6.0\times10^3$ $M^{-1}s^{-1}$ in acetonitrile)[142] and the k_p of the substrate in the liposomes are necessary. Since the k_{inh} of C11-BODIPY$^{581/591}$ and k_p of substrates are dependent on the composition of the biphasic media, investigators often measure the relative activities of unknown RTAs relative to a standard RTA such as Trolox or α-TOH. For example, relative peroxyl radical scavenging activities of antioxidants to that of Trolox could be determined using fluorescent microplate reader assay using Eq. 1.25 in which AUC_{RTA}, AUC_{Trolox} and AUC_0 are the net integration areas under the fluorescence-time curves of the C11-BODIPY$^{581/591}$ fluorescence decay in the presence of the tested RTA, Trolox and in the absence of any RTA, respectively.[139]

$$\frac{k_{\mathrm{inh}}(\mathrm{RTA})}{k_{\mathrm{inh}}(\mathrm{Trolox})} = \frac{(\mathrm{AUC_{RTA}}-\mathrm{AUC_0})[\mathrm{Trolox}]}{(\mathrm{AUC_{Trolox}}-\mathrm{AUC_0})[\mathrm{RTA}]} \qquad \text{Eq. 1.25}$$

It is convenient to evaluate radical scavenging by antioxidants using these fluorogenic probes, however, special precautions are necessary to obtain good quantitative information. For example, suppression of the fluorescence can be due to direct quenching by the RTA in

lieu of suppression of lipid peroxidation.[143] Another drawback of C11-BODIPY$^{581/591}$ is that the rate of reaction of C11-BODIPY$^{581/591}$ with peroxyl radicals is relatively slow, making it impossible to apply it to measure the efficacy of very potent RTAs in liposomes with a small amount of C11-BODIPY$^{581/591}$ to avoid auto quenching and reaching the fluorescence detection limit of the microplate reader.

More recently, Cosa's lab has developed several novel peroxyl radical-trapping fluorescent probes to measure the activities of RTAs in liposomes using a high-throughput fluorescence microplate reader assay.[144,145] These probes are BODIPY conjugates of α-tocopherol, such as the probe H_2B-PMHC shown in **Scheme 1.22**,[145] and rely on an intramolecular photoinduced electron transfer off/on switching mechanism: upon reaction of the phenolic moiety of the probe with peroxyl radicals, the BODIPY fluorescence (λ_{ex} = 485 nm, λ_{em} = 520 nm) is dramatically enhanced.

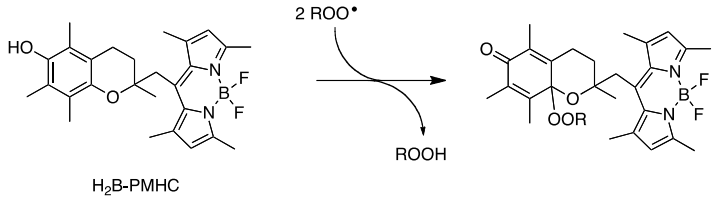

Scheme 1.22. Reaction of H_2B-PMHC probe with peroxyl radicals.

The competition for peroxyl radicals between liposome-embedded H_2B-PMHC and an added RTA enables determination of RTA activity. In the presence of an excellent RTA (**Figure 1.2A**), the increase in fluorescence brought about by reactions of peroxyl radicals with the H_2B-PMHC probe is inhibited until the RTA is consumed. In the presence of a moderate RTA (**Figure 1.2B**), the rate at which the H_2B-PMHC probe is oxidized is merely retarded compared to the uninhibited autoxidation, and the rate of fluorescence increase diminishes with increasing RTA concentration. The intensity-time data in **Figure 1.2B** can also be manipulated to provide quantitative information on relative RTA activities. The ratio of inhibition rate constants of the probe and the added RTA can be obtained from replotting the data in the early part of the oxidation (i.e. prior to the BODIPY moiety undergoing oxidation) according to Eq. 1.26, in which τ is the time at which the fluorescence increases to a maximum (*cf.* **Figure 1.2**).[145]

$$\ln\left(\frac{I_\infty - I_t}{I_\infty - I_0}\right) = \frac{k_{inh}^{H2B-PMHC}}{k_{inh}^{RTA}} \ln\left(1 - \frac{t}{\tau}\right) \qquad \text{Eq. 1.26}$$

The inhibition time τ reflects the stoichiometry of the RTA, i.e. *n*, or how many peroxyl radicals are trapped per molecule of RTA, which can be determined by comparison of the inhibition time corresponding to a given concentration of the RTA under investigation to the inhibition time arising in the presence of the same concentration of a well known RTA, such as α-TOH. For example, by comparing the inhibition time arising from the potent tetrahydronaphthyridinol RTA in **Figure 1.2A** to that arising in the presence of the same concentration of α-TOH in **Figure 1.2B**, it is concluded that the tetrahydronaphthyridinol RTA traps two peroxyl radicals on average, as does α-TOH.

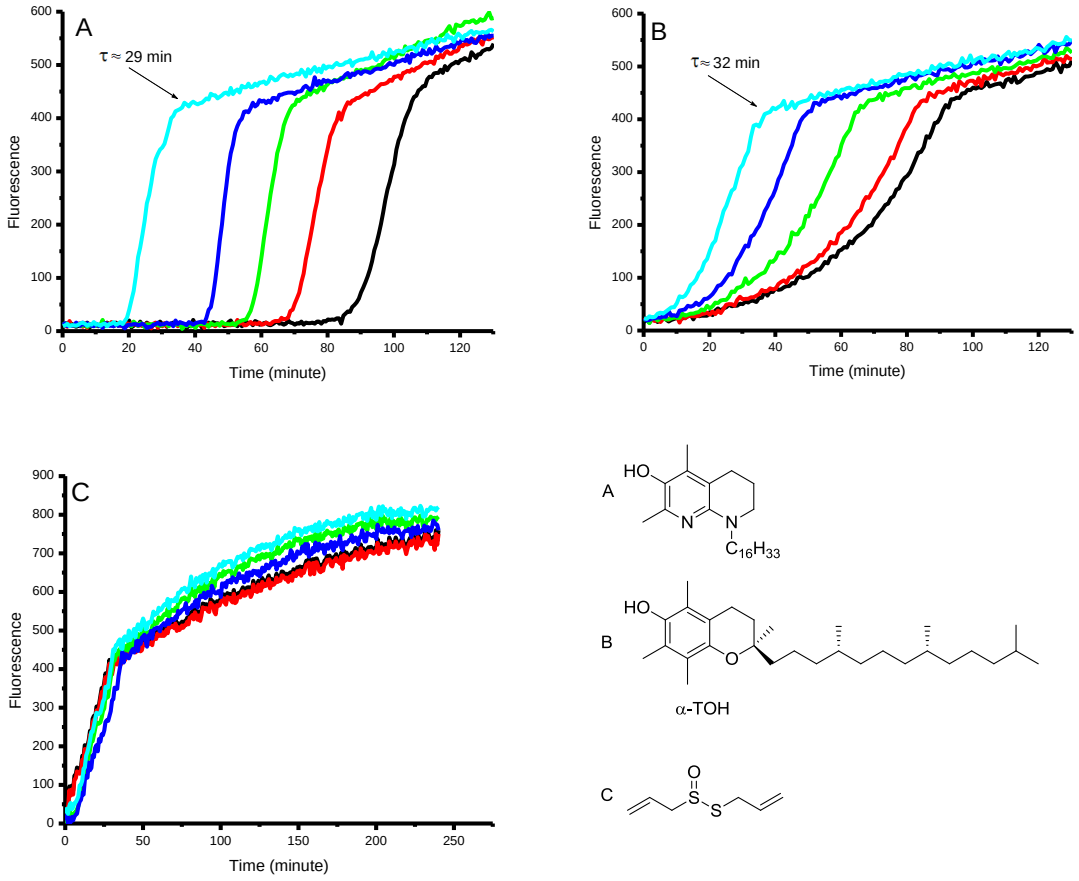

Figure 1.2. Representative fluorescence (at 520 nm) intensity−time profiles from MeOAMVN-mediated (0.68 mM) oxidations of egg phosphatidylcholine liposomes (1 mM in PBS buffer, pH 7.4) containing 0.15 μM H_2B-PMHC and increasing concentrations (1.5 μM, cyan; 3.0 μM, blue; 4.5 μM, green; 6.0 μM, red; and 7.5 μM, black) of RTAs: tetrahydronaphthyridinol C16 (A), α-TOH (B), and allicin (C) (oxidized with 0.2 mM MeOAMVN instead). Inhibition periods are indicated by the arrow for the lowest concentration of the RTAs.

As is the case with all competitive methods, quantitative determination of k_{inh} using this method has limitations when applying to those RTAs that are either too fast or too slow for the H_2B-PMHC probe to compete with because the fluorescence increase is either entirely inhibited or not inhibited at all. An example of the former is the application to study novel tetrahydronaphthyridinol antioxidants (**Figure 1.2A**) (Details please see **Chapter 2** in this thesis).[146] Here, probe oxidation is completely suppressed by the antioxidant, even at very low loadings, corresponding to k_{inh} values at least 30-fold greater than for α-TOH. An example of the latter is the application of the probe to study the RTA activity of allicin and petviercin, the purported antioxidants in garlic and anamu, respectively.[147] Here, there is no effect of allicin or petivericin on probe oxidation, even at very high loadings, corresponding to k_{inh} values at least 100-fold smaller than for α-TOH.

1.4.3 Determining RTA Activity in Cell Culture

Lipid peroxidation arising due to oxidative stress has been linked to the onset of many degenerative diseases, such as atherosclerosis,[148] neurodegenerative disease,[149] and cancer.[150] As such, studies of the effects of RTAs in cell culture have been popular experiments for some time, and have been made much more accessible in recent years due to the development of fluorescent probes alongside microplate, confocal microcopy and flow cytometry technologies. In practice, investigators typically carry out dose-response studies to determine relative RTA efficacies; cells are grown in RTA-supplemented media for a given amount of time, and then lipid peroxidation is initiated following the addition of a fluorescent probe. Lipid peroxidation can be initiated with diethyl maleate (DEM) to deplete glutathione,[151,152] lipopolysaccharide to induce the oxidative burst of immune cells,[153,154] or methyl viologen to promote superoxide formation via uncoupling of the electron transport chain in oxidative phosphorylation.[155,156] Several types of fluorogenic probes have been used to monitor lipid peroxidation, including the aforementioned C11-BODIPY$^{581/591}$ and BODIPY$^{665/676}$ probes.[157,158] For example, idebenone and its pyridinol analogues have been evaluated in cells using C11-BODIPY$^{581/591}$ as lipid peroxidation indicator by Hecht's group by flow cytometry.[152] Quercetin, luteolin and several bromophenols have been examined in HepG2 cells using C11-BODIPY$^{581/591}$.[159]

Because of the high quantum yield and the good spectral separation of the non-oxidized and the oxidized form of C11-BODIPY$^{581/591}$, low concentrations (1 μM) of probe can be used to label membrane systems or living cells.[141]

Probes which are targeted to specific cellular compartments, such as mitochondria, are the focus of more recent developments. For example, Cosa's group have recently reported a mitochondria-targeted analog of the aforementioned H_2B-PMHC probe, Mito-BODIPY-TOH, that was used to monitor the antioxidant status within the inner mitochondrial membranes of live cells by confocal microscopy,[156] and has great potential to evaluate RTA effects on mitrochondrial lipid peroxidation in cells.

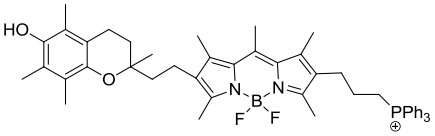

Mito-Bodipy-TOH

It must be acknowledged that 2',7'-dichlorodihydrofluorescein diacetate (DCFH-DA) is often used as a fluorogenic probe to determine the efficacy of RTAs in cells.[160] Following cellular uptake, the acetyl groups in DCFH-DA are cleaved by intracellular esterases to reactive DCFH which can be oxidized to the highly fluorescent dichlorofluorescein (DCF). For example, Niki has used DCFH-DA to compare the activities of PMC, Trolox, α-tocotrienol and α-TOH in cells using flow cytometry.[161] The main drawback of using DCFH-DA is that DCFH has a small partition coefficient (2.52) which precludes its localization in hydrophobic membranes, where it reacts much more slowly with lipid peroxyl radicals than it does with aqueous peroxyl radicals in the surrounding medium.[142] As a result of its partitioning to, and greater reactivity in, water (presumably due to the electron transfer mechanisms which govern its reactivity), there is also a concern that it may be competitively oxidized by hydrogen peroxide (catalyzed by peroxidases),[162] peroxynitrite[163] and other water soluble oxidants.[164]

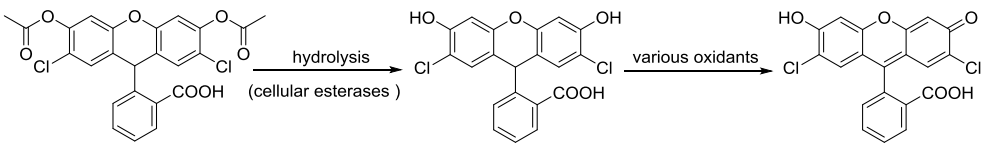

DCFH-DA DCFH DCF

Scheme 1.23. Activation of DCFH and its oxidation to DCF.

1.5 Research Objectives

1.5.1 Besting Vitamin E: Exploring the Reactivity of Tetrahydronaphthyridinol Antioxidants from Solution to Lipid Bilayers and Cells

An ongoing aim of research on antioxidants is to design and synthesize radical-trapping antioxidants that have superior activities compared to nature's best, α-TOH. Previous work in the Pratt laboratory has involved the design of aza analogs of α-TOH (so-called tetrahydronaphthyridinols) that have been shown to trap peroxyl radicals in the inhibited autoxidation of styrene (performed in benzene) with a rate constant 28-time that of α-TOH.[165] In fact, the measured rate constant, k_{inh} = 8.8 × 10^7 M^{-1} s^{-1}, is approaching the purported pre-exponential factor for the reaction of phenolic RTAs with peroxyl radicals, suggesting that it occurs without enthalpic barrier.[165] However, inherent chemical reactivity toward peroxyl radicals is not the only factor that contributes to the activity of antioxidants in heterogeneous systems, such as in the lipid membranes and lipoproteins found *in vivo*. Localization, mobility, as well as accessibility to peroxyl radicals are equally important - if not more so.

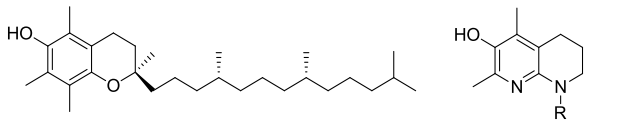

α-TOH tetrahydronaphthyridinol

With this in mind, we have identified the following objectives:

1) Develop a more efficient synthetic method to build up a small library of tetrahydronaphthyridinol radical-trapping antioxidants with varying lipophilicity.
2) Determine the optimal tetrahydronaphthyridinol side chain substitution for radical-trapping activity in heterogeneous lipid bilayers.
3) Determine how systematic changes in the lipophilicity of tetrahydronaphthyridinols impact their regeneration by water-soluble reductants.
4) Determine whether the different activities of tetrahydronaphthyridinols with different lipophilicities in liposome models translate into mammalian cell culture models. Moreover, to compare their lipid peroxidation inhibition activities to those of nature's best RTA, α-TOH, and the recently discovered ferroptosis inhibitors ferrostatin-1 and

liproxstatin-1.

1.5.2. Exploring the Molecular Mechanism of Medicinal Thiosulfinates from Garlic and Petiveria

The "antioxidant" activities of allicin and petivericin, which are thiosulfinates widely believed responsible for the medicinal properties of garlic and petiveria, are a controversial topic. Many reports show that allicin traps radicals[166] or induce gene expression of phase II antioxidant enzymes, [167,168] but others suggest that it is highly cytotoxic in human cancer cells such as colon carcinoma cells, glioblastoma cells and leukemia tumor cells.[169,170] To date, the molecular mechanism of thiosulfinates is not clear. In recent work, the Pratt lab showed that despite the fact that they lack any structural features common to good RTAs, allicin and petivericin are good RTAs in homogeneous organic solution because they readily undergo Cope elimination to produce sulfenic acids – which they showed to be potent H-atom transfer agents.[171] The goal of the current project is to understand the medium dependence of this activity in liposomes and investigate whether the above-mentioned proposed mechanism is relevant in live cells.. The cytotoxicities of the thiosulfinates were determined in parallel in an attempt to provide insight on the apparently contradictory reports on their biological activity.

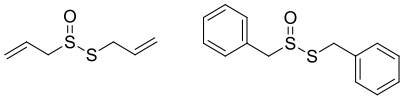

allicin petivericin

1.5.3. Toward a Molecular Level Understanding of the Biological Activities of Resveratrol, its Natural Oligomers and their Synthetic Derivatives

Resveratrol and its oligomers are a diverse set of phenolic natural compounds believed to have health-promoting potential due to their radical-trapping activities. However, the molecular mode of action on how resveratrol and its oligomers work *in vivo* is not yet clear. Systematic studies of radical-trapping activities of resveratrol and its natural oligomers are lacking in the literature, and no kinetic measurement of peroxyl radical trapping activity of resveratrol oligomers has been achieved to date.

To provide some insights on whether the health promoting benefits of resveratrol and its oligomers can be due to their radical-trapping activities and to elucidate their biological mechanism of action, the first stage of this project is set up to systematically evaluate the radical-trapping activities of resveratrol, it natural dimers pallidol and quadrangularin A and their synthetic derivatives in organic solution, heterogeneous lipid bilayers and live mammalian cells. Extending upon this, experiments were also carried out to study the electrophilic potential of the resveratrol autoxidation products – which may induce gene expression of phase II antioxidant enzymes.

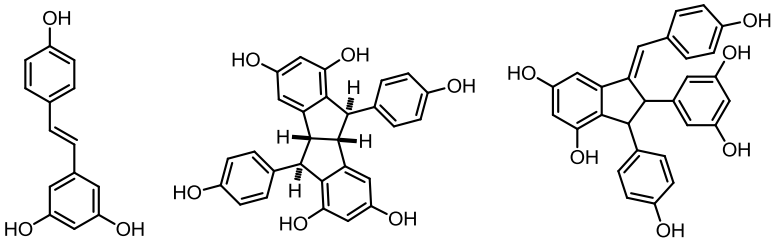

Overall, the inhibition of free radical-mediated oxidation of unsaturated lipids has been the focus of intensive research over the past 40 years. Many research projects have been focused on developing superior synthetic RTAs compared to nature's best lipophilic RTA α-TOH. Another big area in this field has been focused on screening natural compounds and studying their "antioxidant" activities. Previous research to determine the efficacy of antioxidant activities was done by different labs using various methods, which leads to difficulties comparing the various series of compounds directly. In this thesis, the peroxyl radical-trapping activities of three types of compounds – either synthesized or natural – from organic solution to heterogeneous lipid bilayers and finally to live mammalian cells were systematically studied using identical analytical methods. A global picture of what is important in the design of better radical-trapping antioxidants and insight into biological activities of natural thiosulfinates, and resveratrol and its dimers are discussed.

1.6 References

[1] Davies, K. J. *Biochem. Soc. Symp.* **1995,** *61*, 1-31.

[2] Sawyer, D. T.; Valentine, J. S. *Acc. Chem. Res.* **1981,** *14* (2), 393-400.

[3] Slater, E. C. *Trends Biochem. Sci.* **1983,** *8* (7), 239-242.

[4] Bayir, H. *Crit. Care Med.* **2005,** *33* (12 Suppl), S498-501.

[5] Koppenol, W. H.; Kissner, R. *Chem. Res. Toxicol.* **1998,** *11* (2), 87-90.

[6] Ames, B. N.; Shigenaga, M. K.; Hagen, T. M. *Proc. Natl. Acad. Sci. U S A* **1993,** *90* (17), 7915-7922.

[7] Benz, C. C.; Yau, C. *Nat. Rev. Cancer* **2008,** *8* (11), 875-879.

[8] Jena, N. R. *J. Biosci.* **2012,** *37* (3), 503-517.

[9] Jena, N. R.; Mishra, P. C. *Free Radic. Biol. Med.* **2012,** *53* (1), 81-94.

[10] Berlett, B. S.; Stadtman, E. R. *J. Biol. Chem.* **1997,** *272* (33), 20313-20316.

[11] Yin, H.; Xu, L.; Porter, N. A. *Chem. Rev.* **2011,** *111* (10), 5944-5972.

[12] Wang, M. Y.; Liehr, J. G. *Arch. Biochem. Biophys.* **1995,** *316* (1), 38-46.

[13] Frankel, E. N. *Chem. Phys. Lipids* **1987,** *44* (2-4), 73-85.

[14] Bolland, J. L.; Gee, G. *Trans. Faraday Soc.* **1946,** *42* (3-4), 244-252.

[15] Maillard, B.; Ingold, K. U.; Scaiano, J. C. *J. Am. Chem. Soc.* **1983,** *105* (15), 5095-5099.

[16] Russell, G. A. *Chem. Ind.* **1956,** (49), 1483-1483.

[17] Howard, J. A. *Adv. Free Radical Chem.* **1972,** *4*, 49-173.

[18] Porter, N. A.; Wujek, D. G. *J. Am. Chem. Soc.* **1984,** *106* (9), 2626-2629.

[19] Porter, N. A. *Acc. Chem. Res.* **1986,** *19* (9), 262-268.

[20] Tallman, K. A.; Pratt, D. A.; Porter, N. A. *J. Am. Chem. Soc.* **2001,** *123* (47), 11827-11828.

[21] Pizzimenti, S.; Ciamporcero, E.; Daga, M.; Pettazzoni, P.; Arcaro, A.; Cetrangolo, G.; Minelli, R.; Dianzani, C.; Lepore, A.; Gentile, F.; Barrera, G. *Front Physiol.* **2013,** *4*, 242.

[22] Howard, J. A.; Ingold, K. U. *Can. J. Chem.* **1967,** *45* (8), 785-792.

[23] Xu, L.; Davis, T. A.; Porter, N. A. *J. Am. Chem. Soc.* **2009,** *131* (36), 13037-13044.

[24] Staprans, I.; Pan, X. M.; Rapp, J. H.; Feingold, K. R. *Mol. Nutr. Food Res.* **2005,** *49* (11), 1075-1082.

[25] Asano, M.; Adachi, J.; Ueno, Y. *Lipids* **1999,** *34* (6), 557-561.

[26] Ingold, K. U. *Chem. Rev.* **1961,** *61* (6), 563-589.

[27] Ingold, K. U.; Pratt, D. A. *Chem. Rev.* **2014,** *114* (18), 9022-9046.

[28] Kremer, M. L. *Phys. Chem. Chem. Phys.* **1999,** *1*, 3595-3605.

[29] Gray, B.; Carmichael, A. J. *Biochem. J.* **1992,** *281 (Pt 3)*, 795-802.

[30] Halliwell, B. *Annu. Rev. Nutr.* **1996,** *16*, 33-50.

[31] Fukai, T.; Ushio-Fukai, M. *Antioxid. Redox Signal* **2011,** *15* (6), 1583-1606.

[32] Chelikani, P.; Fita, I.; Loewen, P. C. *Cell Mol. Life Sci.* **2004,** *61* (2), 192-208.

[33] Prabhakar, R.; Vreven, T.; Morokuma, K.; Musaev, D. G. *Biochemistry* **2005,** *44* (35), 11864-11871.

[34] Yant, L. J.; Ran, Q.; Rao, L.; Van Remmen, H.; Shibatani, T.; Belter, J. G.; Motta, L.; Richardson, A.; Prolla, T. A., *Free Radic. Biol. Med.* **2003,** *34* (4), 496-502.

[35] Brigelius-Flohe, R.; Maiorino, M. *Biochim. Biophys. Acta.* **2013,** *1830* (5), 3289-3303.

[36] Buxton, G. V.; Greenstock, C. L.; Helman, W. P.; Ross, A. B., *J. Phys. Chem. Ref. Data* **1988,** *17* (2), 513-886.

[37] Koppenol, W. H.; Liebman, J. F. *J. Phys. Chem.* **1984,** *88* (1), 99-101.

[38] Burton , G. W.; Ingold, K. U. *Acc. Chem. Res.* **1986,** *19* (7), 194-201.

[39] Niki, E. *Chem. Phys. Lipids* **1987,** *44* (2-4), 227-253.

[40] Foti, M. C. *J. Pharm. Pharmacol.* **2007,** *59* (12), 1673-1685.

[41] Foti, M. C.; Amorati, R. *J. Pharm. Pharmacol.* **2009,** *61* (11), 1435-1448.

[42] Frei, B.; England, L.; Ames, B. N. *Proc. Natl. Acad. Sci. U S A.* **1989,** *86* (16), 47 6377-6381.

[43] Kerksick, C.; Willoughby, D. *J. Int. Soc. Sports Nutr.* **2005,** *2*, 38-44.

[44] Steinhubl, S. R. *Am. J. Cardiol.* **2008,** *101* (10), S14-S19.

[45] Steinberg, D.; Witztum, J. L. *Circulation* **2002,** *105* (17), 2107-2111.

[46] Steinhubl, S. R. *Am. J. Cardiol.* **2008**, *101* (10A), 14D-19D.

[47] Tang, F.; Lu, M.; Zhang, S.; Mei, M.; Wang, T.; Liu, P.; Wang, H. *Lipids* **2014**, *49* (12), 1215-1223.

[48] Bowry, V. W.; Stocker, R. *J. Am. Chem. Soc.* **1993**, *115* (14), 6029-6044.

[49] Kontush, A.; Finckh, B.; Karten, B.; Kohlschutter, A.; Beisiegel, U. *J. Lipid Res.* **1996**, *37* (7), 1436-1448.

[50] Carr, A.; Frei, B. *FASEB J.* **1999**, *13* (9), 1007-1024.

[51] Burton, G. W.; Ingold, K. U. *Science* **1984**, *224* (4649), 569-573.

[52] Mehta, R. G.; Murillo, G.; Naithani, R.; Peng, X. *Pharm. Res.* **2010**, *27* (6), 950-961.

[53] Jovanovic, S. V.; Steenken, S.; Tosic, M.; Marjanovic, B.; Simic, M. G., *J. Am. Chem. Soc.* **1994**, *116* (11), 4846-4851.

[54] Howard, J. A.; Ingold, K. U. *Can. J. Chem.* **1963**, *41* (7), 1744-1751.

[55] Brown, H. C.; Okamoto, Y. *J. Am. Chem. Soc.* **1958**, *80* (18), 4979-4987.

[56] Valgimigli, L.; Pratt, D. A., Antioxidants in chemistry and biology. Encyclopedia of radicals in chemistry, biology and materials (Chatgilialoglu, C; Studer, A., eds.) **2012**, 3, 1623-1677.

[57] Valgimigli, L.; Pratt, D. A. *Acc. Chem. Res.* **2015**, *48* (4), 966-975.

[58] Mulder, P.; Korth, H. G.; Pratt, D. A.; DiLabio, G. A.; Valgimigli, L.; Pedulli, G. F.; Ingold, K. U. *J. Phys. Chem. A.* **2005**, *109* (11), 2647-2655.

[59] Benson, S. W.; Cohen, N. The thermochemistry of peroxides and polyoxides, and their free radicals. The Chemistry of Free Radicals: Peroxyl Radicals, eds Z. Alfassi, John Wiley & Sons, Ltd, Chichester **1997**.

[60] Howard, J. A.; Ingold, K. U. *Can. J. Chem.* **1963**, *41* (11), 2800-2806.

[61] Pratt, D. A.; DiLabio, G. A.; Mulder, P.; Ingold, K. U. *Acc. Chem. Res.* **2004**, *37* (5), 334-340.

[62] Burton, G. W.; Doba, T.; Gabe, E. J.; Hughes, L.; Lee, F. L.; Prasad, L.; Ingold, K. U. *J. Am. Chem. Soc.* **1985**, *107* (24), 7053-7065.

[63] Litwinienko, G.; Ingold, K. U. *Acc. Chem. Res.* **2007**, *40* (3), 222-230.

[64] Snelgrove, D. W.; Lusztyk, J.; Banks, J. T. ; Mulder, P.; Ingold, K. U. *J. Am. Chem. Soc.* **2001**, *123*, 469-477.

[65] Pratt, D. A.; de Heer, M. I.; Mulder, P.; Ingold, K. U. *J. Am. Chem. Soc.* **2001**, *123* (23), 5518-5526.

[66] Zavitsas, A. A.; Chatgilialglu, C. *J. Am. Chem. Soc.* **1995**, *117* (43), 10645-10654.

[67] Mayer, J. M.; Hrovat, D. A.; Thomas, J. L.; Borden, W. T. *J. Am. Chem. Soc.* **2002**, *124* (37), 11142-11147.

[68] Isborn, C.; Hrovat, D. A.; Borden, W. T.; Mayer, J. M.; Carpenter, B. K. *J. Am. Chem. Soc.* **2005**, *127* (16), 5794-5795.

[69] DiLabio, G. A.; Johnson, E. R. *J. Am. Chem. Soc.* **2007**, *129* (19), 6199-6203.

[70] Litwinienko, G.; Ingold, K. U. *J. Org. Chem.* **2003**, *68* (9), 3433-3438.

[71]Valgimigli, L.; Amorati, R.; Petrucci, S.; Pedulli, G. F.; Hu, D.; Hanthorn, J. J.; Pratt, D. A. *Angew. Chem. Int. Ed. Engl.* **2009**, *48* (44), 8348-8351.

[72] Forman, H. J.; Davies, K.; Ursini, F. *Free Radic. Biol. Med.* **2014**, *66*, 24-35.

[73] Apak, R.; Guclu, K.; Ozyurek, M.; Karademir, S. E. *J. Agric. Food Chem.* **2004**, *52* (26), 7970-7981.

[74] Re, R.; Pellegrini, N.; Proteggente, A.; Pannala, A.; Yang, M.; Rice-Evans, C., *Free Radic. Biol. Med.* **1999**, *26* (9-10), 1231-1237.

[75] Benzie, I. F.; Strain, J. *J. Anal. Biochem.* **1996**, *239* (1), 70-76.

[76] Blois, M. S. *Nature* **1958**, *181* (4617), 1199-1200

[77] Miller, N. J.; Rice-Evans, C.; Davies, M. J.; Gopinathan, V.; Milner, A. *Clin. Sci. (Lond)* **1993**, *84* (4), 407-412.

[78] Miller, N. J.; Rice-Evans, C.; Davies, M. *J. Biochem. Soc. Trans.* **1993**, *21* (2), 95S.

[79] Amorati, R.; Lynett, P. T.; Valgimigli, L.; Pratt. D. A. *Chem. Eur. J.* **2012**, *18* (20), 6370-6379.

[80] Valgimigli, L.; Amorati, R.; Fumo, M. G.; DiLabio, G. A.; Pedulli, G. F.; Ingold, K. U.; Pratt, D. A. *J. Org. Chem.* **2008**, *73* (5), 1830-1841.

[81] Burton, G. W.; Ingold, K. U. *J. Am. Chem. Soc.* **1981**, *103* (21), 6472-6477.

[82] Noguchi, N.; Yamashita, H.; Gotoh, N.; Yamamoto, Y.; Numano, R.; Niki, E. *Free. Radic. Biol. Med.* **1998**, *24* (2), 259-268.

[83] Cipollone, M.; Palma, C. di.; Pedulli, G. F. *Appl. Magn. Reson*. **1992**, *3* (1), 99-106.

[84] Hay, K. X.; Waisundara, V. Y.; Timmins, M.; Ou, B.; Pappalardo, K.; McHale, N.; Huang, D. *J. Agric. Food. Chem.* **2006**, *54* (15), 5299-5305.

[85] Pang, H.; Kwok, N.; Chow, L. M.; Chi-Hung Yeung, C. Wong, K.; Chen, X.; Wang, X. *Sens. Actuators, B* **2007**, *123* (1), 120-126.

[86] Sully, B. D. *Analyst.* **1954**, *79* (935), 86-90.

[87] Zinbo, M.; Jensen, R. K. *Anal. Chem.* **1985**, *57* (1), 315-319.

[88] Jensen, R. K.; Korcek, S.; Zinbo, M. Int. *J. Chem. Kinet.* **1994**, *26* (6), 673-680.

[89] Halket, J. M.; Zaikin, V. G. *Eur. J. Mass. Spectrom.* (Chichester, Eng) **2006**, *12* (1), 1-13.

[90] Akasakaa, K.; Suzuki, T.; Ohruia, H.; Meguro, H. *Anal. Lett.* **1987**, *20* (5), 731-745.

[91] Akasakaa, K.; Suzuki, T.; Ohruia, H. ; Meguro, H. *Anal. Lett.* **1987**, *20* (5), 797-807.

[92] Soh, N.; Ariyoshi, T.; Fukaminato, T.; Nakajima, H.; Nakano, K.; Imato, T. *Org. Biomol. Chem.* **2007**, *5* (23), 3762-3768.

[93] Hanthorn, J. J.; Haidasz, E.; Gebhardt, P.; Pratt, D. A. *Chem. Commun. (Camb)* **2012**, *48* (81), 10141-10143.

[94] Jensen, R. K.; Korcek, S.; Mahoney, L. R.; Zinbo, M. *J. Am. Chem. Soc.* **1979**, *101* (25), 7574-7584.

[95] Wijtmans, M.; Pratt, D. A.; Brinkhorst, J.; Serwa, R.; Valgimigli, L.; Pedulli, G. F.; Porter, N. A. *J. Org. Chem.* **2004**, *69* (26), 9215-9223.

[96] Amorati, R.; Ferroni, F.; Pedulli, G. F.; Valgimigli, L. *J. Org. Chem.* **2003**, *68* (25), 9654-9658.

[97] Brownlie, I. T.; Ingold, K. U. *Can. J. Chem.* **1966**, *44* (8), 861-868.

[98] Valgimigli, L.; Bartolomei, D.; Amorati, R.; Haidasz, E.; Hanthorn, J. J.; Nara, S. J.; Brinkhorst, J.; Pratt, D. A. *Beilstein J. Org. Chem.* **2013**, *9*, 2781-2792.

[99] Valgimigli, L.; Brigati, G.; Pedulli, G. F.; DiLabio, G. A.; Mastragostino, M.; Arbizzani, C.; Pratt, D. A. *Chemistry* **2003**, *9* (20), 4997-5010.

[100] Hanthorn, J. J.; Amorati, R.; Valgimigli, L.; Pratt, D. A. *J. Org. Chem.* **2012**, *77* (16), 6895-6907.

[101] Griller, D.; Ingold, K. U. *Acc. Chem. Res.* **1980**, *13* (9), 317-323.

[102] Chatgilialoglu, C.; Ingold, K. U.; Scaiano, J. C. *J. Am. Chem. Soc.* **1981**, *103* (26), 7739-7742.

[103] Pratt, D. A.; Tallman, K. A.; Porter, N. A. *Acc. Chem. Res.* **2011**, *44* (6), 458-467.

[104] Roschek, B., Jr.; Tallman, K. A.; Rector, C. L.; Gillmore, J. G.; Pratt, D. A.; Punta, C.; Porter, N. A. *J. Org. Chem.* **2006**, *71* (9), 3527-3532.

[105] Hanthorn, J. J.; Pratt, D. A. *J. Org. Chem.* **2012**, *77* (1), 276-284.

[106] Jha, M.; Pratt, D. A. *Chem Commun (Camb)* **2008**, (10), 1252-1254.

[107] Hanthorn, J. J.; Valgimigli, L.; Pratt, D. A. *J. Am. Chem. Soc.* **2012**, *134* (20), 8306-8309.

[108] Lynett, P. T.; Butts, K.; Vaidya, V.; Garrett, G. E.; Pratt, D. A. *Org. Biomol. Chem.*

2011, *9* (9), 3320-3330.

[109] Valgimigli, L.; Banks, J. T.; Lusztyk, J.; Ingold, K. U. *J. Org. Chem.* **1999**, *64* (9), 3381-3383.

[110] Lalevee, J.; Allonas, X.; Fouassier, J. P.; Ingold, K. U. *J. Org. Chem.* **2008**, *73* (17), 6489-6496.

[111] Alfassi, Z. B.; Huie, R. E.; Neta, P. Kinetic studies of organic peroxyl radicals in aqueous solutions and mixed solvents. The Chemistry of Free Radicals: Peroxyl Radicals, eds Z. Alfassi, John Wiley & Sons, Ltd, Chichester **1997**.

[112] Mosseri, S.; Alfassi. Z. B.; Neta, P. *Int. J. Chem. Kinet.* **1987**, *19* (4), 309-317.

[113] Niki, E.; Noguchi, N. *Acc. Chem. Res.* **2004**, *37* (1), 45-51.

[114] Barclay, L. R.; Vinqvist, M. R. *Free Radic. Biol. Med.* **1994**, *16* (6), 779-788.

[115] Barclay, L. R. C.; Ingold, K. U. *J. Am. Chem. Soc.* **1981**, *103* (21), 6478-6485.

[116] Barclay, L. R. C.; Locke, S. J.; MacNeil, J. M.; VanKessel , J.; Burton, G. W.; Ingold, K. U. *J. Am. Chem. Soc.* **1984**, *106* (8), 2479–2481.

[117] Castle, L.; Perkins, M. J. *J. Am. Chem. Soc.* **1986**, *108* (20), 6381-6382.

[118] Barclay, L. R. C.; Baskin, K. A.; Dakin, K. A.; Locke, S. J.; Vinqvist, M. R. *Can. J. Chem.* **1990**, *68* (12), 2258.

[119] Culbertson, S. M.; Antunes, F.; Havrilla, C. M.; Milne, G. L.; Porter, N. A. *Chem. Res. Toxicol.* **2002**, *15* (6), 870-876.

[120] Valgimigli, L.; Ingold, K. U.; Lusztyk, J. *J. Am. Chem. Soc.* **1996**, *118* (15), 3545-3549.

[121] Barclay, L. R.; Antunes, F.; Egawa, Y.; McAllister, K. L.; Mukai, K.; Nishi, T.; Vinqvist, M. R. *Biochim. Biophys. Acta.* **1997**, *1328* (1), 1-12.

[122] Brigati, G.; Franchi, P.; Lucarini, M.; Pedulli, G. F.; Valgimigli, L. *Res. Chem. Intermed.* **2002**, *28* (2-3), 131-141.

[123] Culbertson, S. M.; Porter, N. A. *J. Am. Chem. Soc.* **2000**, *122* (17), 4032-4038.

[124] Bowry, V. W.; Ingold, K. U.; Stocker, R. *Biochem. J.* **1992**, *288* (Pt 2), 341-344.

[125] Barclay, L. R. C.; Locke, S. J.; MacNeil, J. M.; Vankessel, J., *Can. J. Chem.* **1985**, *63* (10), 2633-2638.

[126] Antunes, F.; Pinto, R. E.; Barclay, L. R. C.; Vinqvist, M. R., *Int. J. Chem. Kinet.* **1998**,

30 (10), 753-767.

[127] Niki, E.; Takahashi, M.; Komuro, E., *Chem. Lett.* **1986**, *15* (9), 1573-1576.

[128] Barclay, L. R. C.; Baskin, K. A.; Kong, D.; Locke, S. J. *Can. J. Chem.* **1987**, *65* (11), 2541-2550.

[129] Liu, W.; Yin, H.; Akazawa, Y. O.; Yoshida, Y.; Niki, E.; Porter, N. A. *Chem. Res. Toxicol.* **2010**, *23* (5), 986-995.

[130] Milne, G. L.; Porter, N. A. *Lipids* **2001**, *36* (11), 1265-1275.

[131] Serwa, R.; Nam, T. G.; Valgimigli, L.; Culbertson, S.; Rector, C. L.; Jeong, B. S.; Pratt, D. A.; Porter, N. A. *Chemistry* **2010**, *16* (47), 14106-14114.

[132] Kondo, Y.; Miyazawa, T.; Mizutani, J. *Biochim. Biophys. Acta.* **1992**, *1127* (3), 227-232.

[133] Barclay, L. R. C.; Vinqvist, M. R.; Antunes, F.; Pinto, R. E. *J. Am. Chem. Soc.* **1997**, *119* (24), 5764-5765.

[134] Xu, L.; Davis, T. A.; Porter, N. A. *J. Am. Chem. Soc.* **2009**, *131* (36), 13037-13044.

[135] Sklar, L. A.; Hudson, B. S.; Simoni, R. D. *Proc. Natl. Acad. Sci.* **1975**, *72* (5), 1649-1653.

[136] Pap, E. H.; Drummen, G. P.; Post, J. A.; Rijken, P. J.; Wirtz, K. W. *Methods Enzymol.* **2000**, *319*, 603-612.

[137] Drummen, G. P.; van Liebergen, L. C.; Op den Kamp, J. A.; Post, J. A. *Free Radic. Biol. Med.* **2002**, *33* (4), 473-490.

[138] Naguib, Y. M. *Anal. Biochem.* **1998**, *265* (2), 290-298.

[139] Naguib, Y. M. *J. Agric. Food. Chem.* **2000**, *48* (4), 1150-1154.

[140] Pap, E. H.; Drummen, G. P.; Winter, V. J.; Kooij, T. W.; Rijken, P.; Wirtz, K. W.; Op den Kamp, J. A.; Hage, W. J.; Post, J. A. *FEBS Lett.* **1999**, *453* (3), 278-282.

[141] Yoshida, Y.; Shimakawa, S.; Itoh, N.; Niki, E. *Free. Radic. Res.* **2003**, *37* (8), 861-872.

[142] Itoh, N.; Cao, J.; Chen, Z. H.; Yoshida, Y.; Niki, E. *Bioorg. Med. Chem. Lett.* **2007**, *17* (7), 2059-2063.

[143] Oleynik, P.; Ishihara, Y.; Cosa, G. *J. Am. Chem. Soc.* **2007**, *129* (7), 1842-1843.

[144] Khatchadourian, A.; Krumova, K.; Boridy, S.; Ngo, A. T.; Maysinger, D.; Cosa, G.

Biochemistry **2009**, *48* (24), 5658-5668.

[145] Krumova, K.; Friedland, S.; Cosa, G. *J. Am. Chem. Soc.* **2012**, *134* (24), 10102-10113.

[146] Li, B.; Harjani, J. R.; Cormier, N. S.; Madarati, H.; Atkinson, J.; Cosa, G.; Pratt, D. A. *J. Am. Chem. Soc.* **2013**, *135* (4), 1394-1405.

[147] Zheng, F.; Pratt, D. A. *Chem. Commun. (Camb)* **2013**, *49* (74), 8181-8183.

[148] Witztum, J. L. *Lancet* **1994**, *344* (8925), 793-795.

[149] Simonian, N. A.; Coyle, J. T. *Annu. Rev. Pharmacol.Toxicol.* **1996**, *36*, 83-106.

[150] Benz, C. C.; Yau, C. *Nat. Rev. Cancer.* **2008**, *8* (11), 875-879.

[151] Stacey, N. H.; Klaassen, C. D. *J. Toxicol. Environ. Health.* **1982**, *9* (3), 439-450.

[152] Arce, P. M.; Goldschmidt, R.; Khdour, O. M.; Madathil, M. M.; Jaruvangsanti, J.; Dey, S.; Fash, D. M.; Armstrong, J. S.; Hecht, S. M. *Bioorg. Med. Chem.* **2012**, *20* (17), 5188-5201.

[153] Skibska, B.; Jozefowicz-Okonkwo, G.; Goraca, A. *Pharmacol. Rep.* **2006**, *58* (3), 399-404.

[154] Bhattacharyya, J.; Datta, A. G. *J. Physiol. Pharmacol.* **2001**, *52* (1), 145-152.

[155] Bus, J. S.; Aust, S. D.; Gibson, J. E. *Environ. Health Perspect.* **1976**, *16*, 139-146.

[156] Krumova, K.; Greene, L. E.; Cosa, G. *J. Am. Chem. Soc.* **2013**, *135* (45), 17135-17143.

[157] Khdour, O. M.; Lu, J.; Hecht, S. M. *Pharm. Res.* **2011**, *28* (11), 2896-2909.

[158] Castell, J. V.; Tolosa, L.; Pinto, S.; Donato, M.T.; O' Connor, J.E.; Gómez-Lechón, M. *J. Toxicol. Lett.* **2010**, *196* (S17), S137-138.

[159] Olsen, E. K.; Hansen, E.; Isaksson, J.; Andersen, J. H. *Mar. Drugs.* **2013**, *11* (8), 2769-2784.

[160] Bass, D. A.; Parce, J. W.; Dechatelet, L. R.; Szejda, P.; Seeds, M. C.; Thomas, M. *J. Immunol.* **1983**, *130* (4), 1910-1917.

[161] Saito, Y.; Nishio, K.; Akazawa, Y. O.; Yamanaka, K.; Miyama, A.; Yoshida, Y.; Noguchi, N.; Niki, E. *Free. Radic. Biol. Med.* **2010**, *49* (10), 1542-1549.

[162] LeBel, C. P.; Ischiropoulos, H.; Bondy, S. C. *Chem. Res. Toxicol.* **1992**, *5* (2), 227-231.

[163] Kooy, N. W.; Royall, J. A.; Ischiropoulos, H. *Free Radic. Res.* **1997**, *27* (3), 245-254.

[164] Myhre, O.; Andersen, J. M.; Aarnes, H.; Fonnum, F. *Biochem.l Pharmacol.* **2003**, *65* (10), 1575-1582.

[165] Wijtmans, M.; Pratt, D. A.; Valgimigli, L.; DiLabio, G. A.; Pedulli, G. F.; Porter, N. A. *Angew. Chem. Int. Ed. Engl.* **2003**, *42* (36), 4370-4373.

[166] Okada, Y.; Tanaka, K.; Sato, E.; Okajima, H. *Org. Biomol. Chem.* **2006**, *4* (22), 4113-4117.

[167] Horev-Azaria, L.; Eliav, S.; Izigov, N.; Pri-Chen, S.; Mirelman, D.; Miron, T.; Rabinkov, A.; Wilchek, M.; Jacob-Hirsch, J.; Amariglio, N.; Savion, N. *Eur. J. Nutr.* **2009**, *48* (2), 67-74.

[168] Li, X. H.; Li, C. Y.; Lu, J. M.; Tian, R. B.; Wei, *J. Neurosci. Lett.* **2012**, *514* (1), 46-50.

[169] Jakubikova, J.; Sedlak, J. *Neoplasma* **2006**, *53* (3), 191-199.

[170] Arditti, F. D.; Rabinkov, A.; Miron, T.; Reisner, Y.; Berrebi, A.; Wilchek, M.; Mirelman, D. *Mol. Cancer. Ther.* **2005**, *4* (2), 325-331.

[171] Vaidya, V.; Ingold, K. U.; Pratt, D. A. *Angew. Chem. Int. Ed. Engl.* **2009,** *48* (1), 157-160.

Chapter 2:

Evaluating the Role of Sidechain Substitution on the Reactivity of Tetrahydronaphthyridinol Antioxidants in Lipid Bilayers

2.1 Preface

This chapter is presented largely as it was in the manuscript that was published in the Journal of the American Chemical Society (Li, B.; Harjani, J. R.; Cormier, N. S.; Madarati, H.; Atkinson, J.; Cosa, G. and Pratt, D. A. Besting Vitamin E: Sidechain Substitution is Key to the Reactivity of Naphthyridinol Antioxidants in Lipid Bilayers, *J. Am. Chem. Soc.*, **2013**, *135* (4), pp 1394–1405), but includes supplementary results. The synthesis of the tetrahydronaphthyridinols was originally carried out by Dr. Jitendra R. Harjani, a post-doctoral fellow in the Pratt group, and subsequently repeated several times by myself and undergraduate students under my immediate supervision, including Nicholas Cormier and Elise Malek-Adamian. Effective dissociation constants determined for binding of the tetrahydronaphthyridinols to recombinant human tocopherol transport protein were determined by our collaborator, Prof. Jeffrey Atkinson and his student, Hasam Madarati, at Brock University.

2.2 Introduction

The oxidative modification of proteins, DNA and other biomolecules by electrophilic products of polyunsaturated lipid peroxidation has been implicated in the onset of essentially all degenerative diseases, including atherosclerosis,[1,2] neurodegenerative disease,[3,4] and cancer.[5,6] Peroxidation of polyunsaturated lipids proceeds by the prototypical free radical chain reaction as described in Chapter 1 (**Scheme 2.1**),[7,8] and can be inhibited by RTAs, such as α-TOH,[9] which interrupts the chain sequence by reaction with chain-carrying peroxyl radicals.

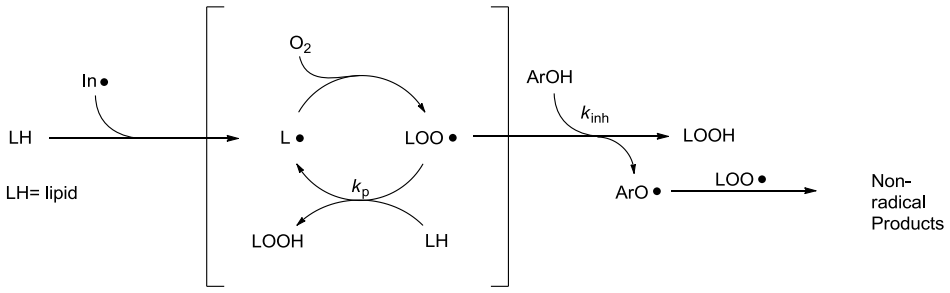

Scheme 2.1. Mechanism of lipid peroxidation.

α-TOH, the most biologically active congener of vitamin E (k_{inh} = 3.2×10^6 M^{-1} s^{-1} at 30 °C),[9] is the major lipid-soluble RTA in human plasma and circulating lipoproteins.[10] It is well established as one of the most reactive RTAs *in vitro* and is commonly used as the standard against which others are evaluated.[11] Given its high reactivity as an inhibitor of lipid peroxidation and the implication of this process in the pathogenesis of degenerative disease, a staggering number of clinical trials employing α-TOH in a therapeutic and/or preventive capacity have been conducted over the past 30 years (the NIH clinical trials database (www.clinicaltrials.gov) currently lists well over 400 relating to cancer and cardiovascular and neurodegenerative diseases alone). The results have been largely disappointing, leading researchers to question whether oxidative damage has a causal or consequential role in the onset and development of degenerative disease.[12,13] Perhaps a more appropriate question is: Is α-TOH the best compound to study, or is it simply convenient to do so?

To determine whether a given compound can effectively inhibit peroxidation, the rate at which an antioxidant traps peroxyl radicals must outcompete the rate at which chain propagation occurs, i.e., k_{inh}[ArOH] ≥ k_p[R-H]. To minimize the amount of RTA needed to protect oxidizable substrates (i.e. lipids), the rate constant at which antioxidants trap peroxyl radicals (k_{inh}) needs to be maximized. Initial exploration of structure-activity relationships of α-TOH revealed that k_{inh} increased with increasing electron-donating abilities of the substituents on the phenolic ring in phenolic RTAs.[9] Thus, Ingold and co-workers examined the impact of replacing the O atom in α-TOH with the more electron donating N atom.[14] Unfortunately, this compound was unstable in air, leading to a lower than expected k_{inh} and poor stoichiometry for its reactions with peroxyl radicals. Indeed, while substitution of the phenolic ring with stronger EDGs can decrease the O-H BDE, it

also leads to a decrease in the ionization potential. As a result, the RTAs are easily oxidized in the presence of O_2 and produce hydroperoxyl radicals, which render them pro-oxidants instead of antioxidants (**Scheme 2.2**).[14]

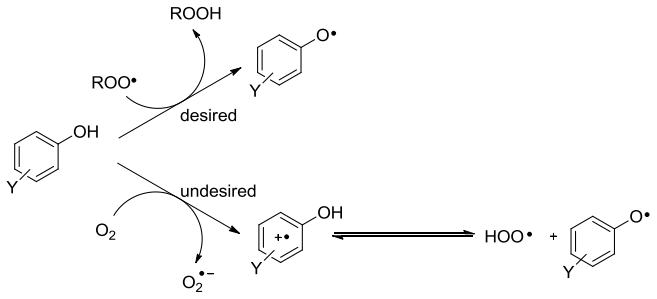

Scheme 2.2. Desired antioxidant radical-trapping reaction and undesired pro-oxidant reactions of electron-rich phenolic compounds

Some time ago, the Pratt group and his collaborators showed that incorporation of nitrogen atoms into the aromatic ring of phenolic RTAs at the 3 and/or 5 positions relative to the hydroxyl group increases their stability towards one electron oxidation by increasing the ionization potential, but do so with a minor impact on their O-H BDE.[15,16] The incorporation of the more electronegative N-atom in the aromatic ring in lieu of carbon destabilizes the radical cation formed upon one-electron oxidation relative to the radical formed upon transferring an H-atom to a peroxyl radical. For example, calculated results show that the IP of 3-pyridinol increases by 11 kcal/mol compared to phenol, where the O-H BDE increased only 1.1 kcal/mol. The IP of 5-pyrimidinol increased by 24.3 kcal/mol and BDE only increased 2.5 kcal/mol (**Table 2.1**).[15]

Table 2.1. Calculated O-H bond dissociation enthalpies and ionization potentials of phenol, 3-pyridinol and 5-pyrimidinol (kcal/mol).[15]

Compounds	O-H BDE	IP
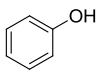	87.1	195.4
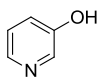	88.2	206.4
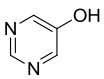	89.6	219.7

As a result, the phenol-like 3-pyridinol and 5-pyrimidinol compounds can be substituted with very strong EDGs at the ortho- and para- position relative to the hydroxyl group (e.g., N,N-diakylamino) to weaken the O−H bond,[17] resulting in some of the fastest RTAs described to date.[15,16] For example, aminopyrimidinol **1** and aminopyridinol **2** (**Chart 2.1**) react 2- and 5-fold faster with peroxyl radicals in organic solution than α-TOH.[15,16,18] The bicyclic pyridinol compounds **3** and **4** are even more reactive, with rate constants measuring 28- and 88-fold greater than that of α-TOH in organic solution, respectively.[16,18] Our lab has recently extended this idea to maximize the reactivity of diarylamine RTAs that are commonly used in additives to petroleum-derived products.[19-21]

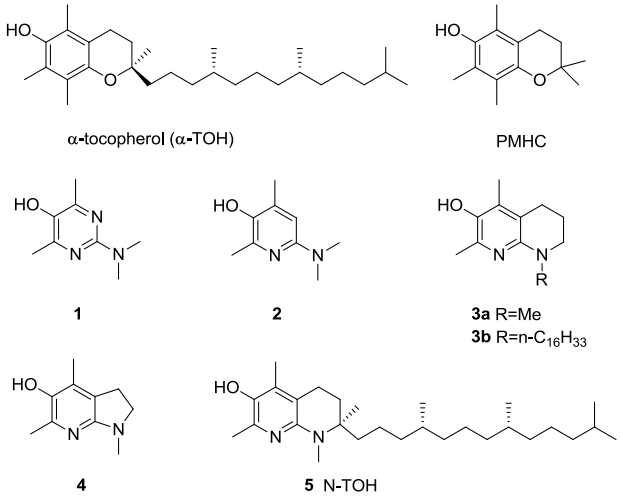

Chart 2.1. Highly reactive radical-trapping antioxidants.

While **4** has limited stability in aerated solutions, **3a** can be more easily manipulated, suggesting that it is a better compromise between activity and stability. Its lipophilic analog **3b**[22] and the tocopherol analog **5**[23] (which was dubbed N-TOH) are both excellent inhibitors of cholesterol ester oxidation in human low-density lipoprotein (LDL), and the latter was found to bind to recombinant human tocopherol transport protein (hTTP) at least as well as α-TOH.[23] Despite these exciting results, further experimentation with **5** has been all but impossible due to its lengthy synthesis, which required 17 chemical steps. Since **3b** has similar activity to **5** in LDL, but is more synthetically accessible, it is a much better candidate for further studies.

It is well-known that the localization and mobility of tocopherols and their analogs can play at least as important a role in their antioxidant activity as their inherent chemical

reactivity upon moving from homogeneous organic solvents to the heterogeneous environment of a lipid bilayer.[24] While we have worked hard over the years to optimize the chemical reactivity of the phenolic headgroup towards peroxyl radicals in homogeneous solution during the development of **3** (and **5**), we had yet to undertake a detailed study of their reactivities in lipid bilayers and determine how changes in their physical properties will impact their activities. Furthermore, since the pyridinoxyl radicals derived from **3** (and **5**) are more stable than the tocopheroxyl radical derived from α-TOH,[16,23] it is unknown whether they will be regenerated by co-antioxidants in the aqueous medium surrounding the lipid bilayers. Indeed, the cooperativity displayed between water-soluble antioxidants, such as ascorbate (vitamin C), and α-TOH has long been thought to be key to the activity of both compounds *in vivo*.[25,26] Furthermore, the impact of changes in the lipophilic sidechain of tocopherols (or any tocopherol-like ligands) on their affinity for the TTP has never been systematically surveyed, and it remains to be determined whether the simpler tetrahydronaphthyridinol (THN) **3** will bind at all, given the removal of the quaternary carbon (whose stereochemistry is known to be important in binding the tocopherols)[27-29] and the relocation of the lipophilic sidechain to a position α to the aromatic ring.

Herein we describe the preparation of a small library of THNs with sidechains of varying length and branching, the results of high-throughput competitive kinetic studies of their reactivities in phosphatidylcholine liposomes under various conditions and the determination of their abilities to bind to recombinant hTTP. Together, these data provide a clear picture of the vital role of the sidechain on the reactivity and potential bioavailability of THN antioxidants and set the stage for experiments *in vivo*.

2.3 Results

2.3.1 Synthesis of Tetrahydronaphtyridinols with Different Sidechain Substitutions

In previous work, our group and others have accessed the THN core structure of **3a, 3b** and **5** starting from either 2-amino-4,6-lutidine[16,30] or pyridoxine (vitamin B_6).[31] The former approach (6 steps) featured two very low-yielding reactions: the (initial) ring annulation (23%) and the (final) installation of the pyridinol moiety via a low-yielding

lithiation/oxidation sequence (25%). This served as motivation for the development of the latter approach (11 steps), which carried the pyridinol moiety through the synthesis, and although longer, did not suffer a single low-yielding step. In parallel, our group found that a Cu-mediated alkoxylation/hydrogenolysis sequence was a much better option than the lithiation/oxidation approach.[32] In addition, Hecht's group provided a concise route to the THN core from 2-piperidinone – a shorter, higher-yielding approach than our earlier annulation strategy.[33] This prompted us to consider a combination of these two developments to prepare our small library of THNs having different sidechain substitution.

Since a variety of substitutions at the amine nitrogen was desired, it was ideal to carry out the alkylation in the final step. Therefore, we elected to benzylate the piperidone to protect this nitrogen through the annulation and aryl substitution steps, after which it could be removed and the amine alkylated with different sidechains. The target compounds are shown as **12a-h**, the oxalic acid addition salts of THNs (**Scheme 2.3**). We chose increments of 4 carbons for the linear sidechains (n-butyl, n-octyl, n-dodecyl, n-hexadecyl) and increments of 5 carbons for the branched sidechains, including one, two and three of the isoprene units found in the phytyl sidechain of α-TOH, in addition to the derivative lacking a sidechain. This range of sidechain lengths provides a range of over 7 orders of magnitude in predicted values of log*P* (**Table 2.2**).

Briefly, 2-piperidinone was first protected with a benzyl moiety to provide **6**, which was ketalized with dimethyl sulfate/sodium methoxide and then condensed with 4-aminopent-3-en-2-one to give **7**. The naphthyridine was halogenated with N-bromosuccinimide and then methoxylated to provide **9**. While we had initially attempted the alkoxylation with benzyl alcohol, as we had in the preparation of **1** and **2**,[32] we found much lower yields for benzyloxylation of **8** presumably due to its greater electron richness, unless we pushed the reactions with large concentrations of CuI and Cs_2CO_3, which we deemed impractical. The benzyl protecting group was then removed by hydrogenolysis and the key intermediate **10** was alkylated with various alkyl bromides to afford the *O*-methylated THNs **11b-h**. Removal of the *O*-methyl group using the dimethylsulfide complex of boron tribromide (BBr_3•Me_2S) followed by addition of oxalic acid provided the ammonium oxalate salts of the THNs **12a-h**. Unlike the free THNs **3**, these derivatives are

indefinitely stable at room temperature in an aerobic atmosphere.

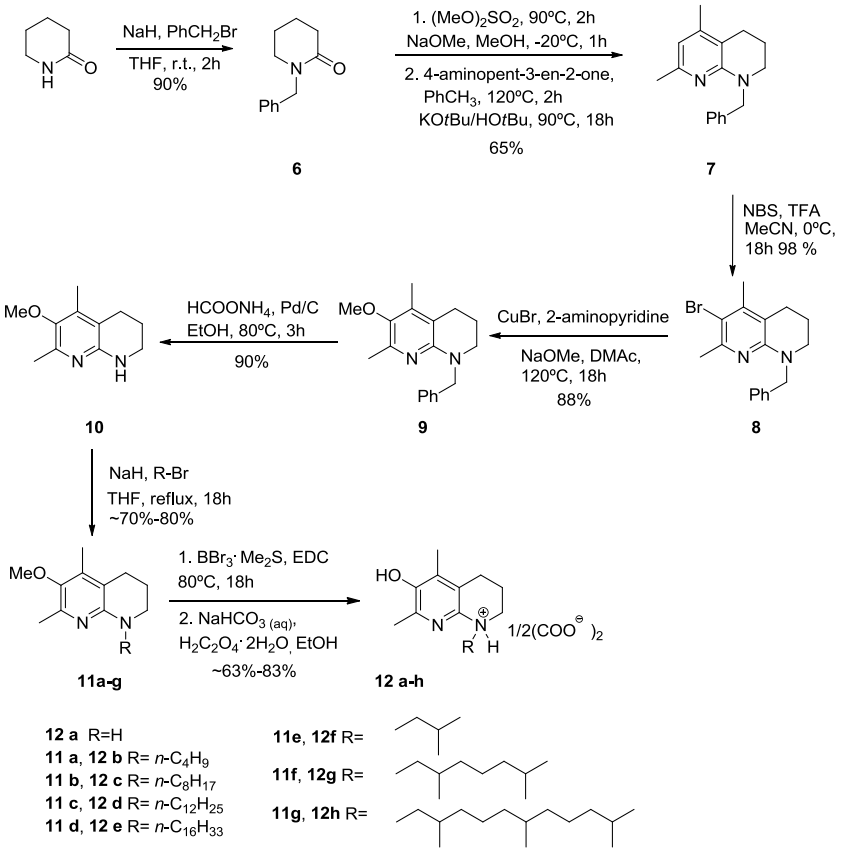

Scheme 2.3. Synthesis of THN antioxidants.

Table 2. 2. Predicted log*P* values for THNs **12a-h**, PMHC and α-TOH.

Compound	log*P*[a]
12a	2.11
PMHC	3.42
12b	4.14
12f	4.47
12c	5.81
12g	6.19
12d	7.48
12h	8.47
12e	9.14
α-TOH	9.98

[a]Predicted for the free base using ChemBioDraw Ultra 12 from Cambridgesoft.

2.3.2 Effect of THNs on Phosphatidylcholine Liposome Oxidations – Competition with the H_2B-PMHC Probe

The peroxyl radical-trapping activities of the THNs were assayed in unilamellar liposomes prepared from egg phosphatidylcholine (EggPC) using the fluorogenic H_2B-PMHC (**Scheme 2.4**) probe (λ_{ex} = 485 nm; λ_{em} = 520 nm).[34] H_2B-PMHC features a BODIPY fluorophore conjugated to 2,2,5,7,8-pentamethyl-6-hydroxychroman (PMHC), an analog of α-TOH which lacks the lipophilic phytyl sidechain. The function of the probe is straightforward: in the 'off' state, the fluorescence of the BODIPY moiety is quenched by photoinduced electron transfer from the electron rich PMHC group, whereas upon reaction of the phenol with peroxyl radicals (**Scheme 2.4**), the fluorescence of the probe is turned 'on' since the resultant chromanone is not sufficiently electron rich to reduce the BODIPY moiety upon excitation.[35,36] The probe was recently used in a high-throughput approach utilizing a microplate reader to monitor the antioxidant status (α-TOH and PMHC) in liposomes of different phospholipid composition; the probe, the fluorescence assay and the data analysis provides a new method to obtain, in a rapid parallel format, relative antioxidant activities in phospholipid membranes.[34] These studies suggested that it would be ideal to survey the relative activities of **12a-h**.

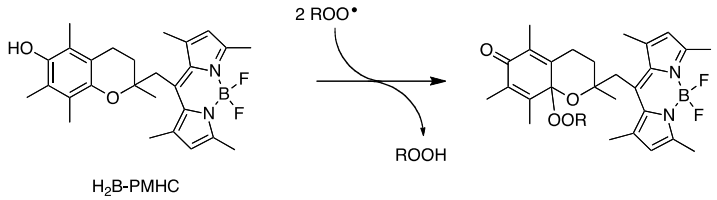

Scheme 2.4. Reaction of H_2B-PMHC probe with peroxyl radicals.

Representative results of oxidations of solutions of H_2B-PMHC-supplemented liposomes containing different concentrations of added antioxidant are shown in **Figure 2.1**. These results were obtained from oxidations mediated by the hydrophilic azo-compound 2,2'-azobis-(2-amidinopropane) monohydrochloride (AAPH) (2.7 mM), which yields water-soluble peroxyl radicals with a rate of $R_i = 2ek_d[\text{AAPH}] = 3.1 \times 10^{-9}$ M s^{-1} under these conditions.[37] Representative data corresponding to oxidations inhibited by the highly lipophilic derivative **12e** and the more hydrophilic derivative

12b are shown in panels A and C, respectively, while data for oxidations inhibited by α-TOH and its truncated analog PMHC are shown for comparison in panels B and D, respectively.

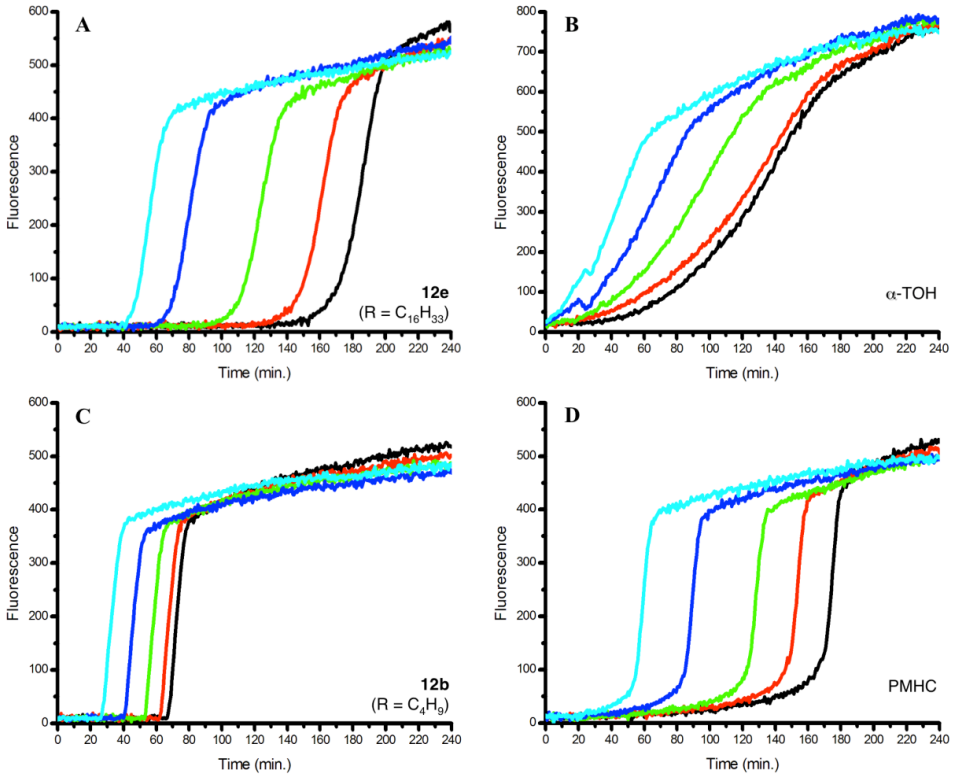

Figure 2.1. Representative fluorescence (at 520 nm) intensity-time profiles from AAPH-mediated (2.7 mM) oxidations of EggPC liposomes (1 mM in PBS buffer, pH 7.4) containing 0.15 μM H_2B-PMHC and increasing concentrations (1.5 μM - cyan, 3.0 μM - blue, 4.5 μM - green, 6.0 μM - red and 7.5 μM - black) of **12e (**A), α-TOH (B), **12b** (C) and PMHC (D).

Five concentrations of each antioxidant were examined from which a clear dose-response relationship is evident. That is, with the addition of increasing amounts of antioxidant, the time required to achieve the maximum rate of fluorescence increase was extended proportionately. The 'inhibited period', where the oxidation of H_2B-PMHC is inhibited (or retarded) by the added antioxidant, is analogous to the 'inhibited period' that is observed in inhibited autoxidations of hydrocarbons,[38] which are usually monitored by either O_2 consumption or the formation of product hydroperoxides – much more laborious experiments not amenable to high-throughput study. Throughout, we have determined the length of the inhibited period (τ) from the intersection of the lines of best fit to the

maximum rate of increase in fluorescence intensity (due to oxidation of the chromanol moiety of H_2B-PMHC) and the slower subsequent increase in fluorescence intensity (due to follow-up reactions of the fluorophore), as this is the time at which all of the added antioxidant as well as the phenolic moiety of the probe has reacted. The inhibited period provides important insight into the reactivities of the antioxidants under investigation, as its duration reflects the relative stoichiometries of the reactions of the antioxidants with peroxyl radicals, since the probe is present in a constant amount in all experiments.[34]

The inhibited periods observed in **Figure 2.1** are very similar for the same concentration of **12e** (**Figure 2.1A**), α-TOH (**Figure 2.1B**) and PMHC (**Figure 2.1D**), becoming longer with increasing antioxidant concentration. In contrast, the inhibited periods observed for **12b** (**Figure 2.1C**) are comparably shorter and do not increase to the same extent with increasing antioxidant concentration. This is representative of the trends observed with all of the THNs (see **Figure 2.2**): the more lipophilic derivatives ($C_{10}H_{21}$ or longer) have similar inhibited periods to α-TOH and PMHC, the more hydrophilic compounds (C_5H_{11} or shorter) have much shorter inhibited periods (less than half at higher concentrations) and the octylated derivative is roughly intermediate between the two groups.

In addition to relative stoichiometry, the data provide insight into the relative rates for the reactions of peroxyl radicals with the different antioxidants *versus* the fluorogenic H_2B-PMHC, since the rate of fluorescence increase during the inhibited period represents the competition of the added antioxidant and H_2B-PMHC for peroxyl radicals. Focusing on this part of the data, it is clear that α-TOH is by far the least reactive compound (**Figure 2.1B**), as it barely retards H_2B-PMHC oxidation, except perhaps in the first few minutes of the experiment when the highest antioxidant concentration is used (7.5 μM). PMHC is more reactive (**Figure 2.1D**), as is clear from the more obvious inhibited periods. A kinetic analysis based on the initial rates of H_2B-PMHC oxidation in the presence and absence of added antioxidant has been carried out to provide an expression useful for the quantification of the relative rate constants in this competition (**Eq. 2.1**):[34]

$$\ln\left(\frac{I_\infty - I_t}{I_\infty - I_0}\right) = \frac{k_{inh}^{H2B-PMHC}}{k_{inh}^{RTA}} \ln\left(1 - \frac{t}{\tau}\right) \qquad \text{Eq. 2.1}$$

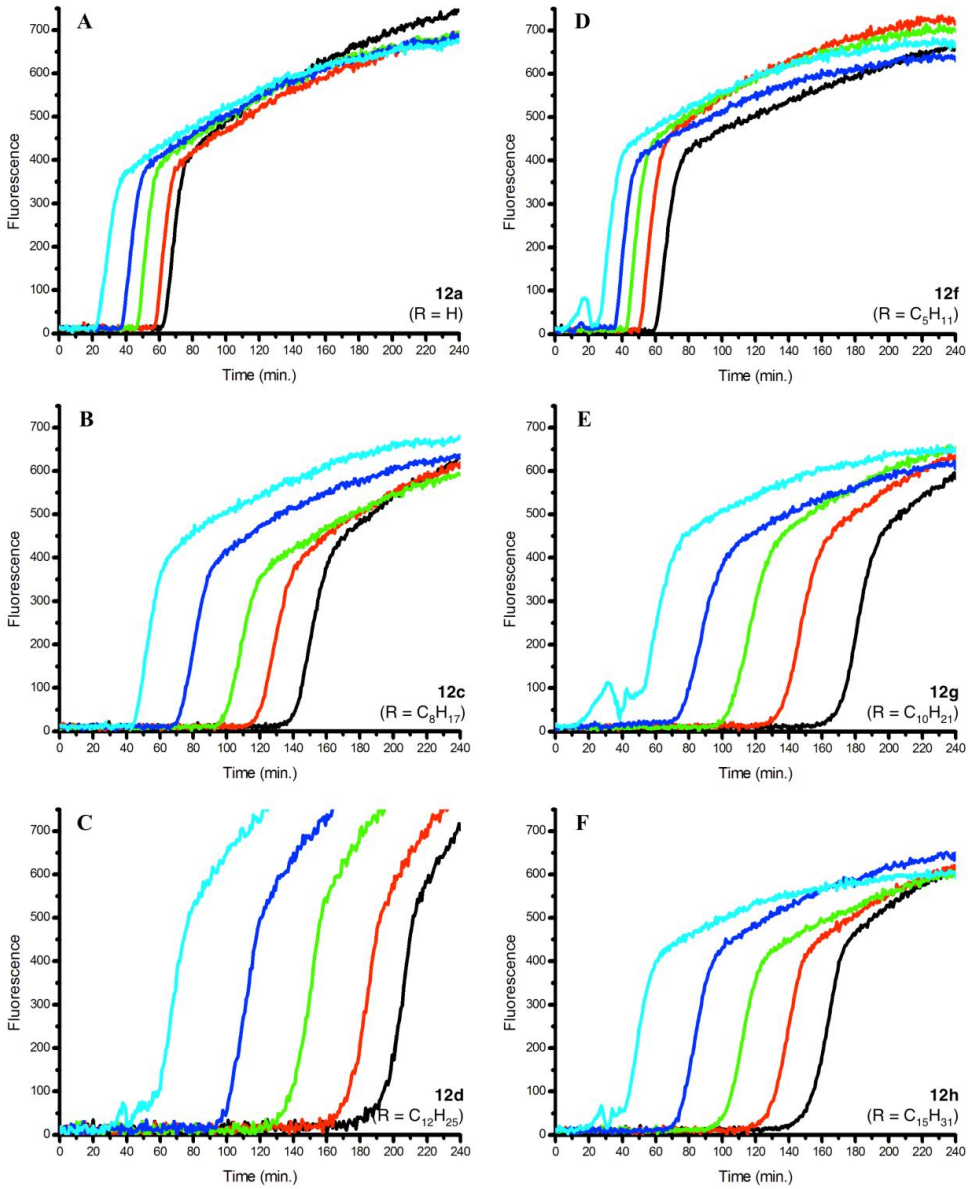

Figure 2.2. Representative fluorescence intensity-time profiles from AAPH-mediated (2.7 mM) oxidations of EggPC liposomes (1 mM) containing 0.15 μM H_2B-PMHC and increasing concentrations (1.5 μM - cyan, 3.0 μM - blue, 4.5 μM - green, 6.0 μM - red and 7.5 μM - black) of **12a** (A), **12c** (B), **12d** (C), **12f** (D), **12g** (E) and **12h** (F). Fluorescence (λ_{ex} = 485 nm; λ_{em} = 520 nm) was recorded every 50 s.

Thus, from a plot of $\ln[(I_\infty - I_t)/(I_\infty - I_0)]$ vs $\ln(1\text{-}t/\tau)$, the relative rate constant can be determined (see **Figure 2.3** and **Table 2.3)**. This analysis indicates a ca. 10-fold increase in the rate constant for the reaction of PMHC and hydrophilic radicals compared to α-TOH under these conditions.[34] Interestingly, the THNs **12e** (**Figure 2.1A**) and **12b** (**Figure 2.1C**) clearly display much faster rates of reaction with peroxyl radicals than both α-TOH and

PMHC, as they completely suppress H_2B-PMHC oxidation throughout the inhibited periods. In fact, the same is true of all of the other substituted THNs (**Figure 2.2**). Based on the lack of any emission enhancement during the inhibited periods observed in the presence of the THNs, the relative rate constants for H-atom transfer from the THNs to peroxyl radicals cannot be derived from Eq. 2.1. However, it can be estimated to at least 30-fold than for H_2B-PMHC (which has essentially the same rate constant for reaction with peroxyl radicals as does α-TOH).

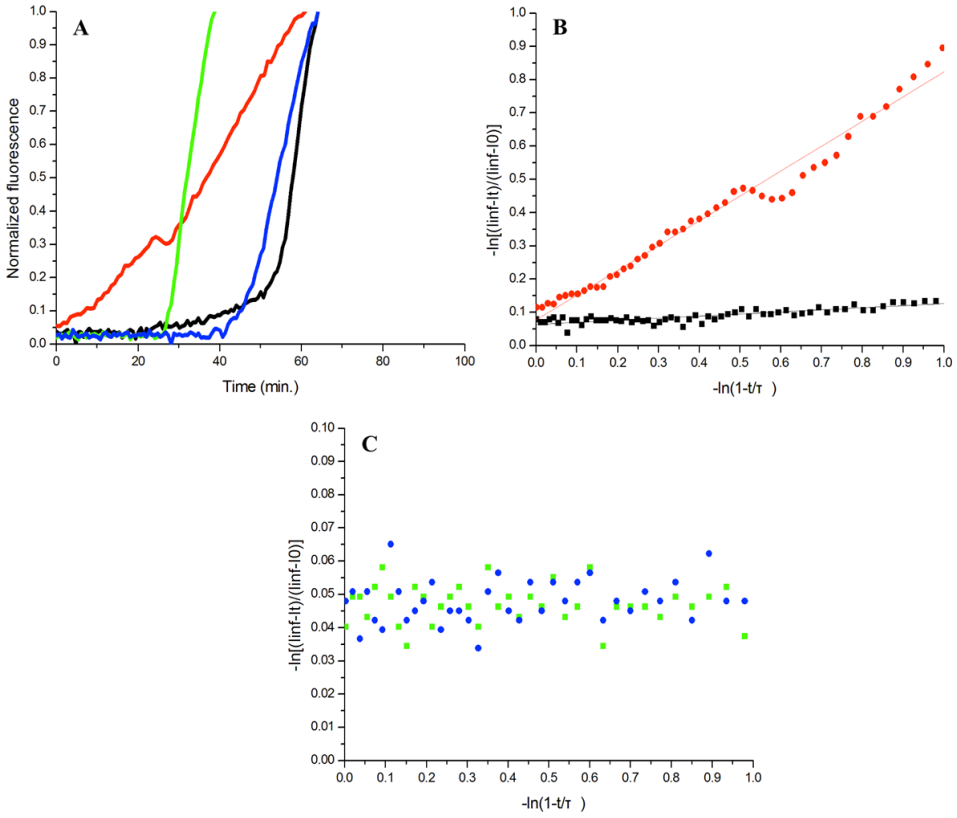

Figure 2.3. (A) Normalized fluorescence (at 520 nm) intensity-time profiles from AAPH-mediated (2.7 mM) oxidations of EggPC liposomes (1 mM in PBS buffer, pH 7.4) containing 0.15 μM H_2B-PMHC and 1.5 μM of **12e** (blue), α-TOH (red), **12b** (green) and PMHC (black). (B) The data in (A) plotted according to **Eq. 2.1** for α-TOH (red) and PMHC (black). (C) The data in (A) plotted according to **Eq. 2.1** for **12e** (blue) and **12b** (green).

Analogous results were obtained when experiments were carried out using the hydrophobic azo-compound 2,2'-azobis(4-methoxy-2,4-dimethylvaleronitrile) (MeOAMVN) (see **Figure 2.4, 2.5**). The relative rate constant can be determined from a plot of $\ln[(I_\infty - I_t)/(I_\infty - I_0)]$ vs $\ln(1-t/\tau)$ as well (see **Table 2.4**).

Table 2.3. Relative rate constants for the reactions of PMHC and α-TOH with AAPH-derived peroxyl radicals derived from data in Figure 2.1B and 2.1D (and two other runs not shown) using Eq. 2.1.

[Antioxidant] (μM)	$k_{inh}^{H2B\text{-}PMHC}/k_{inh}^{TOH}$	$k_{inh}^{H2B\text{-}PMHC}/k_{inh}^{PMHC}$	$k_{inh}^{PMHC}/k_{inh}^{TOH}$
1.5	0.87±0.16	0.074±0.012	11.7±0.4
3.0	0.79±0.13	0.063±0.010	12.5±0.07
4.5	0.78±0.08	0.061±0.007	12.8±1.0
6.0	0.72±0.07	0.062±0.011	11.9±1.2
7.5	0.71±0.06	0.061±0.009	11.8±1.2
		average	**12.2±0.5**

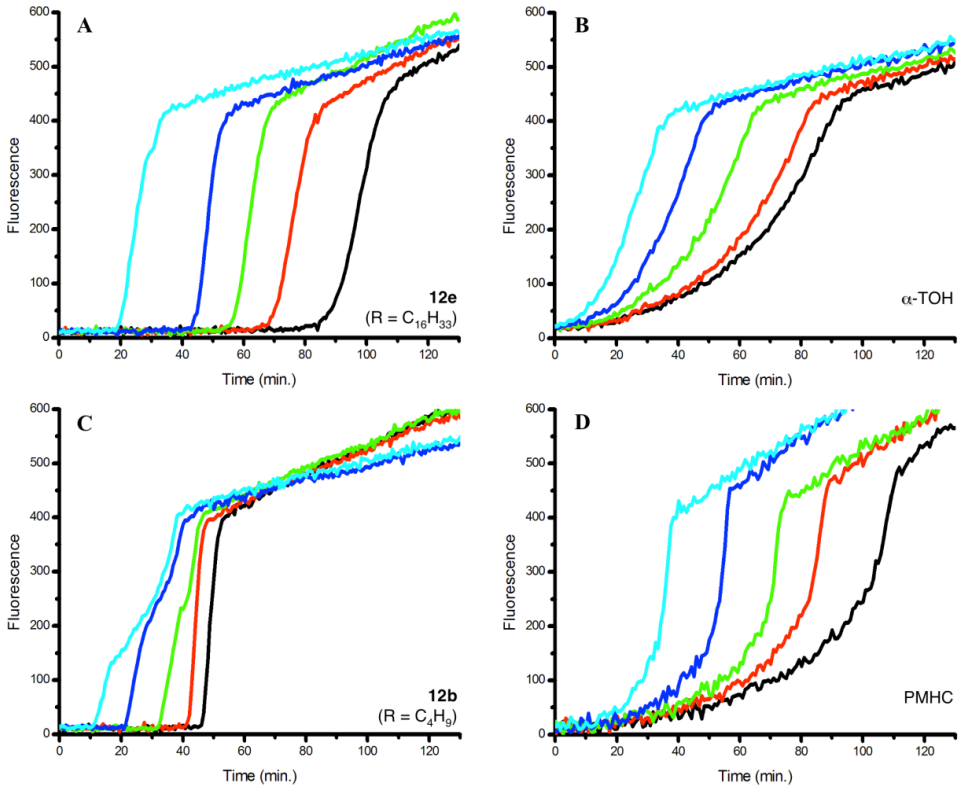

Figure 2.4. Representative fluorescence intensity-time profiles from MeOAMVN-mediated (0.68 mM) oxidations of EggPC liposomes (1 mM) containing 0.15 μM H_2B-PMHC and increasing concentrations (1.5 μM - cyan, 3.0 μM - blue, 4.5 μM - green, 6.0 μM - red and 7.5 μM - black) of **12e** (A), α-TOH (B), **12b** (C) and PMHC (D). Fluorescence (λ_{ex} = 485 nm; λ_{em} = 520 nm) was recorded every 50 s.

Table 2.4. Relative rate constants for the reactions of PMHC and α-TOH with MeOAMVN-derived peroxyl radicals derived from data in Figure 2.4B and 2.4D (and two other runs not shown) using Eq. 2.1.

[Antioxidant] (μM)	$k_{inh}^{H2B\text{-}PMHC}/k_{inh}^{TOH}$	$k_{inh}^{H2B\text{-}PMHC}/k_{inh}^{PMHC}$	$k_{inh}^{PMHC}/k_{inh}^{TOH}$
1.5	0.70±0.10	0.19±0.04	3.6±0.24
3.0	0.56±0.14	0.18±0.03	3.1±0.33
4.5	0.57±0.08	0.19±0.02	3.1±0.35
6.0	0.51±0.01	0.20±0.02	2.6±0.30
7.5	0.51±0.05	0.22±0.01	2.3±0.13
		average	**2.9±0.5**

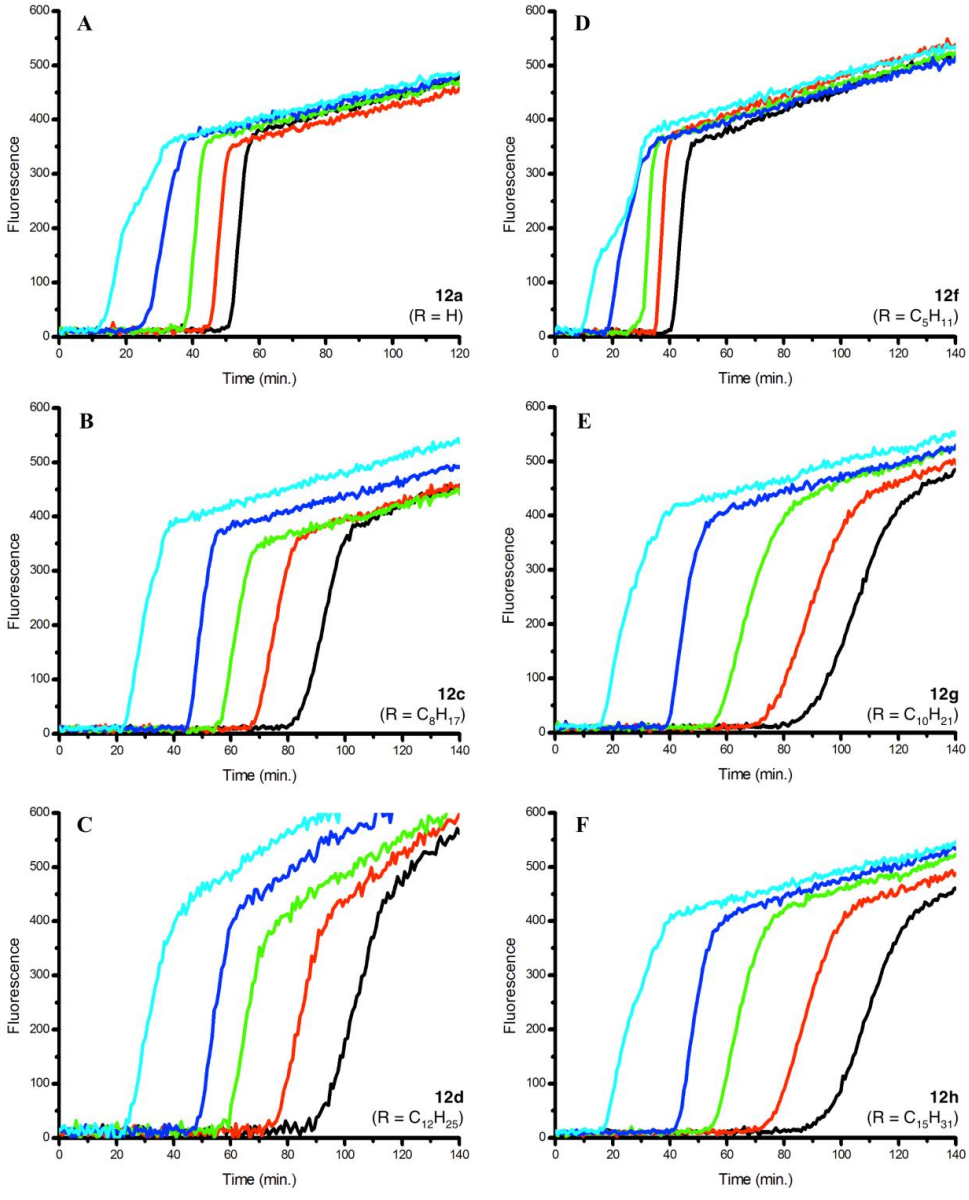

Figure 2.5. Representative fluorescence intensity-time profiles from MeOAMVN-mediated (0.68 mM)

oxidations of EggPC liposomes (1 mM) containing 0.15 μM H_2B-PMHC and increasing concentrations (1.5 μM - cyan, 3.0 μM - blue, 4.5 μM - green, 6.0 μM - red and 7.5 μM - black) of **12a** (A), **12c** (B), **12d** (C), **12f** (D), **12g** (E) and **12h** (F). Fluorescence (λ_{ex} = 485 nm; λ_{em} = 520 nm) was recorded every 50 s.

The inhibited periods for all of the THNs, as well as α-TOH and PMHC, are summarized in **Figure 2.6** for the five concentrations that were studied, alongside the corresponding data for the oxidations with lipophilic peroxyl radicals. Presented in this way it is clear that increasing the concentration of the less lipophilic THNs has very little effect on the observed inhibited periods, while increasing the concentration of the more lipophilic THNs, PMHC or α-TOH leads to a substantial increase in inhibited periods.

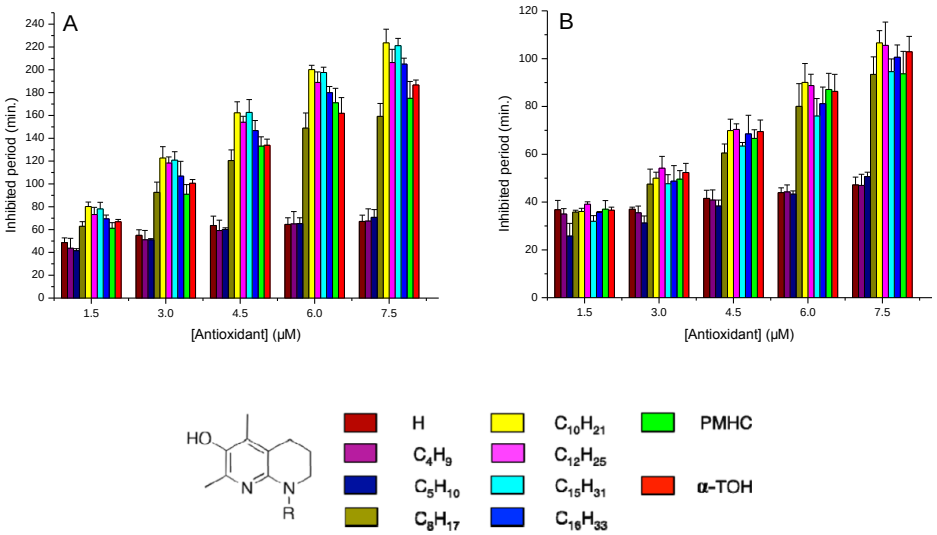

Figure 2.6. Inhibited periods (averages of at least three measurements) observed for THNs **12a-h**, PMHC and α-TOH as a function of antioxidant concentration when EggPC liposomes were oxidized with hydrophilic (A) or lipophilic (B) peroxyl radicals.

In order to ensure that the antioxidants and the H_2B-PMHC probe were incorporated into the liposomes prior to initiation of oxidation, a series of control experiments were carried out. Thus, liposome suspensions to which H_2B-PMHC and a representative concentration (4.5 μM) of **12e** or α-TOH were added was filtered using Amicon ultracentrifuge membranes (10 kDa cutoff) prior to oxidation with MeOAMVN. No significant difference was observed in the reaction profiles compared to the oxidation of

liposomes without filtration (**Figure 2.7**).

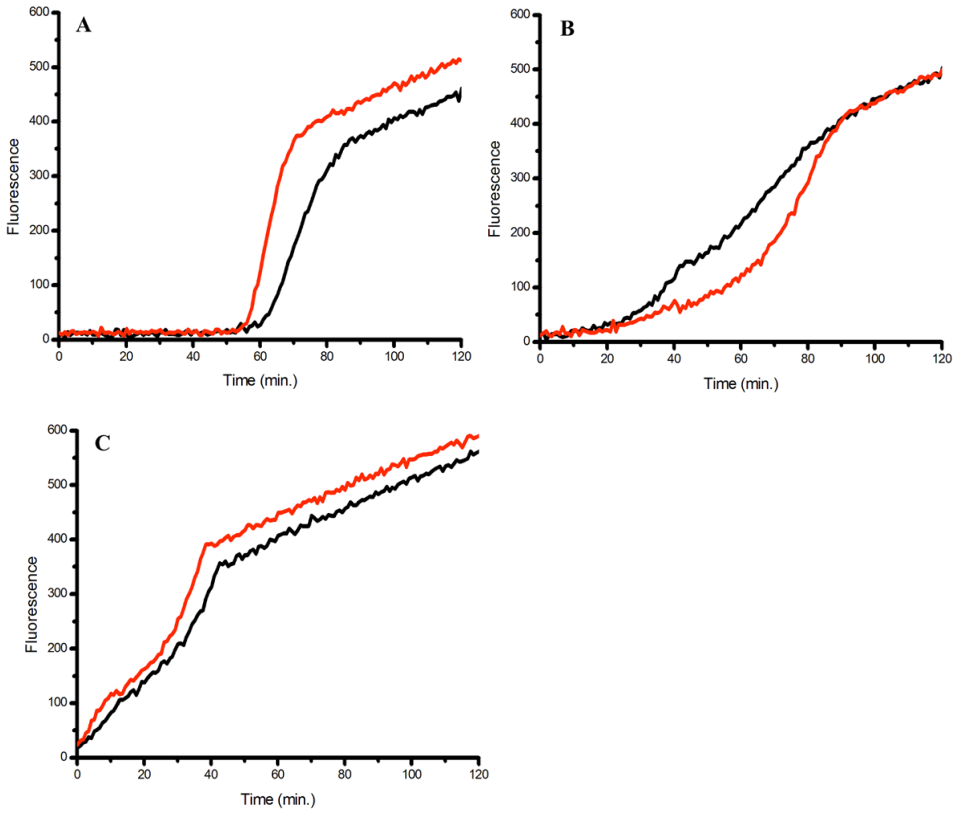

Figure 2.7. Representative fluorescence intensity-time profiles from MeOAMVN-mediated (0.68 mM) oxidations of EggPC liposomes (1 mM) containing 0.15 μM H_2B-PMHC and 4.5 μM of either **12e** (A), α-TOH (B) or no antioxidant (C) with filtration (black) or no filtration (red) through Amicon Ultracentrifuge membrane (10 kDa cutoff). Fluorescence (λ_{ex} = 485 nm; λ_{em} = 520 nm) was recorded every 50 s.

2.3.3 Effect of THNs on Egg Phosphatidylcholine Liposome Oxidation – Competition with the C11-BODIPY$^{581/591}$ Probe

The activity of the compounds was also assayed using the more widely used and commercially available lipid peroxidation indicator C11-BODIPY$^{581/591}$. The 620 nm fluorescence of C11-BODIPY$^{581/591}$ decreases upon peroxyl radical addition to the 1-phenyl-1,3-butadiene sidechain (**Scheme 2.5**).

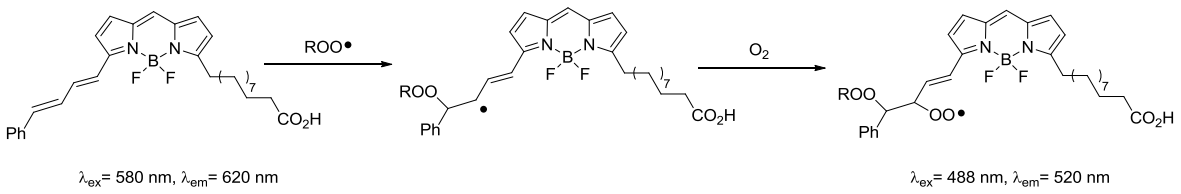

Scheme 2.5. Autoxidation of C11-BODIPY$^{581/591}$.

Results from the autoxidation of EggPC liposomes supplemented with the C11-BODIPY$^{581/591}$ probe and five concentrations of selected RTAs initiated by AAPH are shown in **Figure 2.8**. Representative data from oxidations inhibited by the highly hydrophilic THN **12b** and the highly lipophilic THN **12e** are shown in **Figure 2.8A** and **Figure 2.8B**, respectively. Corresponding data for oxidations inhibited by α-TOH and PMHC are shown in **Figure 2.8C** and **Figure 2.8D** for comparison. Similar to the results obtained with the H_2B-PHMC probe, a clear dose-response relationship is evident for **12e**, α-TOH and PMHC; there is a delay in the time required for the fluorescence of C11-BODIPY$^{581/591}$ to decay that is proportional to the concentration of added antioxidant. This trend is less obvious for the hydrophilic THN **12b**. Similar to the results obtained with the H_2B-PHMC probe, the reaction profile is biphasic; the initial decay reflects the relative rates for the reactions of peroxyl radicals with the different RTAs vs the fluorogenic C11-BODIPY$^{581/591}$ whereas the second phase appears to occur with the same rate regardless of the RTA, and therefore likely takes place after the RTA is consumed. The variability in the initial fluorescence reading between trials and RTAs makes quantitative analysis of these results difficult. Moreover, even qualitiative analysis of the results in the presence of **12e** (e.g. 7.5 μM in **Figure 2.8 B**) is difficult, as the reaction profile appears triphasic; that is, the initial decay of the fluorescence seems to be independent of the concentration of **12e** implying that it does not simply reflect the competition between **12e** and the probe for peroxyl radicals.

Similar trends were observed using the hydrophobic initiator MeOAMVN (**Figure 2.9**). A dose-response relationship is evident for **12e**, α-TOH and PMHC, but not for **12b**. α-TOH and PMHC were able to completely inhibit fluorescence decay at high concentration (7.5 μM in **Figure 2.9C** and **2.9 D**). However, the triphasic behavior of **12e** is even more obvious in the MeOAMVN mediated oxidation in the presence of 6 μM and 7.5 μM **12e** (**Figure 2.9B**); the initial decay of fluorescence is fast and independent of the

concentration of **12e**, followed by complete inhibition of fluorescence decay.

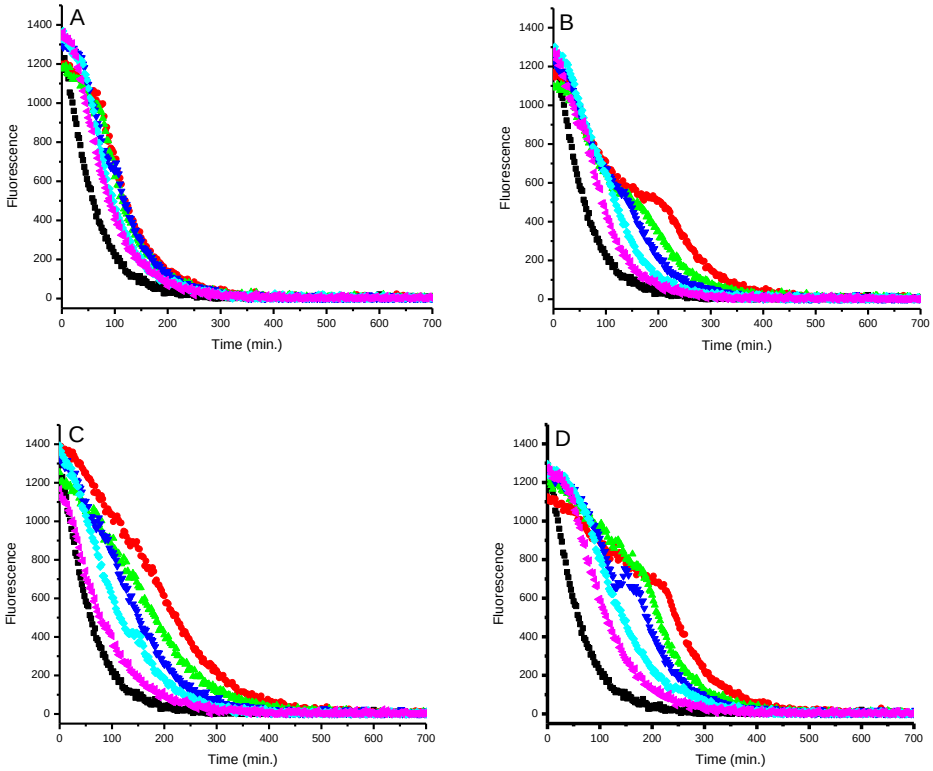

Figure 2.8. Representative fluorescence intensity-time profiles from AAPH-mediated (1.35 mM) oxidations of unilamellar EggPC liposomes (1 mM) containing 0.05 μM C11-BODIPY$^{581/591}$ and increasing concentrations (0 μM - black, 1.5 μM - pink, 3.0 μM - cyan, 4.5μM - blue, 6 μM - green, 7.5 μM - red) of **12b** (A), **12e** (B), α-TOH (C), and PMHC (D). Fluorescence (λ_{ex} = 580 nm; λ_{em} = 620 nm) was recorded every 2 min.

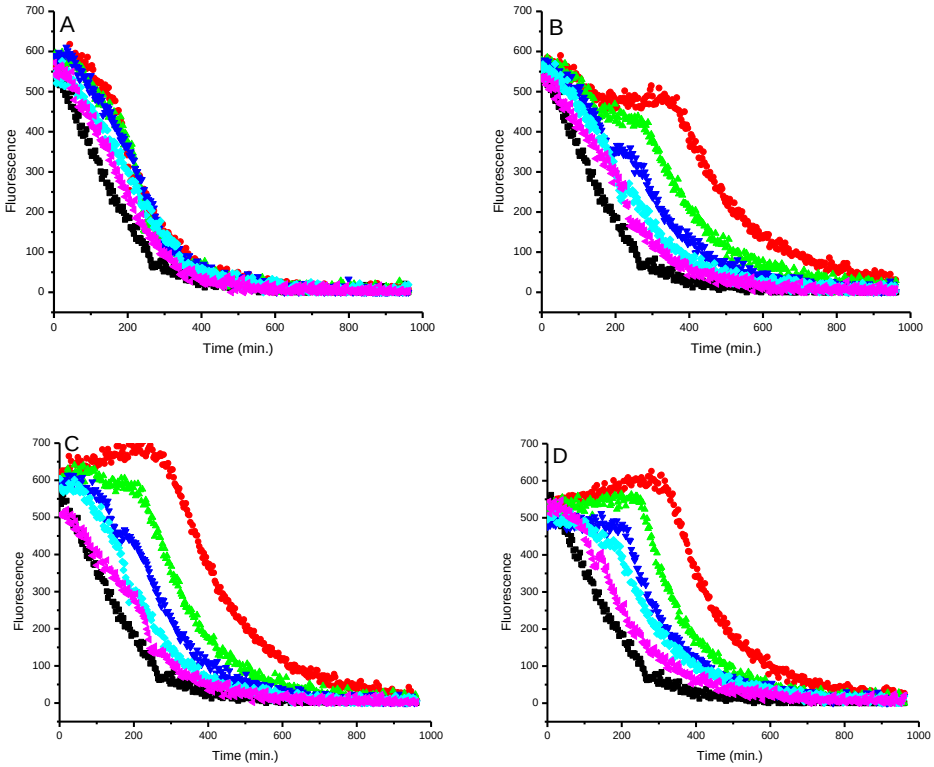

Figure 2.9. Representative fluorescence intensity-time profiles from MeO-AMVN mediated (88.75 μM) oxidations of unilamellar EggPC liposomes (1 mM) containing 0.05 μM C11-BODIPY$^{581/591}$ and increasing concentrations (0 μM - black, 1.5 μM - pink, 3.0 μM - cyan, 4.5μM - blue, 6 μM - green, 7.5 μM - red) of **12b** (A), **12e** (B), α-TOH (C), and PMHC (D). Fluorescence (λ_{ex} = 580 nm; λ_{em} = 620 nm) was recorded every 2 min.

2.3.4 Effect of THNs on PLPC Liposome Oxidations – Determination of Hydroperoxides

In order to corroborate the foregoing results with those from an experiment wherein lipid hydroperoxide formation was also monitored directly, we selected a representative set of RTAs and carried out oxidations of liposomes made exclusively from a polyunsaturated phospholipid 1-palmitoyl-2-linoleyl-sn-glycero-3-phosphocholine (PLPC). Lipid peroxidation was initiated using either the water-soluble initiator 2'-azobis[2-(2-imidazolin-2-yl)propane]dihydrochloride (AIPH) or the lipid-soluble initiator MeOAMVN. PLPC was synthesized according to the previous paper by reacting 1-palmitoyl-2-lyso-sn-glycero-3-phosphocholine and linoleic acid (**Scheme 2.6**).[39]

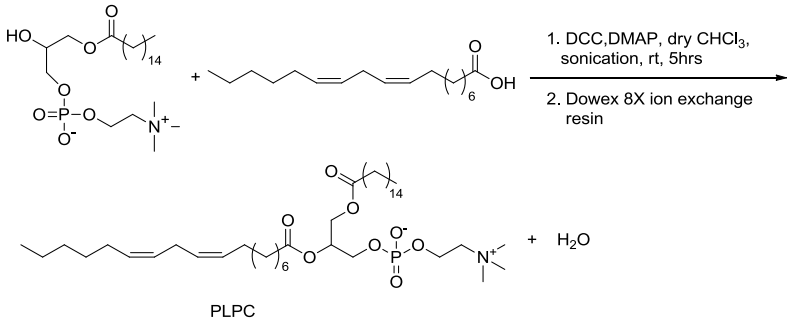

Scheme 2.6. Synthesis of PLPC.

A recently developed coumarin-triarylphosphine conjugate[40] (**Scheme 2.7**) was used to quantify the amount of hydroperoxides formed by using the initial rates for its reaction with lipid hydroperoxides with a rate constant of 9.1 $M^{-1}s^{-1}$ in methanol at 37°C (λ_{ex} = 340 nm; λ_{em} = 425 nm, **Scheme 2.7**).[40] This probe has been shown to provide hydroperoxide concentrations in inhibited hydrocarbon autoxidations that are indistinguishable from those derived using conventional methods such as iodometry or HPLC with UV detection.[40] Initial experiments were carried out in unilamellar PLPC liposomes for closer comparison to the data obtained using the H_2B-PMHC and C11-BODIPY$^{581/591}$ probes.

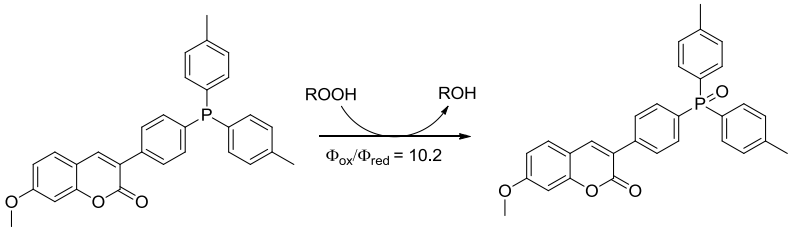

Scheme 2.7. The coumarin-conjugated triarylphosphine probe for hydroperoxide determination.

However, we observed that the more highly oxidizable PLPC lipids were readily autoxidized during the extrusion process leading to spurious results. Hence, we avoided the extrusion process and carried out the autoxidations on multilamellar liposomes instead. However, no inhibition of lipid peroxidation was observed upon addition of the antioxidants to the multilamellar liposome suspensions. We surmised that this was due to poor incorporation of the added antioxidants and poor interlamellar diffusion. In the end, co-evaporation of the PLPC and antioxidants prior to liposome self-assembly afforded the expected inhibited autoxidation profiles, which are shown in **Figure 2.10** and **Figure 2.11** for oxidations initiated with AIPH and MeOAMVN, respectively.

In **Figure 2.10** and **2.11** are shown the uninhibited autoxidation (black), which displays

a linear growth in lipid hydroperoxide concentration with time. In each case, there is an obvious inhibited period, where hydroperoxide formation is completely suppressed, precluding the determination of any relative kinetic information. However, the duration of the inhibited period, which was determined from the intersection of the lines of best fit of the inhibited (green) and uninhibited (red) portions of the data, does depend on the identity of the RTA. In the AIPH-mediated oxidations, the hydrophilic THN **12b** exhibited a shorter inhibited period (48 min), while more lipophilic **12e** exhibited similar inhibited period compared to PMHC and α-TOH (76 min for **12e**, 80 min for PMHC and 69 min for α-TOH, respectively). Similarly, in the MeOAMVN-mediated oxidations, **12b** also exhibited the shorter inhibited period (79 min), while the more lipophilic THN **12e** exhibited similar inhibited period compared to PMHC and α-TOH (98 min for **12e**, 97 min for PMHC and 96 min for α-TOH, respectively).

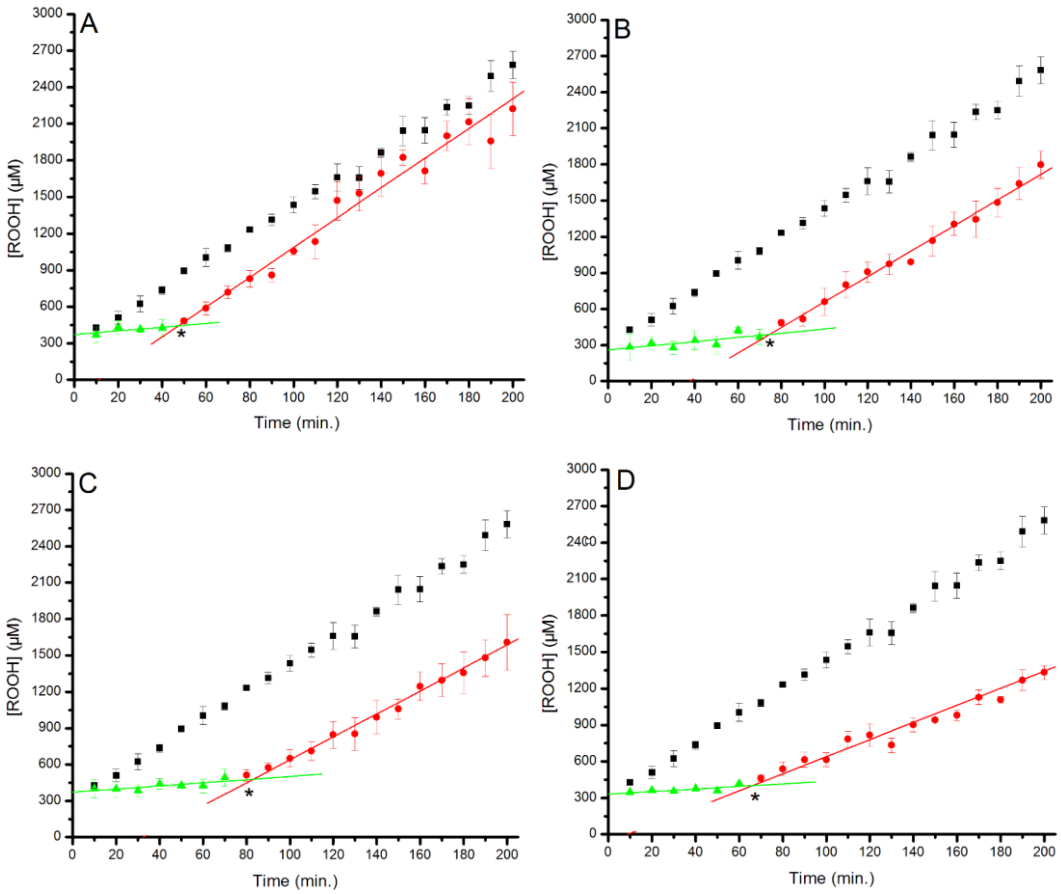

Figure 2.10. Autoxidation of 13.3 mM PLPC multilamellar liposomes at pH 7.4 initiated with 0.36 mM of AIPH, and its inhibition with 3 μM of **12b** (A), **12e** (B), PMHC (C) and α-TOH(D) at 37 °C. The inhibition time, determined from the intersection of the lines of best fit of the inhibited and uninhibited portions of the data are indicated with an asterisk.

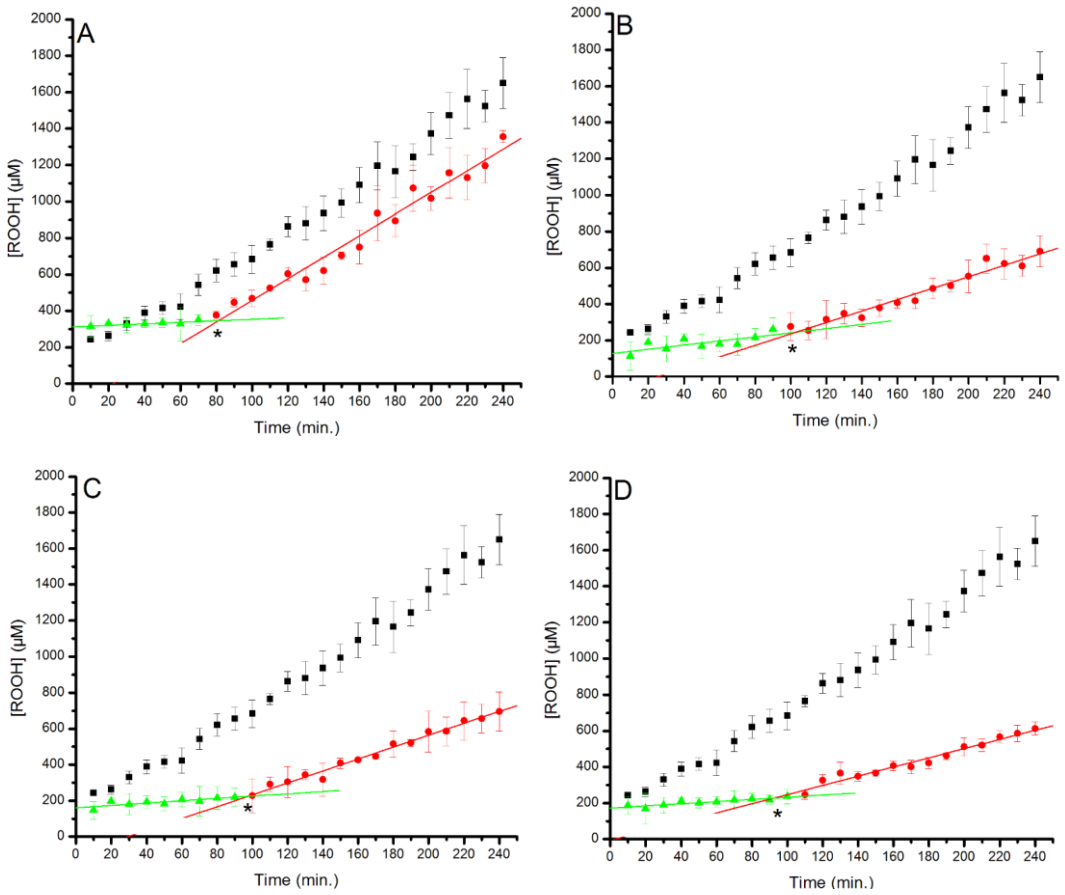

Figure 2.11. Autoxidation of 13.3 mM PLPC multilamellar liposomes at pH 7.4 initiated with 0.15 mM of MeOAMVN, and its inhibition with 5 μM of **12b** (A), **12e** (B), PMHC (C) and α-TOH(D) at 37 °C. The inhibition time, determined from the intersection of the lines of best fit of the inhibited and uninhibited portions of the data are indicated with an asterisk.

2.3.5 Effect of THNs on Egg Phosphatidylcholine Liposome Oxidations – Competition with the H_2B-PMHC Probe as a Function of pH

In an attempt to shed light on the origin of the shorter inhibited periods for the less hydrophobic THNs, additional oxidations were carried out in a buffer of different pH. AAPH- and MeOAMVN-mediated oxidations at pH 5.8 and 7.4 with two different concentrations of either THN **12b** or PMHC (4.5 and 7.5 μM) were carried out in parallel. Representative results are shown in **Figure 2.12** for the AAPH-mediated oxidations with 7.5 μM of either **12b** or PMHC (others are included in **Figure 2.13** and **2.14**). It is important to note that the change in pH had no effect on the rate of H_2B-PMHC oxidation either alone (**Figure 2.15**) or in the presence of PMHC. However, a marked increase in the

inhibition period was clear for **12b** with a decrease in pH. The increase in inhibited period was almost two-fold when the oxidation was carried out with hydrophilic radicals, and 1.5-fold when the oxidation was carried out with hydrophobic radicals (**Figure 2.12-14**).

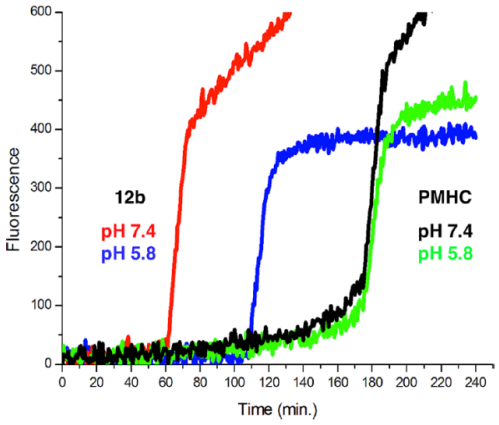

Figure 2.12. Representative fluorescence (at 520 nm) intensity−time profiles from oxidations of EggPC liposomes (1 mM in PBS buffer, pH 7.4) containing 0.15 μM H_2B-PMHC with 2.7 mM AAPH in the presence of 7.5 μM of **12b** (blue, pH 5.8; red, pH 7.4) or PMHC (green, pH 5.8; black, pH 7.4).

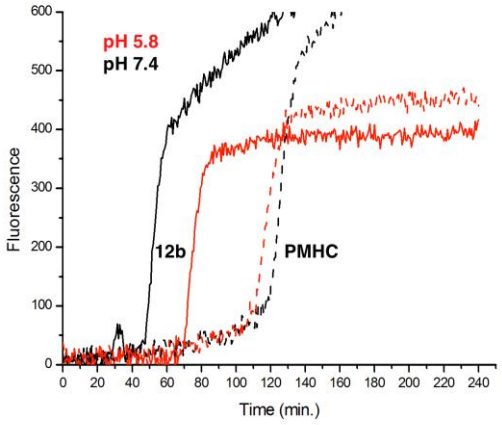

Figure 2.13. Representative fluorescence (at 520 nm) intensity-time profiles from oxidations of EggPC liposomes (1 mM in PBS buffer, pH 7.4) containing 0.15 μM H_2B-PMHC with 2.7 mM AAPH in the presence of 4.5 μM of **12b** (solid lines) or PMHC (dotted lines) at pH 5.8 (red) and 7.4 (black).

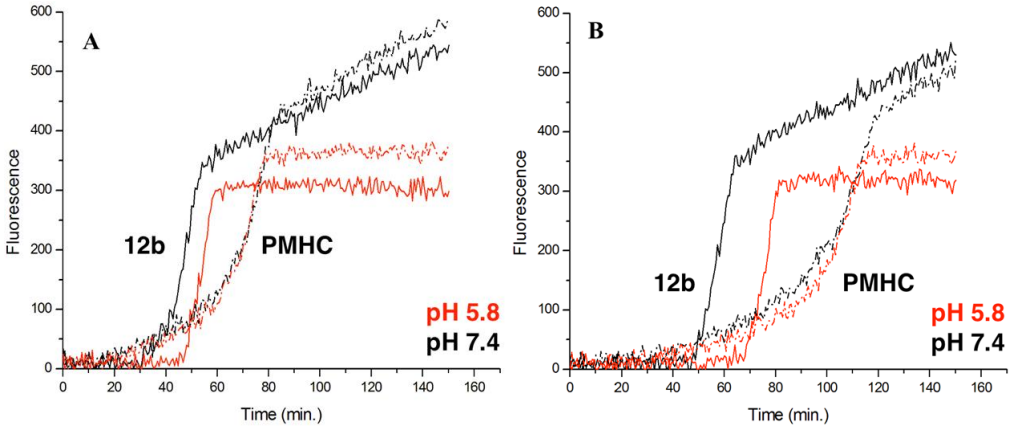

Figure 2.14. Representative fluorescence (at 520 nm) intensity-time profiles from oxidations of EggPC liposomes (1 mM in PBS buffer, pH 7.4) containing 0.15 μM H_2B-PMHC with 0.68 mM MeOAMVN in the presence of either 4.5 μM (A) or 7.5 μM (B) of **12b** (solid lines) or PMHC (dotted lines) at pH 5.8 (red) and 7.4 (black).

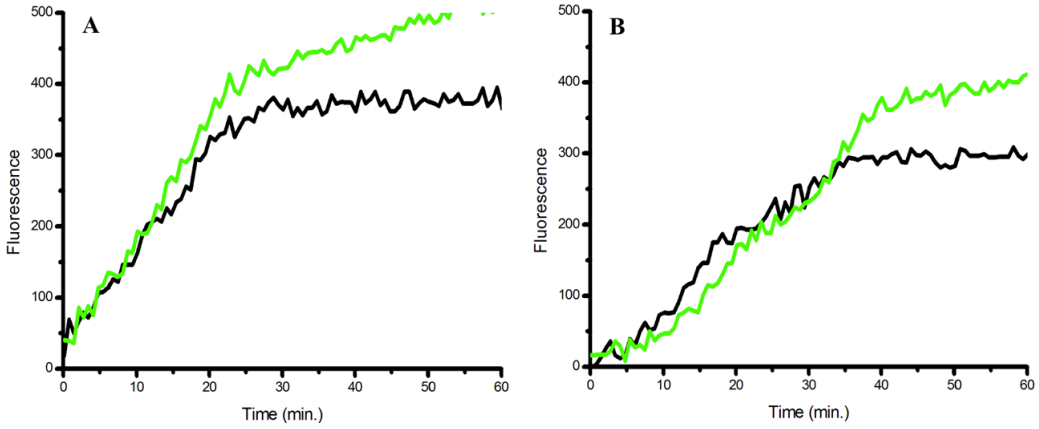

Figure 2.15. Representative fluorescence intensity-time profiles from oxidations of EggPC liposomes (1 mM) containing 0.15 μM H_2B-PMHC with 2.7 mM AAPH-mediated (A) and 0.68 mM MeOAMVN mediated (B) at pH 5.8 (black) and pH 7.4 (green). Fluorescence (λ_{ex} = 485 nm; λ_{em} = 520 nm) was recorded every 50 s.

2.3.6 Peroxyl Radical Trapping by Pyri(mi)dinols in Liposomes

To provide further structure-reactivity data to help understand the origin of the shorter inhibited periods for the less hydrophobic THNs, analogous liposome oxidations inhibited by the less reactive pyrimidinol **1** and pyridinol **2** were carried out with both hydrophilic and lipophilic peroxyl radicals (see **Figure 2.16** and **2.17** for the fluorescence intensity-time traces). The inhibited periods, determined as a function of antioxidant

concentration, are presented in **Figure 2.18**, alongside those for THN **12a** and PMHC for comparison. Clearly, the THN has the shortest inhibition periods, followed by the pyridinol **2**, the pyrimidinol **1**, and finally, PMHC. The inhibited periods follow the trend in the standard potentials ($E°$) of each of the compounds, which were determined from their corresponding cyclic voltammagrams (see **Figure 2.19**), and are given alongside the structures in **Figure 2.18**. Additional experiments were also carried out with lipophilic analogs of pyrimidinol **1** and pyridinol **2** (compounds **13** and **14**, respectively) show significantly longer inhibited periods in corresponding liposome oxidations (**Figure 2.16** and **2.17**).

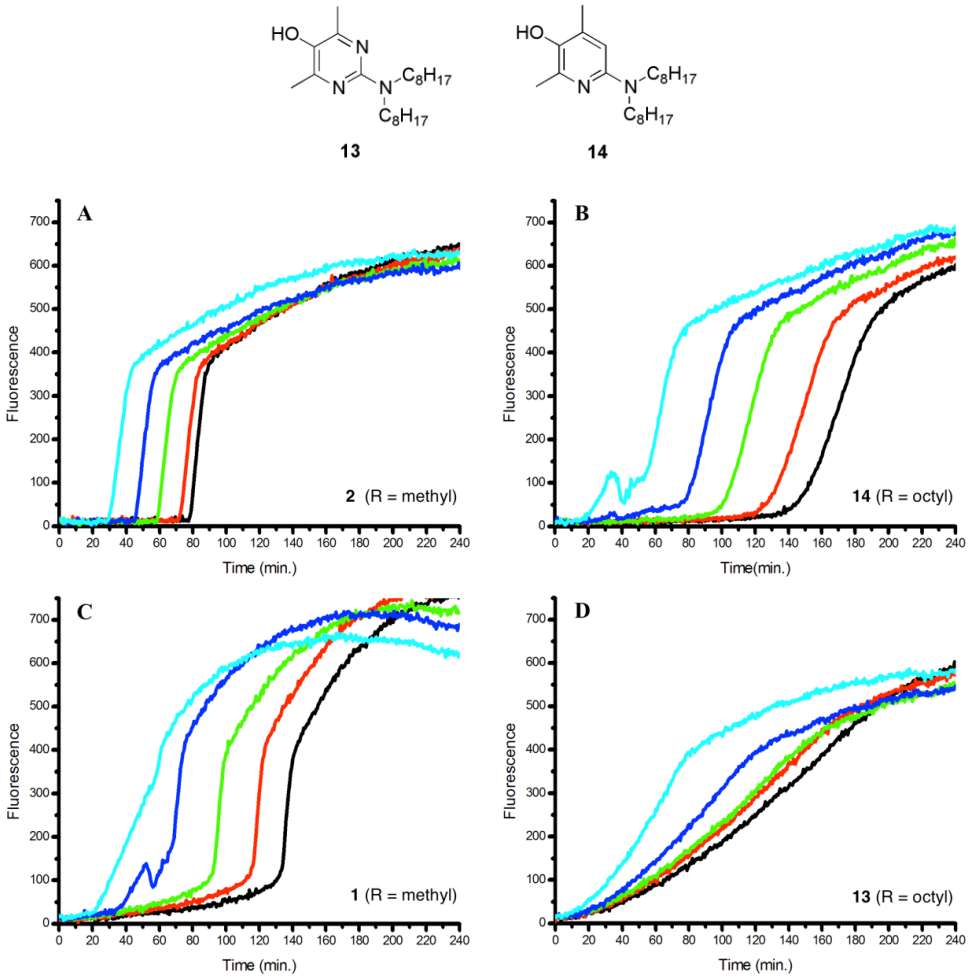

Figure 2.16. Representative fluorescence intensity-time profiles from AAPH-mediated (2.7 mM) oxidations of EggPC liposomes (1 mM) containing 0.15 μM H_2B-PMHC and increasing concentrations (1.5 μM - cyan, 3.0 μM - blue, 4.5 μM - green, 6.0 μM - red and 7.5 μM - black) of **2** (A), **14** (B), **1** (C) and **13** (D). Fluorescence (λ_{ex} = 485 nm; λ_{em} = 520 nm) was recorded every 50 s.

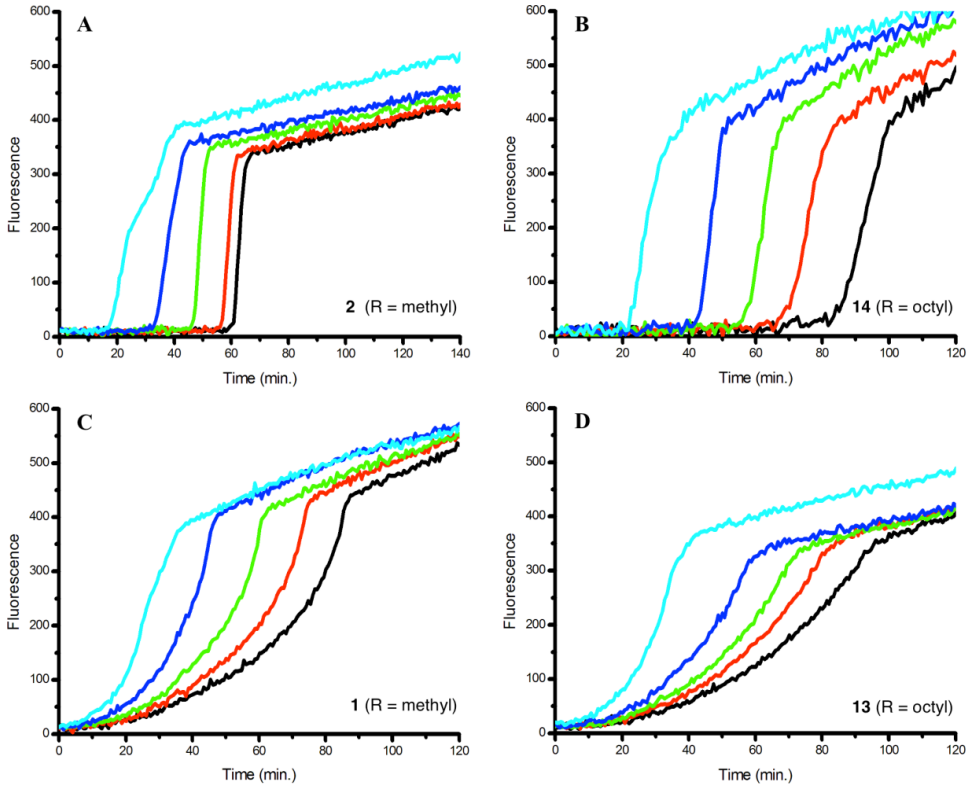

Figure 2.17. Representative fluorescence intensity-time profiles from MeOAMVN-mediated (0.68 mM) oxidations of EggPC liposomes (1 mM) containing 0.15 μM H_2B-PMHC and increasing concentrations (1.5 μM - cyan, 3.0 μM - blue, 4.5 μM - green, 6.0 μM - red and 7.5 μM - black) of **2** (A), **14** (B), **1** (C) and **13** (D). Fluorescence (λ_{ex} = 485 nm; λ_{em} = 520 nm) was recorded every 50 s.

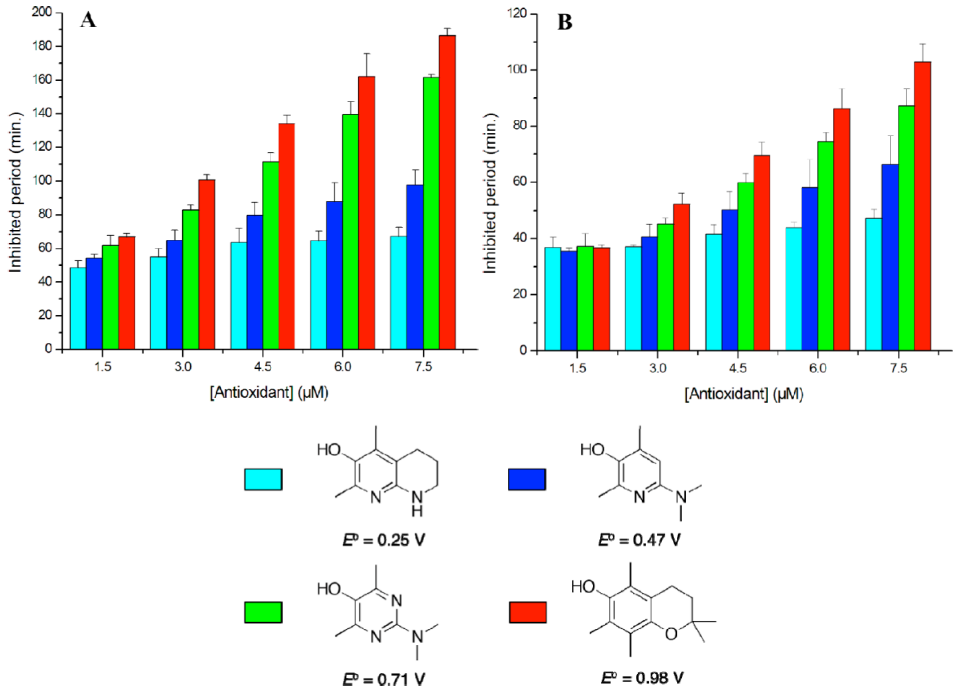

Figure 2.18. Inhibited periods (averages of at least three measurements) observed for pyrimidinol **1**,

pyridinol **2**, THN **12a**, and PMHC as a function of antioxidant concentration when EggPC liposomes were oxidized with hydrophilic (A) or lipophilic (B) peroxyl radicals. Standard potentials (vs NHE at 298K in CH_3CN) are given in the legend.

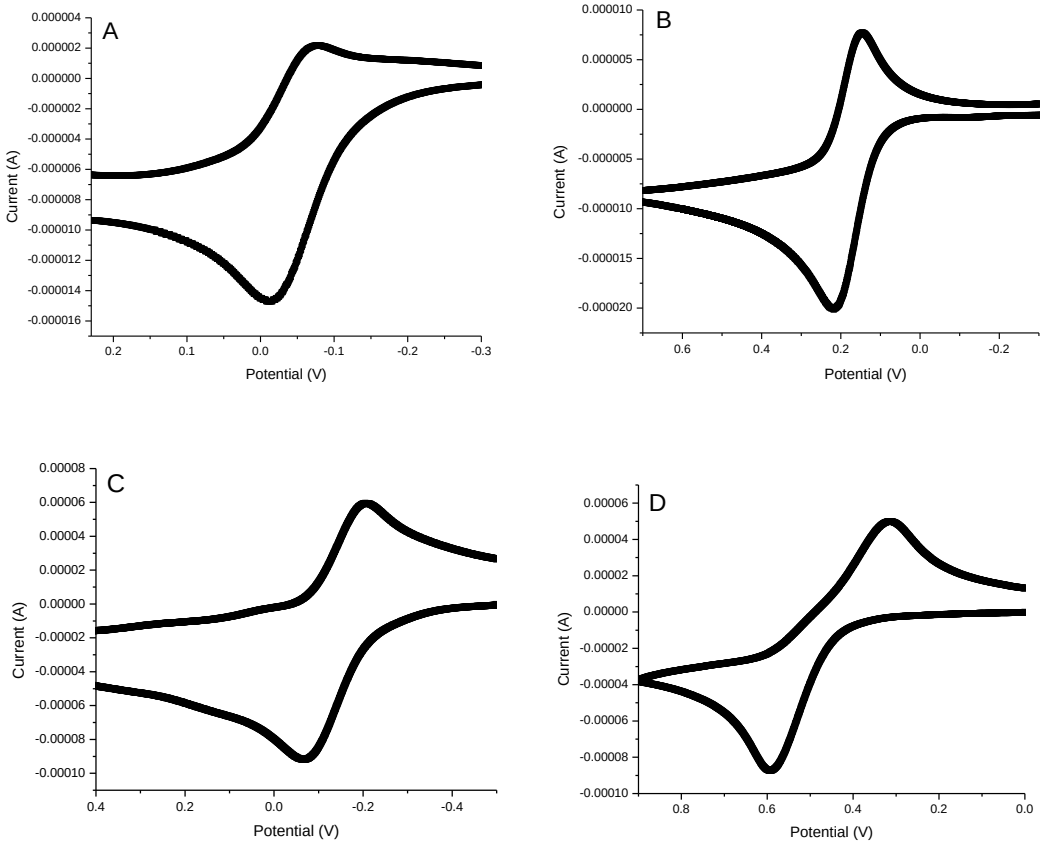

Figure 2.19. Cyclic voltammagram of **1** @100 mV/s ($E_{1/2}$ = E° = 0.71 V vs NHE) (A), **2** @100 mV/s ($E_{1/2}$ = E° = 0.47 V vs NHE) (B), **12a** @ 3 V/s ($E_{1/2}$ = E° = 0.25 V vs NHE) (C), PMHC @500 mV/s ($E_{1/2}$ = E° = 0.98 V vs NHE) (D).

2.3.7 Cooperativity with Water-Soluble Antioxidants

In order to evaluate the interaction of the THNs with water-soluble reductants, oxidations of H_2B-PMHC-loaded liposomes supplemented with a relatively small and constant concentration (1.5 μM) of the most lipophilic (hexadecylated) THN **12e** were carried out in buffered solutions to which were added increasing amounts of water-soluble antioxidants (ascorbate, *N*-acetylcysteine or urate; 1.5-15 μM). Representative results are shown in **Figure 2.20**. The oxidations were carried out using only the lipid-soluble radical initiator MeOAMVN since the water-soluble antioxidants react directly with hydrophilic peroxyl radicals generated from the water-soluble initiator AAPH and therefore do not provide any

information on potential cooperativity between them and the THNs. In addition to these series of experiments, oxidations of liposomes to which no lipophilic antioxidant **12e** was added were carried out in parallel in order to account for *either* the interaction of the water-soluble reductants and lipophilic peroxyl radicals *or* the probe-derived phenoxyl radical (formed from reaction of H_2B-PMHC with lipophilic peroxyl radicals) at the aqueous/lipid interface. The results of these control experiments reveal that neither *N*-acetylcysteine nor urate are particularly effective at inhibiting H_2B-PMHC oxidation under these conditions (see **Figure 2.21**). In contrast, ascorbate is quite effective (**Figure 2.20D**), yielding a clear inhibited period, which increases with increasing concentration of ascorbate. The addition of a small (constant) amount of **12e** to the oxidations carried out in the presence of increasing amounts of either *N*-acetylcysteine and urate (**Figure 2.20B** and **2.20C**) led to a complete suppression in the rate of probe oxidation similar to what is observed when **12e** is used alone in increasing amounts under these conditions. (**Figure 2.4A**). Smaller, but reproducible, differences were observed upon addition of a small (constant) amount of **12e** to the oxidations in the presence of increasing ascorbate concentration, in that the inhibited period was elongated and the rate of inhibited oxidation of the probe was nil when both **12e** and ascorbate were present (compare **Figure 2.20A** to **Figure 2.20D**), as is the case for **12e** alone.

The inhibited periods can be plotted as a function of co-antioxidant concentration in the presence of THN **12e** (see **Figure 2.22**) from which it is clear that the inhibited periods increase linearly with co-antioxidant (i.e. water-soluble reductant) concentration. Furthermore, the magnitudes of the correlations indicate that ascorbate extends the inhibited periods more effectively (7.6 min/μM) than both *N*-acetylcysteine (2.6 min/μM) and urate (2.4 min/μM). All three correlations have smaller magnitudes than that between the inhibited period and concentration of **12e** alone (10.8 min/μM).

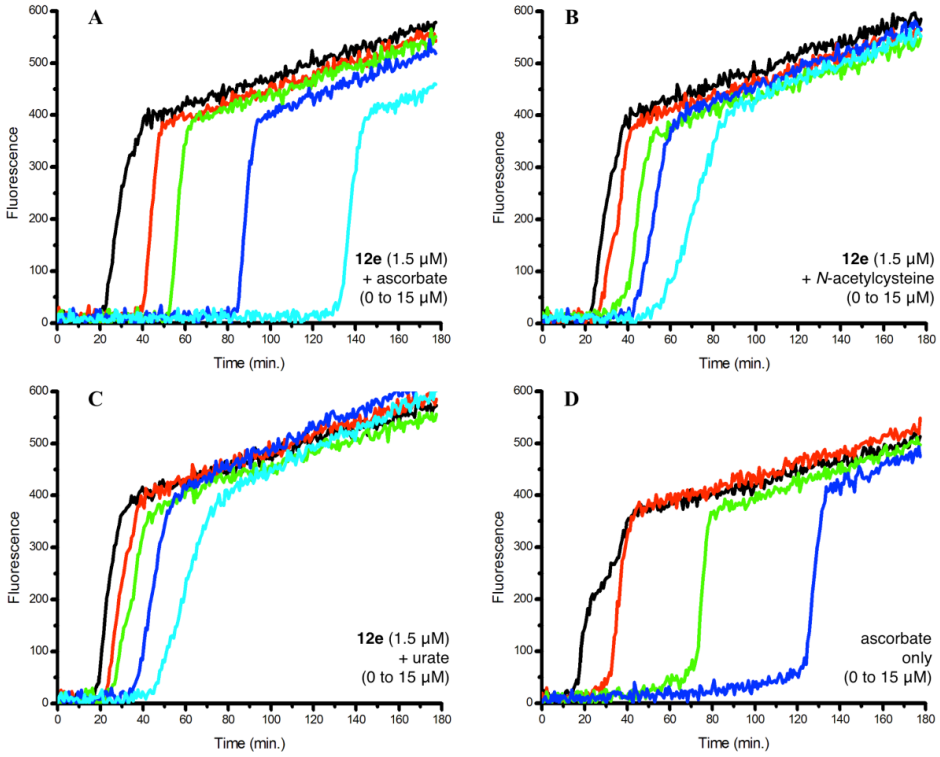

Figure 2.20. Representative fluorescence (at 520 nm) intensity-time profiles from MeOAMVN-mediated (0.68 mM) oxidations of EggPC liposomes (1 mM in PBS buffer, pH 7.4) containing 0.15 μM H_2B-PMHC and 1.5 μM of THN **12e** in the presence of various concentrations (0 μM - black, 1.5 μM - red, 3.0 μM - green, 7.5 μM - blue and 15 μM - cyan) of A) ascorbate, B) N-acetylcysteine and C) urate. Results of corresponding experiments lacking **12e** are shown for ascorbate in D, whereas those for N-acetylcysteine and urate, which show no interaction between them and H_2B-PMHC are included in the Figure 2.21.

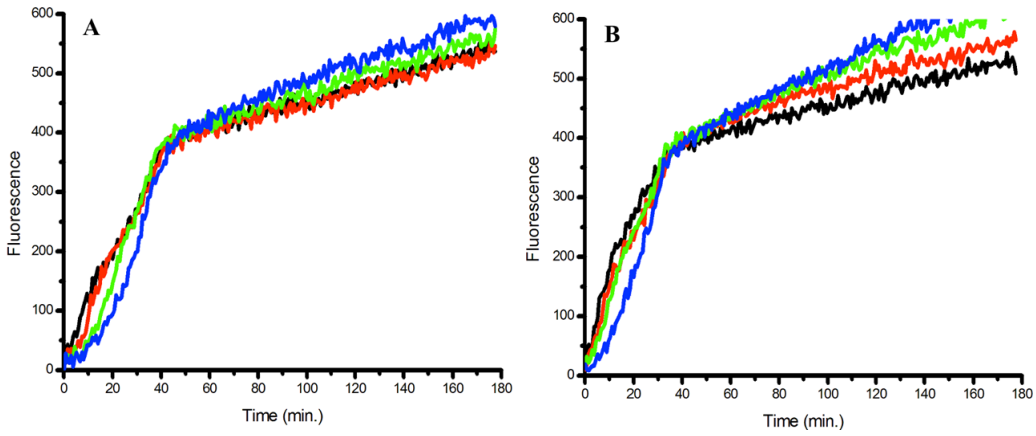

Figure 2.21. Representative fluorescence (at 520 nm) intensity-time profiles from MeOAMVN-mediated (0.68 mM) oxidations of EggPC liposomes (1 mM in PBS buffer, pH 7.4)

containing 0.15 μM H_2B-PMHC and various concentrations (0 μM - black, 1.5 μM - red, 3.0 μM - green, 7.5 μM - blue and 15 μM - cyan) of *N*-acetylcysteine (A) and urate (B).

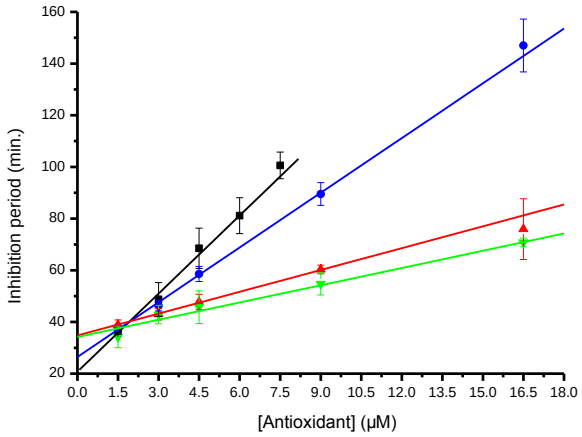

Figure 2.22. Inhibited periods observed when ascorbate (blue), *N*-acetylcysteine (red) or urate (green) were added to EggPC liposome (1 mM in PBS buffer, pH 7.4) suspensions containing 1.5 μM of **12e** and oxidized with 0.68 mM MeOAMVN. Inhibited periods for the addition of increasing amounts of **12e** alone are given in black.

2.3.8 Binding to the Tocopherol Transport Protein

The binding of the THNs **12b-h** to the tocopherol transport protein (TTP) was assayed using the fluorescent tocopherol analogue NBD-Toc (**Figure 2.23** and **2.24**).[35] The fluorescence of NBD-Toc (λ_{ex} = 470 nm; λ_{em} = 535 nm) diminishes upon its displacement from TTP's binding site by competitive ligands due to intramolecular quenching from the benzochromanol moiety. From the fluorescent titration of TTP with NBD-Toc, a dissociation constant (K_d) of 45±15 nM is obtained.[35] By way of comparison, a radioligand binding assay with ^{3}H-α-TOH gives a K_d of 25 nM for α-TOH binding to TTP, which demonstrates the validity of the fluorescence assay. Effective dissociation constants ($K_{d,eff}$) for the various THNs are given in **Table 2.5** as is the value obtained for α-TOH, which is provided for comparison.

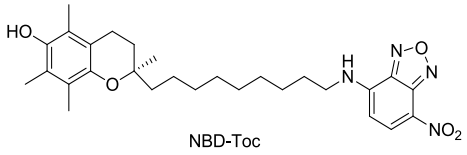

NBD-Toc

Table 2.5. Effective dissociation constants ($K_{d,eff}$) for THN binding to recombinant human tocopherol transport protein measured by competition with fluorogenic NBD-Toc (1 μM) in SET buffer, pH 7.4 at 20°C.

Antioxidant	$K_{d,eff}$ (μM)
12b	*nc*[a]
12c	3.7±0.4
12d	1.3±0.2
12e	1.0±0.2
12f	*nc*[a]
12g	1.0±0.1
12h	0.1±0.1
α-TOH	1.1±0.2

nc[a] = noncompetitive with NBD-Toc.

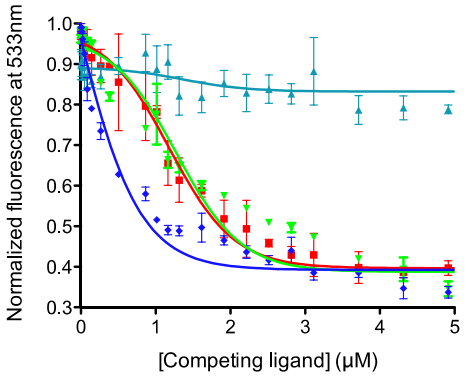

Figure 2.23. Competitive binding curves for the branched chain substituted THNs **12f** (▲), **12g** (▼) and **12h** (◆) obtained using the NBD-Toc probe. The corresponding data obtained alongside for α-TOH is also shown (■).

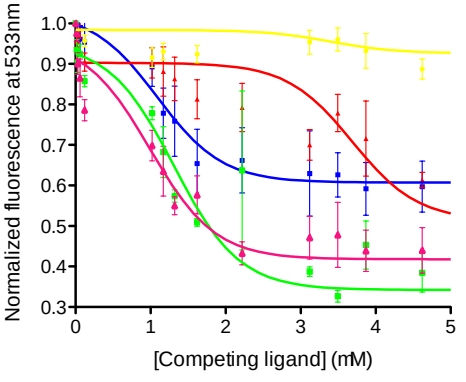

Figure 2.24. Competitive binding curves for the linear chain substituted THNs **12b** (▼), **12c** (▲) **12d**

(▲) and **12e** (■) obtained using the NBD-Toc probe. The corresponding data obtained alongside for α-TOH is also shown (■).

2.4 Discussion

Excitement surrounding the promise of radical-trapping antioxidants for degenerative disease prevention and/or therapy has receded somewhat in recent years due in large part to the disappointing results of clinical trials with α-TOH, ascorbate and β-carotene, among other less-trumpeted natural products.[12,41] However, it must be pointed out that these compounds have well-documented shortcomings as radical-trapping antioxidants. For instance, in the absence of water-soluble reductants (or reduced coenzyme Q_{10}), α-TOH can mediate the oxidation of polyunsaturated lipids in circulating low-density lipoproteins,[42-44] via the thermodynamically-favourable chain transfer reaction:

$$\alpha\text{-TO}\bullet + \text{L-H} \rightarrow \alpha\text{-TOH} + \text{L}\bullet$$

Hence, under some (physiologically-relevant) conditions, α-TOH can mediate the peroxidation of lipids, rather than inhibit the process. Ascorbate, which is water-soluble, does not inhibit lipid peroxidation directly, but can do so only in a cooperative manner with a lipid-soluble radical-trapping antioxidant such as α-TOH.[26] Furthermore, since ascorbate is such a powerful reductant, it can act as a prooxidant through reactions with product hydroperoxides[44] or O_2.[45] The problems with β-carotene are even more significant; it can only trap peroxyl radicals at low partial pressures of O_2, and at normal levels in lipids it acts as a prooxidant.[46] In light of these chemical facts, one has to wonder if it is wise to downplay the idea that radical-trapping antioxidants may have a preventive and/or therapeutic role to play *in vivo* on the basis of the clinical data collected to date.

Given the foregoing, the ideal peroxyl radical-trapping antioxidant must – *at a minimum* – be a readily accessible lipophilic compound that: 1) is more reactive to peroxyl radicals than α-TOH, 2) is less reactive to chain-transfer than α-TOH, 3) maintains these reactivity differences when embedded in lipid bilayers, 4) is at least as regenerable by phase-separated (i.e. water-soluble) reductants as α-TOH, and 5) has similar affinity for the tocopherol transport protein as α-TOH to ensure good bioavailability and limited metabolism in the liver (*vide infra*). If such a compound were available for *in vivo* study, its

use would almost certainly help in shedding definitive light on whether lipid peroxidation has a causal or consequential role in degenerative disease pathogenesis.

Our work to date on the THNs reveals that they meet the first two of these criteria. The rate constant for the reaction of the THNs **3** with peroxyl radicals is ca. 30-fold greater than that measured for α-TOH in homogeneous organic solution,[16] and likely takes place with a negligible E^a since log$k$ = 7.9 is very close to the expected log$A$ = 8 for this reaction. The O-H BDE of the THN **3a** (76.3 kcal/mol)[16] is ca. 2 kcal/mol lower than the O-H BDE of α-TOH (78.3 kcal/mol),[16] implying that the chain transfer reaction of the THN-derived aryloxyl radical and a polyunsaturated lipid can be expected to be thermoneutral at best (the bis-allylic C-H BDE is ca. 76 kcal/mol).[47] Indeed, THNs **3b**[22] and **5**[23] did not appear to mediate lipid peroxidation to a significant extent in our preliminary studies in low-density lipoproteins under conditions where α-TOH did so. While these results have been highly encouraging, we had yet to address the other three criteria identified above. The recent development of the chromanol-BODIPY conjugates as indicators of the antioxidant status (and indirectly the extent of lipid peroxidation) in lipid bilayers,[34-36] in combination with some synthetic advances,[32,33] prompted us to quantify how effective the THNs are at trapping peroxyl radicals in lipid bilayers and understand the role of sidechain-substitution on their reactivity and regenerability in these systems.

Oxidations of H_2B-PMHC-supplemented liposomes with either hydrophilic or lipophilic peroxyl radicals were completely suppressed by the THNs, regardless of the length or branching of the sidechain. This is in contrast to the results obtained with α-TOH and PMHC, which reveal an obvious sidechain-dependence in that the latter is much more efficient at preventing probe oxidation than the former. The relative rate constants can be determined from the initial rates of fluorescence intensity increase and reveal a difference of almost one order of magnitude (a factor of 9) in the case of hydrophilic radicals and ca. 3-fold in the case of lipophilic radicals.[34] The former can be explained simply by the greater access of PMHC to hydrophilic peroxyl radicals owing to the lack of a lipophilic sidechain,[48] while the latter may be approaching the reproducibility of the measurement. Whilst it could be expected that a corresponding difference should exist for the THNs of different sidechain substitution, it could not be observed using the H_2B-PMHC probe,

presumably because it is not sufficiently reactive to compete for peroxyl radicals with any of the THNs. As a result, only an estimate of the lower bounds of the reactivity of the THNs towards peroxyl radicals of 2 orders of magnitude (relative to the probe) can be derived from these experiments. Since the reactivity of the probe towards peroxyl radicals is essentially the same as that of α-TOH,[34] this provides a direct comparison with the reactivity of α-TOH as well. The much greater activity of the THNs is consistent with their much higher inherent chemical reactivities (*vide supra*), which may be further bolstered by the greater polarity of the THN moiety compared to the benzochromanol moiety found in α-TOH and PMHC. While the THN is not expected to be deprotonated (pK_a of the O-H of **2** is 10.1)[49] or protonated (pK_a of pyridinium derived from **2** is less than 6)[49] to any significant extent at pH 7.4, the two nitrogen atoms are expected to increase the polarity and H-bond accepting ability of the THN compared to the benzochromanol.

While liposomal oxidations of the H_2B-PMHC probe did not reveal any differences in the apparent kinetics of the reactions of the THNs of different sidechain substitution with peroxyl radicals, the differences in the inhibited periods are consistent with significantly different reaction stoichiometries. This, again, is in contrast with α-TOH and PMHC, which gave approximately equal inhibited periods for the various concentrations studied, and is fully consistent with previous work which has demonstrated that both of these phenols react with 2 peroxyl radicals to form non-radical products. [9,26] The fact that the inhibited periods of the less lipophilic THNs approach 1/3 of those observed for PMHC and α-TOH (at the upper-end of the concentrations we studied) implies that only a corresponding fraction of peroxyl radicals are trapped by these derivatives.

The results revealing the significant stoichiometric difference between the hydrophilic and hydrophobic THNs are corroborated by results of the experiments carried out with the commercially available lipid peroxidation indicator C11-BODIPY$^{581/591}$. Although in good qualitative agreement on this point, the results obtained using C11-BODIPY$^{581/591}$ are less clear, and display more complex (biphasic) kinetics – implying that the initial rate is unlikely to reflect a simple competition between the probe and the RTA for peroxyl radicals and precluding the extraction of any meaningful quantitative information. These results highlight the attractiveness of the H_2B-PMHC probe for determining relative reactivities of

RTAs in liposomes. The stoichiometric difference of the hydrophobic and hydrophilic THNs were further confirmed by measuring the lipid hydroperoxide production in the autoxidation of liposomes composed exclusively of polyunsaturated lipids and making use of the coumarin-conjugated triarylphosphine probe recently developed in the Pratt lab.

The reduced stoichiometries of the more hydrophilic THNs can be explained by their direct reaction with O_2 (**Eq. 2.2**), which deplete the antioxidant. Since this reaction can be expected to be faster in aqueous solution, which better supports charge development in the electron transfer reaction, it should be more apparent in the reactions of the more hydrophilic compounds which could partition there.[31] Since the oxidation of phenols in aqueous solution is greatly accelerated upon deprotonation of the phenol to yield its corresponding phenoxide,[50] it was anticipated that this pre-equilibrium would be likely to contribute to the rate. Indeed, results of liposomal oxidations carried out at slightly depressed pH (of 5.8), which would shift any unfavourable, but kinetically relevant, pre-equilibrium and slow the rate of competing autoxidation, support the latter mechanism. Indeed, while there was no change in the inhibited periods observed for PMHC (which has both a higher pK_a and is less oxidizable, *vide infra*), there was a significant increase in the inhibited periods observed for the THN (**12b**) at the lower (more acidic) pH.

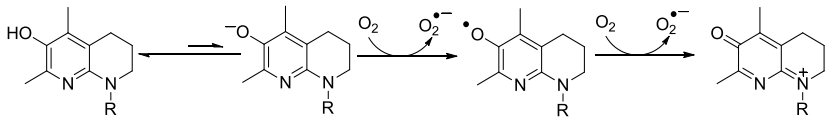

Further evidence for the contribution of THN autoxidation to the shorter inhibited periods observed for the less lipophilic derivatives was provided from the results of liposome oxidations that were carried out on in the presence of pyrimidinol **1** and pyridinol **2**. While these compounds have log*P* values in the same range as THN **12a** and PMHC (logP = 1.13 and 2.50 for compound **1** and **2**, respectively), they have redox potentials which span the range between **12a** ($E°$ = 0.25 V) and PMHC ($E°$ = 0.98 V), at $E°$ = 0.71 and 0.47 V, respectively. Indeed, the inhibited periods for each of the five concentrations we studied follows the trend PMHC > pyrimidinol **1** > pyridinol **2** > THN **12a**, which is clearly consistent with the trends in $E°$; hence, the greater the one-electron oxidizability of the compound, the shorter the inhibited period. Therefore, it would appear that the longer inhibited periods for oxidations inhibited by the more lipophilic compounds arise simply

because their partitioning to the lipid region protects them from autoxidation, which proceeds much faster in the aqueous phase. Consistent with this, additional experiments carried out with lipophilic analogs of pyrimidinol **1** and pyridinol **2** (compounds **13** and **14**, respectively) show significantly longer inhibited periods in corresponding liposome oxidations.

The ability of ascorbate to recycle α-TOH via reduction of the α-tocopheroxyl radical (α-TO•) at the interfacial region of the bilayer is believed to be key to the lipophilic peroxyl radical-trapping antioxidant activity of both compounds *in vivo*. Consistent with this, oxidations of liposome-embedded H_2B-PMHC with lipophilic peroxyl radicals could be inhibited in a dose-dependent manner by added ascorbate, presumably due to scavenging of the probe-derived aryloxyl radical:

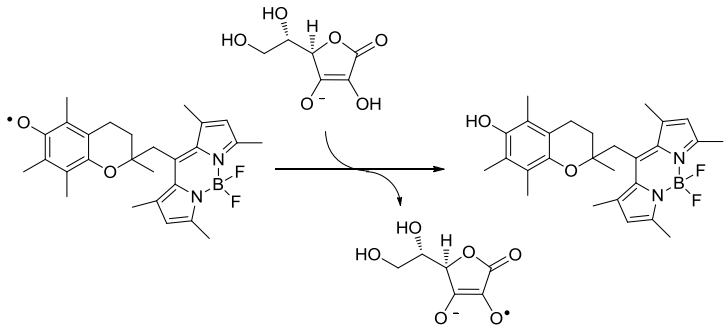

Upon incorporation of a small, constant amount (1.5 μM) of lipid-soluble THN (e.g. the hexadecylated derivative **12e**) into the liposomes, probe oxidation was completely suppressed and the inhibited period could be increased in a dose-dependent manner with increasing ascorbate concentration. In fact, the data were almost indistinguishable from those obtained from oxidations carried out in the presence of increasing concentration of the THN **12e** alone. This provides the first evidence that the THNs can indeed be recycled with ascorbate as is the case for α-TOH, despite the fact that the reaction is less exothermic by 2 kcal/mol (*vide supra*). However, it should be pointed out that the magnitude of the correlation of the inhibited period and co-antioxidant concentration was only ca. 68% of what is observed for the THN alone (*cf.* **Figure 2.22**). Since the THN traps 2 peroxyl radicals, as does PMHC and α-TOH, this means that each molecule of ascorbate is supplying less than 2 reducing equivalents to regenerate the THN (ca. 0.65 × 2 ~1.3). Ingold,[26] Barclay[51] and others have found that while ascorbate can indeed regenerate α-TOH, this process often proceeds without complete fidelity – a fact that has been

explained by the intervention of other competing reactions, such as oxidation of ascorbate or the ascorbyl radical anion by O_2 in competition with either the disproportionation of the ascorbyl radical anion or its reaction with an aryloxyl (such as α-TO•) – thereby effectively wasting reducing equivalents.

When analogous experiments were carried out with small amounts (1.5 μM) of the other THNs (**Figure 2.25**), we found the same proportional increase in inhibited period with added ascorbate. However, unlike liposome oxidations inhibited by the THN alone, the inhibited periods were almost independent of the sidechain length. For example, where the inhibited periods decreased from 155 to 125 to 62 minutes as the sidechain of the THN was shortened from *n*-hexadecyl to *n*-octyl to *n*-butyl in oxidations inhibited by 7.5 μM of **12e**, **12c** and **12b**, respectively, when any of the three were used at 1.5 μM along with 6 μM of ascorbate, the inhibited periods were all within a few minutes of each other (104±5) min. At first glance, it would appear that ascorbate is protecting the more hydrophilic THN from autoxidation. However, this would deplete the ascorbate, which would give rise to shorter inhibited periods. However, careful consideration of the data obtained in the absence of ascorbate reveals that, under these conditions, and at a concentration of 1.5 μM, autoxidation of the hydrophilic THNs is not yet competitive with peroxyl radical-trapping. Therefore, since the maximum concentration of **12b** cannot exceed 1.5 μM throughout the experiment regardless of ascorbate concentration, autoxidation is not a problem, and the dependence of the inhibited period on sidechain length is minimized.

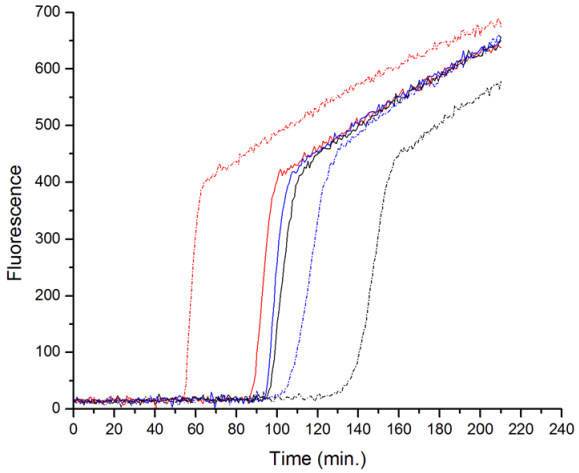

Figure 2.25. Representative fluorescence (at 520 nm) intensity-time profiles from oxidations of EggPC liposomes (1 mM in PBS buffer, pH 7.4) containing 0.15 μM H_2B-PMHC with 0.68 mM MeOAMVN

in the presence of 1.5 μM of **12b** (red), **12c** (blue) or **12e** (black) and 6 μM ascorbate (solid lines). For comparison, dashed lines correspond to 7.5 μM of **12b** (red) **12c** (blue) or **12e** alone.

Analogous experiments were carried out with *N*-acetylcysteine and urate. Glutathione,[52] as well as its biosynthetic precursor cysteine,[53] are very poor co-antioxidants with α-TOH, and urate has not demonstrated any cooperativity at all.[54] Consistent with this, both *N*-acetylcysteine and urate were not effective scavengers of the H_2B-PMHC-derived aryloxyl radical in liposomal oxidations. However, when a small amount of lipophilic THN was incorporated, as was the case with ascorbate, probe oxidation was completely suppressed, and the inhibited periods increased in a dose-dependent fashion with increasing NAC or urate concentration. In this case, the magnitude of the correlation of the length of the inhibited period and co-antioxidant concentration was only ca. 24 and 22% (NAC and urate, respectively) of what is observed with the THN alone, as compared to 68% for ascorbate (*cf.* **Figure 2.22**). This is consistent with the fact that *N*-acetylcysteine and urate are expected to be only one-electron reductants (**Eq. 2.3**), so maximum regeneration would yield a correlation of only half that possible for ascorbate, which is a two-electron reductant. We can only speculate that the increased polarity of the THN is responsible for its greater regenerability by NAC and urate, since the thermodynamics are less favourable than the corresponding reactions for α-TOH (*vide supra*).

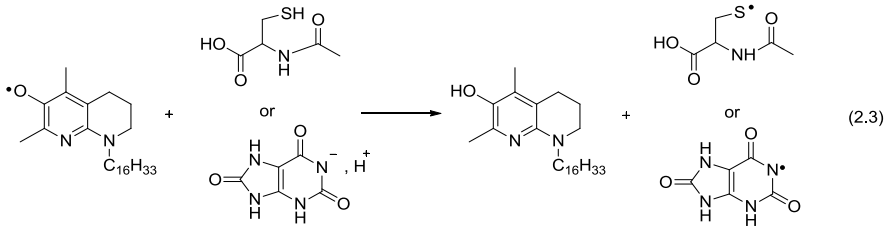

Secretion of α-TOH from hepatic cells for delivery to peripheral tissues and circulating lipoproteins is facilitated by the tocopherol transfer protein (TTP), which displays a clear preference for α-TOH (K_d = 25 nM) over the other tocopherol congeners (β-TOH, γ-TOH and δ-TOH), with relative $1/K_d$'s determined to be 1.0 : 0.20 : 0.09 : 0.04 for α : β : γ : δ, respectively.[29] The three dimensional structure of recombinant human TTP with α-TOH bound has been determined to a resolution of 1.5 Å,[55] and clearly shows that the protein's binding pocket has evolved to bind α-TOH, with close contacts all along the periphery of

the fully methylated phenolic ring (**Figure 2.26**). The phenolic hydroxyl group in α-TOH binds Val182 in TTP through a hydrogen bond.[56] The aromatic methyl groups fit into the pockets formed in TTP.[56] Although it is known that replacement of the 16-carbon phytyl chain in α-TOH with a single carbon carboxylic acid moiety (to give the water-soluble tocopherol analog, Trolox) increases the K_d over 40-fold,[29] there has never been a systematic study of sidechain length on binding to the TTP.

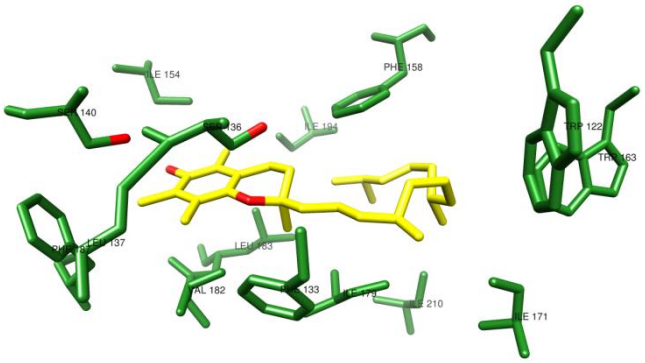

Figure 2.26. Crystallographic positions of amino acid sidechains in hTTP in the vicinity of its ligand, α-TOH.[55]

In previous work, we demonstrated that replacement of the benzochromanol core of α-TOH with the THN core in **5** did not impair its binding to hTTP.[23] In fact, it bound (marginally) better – a result we ascribed to the potential for a strong H-bond between the tertiary amine and Ser136. From the outset of the current study, we were concerned that the attachment of the lipophilic sidechain to the tertiary amine (in lieu of the methyl group in **5**) and the corresponding removal of the quaternary center known to be a key determinant in why synthetic (racemic) and natural (*R*) α-TOH differ significantly in their bioavailabilities,[29] would disrupt binding. However, when we examined the binding of our new compounds to recombinant hTTP we were gratified to learn that these changes did not significantly affect binding. While the butyl- and isopentyl-substituted THNs were non-competitive with the fluorogenic NBD-Toc probe for hTTP's active site (implying very poor affinity) and the octyl-substituted derivative was only a fair competitor, all other derivatives had very similar or better binding than α-TOH itself (*cf.* **Table 2.2**). The most lipophilic linear alkyl-substituted THN (hexadecylated **12e**) had essentially equivalent binding to hTTP as α-TOH ($K_{d,eff}$ = 1.0±0.2 μM *vs.* 1.1±0.2 μM), whereas the most

lipophilic branched alkyl-substituted compound (the farnesol-derived, $C_{15}H_{31}$-substituted **12h**) is roughly 10-fold better ($K_{d,eff}$ = 0.1±0.1 μM). The latter is the best ligand for hTTP reported to date, and presumably demonstrates superior binding to the linear analog because of advantageous interactions between the sidechain methyl substituents and the binding pocket residues evolved to bind the phytyl tail of the tocopherols.[55] Of course, whether superior binding is actually a desirable characteristic of these analogs for *in vivo* studies is unclear, since the ligand must eventually be released to peripheral tissues and circulating lipoproteins in order to serve its purpose as a radical-trapping antioxidant, and the mechanism of ligand release from TTP remains unknown.[57]

While the high affinity of the THN derivatives for the TTP is likely critical to ensure their appropriate systemic distribution in animal models it may also have implications on any potential cytotoxicity of these compounds. The strong binding of α-TOH to TTP is believed to contribute to its slower metabolism compared to the other members of the Vitamin E family, which are rapidly metabolized by hepatic CYP4F2 in order to improve their water-solubility and facilitate excretion.[58-60] Thus, the high affinity of the THNs to TTP may also help protect them from metabolism in the liver.

2.5 Conclusions

Herein we have presented a series of THN analogs of α-TOH with varying sidechain substitution, which were synthesized in an expeditious manner in order to determine how systematic changes in the lipophilicity of these potent antioxidants impact both their radical-trapping activities in lipid bilayers, regenerability by water-soluble reductants and binding to the human tocopherol transport protein (TTP). Liposomes supplemented with the different THNs were oxidized using either hydrophilic or lipophilic peroxyl radicals and consistently revealed a dose-dependent protection of the fluorogenic H_2B-PMHC. In fact, no detectable oxidation of H_2B-PMHC took place in the presence of any of the THNs under conditions where either α-TOH or its truncated analog PMHC were effective only in retarding the rate of oxidation; indicating an unprecedented peroxyl radical-trapping activity in lipid bilayers upwards of two orders of magnitude more effective than α-TOH,

and suggesting that the same difference in reactivity may be expected *in vivo*. While sidechain length and/or branching did not have an effect on the apparent reactivity of the THNs to either hydrophilic or lipophilic peroxyl radicals, it had a dramatic effect on their stoichiometry – with more lipophilic compounds trapping *ca.* 2 peroxyl radicals and more hydrophilic compounds trapping significantly fewer than 1. It is suggested that the more hydrophilic compounds autoxidize in the aqueous phase and that the preferential partitioning of the more lipophilic compounds to the lipid phase protects them from this deleterious pro-oxidative reaction. Studies at more acidic pH as well as with hydrophilic and hydrophobic pairs of less electron-rich pyridinols and related pyrimidinols support this assertion. The cooperativity of the most lipophilic THN with water-soluble reducing agents was also studied in liposomes using H_2B-PMHC. Despite the fact that the THN-derived radical is more stable than the radical derived from α-TOH, it appeared to have better regenerability by each of ascorbate, *N*-acetylcysteine and urate, suggesting that this may be expected *in vivo*. It is suggested that the greater polarity of the THN moiety makes regeneration more efficient than for α-TOH. Binding assays with recombinant human TTP, a key determinant of the bioavailability of the tocopherols, reveal that these compounds have very high affinities. In fact, THNs with sidechains of eight or more carbons were similar (and in one case 10-fold better) ligands for the protein than α-TOH, suggesting that similar bioavailabilities may be expected *in vivo*. We are currently pursuing studies *in vivo*.

2.6 Experimental Section

2.6.1 Synthesis of THNs with Different Sidechain Substitutions 6-19

***Synthesis of Compounds 1-Benzylpiperidin-2-one* (6).** To a solution of NaH (4.84 g, 20.18 mmol, 60 w% suspension in mineral oil) in anhydrous THF (120 mL), was slowly added 2-piperidone (10.00 g, 100.90 mmol) at room temperature to yield the piperidone salt. Benzyl bromide (17.26 g, 100.90 mmol) was added dropwise to the piperidone salt and the reaction was stirred at room temperature for 18 hours until the reaction was found to be complete by TLC. THF was evaporated and the crude product was extracted in Et_2O/H_2O. The ethereal layer was dried over $MgSO_4$ and the solvent was subsequently evaporated to

yield compound **6** as a mixture of product and mineral oil. The product was separated from mineral oil by extracting with hexane (3×50 mL) to afford **6** as a yellow oil (17.16 g, 90 %). ^{1}H NMR (400 MHz; $CDCl_3$): δ 7.28-7.19 (m, 5H), 4.55 (s, 2H), 3.14 (t, J = 5.7 Hz, 2H), 2.41 (t, J = 6.3 Hz, 2H), 1.75-1.70 (m, 4H).^{13}C NMR (100 MHz; $CDCl_3$): δ 169.8, 137.3, 128.5, 128.0, 127.3, 50.0, 47.2, 32.4, 23.2, 21.4. HRMS (EI) calcd for $C_{12}H_{15}NO$ [M] 189.1154, obsd 189.1153.

***1-Benzyl-2,2-dimethoxypiperidine* (7).** A solution of **6** (27.59g, 146.00 mmol) in DCM (50 mL) was dried over anhydrous CaH_2 (+4 mesh) for 48 hours. CaH_2 was then removed and DCM was evaporated by reduced pressure and dimethyl sulfate (18.40g, 146.00 mmol) was added. The solution was refluxed for 2 hours at 90 ^{o}C with sufficient stirring. The resulting ionic liquid was dissolved in 40 mL anhydrous MeOH and slowly transferred to a solution of NaOMe. A solution of NaOMe was prepared by adding MeOH (160 mL) in one portion to Na (3.70 g, 161.00 mmol) under argon atmosphere, using a reflux condenser. The solution of NaOMe was cooled to -20 ^{o}C while being stirred under an argon atmosphere. Following the addition of the ionic liquid, the reaction mixture was slowly warmed to room temperature and allowed to mix at room temperature for 1 hour. The reaction mixture was evaporated under reduced pressure and the product was extracted using dry Et_2O (3×100 mL). The Et_2O extracts were separated from the salts by filtration. The Et_2O extracts were then evaporated under reduced pressure to yield crude lactam acetal of 1-benzyl-2-piperidone containing 25% (by moles) of **6** (quantified by ^{1}H NMR). 4-aminopent-3-en-2-one (6.93 g, 69.99 mmol) and toluene (100 mL) were added to the crude lactam acetal. The reaction mixture was refluxed for 2 hrs. Potassium *tert*-butoxide (12.99 g, 116.00 mmol) and *tert*-butanol (15 mL) were added to the reaction mixture and heated at 90 ˚C for 18 h. The reaction mixture was evaporated under reduced pressure to evaporate toluene and *tert*-butanol. Water (100 mL) was added in to the residual mass. Et_2O (2×100 mL) was used for extraction of the product. The ether extracts were dried over anhydrous $MgSO_4$ and evaporated under reduced pressure to yield the crude product. Pure **7** was separated from the crude product by column chromatography using 2 % EtOAc in hexanes to yield pure **7** as a light yellow oil. (23.91 g, 65 %). ^{1}H NMR (400 MHz; $CDCl_3$): δ 7.30-7.18 (m, 5H), 6.22 (s, 1H), 4.90 (s, 2H), 3.20 (t, J = 5.6 Hz, 2H), 2.58 (t, J = 6.5 Hz,

2H), 2.28 (s, 3H), 2.07 (s, 3H), 1.89-1.83 (m, 2H).^{13}C NMR (100 MHz; $CDCl_3$): δ 155.2, 153.2, 144.5, 139.9, 128.2, 127.9, 126.5, 113.4, 111.7, 51.3, 46.8, 24.11, 23.98, 21.6, 18.8. HRMS (EI) calcd for $C_{17}H_{20}N_2$ [M] 252.1626, obsd 252.1633.

1-Benzyl-6-bromo-5,7-dimethyl-1,2,3,4-tetrahydro-1,8-naphthyridine **(8).** To a solution of compound **7** (4.66 g, 18.49 mmol) in acetonitrile (100 mL), was added trifluoroacetic acid (3.62 g, 20.33 mmol). The reaction mixture was cooled to 0˚C and stirred while N-bromosuccinate (3.62 g, 20.33 mmol) was gradually added over a period of 15 minutes. The reaction vessel was capped with a rubber stopper and the solution was mixed at 0˚C for 18 hours. Acetonitrile was evaporated under reduced pressure to yield a crude material to which Na_2CO_3 (1.00 g in 20 mL of water) was added. The product was extracted with Et_2O/H_2O. The ethereal layer were dried over anhydrous $MgSO_4$ and the solvent was evaporated under reduced pressure to afford the brominated compound **8** as a dark purple oil (6.00 g, 98 %). ^{1}H NMR (300 MHz; $CDCl_3$): δ 7.28-7.18 (m, 5H), 4.86 (s, 2H), 3.21 (t, J = 5.6 Hz, 2H), 2.66 (t, J = 6.5 Hz, 2H), 2.46 (s, 3H), 2.24 (s, 3H), 1.92-1.84 (m, 2H).^{13}C NMR (75 MHz; $CDCl_3$): δ 153.6, 151.8, 143.7, 139.5, 128.3, 127.8, 126.7, 113.9, 110.9, 51.4, 46.6, 25.8, 25.6, 21.7, 19.2. HRMS (EI) calcd for $C_{17}H_{19}N_2Br$ [M] 330.0732, obsd 330.0725.

Benzyl-6-methoxy-5,7-dimethyl-1,2,3,4-tetrahydro-1,8-naphthyridine **(9).** The brominated compound, **8** (6.00 g, 18.20 mmol) was dissolved in 50 mL N,N-dimethylacetamide (DMAc). To this solution was added copper (I) bromide (0.26 g, 1.82 mmol), 2-aminopyridine (0.34 g, 3.64 mmol), and sodium methoxide (35 mL of 25 w% solution, 163.80 mmol). The reaction was refluxed for 24-36 hours, until the reaction was found to be complete by TLC analysis. DMAc was evaporated under reduced pressure to yield a tar-like residual mass. Hexanes (100 mL) was added to the residual mass and the vessel was shaken to dissolve the product from the reaction waste. The hexanes phase was collected by filtration and the solvent was evaporated under reduced pressure to obtain the crude. The crude material was purified by column chromatography using 2% EtOAc in hexanes to afford the pure compound **9** as a transparent yellow oil (4.50 g, 88 %). ^{1}H NMR (400 MHz; $CDCl_3$): δ 7.31-7.21 (m, 5H), 4.87 (s, 2H), 3.64 (s, 3H), 3.19 (t, *J* = 5.6 Hz, 2H), 2.61 (t, *J* = 6.5 Hz, 2H), 2.33 (s, 3H), 2.10 (s, 3H), 1.92-1.89 (m, 2H). ^{13}C NMR (100 MHz;

$CDCl_3$): δ 151.5, 145.6, 144.7, 140.0, 138.0, 128.2, 127.9, 126.5, 113.4, 60.5, 51.4, 46.7, 30.9, 24.8, 21.8, 19.1, 11.8. HRMS (EI) calcd for $C_{18}H_{22}N_2O$ [M] 282.1732, obsd 282.1749.

6-Methoxy-5,7-dimethyl-1,2,3,4-tetrahydro-1,8-naphthyridine **(10).** To a solution of **9** (3.00 g, 10.64 mmol) in 95% ethanol (40 mL) was added ammonium formate (3.35 g, 53.20 mmol) and 5% Pd-C (0.30 g). The reaction mixture was refluxed for 3 hours. Upon completion of the reaction (as monitored by TLC), the ethanolic solution was filtered through celite. The celite was washed with additional ethanol (20 mL). Ethanol was evaporated under reduced pressure to afford a crystalline powder product (1.83 g, 90 %). ^{1}H NMR (300 MHz; $CDCl_3$): δ 4.55 (s, 1H), 3.60 (s, 3H), 3.29 (t, *J* = 4.4 Hz, 2H), 2.57 (t, *J* = 6.5 Hz, 2H), 2.29 (s, 3H), 2.08 (s, 3H), 1.90 (dt, *J* = 11.6, 6.0 Hz, 2H).^{13}C NMR (75 MHz; $CDCl_3$): δ 151.9, 146.2, 145.5, 139.1, 112.9, 60.5, 41.2, 23.8, 21.8, 18.5, 11.5. HRMS (EI) calcd for $C_{11}H_{16}N_2O$ [M] 192.1263, obsd 192.1256.

1-Butyl-6-methoxy-5,7-dimethyl-1,2,3,4-tetrahydro-1,8-naphthyridine **(11b).** Compound **10** (0.50 g, 2.62 mmol) in anhydrous THF (10 mL) was gradually transferred to solution of NaH (0.13 g of 60 w% suspension in mineral oil, 3.25 mmol) in dry THF (10 mL) in an inert atmosphere. Butyl bromide (0.71 g, 0.69 mL, 2.88 mmol) was added and the reaction was refluxed for 18 h under argon. THF was evaporated under reduced pressure and water (10 mL) was added to quench excess hydride. The product was extracted with Et_2O (2×10 mL) and the ethereal layer was dried over anhydrous $MgSO_4$ to yield the crude product. The crude product was purified by column chromatography using 5% EtOAc in hexanes to afford pure product as yellow oil (0.51 g, 78 %). ^{1}H NMR (400 MHz, $CDCl_3$): δ 3.61 (s, 3H), 3.54-3.58 (t, J = 7.4 Hz, 2H), 3.25-3.27 (t, J = 5.6 Hz, 2H), 2.56-2.60 (t, J = 6.8 Hz, 2H), 2.32 (s, 3H), 2.07 (s, 3H), 1.88-1.94 (m, 2H), 1.51-1.58 (m, 2H), 1.29-1.38 (m, 2H), 0.92-0.96 (t, J = 7.4 Hz, 3H). ^{13}C NMR (125 MHz, $CDCl_3$): δ 151.70, 145.55, 144.12, 137.65, 113.30, 60.45, 48.23, 47.35, 29.40, 24.85, 21.93, 20.34, 19.11, 14.09, 11.72. HRMS (EI) calcd for $C_{15}H_{24}N_2O$ [M] 248.1889 , obsd 248.1900.

1-Octyl-6-methoxy-5,7-dimethyl-1,2,3,4-tetrahydro-1,8-naphthyridine **(11c).** The synthesis was completed according to the synthetic procedure used for compound **11b** except 1-bromooctane was used instead of butyl bromide (87 %) ^{1}H NMR (400 MHz,

$CDCl_3$): δ 3.61 (s, 3H), 3.52-3.56 (t, J = 7.4 Hz, 2H), 3.25-3.27 (t, J = 5.4 Hz, 2H), 2.56-2.60 (t, J = 6.4 Hz, 2H), 2.32 (s, 3H), 2.07 (s, 3H), 1.88-1.94 (m, 2H), 1.53-1.56 (m, 2H), 1.27-1.31 (m, 10H), 0.86-0.89 (t, J = 6.8 Hz, 3H). ^{13}C NMR (100 MHz, $CDCl_3$): δ 151.70, 145.57, 137.64, 113.31, 60.45, 48.57, 47.39, 31.92, 29.49, 29.34, 27.14, 27.07, 24.85, 22.70, 21.95, 19.10, 14.14, 11.72. HRMS (EI) calcd for $C_{19}H_{32}N_2O$ [M] 304.2515, obsd 304.2516.

1-Dodecyl-6-methoxy-5,7-dimethyl-1,2,3,4-tetrahydro-1,8-naphthyridine **(11d).** The synthesis was completed according to the synthetic procedure used for compound **11b** except 1-bromododecane was used instead of butyl bromide (70 %) ^{1}H NMR (400 MHz, $CDCl_3$): δ 3.61 (s, 3H), 3.52-3.56 (t, J = 7.4 Hz, 2H), 3.25-3.28 (t, J = 5.8 Hz, 2H), 2.56-2.60 (t, J = 6.4 Hz, 2H), 2.32 (s, 3H), 2.07 (s, 3H), 1.90-1.93 (m, 2H), 1.51-1.58 (m, 2H), 1.26-1.31 (m, 18H), 0.86-0.90 (t, J = 6.8 Hz, 3H). ^{13}C NMR (100 MHz, $CDCl_3$): δ 151.70, 145.58, 144.16, 137.63, 113.30, 60.45, 48.57, 47.39, 31.94, 29.72, 29.69, 29.68, 29.54, 29.37, 27.15, 27.08, 24.86, 22.70, 21.96, 19.12, 14.13, 11.72. HRMS (EI) calcd for $C_{23}H_{40}N_2O$ [M] 360.3141, obsd 360.3169.

1-Hexadecyl-6-methoxy-5,7-dimethyl-1,2,3,4-tetrahydro-1,8-naphthyridine **(11e).** The synthesis was completed according to the synthetic procedure used for compound **11b** except 1-bromohexadecane was used instead of butyl bromide (74 %) ^{1}H NMR (400 MHz, $CDCl_3$): δ 3.63 (s, 3H), 3.53-3.57 (t, J = 7.4 Hz, 2H), 3.26-3.29 (t, J = 5.6 Hz, 2H), 2.58-2.61 (t, J = 6.4 Hz, 2H),2.33 (s, 3H), 2.08 (s, 3H), 1.91-1.96 (m, 2H), 1.54-1.60 (m, 2H), 1.29-1.31 (m, 26H), 0.87-0.91 (t, J = 6.8 Hz, 3H). ^{13}C NMR (100 MHz, $CDCl_3$): δ 151.91, 145.78,. 144.36, 137.84, 113.51, 60.65, 48.78, 47.60, 32.15, 29.93, 29.89, 29.75, 29.59, 27.34, 27.28, 25.06, 22.91, 22.16, 19.33, 14.34, 11.93. HRMS (EI) calcd for $C_{27}H_{48}N_2O$ [M] 416.3767, obsd 416.3756.

1-Isopentyl-6-methoxy-5,7-dimethyl-1,2,3,4-tetrahydro-1,8-naphthyridine **(11f).** The synthesis was completed according to the synthetic procedure used for compound **11b** except 1-bromo-3-methylbutane was used instead of butyl bromide (81 %). ^{1}H NMR (300 MHz; $CDCl_3$): δ 3.62-3.56 (m, 5H), 3.26 (t, *J* = 5.6 Hz, 2H), 2.58 (t, *J* = 6.5 Hz, 2H), 2.32 (s, 3H), 2.07 (s, 3H), 1.93-1.90 (m, 2H), 1.58 (dd, *J* = 13.2, 6.6 Hz, 1H), 1.47-1.40 (m, 2H), 0.94 (d, *J* = 6.5 Hz, 6H). ^{13}C NMR (75 MHz; $CDCl_3$): δ 151.6, 145.5, 144.1, 137.6, 113.3,

60.4, 47.1, 46.7, 36.0, 26.1, 24.8, 22.8, 21.9, 19.1, 11.7. HRMS (EI) calcd for $C_{16}H_{26}N_2O$ [M] 262.2045, obsd 262.2045.

1-(3,7-Dimethyloctyl)-6-methoxy-5,7-dimethyl-1,2,3,4-tetrahydro-1,8-naphthyridine **(11g).** The synthesis was completed according to the synthetic procedure used for compound **11b** except 1-bromo-3,7-dimethyloctane was used instead of butyl bromide (86 %). ^{1}H NMR (300 MHz; $CDCl_3$): δ 3.61-3.55 (m, 5H), 3.26 (t, *J* = 5.6 Hz, 2H), 2.58 (t, *J* = 6.5 Hz, 2H), 2.32 (s, 3H), 2.07 (s, 3H), 1.92 (dt, *J* = 11.6, 6.0 Hz, 2H), 1.59-1.12 (m, 10H), 0.90 (dd, *J* = 21.2, 6.5 Hz, 9H). ^{13}C NMR (75 MHz; $CDCl_3$): δ 151.8, 145.7, 144.3, 137.8, 113.4, 60.6, 47.3, 46.8, 39.5, 37.4, 34.0, 31.0, 28.1, 24.98, 24.84, 22.88, 22.79, 22.1, 20.1, 19.2, 11.9. HRMS (EI) calcd for $C_{21}H_{36}N_2O$ [M] 332.2828, obsd 332.2830.

6-Methoxy-5,7-dimethyl-1-(3,7,11-trimethyldodecyl)-1,2,3,4-tetrahydro-1,8-naphthyridine **(11h).** The synthesis was completed according to the synthetic procedure used for compound **11b** except 1-bromo-3,7,11-trimethyldodecane was used instead of butyl bromide (71 %). ^{1}H NMR (300 MHz; $CDCl_3$): δ 3.60-3.53 (m, 5H), 3.24 (t, *J* = 5.6 Hz, 2H), 2.56 (t, *J* = 6.5 Hz, 2H), 2.30 (s, 3H), 2.05 (s, 3H), 1.90 (dt, *J* = 11.6, 6.0 Hz, 2H), 1.57-1.00 (m, 17H), 0.93-0.81 (m, 12H).^{13}C NMR (75 MHz; $CDCl_3$): δ 151.6, 145.5, 144.1, 137.6, 113.3, 60.4, 47.2, 46.6, 39.4, 37.43, 37.38, 37.33, 33.89, 33.79, 32.8, 30.8, 29.7, 28.0, 24.8, 24.39, 24.36, 22.72, 22.62, 21.9, 19.94, 19.87, 19.75, 19.69, 19.1, 11.7. HRMS (EI) calcd for $C_{26}H_{46}N_2O$ [M] 402.3610, obsd 402.3622.

2,4-Dimethyl-5,6,7,8-tetrahydro-1,8-naphthyridinium-3-ol oxalate **(12a).** To a solution of **10** (0.80 g, 4.17 mmol) in 1,2-dichloroethane (60 mL), was added BBr_3•Me_2S solution (5.20 g, 16.67 mmol, prepared as a solution in 30 mL EDC) under inert atmosphere. The reaction was refluxed for 18 hours under inert atmosphere. The reaction mixture was cooled to 0˚C and subsequently quenched with methanol (30 mL). The solvent was evaporated under reduced pressure, with NaOCl added in the trap to quench evaporated Me_2S. To the resulting material was added aqueous $NaHCO_3$ until the effervescence subsided. The aqueous solution was poured into the separating funnel and the product was extracted with Et_2O (2×20 mL). The crude product was dried over anhydrous $MgSO_4$. To the dried ethereal extracts was added a solution of oxalic acid (0.53 g, 4.17 mmol) in ethanol (25 mL). The solvents were evaporated under reduced pressure to afford the crude

product. The crude product was re-crystallized in acetone at 0˚C to provide the product as a solid (0.37 g, 49 %). ^{1}H NMR (400 MHz; DMSO-d_6): δ 5.50 (s, 1H), 3.35 (s, 3H), 3.13 (dt, J = 7.5, 3.3 Hz, 2H), 2.16 (s, 3H), 2.00 (s, 3H), 1.82-1.76 (m, 2H). ^{13}C NMR (100 MHz; DMSO-d_6): δ 164.3, 14, 6.6, 144.4, 139.9, 130.5, 116.0, 22.7, 19.6, 13.7, 12.7. HRMS (ESI) calcd for $C_{10}H_{14}N_2O$ [M-C_2HO_4] $^{+}$ 179.1184, obsd 179.1181.

8-Butyl-2,4-dimethyl-5,6,7,8-tetrahydro-1,8-naphthyridinium-3-ol oxalate **(12b).** The synthesis was completed according to the synthetic procedure used for compound **12a** except **11b** was used as the starting material (72 %). ^{1}H NMR (400 MHz, DMSO-d_6): δ 3.45-3.49 (t, J = 7.4 Hz, 2H), 3.21-3.24 (t, J = 5.4 Hz, 2H), 2.54-2.57 (t, J = 6.4 Hz, 2H), 2.23 (s, 3H), 2.02 (s, 3H), 1.80-1.87 (m, 2H), 1.44-1.51 (m, 2H), 1.22-1.31 (m, 2H), 0.88-0.92 (t, J = 7.4 Hz, 3H). ^{13}C NMR (100 MHz, DMSO-d_6): δ 162.57, 147.78, 139.90, 137.06, 136.81, 114.49, 48.04, 47.24, 28.45, 23.99, 21.07, 19.56, 17.74, 13.80, 12.14. HRMS (ESI) calcd for [M-C_2HO_4]$^{+}$ 235.1810, obsd 235.1816.

8-Octyl-2,4-dimethyl-5,6,7,8-tetrahydro-1,8-naphthyridinium-3-ol oxalate **(12c).** The synthesis was completed according to the synthetic procedure used for compound 1**2a** except **11c** was used as the starting material (63 %). ^{1}H NMR (400 MHz, DMSO-d_6): δ 3.46-3.49 (t, J = 7.2 Hz, 2H), 3.23-3.26 (t, J = 5.6 Hz, 2H), 2.55-2.58 (t, J = 6.4 Hz, 2H), 2.25 (s, 3H), 2.04 (s, 3H), 1.80-1.86 (m, 2H), 1.47-1.52 (m, 2H), 1.25-1.27 (m, 10H), 0.84-0.87 (t, J = 6.8 Hz, 3H). ^{13}C NMR (100 MHz, DMSO-d_6): δ 162.78, 147.49, 140.03, 138.29, 135.93, 115.16, 48.60, 47.51, 31.29, 28.84, 28.69, 26.34, 26.15, 24.03, 22.12, 20.98, 17.20, 13.97, 12.39. HRMS (ESI) calcd for $C_{18}H_{31}N_2O$ [M-C_2HO_4]$^{+}$ 291.2436, obsd 291.2429.

8-Dodecyl-2,4-dimethyl-5,6,7,8-tetrahydro-1,8-naphthyridinium-3-ol oxalate **(12d).** The synthesis was completed according to the synthetic procedure used for compound **12a** except **11d** was used as the starting material (68 %). ^{1}H NMR (400 MHz, DMSO-d_6): δ 3.46-3.50 (t, J = 7.0 Hz, 2H), 3.24-3.26 (t, J = 6.0 Hz, 2H), 2.56-2.59 (t, J = 6.6 Hz, 2H), 2.26 (s, 3H), 2.04 (s, 3H), 1.80-1.84 (m, 2H),1.46-1.52 (m, 2H), 1.23-1.28 (m, 18H), 0.84-0.87 (t, J = 7.0 Hz, 3H). ^{13}C NMR (100 MHz, CD_3OD): δ 166.64, 147.24, 146.63, 141.85, 131.51, 119.92, 51.07, 50.03, 33.06, 30.75, 30.70, 30.58, 30.45, 27.73, 27.55, 25.11, 23.72, 21.36, 14.44, 13.75, 13.45. HRMS (ESI) calcd for $C_{22}H_{39}N_2O$ [M-C_2HO_4]$^{+}$

347.3062, obsd 347.3058.

***8-Hexadecyl-2,4-dimethyl-5,6,7,8-tetrahydro-1,8-naphthyridinium-3-ol oxalate* (12e).** The synthesis was completed according to the synthetic procedure used for compound **12a** except **11e** was used as the starting material (83 %). ^{1}H NMR (400 MHz, CD_3OD): δ 3.56-3.60 (t, J = 7.8 Hz, 2H), 3.47-3.50 (t, J = 5.6 Hz, 2H), 2.72-2.76 (t, J = 6.6 Hz, 2H), 2.45 (s, 3H), 2.25 (s, 3H), 1.95-2.01 (m, 2H), 1.61-1.68 (m, 2H), 1.28-1.36 (m, 26H), 0.88-0.91 (t, J = 7.0 Hz, 3H). ^{13}C NMR (100 MHz, CD_3OD): δ 166.61, 147.28, 146.73, 141.94, 131.47, 120.02, 51.09, 50.07, 33.09, 30.79, 30.77, 30.76, 30.72, 30.60, 30.49, 27.76, 27.57, 25.13, 23.75, 21.40, 14.46, 13.77, 13.48. HRMS (ESI) calcd for $C_{26}H_{47}N_2O$ $[M\text{-}C_2HO_4]^+$ 403.3688, obsd 403.3683.

***Isopentyl-2,4-dimethyl-5,6,7,8-tetrahydro-1,8-naphthyridinium-3-ol oxalate* (12f).** The synthesis was completed according to the synthetic procedure used for compound **12a** except **11f** was used as the starting material (81 %). ^{1}H NMR (300 MHz; DMSO-*d*$_6$): δ 3.48 (t, *J* = 7.5 Hz, 2H), 3.20 (t, *J* = 5.5 Hz, 2H), 2.53 (t, *J* = 6.4 Hz, 2H), 2.22 (s, 3H), 2.00 (s, 3H), 1.80 (quintet, *J* = 5.7 Hz, 2H), 1.50 (dquintet, *J* = 13.2, 6.6 Hz, 1H), 1.34 (q, *J* = 7.3 Hz, 2H), 0.86 (d, *J* = 6.5 Hz, 6H). ^{13}C NMR (75 MHz; DMSO-d_6): δ 161.9, 148.1, 140.0, 114.3, 47.0, 46.6, 35.2, 25.5, 24.1, 22.6, 21.3, 12.1, 0.1. HRMS (ESI) calcd for $C_{15}H_{25}N_2O$ $[M\text{-}C_2HO_4]^+$ 249.1966, obsd 249.1963.

***8-(3,7-Dimethyloctyl)-2,4-dimethyl-5,6,7,8-tetrahydro-1,8-naphthyridinium-3-ol oxalate* (12g)**. The synthesis was completed according to the synthetic procedure used for compound **12a** except **11g** was used as the starting material (50 %). ^{1}H NMR (300 MHz; DMSO-*d*$_6$): δ 3.53-3.47 (m, 2H), 3.23-3.19 (m, 2H), 2.55 (t, *J* = 6.6 Hz, 2H), 2.22 (s, 3H), 2.01 (s, 3H), 1.83 (dt, *J* = 11.4, 5.9 Hz, 2H), 1.54-0.83 (m, 19H). ^{13}C NMR (100 MHz; DMSO-*d*$_6$): δ 162.4, 147.8, 140.0, 114.9, 47.2, 46.8, 35.2, 25.5, 24.1, 22.6, 21.1, 17.7, 12.3, 0.1. HRMS (ESI) calcd for $C_{20}H_{35}N_2O$ $[M\text{-}C_2HO_4]^+$ 319.2749, obsd 319.2752.

***2,4-Dimethyl-8-(3,7,11-trimethyldodecyl)-5,6,7,8-tetrahydro-1,8-naphthyridinium-3-ol oxalate* (12h).** The synthesis was completed according to the synthetic procedure used for compound **12a** except **11h** was used as the starting material (65 %). ^{1}H NMR (300 MHz; DMSO-*d*$_6$): δ 3.56 (d, *J* = 7.4 Hz, 2H), 3.31 (t, *J* = 4.9 Hz, 2H), 2.60 (t, *J* = 6.2 Hz, 2H), 2.31 (s, 3H), 2.09 (s, 3H), 1.84 (t, *J* = 5.1 Hz, 2H), 1.52-0.80 (m, 29H). ^{13}C NMR (100

MHz; DMSO-d_6): δ 161.7, 146.4, 140.1, 133.1, 47.8, 47.4, 38.8, 36.79, 36.74, 36.69, 36.63, 32.96, 32.86, 32.1, 30.0, 27.4, 24.22, 24.19, 23.76, 23.73, 22.61, 22.52, 19.66, 19.59, 12.9. HRMS (ESI) calcd for $C_{25}H_{45}N_2O$ [M-C_2HO_4]$^+$ 389.3526, obsd 389.3529.

2.6.2 Liposome Oxidations

Liposome Preparation. EggPC was weighed (75 mg) in a dry vial and dissolved in a minimum volume of chloroform. The solvent was then evaporated under argon to yield a thin film on the vial wall. The film was left under vacuum to remove any remaining solvent for 1 hr. The lipid film was then hydrated with 4.83 mL of a 10 mM phosphate buffered-saline (PBS) solution containing 150 mM NaCl (pH 7.4), yielding a 20 mM lipid suspension. The lipid suspension was subjected to 10 freeze-thaw-sonication cycles, where each cycle involved storing the vial with the solution in dry ice for 4 min, thawing at room temperature for 4 min, followed by 4 min of sonication. The lipid suspension was then extruded 20-25 times using a mini extruder equipped with a 100 nm polycarbonate membrane.

Inhibited Oxidations. To individual 21.4 μL aliquots of the 20 mM liposome solution were added increasing amounts (5, 10, 15, 20, and 25 μL, respectively) of a solution the test antioxidant in either aqueous acetonitrile (129 μM) or 5 μL of a solution of H_2B-PMHC in acetonitrile (12.9 μM). Each resultant solution was then diluted to 400 μL with PBS, from which 280 μL of each was loaded into a well of a 96-well microplate. The solution was equilibrated to 37 °C for 5 min, after which 20 μL of a solution of azo compound (40.5 mM in 2,2'-azobis-(2-amidinopropane)monohydrochloride (AAPH) in PBS or 10.1 mM in 2,2'-azobis-(4-methoxy-2,4-dimethylvaleronitrile) (MeO-AMVN) in acetonitrile) was added to each well using the reagent dispenser of the microplate reader. The fluorescence was then monitored for 6 h at 50 s time intervals (λ_{ex} = 485 nm; λ_{em} = 520 nm). The final solutions in each well were 1 mM in lipids, 0.15 μM in H_2B-PMHC, 2.7 mM in AAPH, or 0.68 mM in MeOAMVN and either 1.5, 3.0, 4.5, 6.0, or 7.5 μM in antioxidant. Each liposome contained, on average, 15 fluorophores with an EggPC/fluorophore molar ratio of 6700:1. Under these conditions, no fluorescence self-quenching was expected to occur within the liposome bilayer. Control experiments wherein the liposome solutions were

purified by size exclusion chromatography following supplementation with H_2B-PMHC and lipophilic antioxidants (e.g., α-TOH, 12e) revealed that they are indeed incorporated into the liposomes using the above procedure, as the fluorescence profiles are essentially indistinguishable. Inhibited oxidation of EggPC unilamellar liposome in the presence of C11-BODIPY$^{581/591}$ was done using the same procedure except that different initiator was added. The fluorescence was then monitored at 120 s time intervals (λ_{ex} = 580 nm; λ_{em} = 610 nm). The final solutions in each well were 1 mM in lipids, 0.05 μM in C11-BODIPY$^{581/591}$, 1.35 mM in AAPH or 0.08875 mM in MeOAMVN and 1.5 μM, 3.0 μM, 4.5 μM, 6.0 μM and 7.5 μM in antioxidant, respectively.

Inhibited autoxidation of multilamellar PLPC liposomes. 1-palmitoyl-2-linoleyl-sn-glycero-3-phosphocholine **(**PLPC) was synthesized according to the previous procedure by reacting 1-palmitoyl-2-lyso-sn-glycero-3-phosphocholine (purchased from GordenPharma) and linoleic acid.[39] PLPC was purified by column chromatography using $CHCl_3$: MeOH: H_2O (65:25:4) once again right before using to remove the oxidized product formed upon storage. Stock solution of PLPC in chloroform and stock solution of antioxidant in chloroform were mixed and the solvent was evaporated under Argon to form a thin film in the small vial. PLPC multilamellar liposomes were then formed by adding the pH 7.4 10 mM PBS buffer with 150 mM NaCl, vortexing 3 min, and stirring for 3 min. AIPH (in pH 7.4 PBS buffer) or MeOAMVN (in acetonitrile) was then added to initiate lipid peroxidation. The reaction mixtures were stirred at 37°C in an aluminum heating block. The final concentrations of PLPC, AIPH and MeOAMVN were 13.3 mM, 0.36 mM and 0.15 mM, respectively. Antioxidant concentration is 3 μM for AIPH initiated reaction or 5 μM for MeOAMVN initiated reaction. Every 10 minutes, 10 μL of the reaction mixture was withdrawn from the reaction mixture and transferred to a well of a Nunc 96-well polypropylene microplate and 165 μL of HPLC grade MeOH containing butylated hydroxytoluene (45 mM) was added to destroy the liposome and prevent adventitious oxidation. Using the reagent dispenser of the microplate reader, 25 μL of a solution of fluorescent probe in acetonitrile (160 μM) was added to each well and the initial rate of the reaction was obtained by measuring the fluorescence (λ_{ex} = 340 nm; λ_{em} = 425 nm) for 50 s using a Biotek Synergy H1 Hydrid microplate reader at gain 85. The lipid

hydroperoxide concentration was calculated based on the initial rate of the reaction.[40]

Co-Inhibited Oxidations. To individual 21.4 μL aliquots of the 20 mM liposome solution were added 5 μL of a solution of 12e in aqueous acetonitrile (129 μM) or simply 5 μL of acetonitrile only, followed by 5 μL of a solution of H_2B-PMHC in acetonitrile (12.9 μM). To the aliquots of the two sets of samples were then added increasing amounts (0, 5, 10, 25, and 50 μL) of solutions of water-soluble reducing agent (ascorbate, urate, or N-acetylcysteine) in PBS (129 μM). Each resultant solution was then diluted to 400 μL with PBS, from which 280 μL was loaded into a well of a 96-well microplate. The microplate was equilibrated to 37 °C for 5 min, after which 20 μL of a solution of MeO-AMVN in acetonitrile (10.1 mM) was added to each well using the reagent dispenser of the microplate reader. The fluorescence was then monitored for 6 h at 50 s time intervals (λ_{ex} = 485 nm; λ_{em} = 520 nm). The final solutions in each well were 1 mM in lipids, 0.15 μM in H_2B-PMHC, 0.68 mM in MeOAMVN, 0 or 1.5 μM in 12e μM and either 0, 1.5, 3.0, 7.5, or 15 μM in water-soluble reducing agent.

2.6.3 Voltammetry

Standard potentials for the oxidation of **1**, **2**, **12a**, and PMHC were determined from cyclic voltammagrams measured using a three-electrode cell equipped with a glassy carbon working electrode, a platinum counter electrode, and an Ag/$AgNO_3$ reference electrode. Voltammagrams were obtained at a scan rate of 100 mV/s in dry acetonitrile using Bu4N·PF6 (0.1 M) as electrolyte at 25 °C. All potentials are reported vs the normal hydrogen electrode (NHE) via reference to the ferrocene/ferrocenium couple.

2.6.4 hTTP Binding Affinity by Competition Studies

Recombinant hTTP (0.35 μM) was incubated with 1.0 μM NBD-Toc in SET buffer (250 mM sucrose, 1 mM EDTA, 50 mM Tris, pH 7.4) at approximately 20 °C. After reaching equilibrium, the maximum fluorescence was recorded, and a small aliquot of competitor dissolved in EtOH was added. Approximately 10 min was required for the competitor to reach equilibrium again before the new fluorescence value was recorded. The competitor aliquots were added in increasing concentrations, and the total volume of the

competitor added did not go above 1% of the total volume of the solution in the cuvette. Data were plotted using the Prism software package (Prism GraphPad v4.0) and analyzed using nonlinear regression for a one-site competition model, from which effective dissociation constants, $K_{d,eff}$, were calculated for competing ligands **12c−e**, **12g**, and **12h** as well as α-TOH.

2.7 References

[1] Steinberg, D.; Parthasarathy, S.; Carew, T. E.; Khoo, J. C.; Witztum, J. L. *New Engl. J. Med.* **1989,** *320* (14), 915-924.

[2] Witztum, J. L.; Steinberg, D *J. Clin. Invest.* **1991,** *88* (6), 1785-1792.

[3] Simonian, N. A.; Coyle, J. T. *Annu. Rev. Pharmacol.Toxicol.* **1996,** *36*, 83-106.

[4] Barnham, K. J.; Masters, C. L.; Bush, A. I. *Nat. Rev. Drug Discov.* **2004,** *3* (3), 205-214.

[5] Marnett, L. J. *Carcinogenesis* **2000,** *21* (3), 361-370.

[6] Benz, C. C.; Yau, C. *Nat. Rev. Cancer.* **2008,** *8* (11), 875-879.

[7] Porter, N. A. *Acc. Chem. Res.* **1986,** *19* (9), 262-268.

[8] Pratt, D. A.; Tallman, K. A.; Porter, N. A. *Acc. Chem. Res.* **2011,** *44* (6), 458-467.

[9] Burton , G. W.; Ingold, K. U. *Acc. Chem. Res.* **1986,** *19* (7), 194-201.

[10] Burton, G. W.; Joyce, A.; Ingold, K. U. *Arch. Biochem. Biophys.* **1983,** *221* (1), 281-290.

[11] Valgimigli, L.; Pratt, D. A., Antioxidants in chemistry and biology. *Encyclopedia of radicals in chemistry, biology and materials (Chatgilialoglu, C; Studer, A., eds.)* **2012,** *3*, 1623-1677.

[12] Lonn, M. E.; Dennis, J. M.; Stocker, R. *Free Radic. Biol. Med.* **2012,** *53* (4), 863-884.

[13] Steinhubl, S. R. *Am. J. Cardiol.* **2008,** *101* (10), S14-S19.

[14] Burton, G. W.; Dota, T.; Gabe, E. J.; Hughes, L.; Lee, F. L.; Prasad, L.; Ingold, K. U. *J. Am. Chem. Soc.* **1985,** *107* (24), 7053-7065.

[15] Pratt, D. A.; DiLabio, G. A.; Brigati, G.; Pedulli, G. F.; Valgimigli, L. *J. Am. Chem. Soc.* **2001,** *123* (19), 4625-4626.

[16] Wijtmans, M.; Pratt, D. A.; Valgimigli, L.; DiLabio, G. A.; Pedulli, G. F.; Porter, N. A.

Angew. Chem. Int. Ed. Engl. **2003,** *42* (36), 4370-4373.

[17] Pratt, D. A.; DiLabio, G. A.; Mulder, P.; Ingold, K. U. *Acc. Chem. Res.* **2004,** *37* (5), 334-340.

[18] Valgimigli, L.; Brigati, G.; Pedulli, G. F.; DiLabio, G. A.; Mastragostino, M.; Arbizzani, C.; Pratt, D. A. *Chemistry* **2003,** *9* (20), 4997-5010.

[19] Hanthorn, J. J.; Valgimigli, L.; Pratt, D. A. *J. Am. Chem. Soc.* **2012,** *134* (20), 8306-8309.

[20] Hanthorn, J. J.; Amorati, R.; Valgimigli, L.; Pratt, D. A. *J. Org. Chem.* **2012,** *77* (16), 6895-6907.

[21] Shah, R.; Haidasz, E. A.; Valgimigli, L.; Pratt, D. A. *J. Am. Chem. Soc.* **2015,** *137* (7), 2440-2443.

[22] Kim, H. Y.; Pratt, D. A.; Seal, J. R.; Wijtmans, M.; Porter, N. A. *J. Med. Chem.* **2005,** *48* (22), 6787-6789.

[23] Nam, T. G.; Rector, C. L.; Kim, H. Y.; Sonnen, A. F.; Meyer, R.; Nau, W. M.; Atkinson, J.; Rintoul, J.; Pratt, D. A.; Porter, N. A. *J. Am. Chem. Soc.* **2007,** *129* (33), 10211-10219.

[24] Niki, E.; Noguchi, N. *Acc. Chem. Res.* **2004,** *37* (1), 45-51.

[25] Frei, B. E., L.; Ames, B. N. *Proc. Natl. Acad. Sci. U S A.* **1989,** *86* (16), 6377-6381.

[26] Doba, T.; Burton, G. W.; Ingold, K. U. *Biochim. Biophys. Acta.* **1985,** *835* (2), 298-303.

[27] Traber, M. G.; Burton, G. W.; Ingold, K. U.; Kayden, H. J. *J. Lipid Res.* **1990,** *31* (4), 675-685.

[28] Burton, G. W.; Traber, M. G.; Acuff, R. V.; Walters, D. N.; Kayden, H.; Hughes, L.; Ingold, K. U. *Am. J. Clin. Nutr.* **1998,** *67* (4), 669-684.

[29] Panagabko, C.; Morley, S.; Hernandez, M.; Cassolato, P.; Gordon, H.; Parsons, R.; Manor, D.; Atkinson, J. *Biochemistry* **2003,** *42* (21), 6467-6474.

[30] Wijtmans, M.; Pratt, D. A.; Brinkhorst, J.; Serwa, R.; Valgimigli, L.; Pedulli, G. F.; Porter, N. A. *J. Org. Chem.* **2004,** *69* (26), 9215-9223.

[31] Serwa, R.; Nam, T. G.; Valgimigli, L.; Culbertson, S.; Rector, C. L.; Jeong, B. S.; Pratt, D. A.; Porter, N. A. *Chemistry* **2010,** *16* (47), 14106-14114.

[32] Nara, S. J.; Jha, M.; Brinkhorst, J.; Zemanek, T. J.; Pratt, D. A. *J. Org. Chem.* **2008,** *73* (23), 9326-9333.

[33] Lu, J.; Cai, X.; Hecht, S. M. *Org. Lett.* **2010,** *12* (22), 5189-5191.

[34] Krumova, K.; Friedland, S.; Cosa, G. *J. Am. Chem. Soc.* **2012,** *134* (24), 10102-10113.

[35] Krumova, K.; Oleynik, P.; Karam, P.; Cosa, G. *J. Org. Chem.* **2009,** *74* (10), 3641-3651.

[36] Oleynik, P.; Ishihara, Y.; Cosa, G. *J. Am. Chem. Soc.* **2007,** *129* (7), 1842-1843.

[37] Barclay, L. R. C.; Locke, S. J.; MacNeil, J. M.; VanKessel , J.; Burton, G. W.; Ingold, K. U. *J. Am. Chem. Soc.* **1984,** *106* (8), 2479–2481.

[38] Burton, G. W.; Ingold, K. U. *J. Am. Chem. Soc.* **1981,** *103* (21), 6472-6477.

[39] O'Neil, E. J.; DiVittorio, K. M.; Smith, B. D. *Org. Lett.* **2007,** *9* (2), 199-202.

[40] Hanthorn, J. J.; Haidasz, E.; Gebhardt, P.; Pratt, D. A. *Chem. Commun. (Camb)* **2012,** *48* (81), 10141-10143.

[41] Steinhubl, S. R. *Am. J. Cardiol.* **2008,** *101* (10), S14-S19.

[42] Bowry, V. W.; Ingold, K. U. *Acc. Chem. Res.* **1999,** *32* (1), 27-34.

[43] Bowry, V. W.; Stocker, R. *J. Am. Chem. Soc.* **1993,** *115* (14), 6029-6044.

[44] Ingold, K. U.; Bowry, V. W.; Stocker, R.; Walling, C. *Proc. Natl. Acad. Sci. U S A* **1993,** *90* (1), 45-49.

[45] Lee, S. H.; Oe, T.; Blair, I. A. S*cience* **2001,** *292* (5524), 2083-2086.

[46] Burton, G. W.; Ingold, K. U. *Science* **1984,** *224* (4649), 569-573.

[47] Lucarini, M. P., G. F.; Cipollone, M. *J. Org. Chem.* **1994,** *59* (17), 5063-5070.

[48] Kagan, V. E.; Serbinova, E. A.; Bakalova, R. A.; Stoytchev, T. S.; Erin, A. N.; Prilipko, L. L.; Evstigneeva, R. P. *Biochem. Pharmacol.* **1990,** *40* (11), 2403-2413.

[49] Nam, T. G.; Nara, S. J.; Zagol-Ikapitte, I.; Cooper, T.; Valgimigli, L.; Oates, J. A.; Porter, N. A.; Boutaud, O.; Pratt, D. A. *Org. Biomol. Chem.* **2009,** *7* (24), 5103-5112.

[50] Weinberg, D. R.; Gagliardi, C. J.; Hull, J. F.; Murphy, C. F.; Kent, C. A.; Westlake, B. C.; Paul, A.; Ess, D. H.; McCafferty, D. G.; Meyer, T. J. *Chem. Rev.* **2012,** *112* (7), 4016-4093.

[51] Barclay, L. R. C.; Locke, S. J.; MacNeil, J. M., *Can. J. Chem.* **1983,** *61* (6), 1288-1290.

[52] Barclay, L. R. *J. Biol. Chem.* **1988,** *263* (31), 16138-16142.

[53] Motoyama, T.; Miki, M.; Mino, M.; Takahashi, M.; Niki, E. *Arch. Biochem. Biophys.* **1989,** *270* (2), 655-661.

[54] Niki, E.; Saito, M.; Yoshikawa, Y.; Yamamoto, Y.; Kamiya, Y. *Bull. Chem. Soc. Jpn.* **1986,** *59* (2), 471-477.

[55] Min, K. C.; Kovall, R. A.; Hendrickson, W. A. *Proc. Natl. Acad. Sci. U S A* **2003,** *100* (25), 14713-14718.

[56] Meier, R.; Tomizaki, T.; Schulze-Briese, C.; Baumann, U.; Stocker, A. *J. Mol. Biol.* **2003,** *331* (3), 725-734.

[57] Morley, S.; Cecchini, M.; Zhang, W.; Virgulti, A.; Noy, N.; Atkinson, J.; Manor, D. *J. Biol. Chem.* **2008,** *283* (26), 17797-17804.

[58] Birringer, M.; Drogan, D.; Brigelius-Flohe, R. *Free Radic. Biol. Med.* **2001,** *31* (2), 226-232.

[59] Sontag, T. J.; Parker, R. S. *J. Biol. Chem.* **2002,** *277* (28), 25290-25296.

[60] Sontag, T. J.; Parker, R. S. *J. Lipid Res.* **2007,** *48* (5), 1090-1098.

Chapter 3:

Inhibition of Lipid Peroxidation by Tetrahydronaphthyridinol Analogs of Vitamin E in Mammalian Cell Culture

3.1 Preface

In the previous chapter we introduced the tetrahydronaphthyridinols (THNs), compounds designed to supplant α-tocopherol (α-TOH), the most biologically active form of Vitamin E, as the most potent lipid-soluble radical-trapping antioxidants (RTAs) known. THNs were demonstrated to be ca. 30-fold more reactive in organic solution and in the lipid bilayers of liposomes than α-TOH. Herein we demonstrate that this unprecedented reactivity translates to mammalian cell culture, where lipophilic THNs are found to be significantly better inhibitors of lipid peroxidation than α-TOH (e.g. EC_{50} values as low as 17 nM have been determined for THNs in Tf1a erythroblasts, compared to ca. 1 μM for α-TOH under the same conditions). Consistent with the results in liposomes, hydrophilic THNs are not potent. Interestingly, the lipophilic THNs were found to be similarly potent to ferrostatin-1 (Fer-1) and liproxstatin-1 (Lip-1), compounds recently uncovered in screening efforts to identify potent inhibitors of ferroptosis, a form of cell death associated with the iron-dependent accumulation of lipid hydroperoxides. In fact, the lipophilic THNs performed at least as well as Fer-1 and Lip-1 at subverting ferroptosis induced by glutathione peroxidase-4 (GPx4) inhibition in mouse fibroblasts or glutathione (GSH) depletion by glutamate in mouse hippocampal cells – models of kidney and neurodegenerative disease, respectively. While the THNs likely inhibit lipid peroxidation and subvert ferroptosis by their unrivalled reactivity as RTAs, Fer-1 and Lip-1 appear to operate via a distinct mechanism. Higher potency of THNs compared to α-TOH translated from lipid bilayers to mammalian cells, suggesting that they are excellent candidates for study in animal models of disease in which ferroptosis and/or accumulation of lipid hydroperoxides have been implicated. Inhibition of ferroptosis induced by GPx4 inhibition in mouse fibroblasts, and glutathione depletion by glutamate in mouse hippocampal cells were carried out by our collaborator Dr. Jose Pedro

Friedmann Angeli at the Institute of Developmental Genetics, of the German Research Centre for Environmental Health (Helmholtz Zentrum) in Munich, Germany. Measurements of rate constants at which THN-C15, α-TOH, Lip-1 and Fer-1 trap peroxyl radicals in organic solution and their oxidation potentials were carried out by Omkar Zilka, a graduate student in the Pratt laboratory.

3.2 Introduction

The accumulation of lipid hydroperoxides (LOOH) has long been implicated in cell death and dysfunction, leading to aging, the onset and progression of degenerative disease and cancer.[1,2] Apoptosis, necrosis and autophagy are the established primary mechanisms of cell death, with each being characterized by distinct biochemical events and morphological changes.[3,4] In 2012, a fourth distinct mechanism was identified and named 'ferroptosis' owing to the unique iron-dependent accumulation of LOOH that precedes cell death.[5,6] Interestingly, initial lipid peroxidation in ferroptosis takes place outside of the mitochondria – the principle source of peroxidation-initiating reactive oxygen species in the cell – and outer mitochondrial membrane rupture has been identified as a downstream event in ferroptosis.[7] Two primary mechanisms of ferroptosis induction have been identified. The first comprises GSH depletion agents such as erastin (**Chart 3.1**). Erastin prevents the uptake of cystine (oxidized cysteine), starving glutathione peroxidase (GPx) of its co-substrate for the reduction of hydrogen peroxide to water and lipid hydroperoxides to the corresponding alcohol.[8] The second type of ferroptosis inducing agent, such as (*1S,3R*)-RSL3 (**Chart 3.1**), inhibits GPx4 directly,[8] resulting in increased levels of intracellular lipid hydroperoxides, but has no effect on GSH levels at lethal concentrations.[5,8] Considerable excitement has surrounded this discovery, since the induction of ferroptosis offers a new strategy for killing cancer cells, and a novel pathway to disrupt the regulatory framework that may contribute to the pathogenesis of degenerative diseases in which LOOH accumulation has been implicated, such as cardiovascular, neurodegenerative, kidney and respiratory disease.[1,2,9]

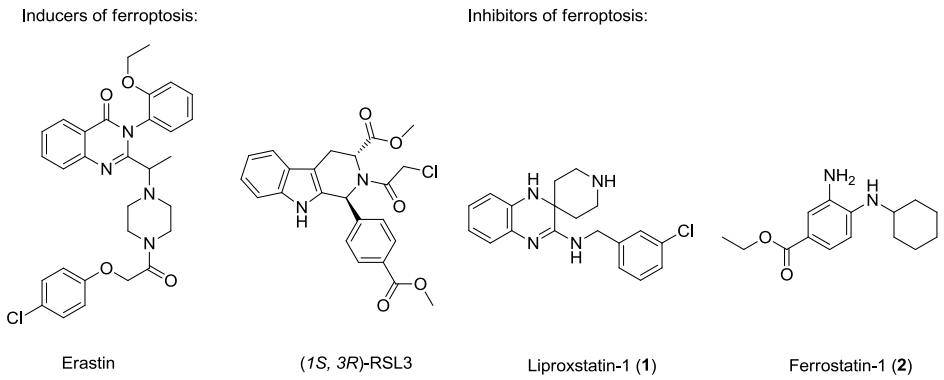

Chart 3.1. Potent inducers and inhibitors of ferroptosis.

The formation of cellular LOOH occurs by two primary mechanisms: a spontaneous peroxyl radical-mediated process called lipid autoxidation (lipid peroxidation) and enzyme-mediated processes catalyzed by lipoxygenases (LOs).[10,11] Accordingly, compounds that inhibit either *or both* of these processes have great potential to inhibit ferroptosis and may provide important leads for preventive and/or therapeutic agents to combat degenerative disease. Very recently, the Stockwell and Conrad groups independently discovered the first potent inhibitors of ferroptosis: ferrostatin-1 (Fer-1)[5] and liproxstatin-1 (Lip-1) (**Chart 3.1**).[7] Fer-1 has been identified as small molecule inhibitor of ferroptosis in cancer cells and glutamate-induced cell death in organotypic rat brain slices.[5] Lip-1, a spiroquinoxalinamine derivative, has been identified as a potent molecule to suppress ferroptosis in cells induced by (*1S, 3R*)-RSL3, in Gpx4 knockout mice, and in a pre-clinical model of ischaemia/reperfusion induced hepatic damage.[7] They were discovered by screening libraries of thousands of compounds in cell assays where ferroptosis was induced by either knocking down expression of the gene encoding the LOOH-detoxifying enzyme Gpx4[7] or inhibition of Gpx4 with RSL3.[5] Both compounds were found to reduce LOOH levels,[7,12] but the mechanism by which they do so is currently unknown.

Since lipid autoxidation is one of the two processes that contribute directly to cellular LOOH production, compounds that have been designed specifically to trap the lipid peroxyl radicals that propagate the radical chain reaction, i.e. radical-trapping antioxidants (RTAs),[13] should be highly potent inhibitors of ferroptosis. Interestingly, both the Conrad

and Stockwell groups found that α-tocopherol (α-TOH, **Chart 3.2**), the most biologically active form of Vitamin E and Nature's premier lipid-soluble radical-trapping antioxidant,[14] is a comparatively poor inhibitor of ferroptosis, with ~10 fold higher EC_{50} than either Fer-1 or Lip-1 in Pf1a mouse fibroblasts.[12] These results suggest that the inhibition of lipid peroxidation may not be at the root of the activity of Fer-1 and Lip-1.

Over the years, we have made use of our comprehensive understanding of the structure-reactivity relationships in RTAs to "optimize" the reactivity of α-TOH.[15-17] The so-called tetrahydronaphthyridinols (THNs) introduced in Chapter 2 (**Chart 3.2**) are ca. 30-fold more reactive than α-TOH in organic solution[15-18] and in lipid bilayer models of the cell membrane (liposomes).[19] Accordingly, if preventing LOOH accumulation by autoxidation of lipid is important in subverting ferroptosis, it follows that the THNs should be highly potent inhibitors. However, to date these derivatives have not been systematically studied in cell culture.

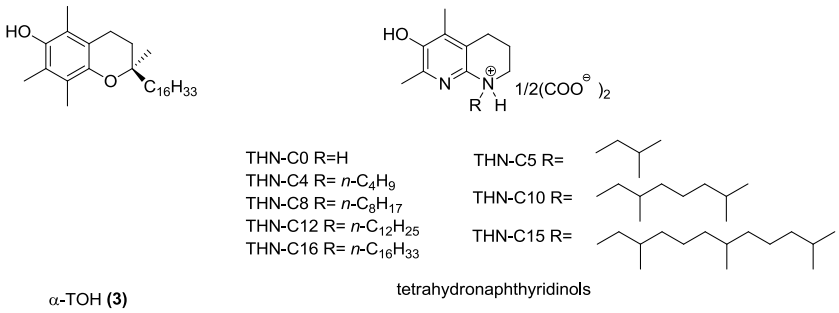

Chart 3.2. α-TOH and tetrahydronaphthyridinol (THN) radical-trapping antioxidants.

Herein, we report on the ability of a series of THNs to inhibit lipid peroxidation in mammalian cells. Our studies reveal that their superior reactivity compared to α-TOH translates from organic solution and liposomes to mammalian cells. Moreover, we demonstrate that these compounds are at least as potent at subverting ferroptosis in mouse fibroblasts and hippocampal cells as each of Lip-1 and Fer-1, and with a preferable toxicity profile compared to Lip-1 in HepG2 cells. Lastly, we provide the first mechanistic studies of Lip-1 and Fer-1 activity, and demonstrate that they are unlikely to be kinetically-competent RTAs, suggesting that their mechanism of action in slowing LOOH accumulation and subverting ferroptosis is distinct from that of the lipophilic THNs.

3.3 Results

3.3.1 Inhibition of Lipid Peroxidation in Human Erythroblasts and Embryonic Kidney Cells

To examine whether superior potency of THNs compared to α-TOH translates from liposome models further to human cellular models, the THNs synthesized in **Chapter 2** (**Chart 3.2**) were first assayed for their ability to prevent lipid peroxidation in human Tf1a erythroblasts. C11-BODIPY$^{581/591}$ (**Scheme 3.1,** introduced in **Chapter 2**) was used to probe the extent of lipid peroxidation[20] after incubation of the cells with various concentrations of THNs for either 5 or 22 hours. The probe is oxidized competitively with unsaturated lipids in the cell; its (green) fluorescence (λ_{em} = 520 nm; λ_{ex} = 488 nm) is increased upon reaction with peroxyl radicals.

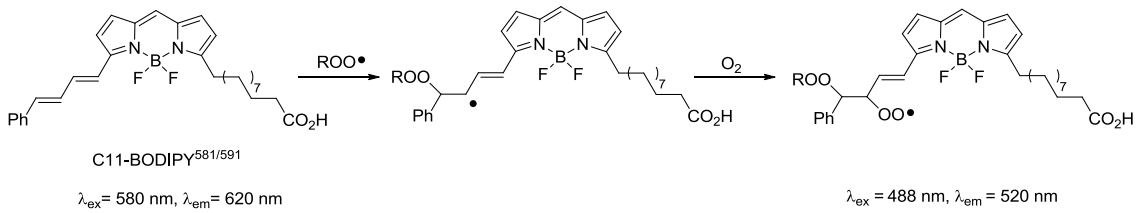

Scheme 3.1. The reaction of C11-BODIPY$^{581/591}$ towards peroxyl radicals.

Lipid peroxidation was induced by glutathione depletion with diethylmaleate (DEM) for 2 hours, after which cells were subjected to flow cytometry to monitor the change in fluorescence intensity of the C11-BODIPY$^{581/591}$ (5×10^5 cells/ mL; λ_{ex} = 488 nm, λ_{em} = 525±25 nm; 10,000 events). Cells from untreated cultures were used as negative control and cells from cultures treated with DEM but no antioxidants were used as positive control. Representative histograms are shown in **Figure 3.1**. Lipid peroxidation was calculated by comparing the mean geometric fluorescence intensity from the histograms for a given antioxidant concentration relative to the negative and positive controls. The corresponding dose response curves for each antioxidant were thus obtained and are shown in **Figure 3.2** and **Figure 3.3**. All experiments were run in triplicate (at minimum).

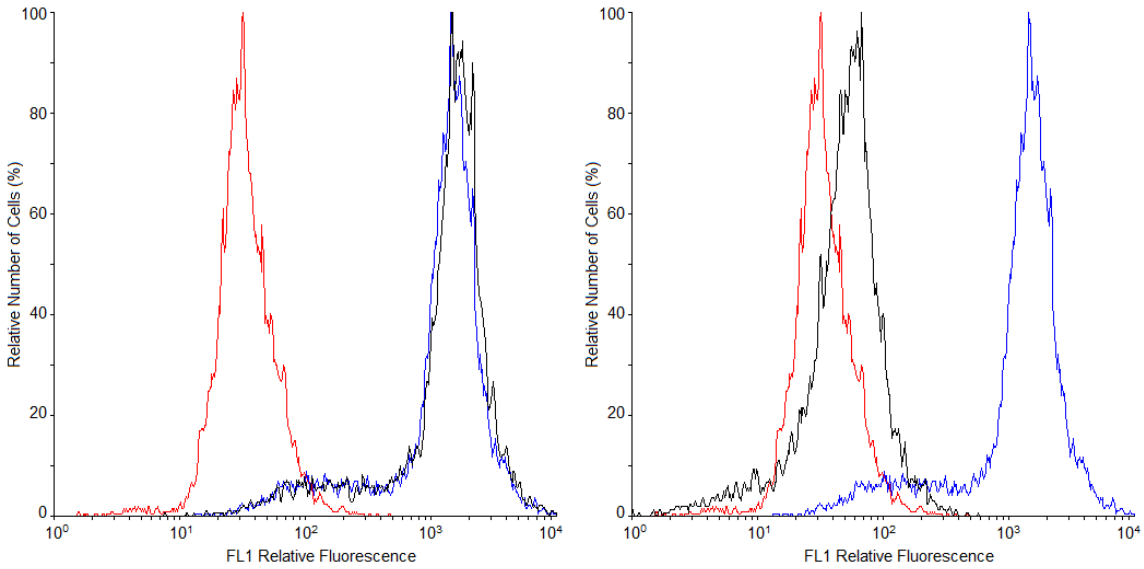

Figure 3.1. Representative histograms obtained from flow cytometry (5×10^5 cells/ mL; λ_{ex} = 488 nm, λ_{em} = 525±25 nm; 10,000 events) following induction of oxidative stress with diethylmaleate (DEM, 9 mM) in Tf1a cells grown in media containing either 0.005 μM or 0.1 μM THN-C15 (black) for 5 hours at 37 °C. Cells were incubated with the lipid peroxidation reporter C11-BODIPY$^{581/591}$ (1 μM) for 30 minutes prior to DEM treatment. Cells not treated with DEM were used as negative control (red). Cells not treated with antioxidants were used as positive control (blue).

Representative data are presented in **Figure 3.2** alongside corresponding data for α-TOH, its truncated analog PMC and each of Fer-1 and Lip-1 (see **Figure 3.3** for all the details**)**. The potency of the THNs varied considerably as a function of the sidechain, with EC_{50} values ranging from greater than 5 μM to as little as 17 nM; the more lipophilic compounds exhibiting significantly higher potency than the more hydrophilic compounds (also in embryonic kidney HEK-293 cells, see **Figure 3.4**) and reaching a maximum for the C12 and C15 sidechains, which are essentially the same length (the C15 sidechain has three tertiary centres, *cf.* **Chart 3.2**).

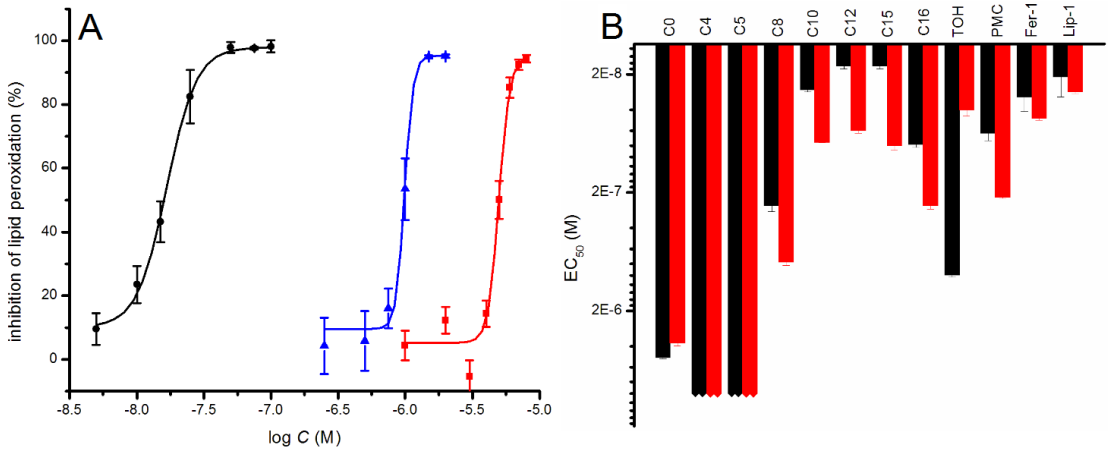

Figure 3.2. (A) Representative dose-response curves obtained from flow cytometry (0.5×10^6 cells/mL; λ_{ex} = 488 nm, λ_{em} = 525±25 nm; 10,000 events) after 5 hours incubation with compounds following induction of oxidative stress with DEM (9 mM) in Tf1a erythroblasts grown in RPMI-1640 media containing THN-C15 (EC_{50} = 0.017±0.001 μM) (black), α-TOH (EC_{50} = 1.0±0.1 μM) (blue) and THN-C0 (EC_{50} = 5.0±0.1 μM) (red); (B) Potency of all THNs as well as PMC, Fer-1 and Lip-1 after 5 hrs incubation period (black) or 22 hrs incubation period (red).

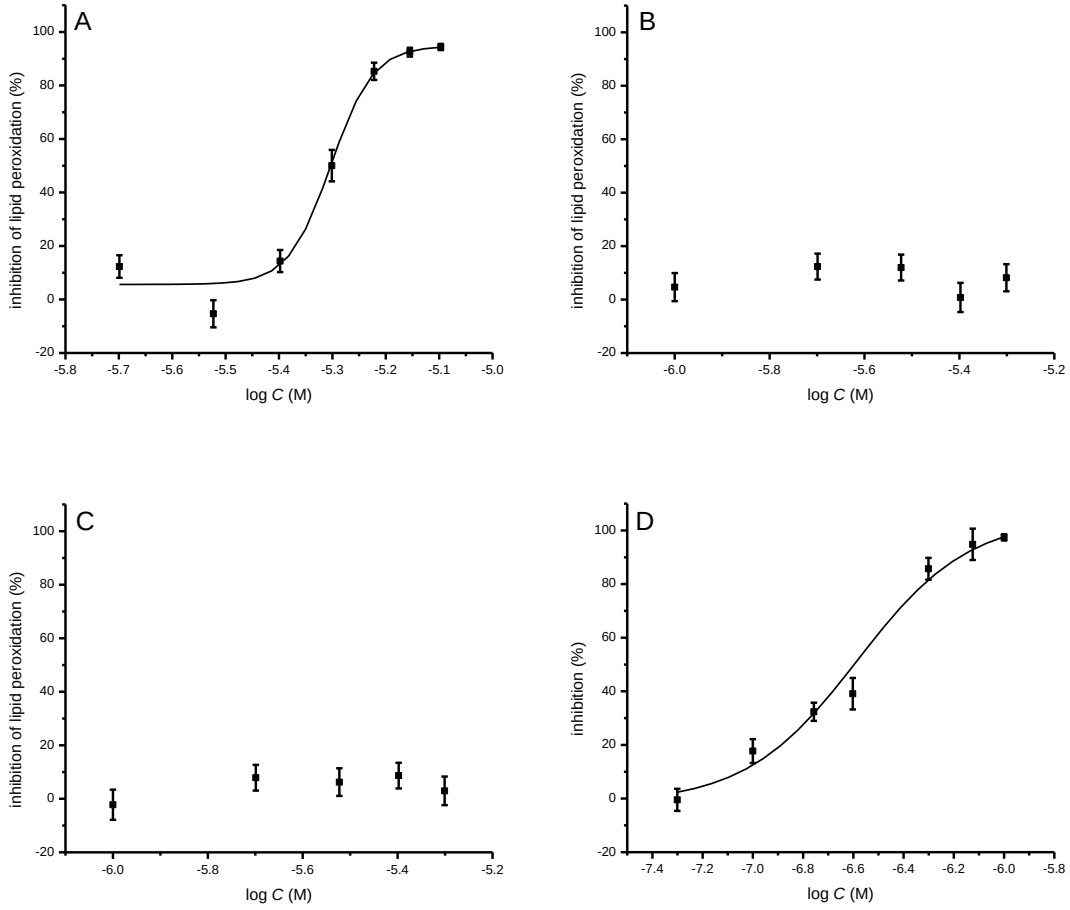

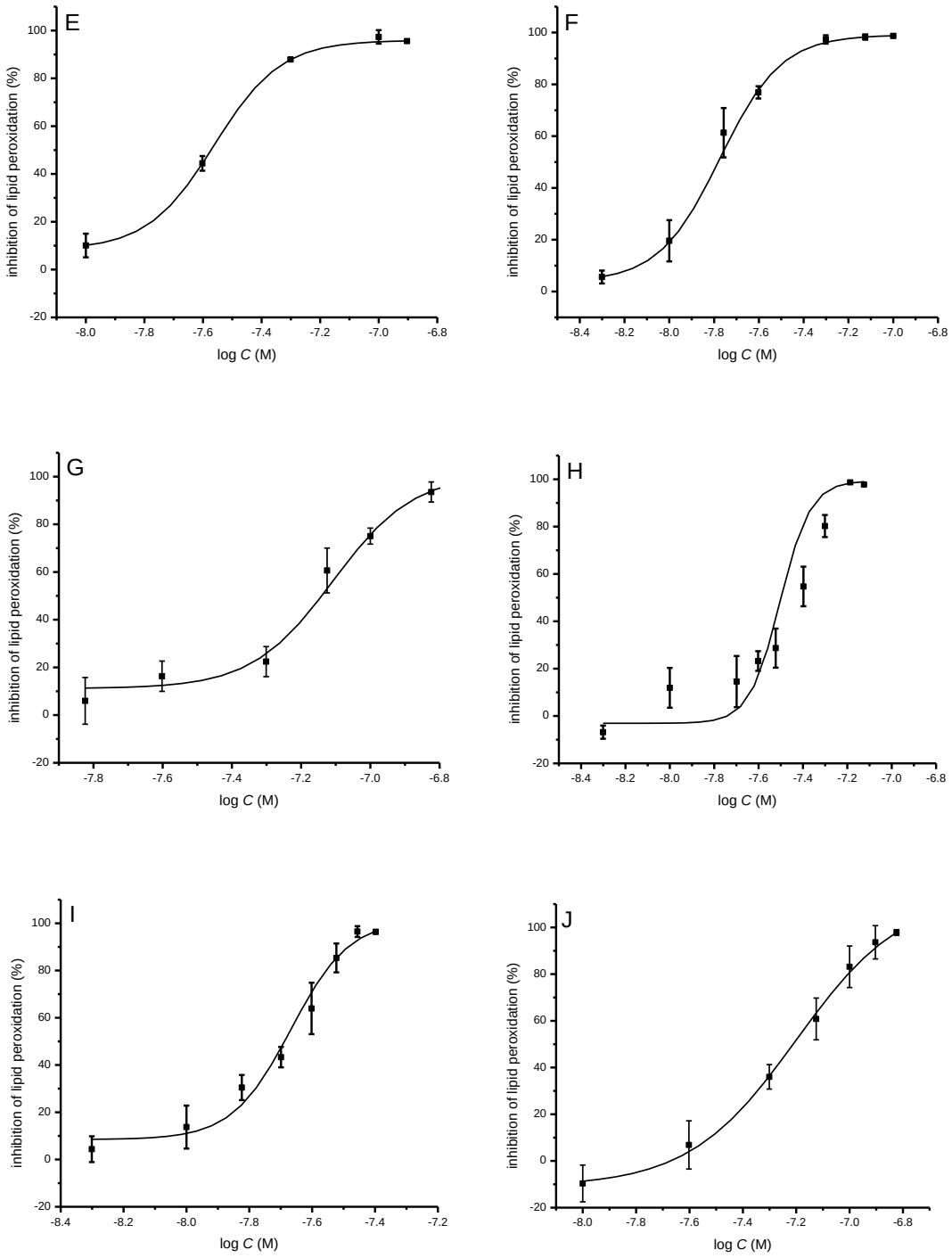

Figure 3.3. Representative dose-response curves obtained from flow cytometry (0.5×10^6 cells/mL; λ_{ex} = 488 nm, λ_{em} = 525±25 nm; 10,000 events) after 5 hrs incubation with antioxidants following induction of oxidative stress with DEM (9 mM) in Tf1a cells grown in RPMI-1640 media containing either THN-C0 (EC_{50} = 5.0 ± 0.1 μM) (A), THN-C4 (B), THN-C5 (C), THN-C8 (EC_{50} = 0.26 ± 0.03 μM) (D), THN-C10 (EC_{50} = 0.027 ± 0.001 μM) (E), THN-C12 (EC_{50} = 0.017 ± 0.001 μM) (F), THN-C16 (EC_{50} = 0.078 ± 0.005 μM) (G), Fer-1 (EC_{50} = 0.031 ± 0.001 μM) (H), Lip-1 (EC_{50} = 0.021 ± 0.001 μM) (I),

PMC (EC_{50} = 0.063 ± 0.001 μM) (J) (0.005-8 μM) at 37 °C. Cells were incubated with the lipid peroxidation reporter C11-BODIPY$^{581/591}$ (1 μM) for 30 minutes prior to DEM treatment.

Moreover, the potency of the compounds varied with the incubation time; at the shorter incubation time (5 hours), the more lipophilic THNs were extremely potent (i.e. EC_{50} = 17±1 nM for C12 and EC_{50} = 17±2 nM for C15) – over 50-fold more so than α-TOH (EC_{50} = 1.0±0.1 μM) and slightly better than Fer-1 (EC_{50} = 31±1 nM) and Lip-1 (EC_{50} = 21±1 nM).[5,7] On the other hand, at the longer incubation time (22 hours) (see **Figure 3.5)**, the potency of the lipophilic THNs decreased roughly 3-fold (i.e. EC_{50} = 60±3 and 80±8 nM for C12 and C15, respectively), while the activity of α-TOH improved (EC_{50} = 42±5 nM). Interestingly, the potency of PMC, an analog of α-TOH with phytyl chain, also decreased about 3-fold (EC_{50} = 220±4 nM at 22 hours incubation *vs.* 63±1 nM at 5 hours incubation), while the ferroptosis inhibitors Fer-1 and Lip-1 were only roughly 50% and 33% less potent at the longer incubation time (i.e. EC_{50} = 47±2 and 28±1 nM at 22 hours).

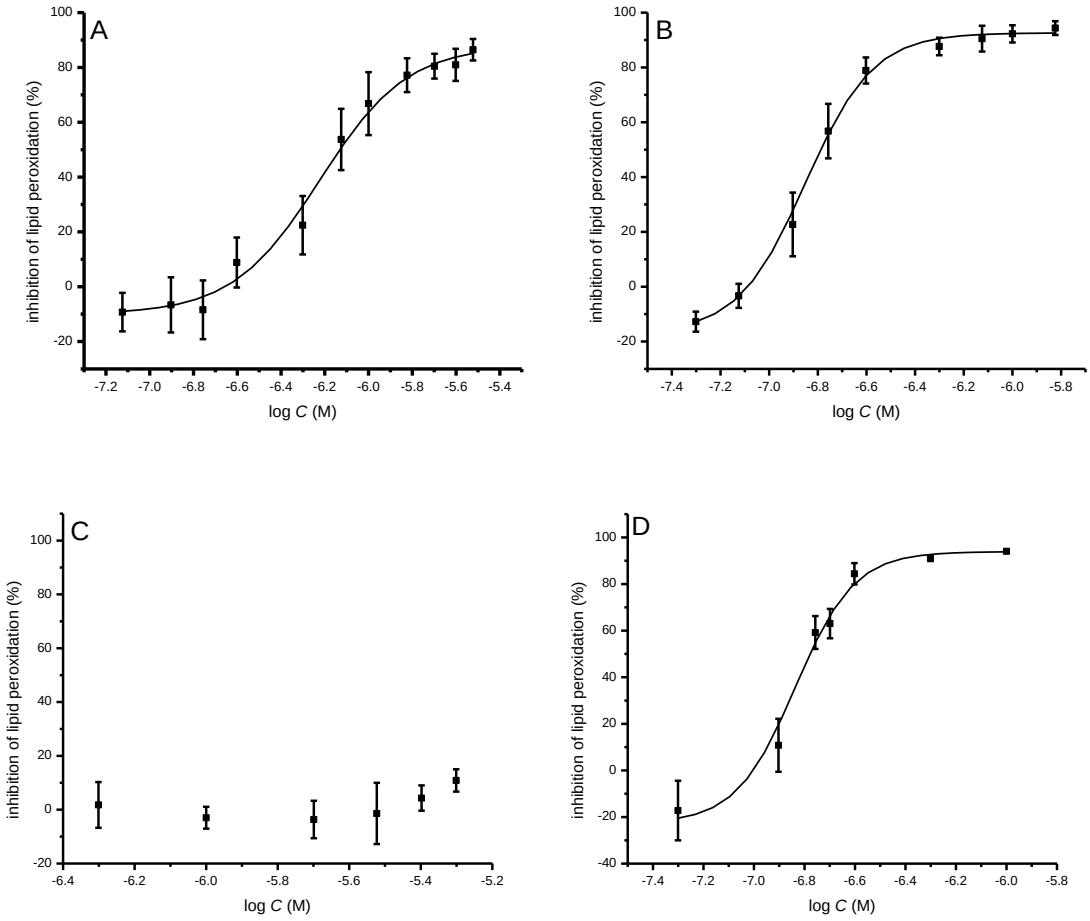

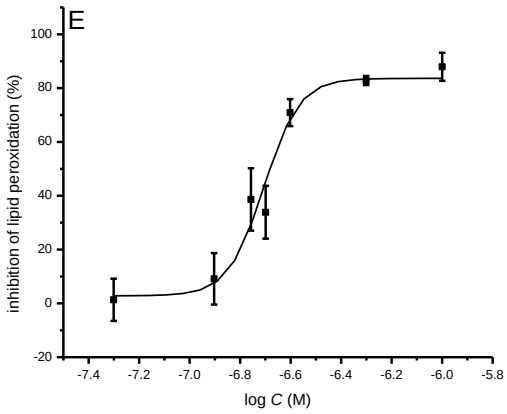

Figure 3.4. Representative dose-response curves obtained from flow cytometry (0.5×10^6 cells/mL; λ_{ex} = 488 nm, λ_{em} = 525±25 nm; 10,000 events) after 22 hrs incubation with antioxidants following induction of oxidative stress with DEM (9 mM) in HEK293 cells grown in MEM media containing either THN-C15 (A) (EC_{50} = 0.6 ± 0.09 μM), THN-C16 (B) (EC_{50} = 0.14 ± 0.01 μM), THN-C4 (C), α-TOH (D) (EC_{50} = 0.15 ± 0.01 μM), PMC (E) (EC_{50} = 0.20 ± 0.01 μM) (0.05-5 μM) at 37 °C. Cells were incubated with the lipid peroxidation reporter C11-BODIPY$^{581/591}$ (1 μM) for 30 minutes prior to DEM treatment.

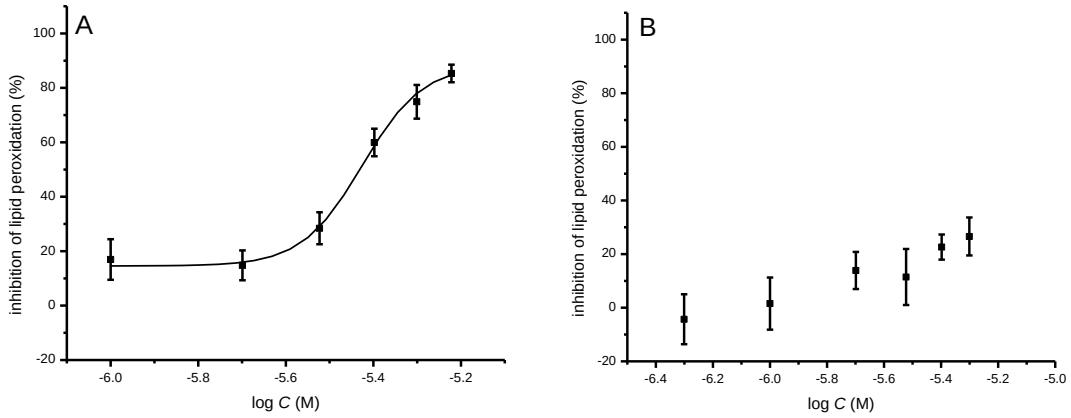

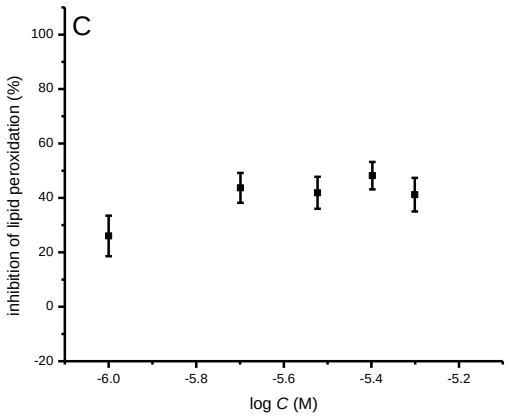
C
inhibition of lipid peroxidation (%)
log C (M)

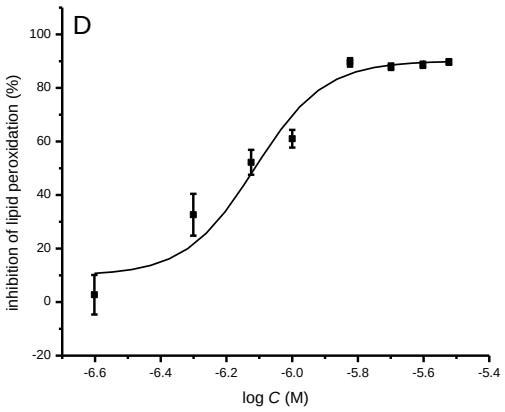
D
inhibition of lipid peroxidation (%)
log C (M)

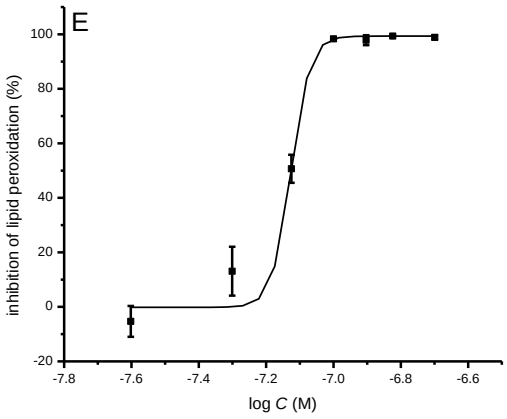
E
inhibition of lipid peroxidation (%)
log C (M)

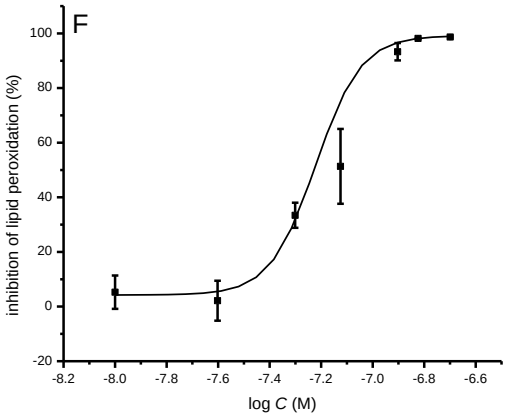
F
inhibition of lipid peroxidation (%)
log C (M)

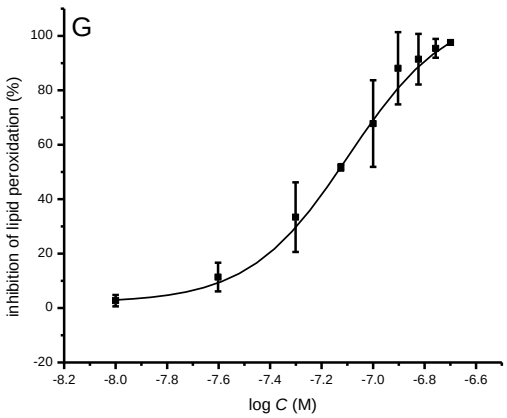
G
inhibition of lipid peroxidation (%)
log C (M)

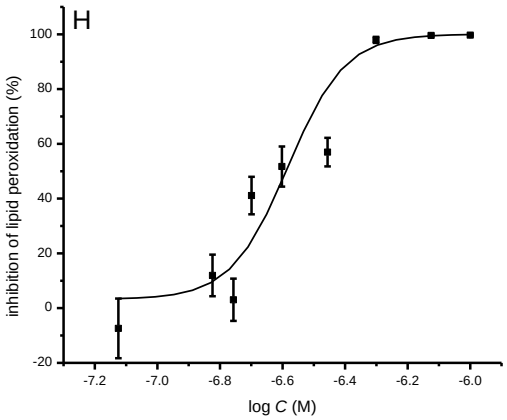
H
inhibition of lipid peroxidation (%)
log C (M)

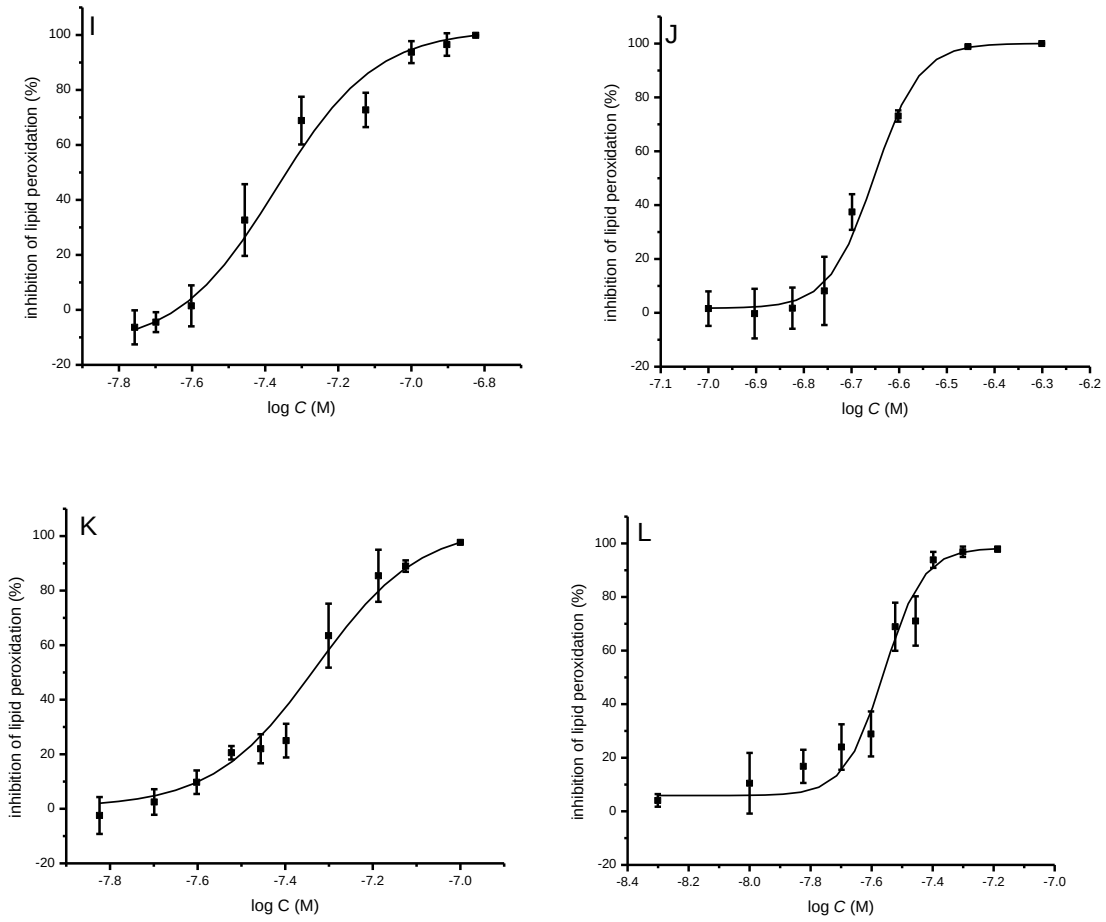

Figure 3.5. Representative dose-response curves obtained from flow cytometry (0.5×10^6 cells/mL; λ_{ex} = 488 nm, λ_{em} = 525±25 nm; 10,000 events) after 22 hrs incubation with antioxidants following induction of oxidative stress with DEM (9 mM) in Tf1a cells grown in RPMI-1640 media containing either THN (C0) (EC_{50} = 3.75 ± 0.2 μM) (A), THN-C4 (B), THN-C5 (C), THN-C8 (EC_{50} = 0.77 ± 0.05 μM) (D), THN-C10 (EC_{50} = 0.075 ± 0.001 μM) (E), THN-C12 (EC_{50} = 0.06 ± 0.003 μM) (F), THN-C15 (EC_{50} = 0.08 ± 0.008 μM) (G), THN-C16 (EC_{50} = 0.26 ± 0.017 μM) (H), α-TOH (EC_{50} = 0.04 ± 0.005 μM) (I), PMC (EC_{50} = 0.22 ± 0.004 μM) (J) (0.005-8 μM), Fer-1 (EC_{50} = 0.047 ± 0.002 μM) (K), Lip-1 (EC_{50} = 0.028 ± 0.001 μM) (L) at 37 °C. Cells were incubated with the lipid peroxidation reporter C11-BODIPY$^{581/591}$ (1 μM) for 30 minutes prior to DEM treatment.

3.3.2 Inhibition of Ferroptosis Induced by Gpx4 Inhibition

Given the similar potency of the THNs to Fer-1 and Lip-1 in inhibiting lipid peroxidation, the anti-ferroptotic potential of the THNs was determined by our collaborator, Dr. Jose Pedro Friedmann Angeli. Ferroptosis was induced in Pfa-1 mouse fibroblasts with the

recently identified Gpx4 inhibitor (*1S,3R*)-RSL3,[5] which was co-administered with the test compounds. Cell viability was measured 6 hours post-induction using AquaBluer.[7] The data are presented in **Figure 3.6**. Fully consistent with the foregoing experiments in Tf1a cells (with the shorter incubation time), the hydrophilic THNs were not potent, and the most potent THNs were THN-C12 and THN-C15 with EC_{50} values of 13±5 and 50±2 nM, respectively. Fer-1 and Lip-1 were also highly potent, with EC_{50} values of 45±5 and 38±3 nM, respectively, while α-TOH was a poor inhibitor (EC_{50} = 1.8±0.3 μM).

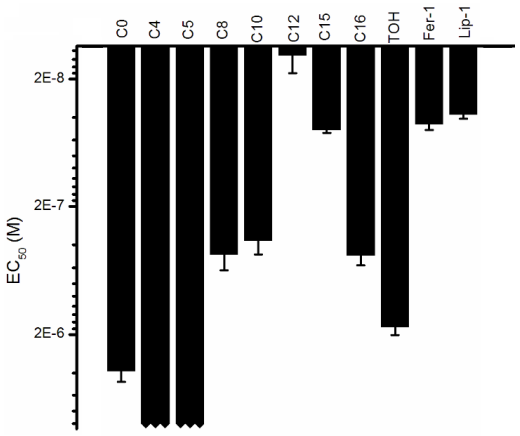

Figure 3.6. Anti-ferroptotic activity of THNs in mouse Pf1a fibroblasts. Ferroptosis was induced by administration of the Gpx4 inhibitor (*1S,3R*)-RSL3 and cell survival was determined 6 hours post-induction. Corresponding data obtained for α-TOH, Fer-1 and Lip-1 is also shown.

3.3.3 Inhibition of Glutamate Toxicity and Cell Death in Mouse Hippocampal Cells

The THNs were also assayed in a cell model of neurodegeneration by our collaborator, Dr. Jose Pedro Friedmann Angeli. HT22 mouse hippocampal cells were challenged with glutamate (5 mM). High concentrations of glutamate inhibits the cystine glutamate antiporter (system xc-), thereby depleting cells of cysteine, resulting in the rapid depletion of GSH and the induction of cell death.[21] Cells treated with β-mercaptoethanol (βMe) were chosen as a positive control. βMe acts by reducing cystine via the formation of a mixed disulfide with cysteine. The βMe/cysteine disulfide is taken up by the cells, independently of system xc-, and subsequently reduced intracellularly providing cysteine for GSH synthesis.[22] Cell viability was assayed using AquaBluer[7] and the results are shown in **Figure 3.7A**.

Consistent with the results in Pf1a fibroblasts, the hydrophilic THNs were not effective in preventing cell death, while the lipophilic THNs (with sidechains of more than 8-carbons) were as potent as Lip-1 and Fer-1. To corroborate that the efficacy of the compounds correlated with the suppression of lipid peroxidation, the C11-BODIPY$^{581/591}$ probe was again employed, yielding the expected results (**Figure 3.7B**). Moreover, the compounds were shown to have no effect on the total glutathione concentration (**Figure 3.7C**).

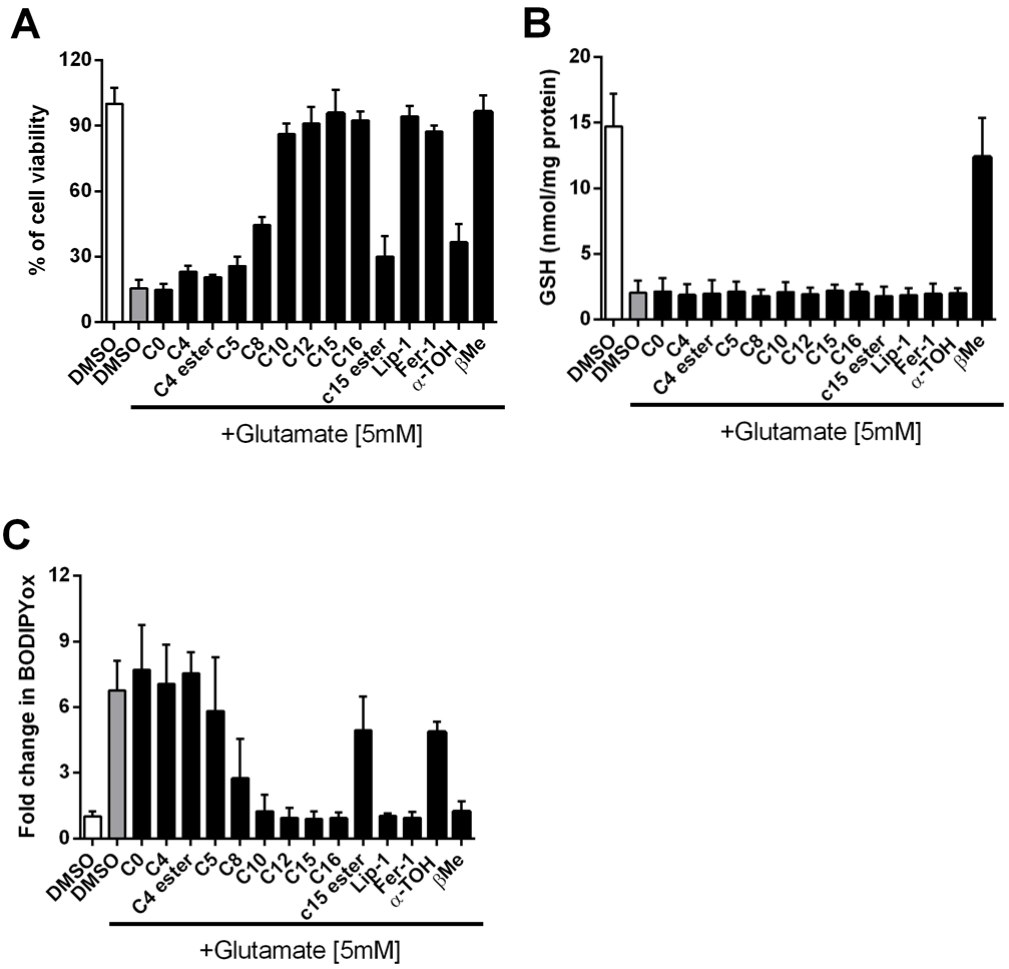

Figure 3.7. Cell viability in HT22 mouse hippocampal cells treated with 5 mM glutamate for 10 hrs (A), total glutathione concentration (B) and fold change in C11-BODIPY$^{581/591}$ fluorescence determined by flow cytometry (C). 100 nM compounds were pre-incubated for 1h before glutamate addition.

3.3.4 Oxidative Stability of the THNs, Fer-1 and Lip-1 in Solution and Cytotoxicities in HepG2 Cells

The stability of a representative THN (C15), Fer-1 and Lip-1 was determined in pH 7.4 PBS buffer at 37°C and compared to α-TOH under the same conditions. The profiles, determined as their conjugate acid by reverse-phase HPLC with ESI-MS detection in positive ion mode or UV-Vis, are shown in **Figure 3.8**. Clearly, the THN is the most labile of the compounds, with a half-life of ca. 3 hours, followed by α-TOH. No degradation of Fer-1 and Lip-1 was observed within an 18-hour period.

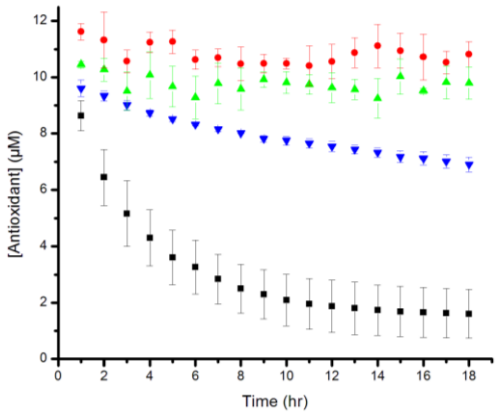

Figure 3.8. Stabilities of a representative THN (THN-C15, black), Fer-1 (red) and Lip-1 (green) in pH 7.4 PBS buffer (10 mM) determined as their conjugate acid by reverse-phase HPLC with ESI-MS detection in positive ion mode. MS (SIR) $[M+H]^+$ for THN-C15 is 389, Fer-1 is 263, Lip-1 is 341. Stability of α-TOH (blue) in pH 7.4 PBS buffer (10 mM) determined by monitoring the decreasing of absorbance at 300 nm.

These results were corroborated with electrochemical oxidations of these compounds. Fer-1 and Lip-1 produced voltammograms with much more oxidizing potentials than the voltammograms obtained for THN-C15 (**Table 3.1**). None of THN-C15, Fer-1 nor Lip-1 showed quasi-reversible voltammagrams at low scan rate (100 mV/s). The first anodic peak potentials were 0.43 V *vs* NHE (THN-C15), 0.73 V *vs* NHE (Lip-1) and 0.85 V *vs* NHE (Fer-1), respectively, when scanned at 100 mV/s. The standard redox potentials ($E°$) can be estimated from the quasi-reversible voltammograms at high scan rates for THN-C15, with $E°$ for THN-C15 to be 0.40 V *vs* NHE at 10 V/s (see **Figure 3.9** for details). Standard redox

potential of α-TOH (estimated from measurement of PMC, the analog of α-TOH without the phytyl sidechain under the same condition) is 0.98 V[19] *vs* NHE.

Table 3.1. Oxidation potentials of α-TOH, THN-C15, Lip-1 and Fer-1 measured by cyclic voltammetry.

RTAs	$E_{pa,1}$ (V vs NHE)[a]	$E°$ (V vs NHE)
α-TOH	1.09[b]	0.98[b]
THN-C15	0.43	0.40[c]
Lip-1	0.73	N/A
Fer-1	0.85	N/A

[a]Cyclicvoltammogram measured @ 100 mV/s; [b]Potentials were estimated from measurement of PMC @ 500 mV/s[19] [c]Obtained from quasi-reversible cyclic voltammograms measured @ 10000 mV/s;

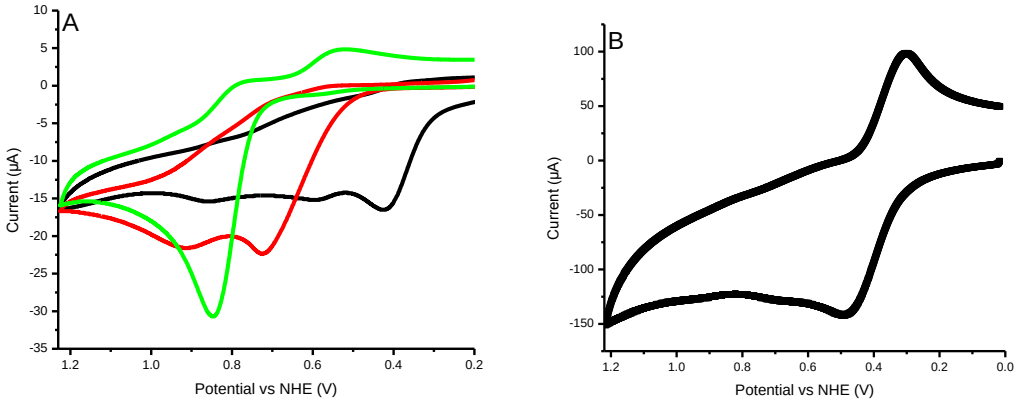

Figure 3.9. Cyclic voltammagram @ 100 mV/s for Fer-1 (green, E_{pa} = 0. 85 V *vs* NHE), Lip-1 (red, E_{pa1} = 0.73 V *vs* NHE), THN-C15 (black, E_{pa1} = 0. 43V *vs* NHE) (A); THN-C15 (B) @ 10000 mV/s ($E_{1/2}$ = $E°$ = 0.40 V *vs* NHE)

Given the highly oxidizable nature of the THNs, their cytotoxicities were determined in HepG2 cells (liver carcinoma) and compared to Fer-1 and Lip-1 as well as α-TOH and PMC using an MTT assay.[23] THN-C15 exhibited less toxicity compared to Lip-1, with TC_{50} values at 85.3 ± 3.8 μM and 41.4 ± 2.13 μM, respectively. Fer-1 had a TC_{50} value of

212.7 ± 27.7 μM. α-TOH was not toxic up to 100 μM, after which it was of dubious solubility in the cell culture medium. In comparison, THN-C16 exhibited similar toxicity to THN-C15, while THN-C4 and PMC were not particularly toxic up to 100 μM. (see **Table 3.2** and **Figure 3.10** for details)

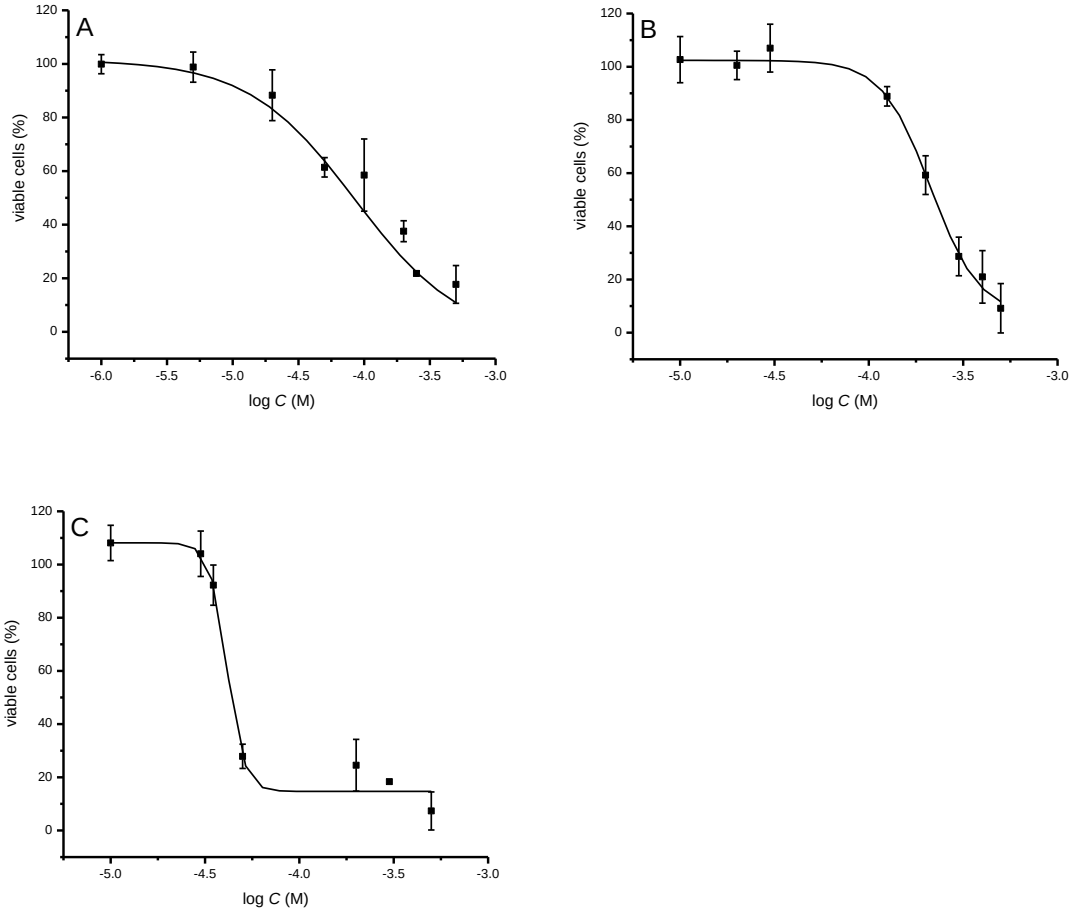

Figure 3.10. Dose-response curves obtained from MTT cell viability studies with HepG2 cells containing varying concentrations of THN-C15 (A) (TC_{50} = 85.3 ± 3.8 μM), Fer-1 (B) (TC_{50} = 212.7 ± 27.7 μM), Lip-1 (C) (TC_{50} = 41.4 ± 2.13 μM) incubated at 37 °C for 22 hrs.

Table 3.2. MTT cell viability studies in HepG2 cells containing varying concentrations of antioxidants.

Compounds	Cell viability at various concentration of compounds (%)		
	5 μM	50 μM	100 μM
α-TOH	97.1±6.1	94.1±9.6	82.4±10.5
THN-C15	98.8±9.1	61.4±3.6	58.5±13.5
THN-C16	102.1±10.4	61.2±4.7	67.2±12.84
THN-C4	102.4±9.1	102.7±8.7	100.7±8.1
PMC	102.2±3.3	97.6±1.7	105.2±12.7

3.3.5 Radical-Trapping Antioxidant Activities of Fer-1 and Lip-1 in Organic Solution

The inherent radical-trapping antioxidant activities of Fer-1 and Lip-1 were determined directly in homogenous organic solution and compared to a representative THN (THN-C15) and α-TOH in order to provide some insight on whether RTA activity figures into the mechanism of their activity in cells. They comprise inhibited co-autoxidations of styrene and PBD-BODIPY, wherein reaction progress is monitored at 591 nm, which corresponds to consumption of the PBD-BODIPY that is added to the styrene as a signal carrier.[24] The absorbance is lost as peroxyl radicals add to the 1-phenylbutadiene moiety in competition with styrene (**Scheme 3.2**).

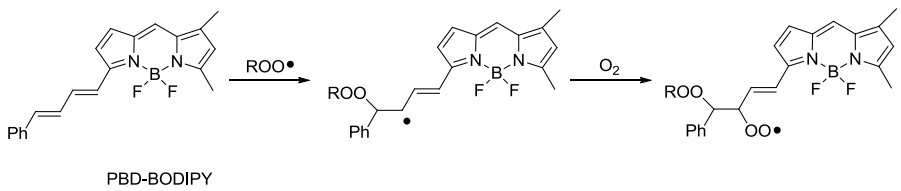

Scheme 3.2. The autoxidation of PBD-BODIPY.

Representative results are shown in **Figure 3.11**. Although THN-C15 fully inhibited

the autoxidation until it was consumed, and α-TOH produced a similar clear inhibited period, Fer-1 and Lip-1 were only able to retard the rate of autoxidation at each of the three concentrations assayed. To quantitate their inherent reactivities, the reaction progress curves were numerically fit to the kinetic scheme for inhibited autoxidation of styrene to obtain the second order rate constants for the reactions of Lip-1, Fer-1 and α-TOH with chain-carrying peroxyl radicals to yield values of $(3.0\pm0.1)\times10^5$, $(3.1\pm0.2)\times10^5$ and $(3.7\pm0.2)\times10^6$ $M^{-1}s^{-1}$, respectively. Since the THN-inhibited reaction is essentially completely inhibited, it is impossible to accurately obtain a rate constant for its reaction with peroxyl radicals from these data. However, previous efforts with a slightly different experimental approach yielded a value of 2.8×10^8 $M^{-1}s^{-1}$ under similar conditions.[16] Since the inhibited period is linearly proportional to the number of radicals trapped per molecule of RTA and α-TOH traps two peroxyl radicals under these conditions,[13,25] the stoichiometries of the THN-C15, Lip-1 and Fer-1 can be estimated to be ~1.9±0.1, ~1.2±0.1 and ~0.9±0.1, respectively.

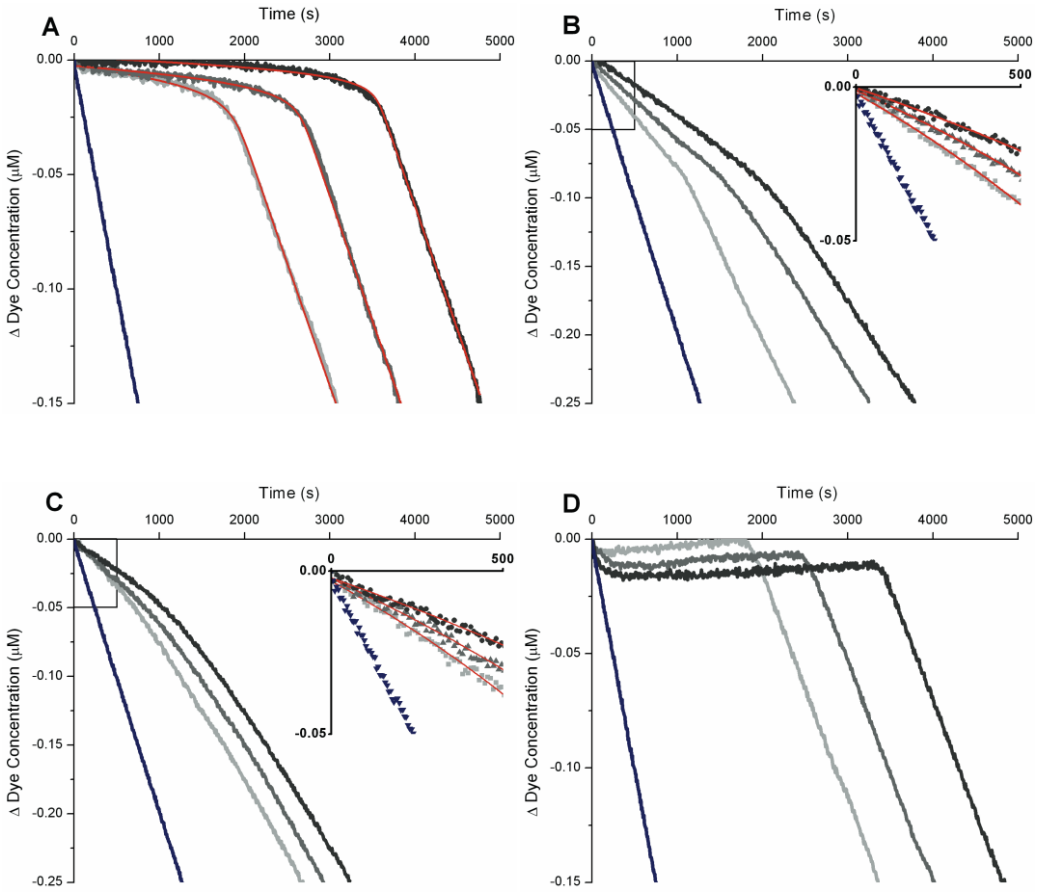

Figure 3.11. Inhibited autoxidations of styrene in chlorobenzene at 37°C initiated by 6 mM AIBN in the

presence of 2, 3, 4 μM α-TOH (A), Lip-1 (B), Fer-1 (C), THN-C15 (D) and uninhibited. Reaction progress was monitored by consumption of PBD-BODIPY at 591 nm.

3.3.6 Radical-Trapping Antioxidant Activities of Fer-1 and Lip-1 in Egg Phosphatidylcholine Liposomes

The reactivity of Fer-1 and Lip-1 toward peroxyl radicals was also assayed in the lipid bilayers of unilamellar liposomes prepared from egg phosphatidylcholine (EggPC) oxidized using the hydrophobic azo-compound 2,2'-azobis(4-methoxy-2,4-dimethylvaleronitrile) (MeO-AMVN). The pro-fluorescent H_2B-PMHC mentioned in **Chapter 2** was used to follow reaction progress (**Scheme 3.3**); the fluorescence (λ_{em} = 520 nm; λ_{ex} = 485 nm) of the probe increases as it reacts with peroxyl radicals owing to interrupted intramolecular quenching by photoinduced electron transfer from the electron-rich chromanol moiety to the BODIPY fluorophore.[26] The suppression of the initial rate at which the fluorescence increases in the presence of a test compound provides the relative rate at which it reacts with peroxyl radicals (n.b. the probe reacts with peroxyl radicals at essentially the same rate as α-TOH).[19]

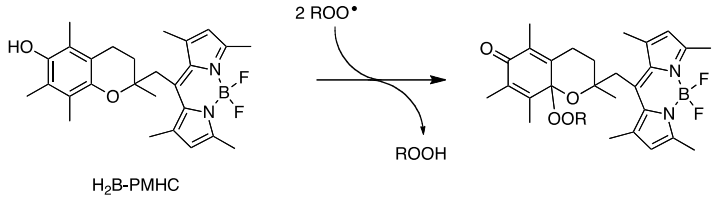

Scheme 3.3 The reaction of H_2B-PMHC with peroxyl radicals.

Representative results are shown in **Figure 3.12** when the EggPC liposomes are supplemented with five concentrations of Fer-1, Lip-1 alongside with THN-C15 and α-TOH for comparison. Again, while the THNs are extremely potent, completely suppressing oxidation of the probe as a dose-response behavior, Fer-1 and Lip-1 are poor radical-trapping antioxidants. In fact, Fer-1 and Lip-1 have essentially no effect on the initial rate of the oxidation up to ratios of Fer-1/Lip-1:H_2B-PMHC of 50:1 (**Figure 3.12A, 3.12B)** suggesting that they are at least 50-fold less reactive than α-TOH – in good agreement with the results in solution. Interestingly, while Fer-1 has essentially no impact

on the rate of the initial oxidation, either it or an oxidation product derived therefrom appears to quench the fluorescence of the probe. Lip-1 displays similar quenching behavior, but to a lesser extent compared to Fer-1. It should be noted that the α-TOH-inhibited oxidations of EggPC liposomes were highly irreproducible. Despite identical experimental protocols, the observed inhibited periods varied significantly between trials and was up to 78% lower than what we observed previously (**Chapter 2**). In sharp contrast, the other inhibited oxidations were highly reproducible, with inhibited periods varying by 10% at most.

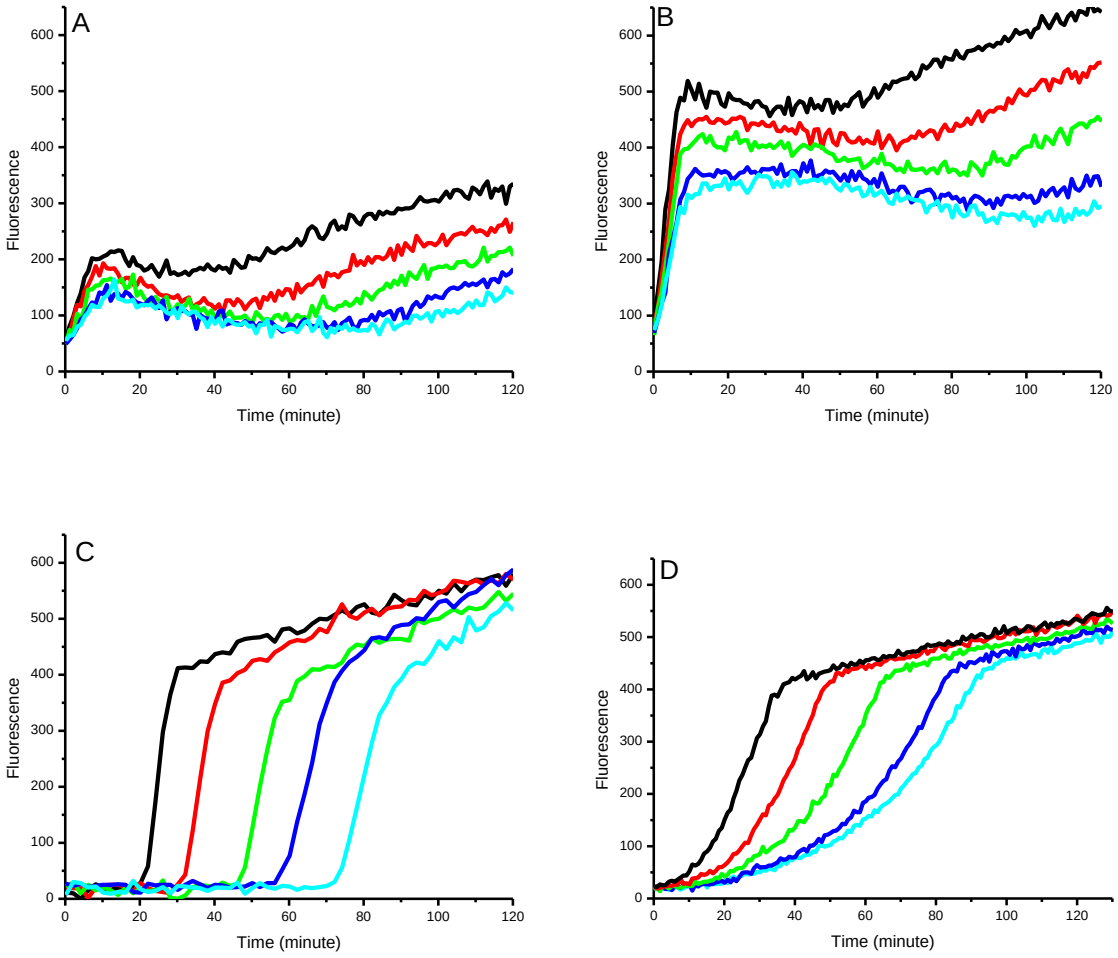

Figure 3.12. Representative fluorescence intensity-time profiles from MeOAMVN-mediated (0.68 mM) oxidations of EggPC liposomes (1 mM) containing 0.15 μM H_2B-PMHC and increasing concentrations (1.5 μM black, 3.0 μM red, 4.5 μM green, 6.0 μM blue and 7.5 μM cyan) of Fer-1 (A), Lip-1 (B), THN-C15 (C) and α-TOH (D). Fluorescence (λ_{ex} = 485 nm; λ_{em} = 520 nm) was recorded every min.

Analogous results were obtained when experiments were carried out using AAPH (see

Figure 3.13 for representative data**)**. Again, the inhibition period observed in the presence of α-TOH was irreproducible and up to 61% lower than what is reported in **Chapter 2**.

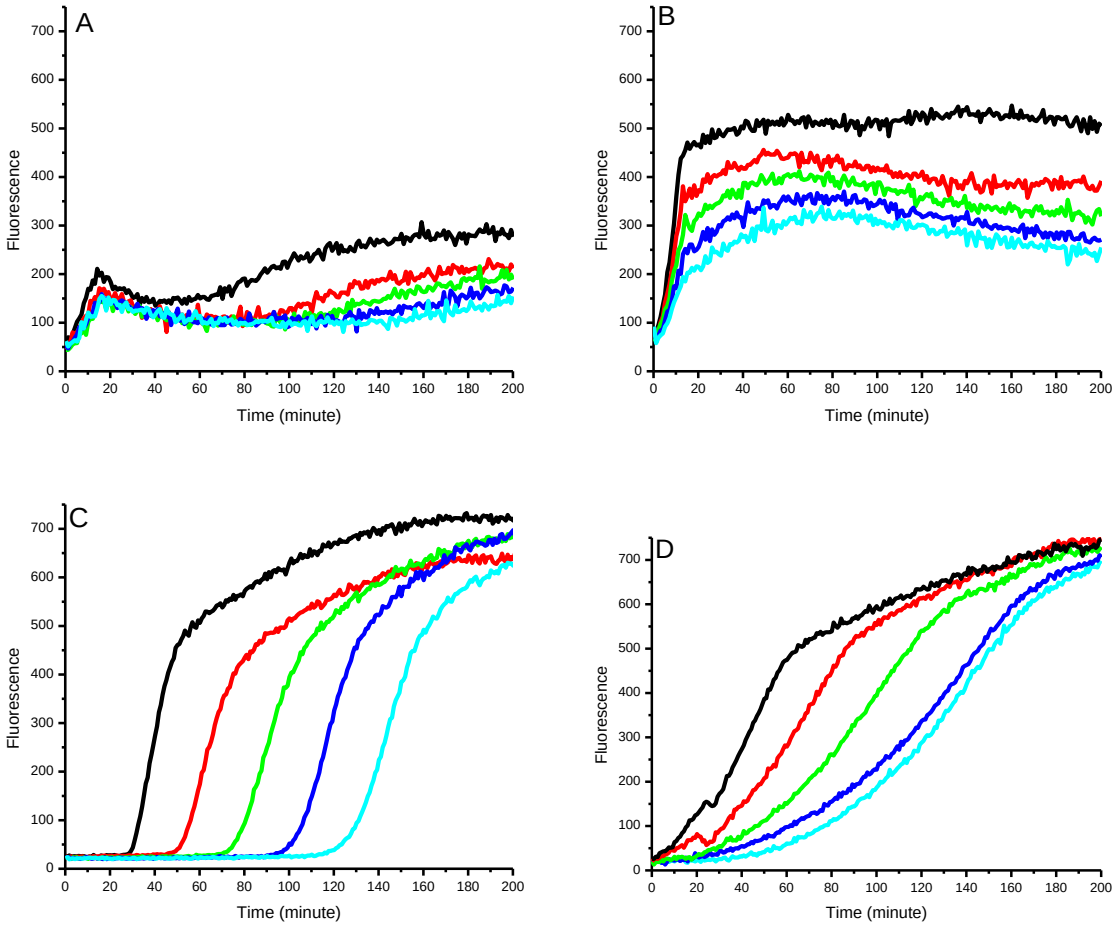

Figure 3.13. Representative fluorescence intensity-time profiles from AAPH-mediated (2.7 mM) oxidations of EggPC liposomes (1 mM) containing 0.15 μM H_2B-PMHC and increasing concentrations (1.5 μM black, 3.0 μM red, 4.5 μM green, 6.0 μM blue and 7.5 μM cyan) of Fer-1 (A), Lip-1 (B), THN-C15 (C) and α-TOH (D). Fluorescence (λ_{ex} = 485 nm; λ_{em} = 520 nm) was recorded every min. Fluorescence (λ_{ex} = 485 nm; λ_{em} = 520 nm) was recorded every minute.

3.3.7 Radical-Trapping Antioxidant Activities in Egg Phosphatidylcholine Liposomes with Different Incubation Period

The increased potency of α-TOH with 22 hours compared to 5 hours in Tf1a cells suggests that α-TOH might be relatively slow to incorporate into the cells. Given the practical difficulties associated with determining cell uptake of the THNs compared to α-TOH, we sought to investigate the effects of changing the length of the incubation period

in the liposome experiments. These experiments will also provide some insight on whether the decreased potency of α-TOH in liposome oxidation is due to slower incorporation caused by different liposome viscosity or fluidity between batches. As a result, we carried out liposome oxidations wherein RTAs were incubated with lipid bilayers for different length of time before lipid peroxidation was initiated with MeOAMVN. Results (**Figure 3.14** for details) showed that for hydrophobic THN-C15, there was no obvious change on inhibition period with prolonged RTA incubation time (with 81 min., 88 min, and 84 min. for 0 hr, 5 hrs and 22 hrs incubation time in the presence of 7.5 μM THN-C15). More interestingly, the efficacy of α-TOH to slow down oxidation of H_2B-PMHC probe was irreproducible. For some trials, the efficacy was better with longer incubation time (with 17 min., 30 min, and 38 min. inhibition periods for 0 hr, 5 hrs and 22 hrs incubation time in the presence of 7.5 μM α-TOH shown in **Figure 3.14D**). But for other trials wherein inhibition time of α-TOH without incubation was longer than what is shown in **Figure 3.14D**, incubation time had no obvious effect on the efficacy of α-TOH (data is not shown). THN-C4 showed clearly shortened inhibition period as incubation time was prolonged (with 56 min., 44 min, and 38 min. for 0 hr, 5 hrs and 22 hrs incubation time in the presence of 7.5 μM THN-C4). While for PMC, whose hydrophilicity is similar to THN-C4 with log*P* ca. 3.42,[19] but is very stable to one electron oxidation (one electron oxidation potential $E_{1/2}$ = $E°$ = 0.98 V *vs* NHE),[19] no decreasing of inhibition period was observed with longer incubation time, with 84 min., 84 min, and 78 min. for 0 hr, 5 hrs and 22 hrs incubation time in the presence of 7.5 μM PMC). No obvious change was monitored for Fer-1 and Lip-1 on varying incubation time.

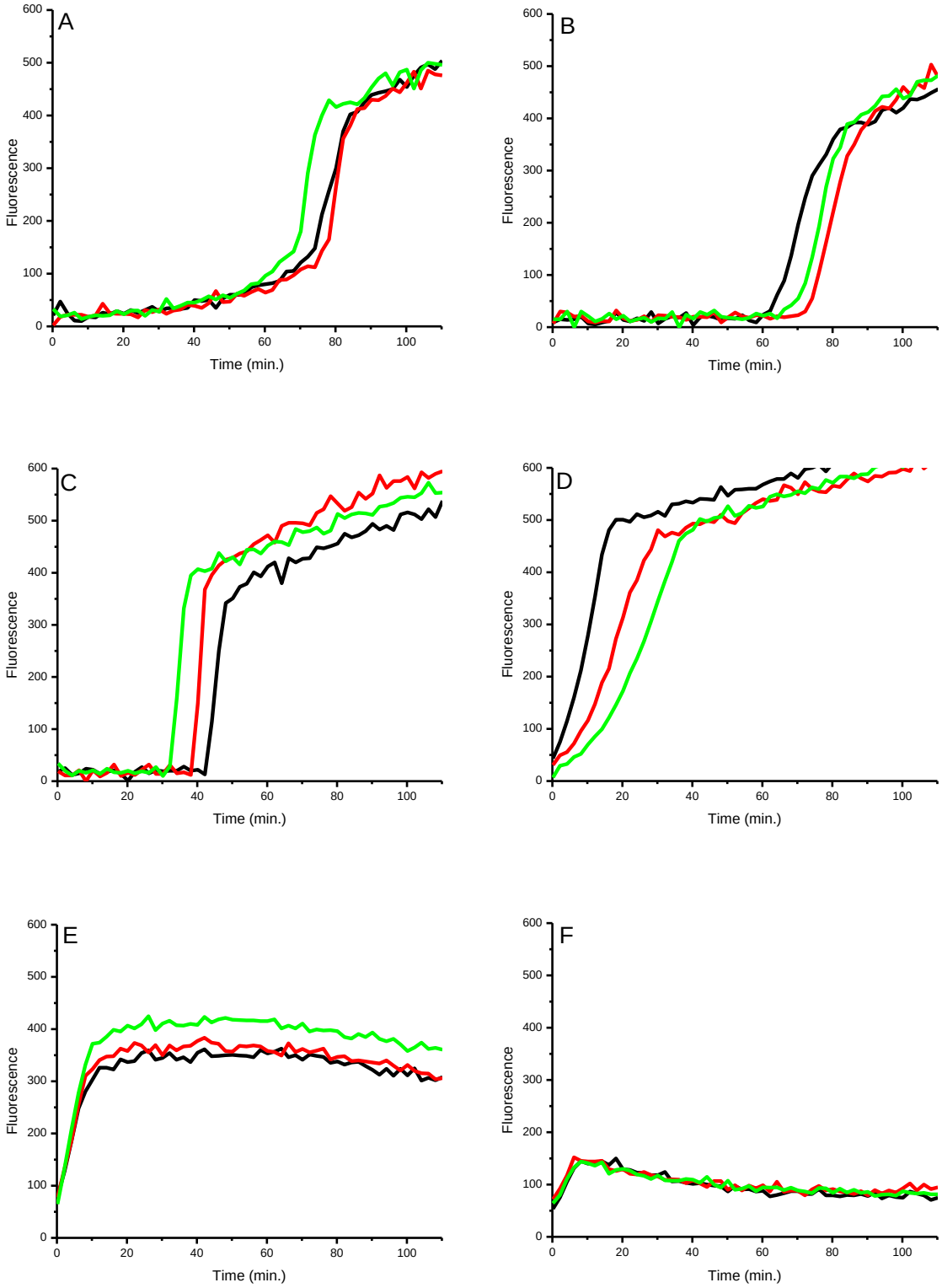

Figure 3.14. Representative fluorescence intensity-time profiles from oxidations of EggPC liposomes (1 mM) containing 0.15 μM H_2B-PMHC and 7.5 μM antioxidants initiated with 0.68 mM MeOAMVN after different incubation time with antioxidants 0 hr (black), 5hr (red), 22 hr (green) PMC (A), THN-C15 (B), THN-C4 (C), α-TOH (D), Lip-1 (E), Fer-1 (F). Fluorescence (λ_{ex} = 485 nm; λ_{em} = 520

nm) was recorded every two minute.

3.4 Discussion

Previous work by the Pratt group demonstrated that the THNs were ca. 30-fold more reactive than α-TOH in homogenous organic solution (i.e. benzene or chlorobenzene).[16] In our subsequent efforts (**Chapter 2**),[19] we designed a small library of THNs with a wide range of lipid solubilities (log*P* ranging from 2.11 to 9.14), and showed that derivatives bearing aliphatic sidechains of at least 8 carbon atoms (log*P* > 6.19) were found to be highly effective inhibitors of lipid peroxidation in phosphatidylcholine lipid bilayers.[19] In fact, they were so reactive we could only assign a lower bounds to their relative reactivity: >30-fold faster than α-TOH. Although hydrophilic THNs had similar reaction kinetics for peroxyl radical-trapping, they were far less efficient (they trapped less than half as many radicals). We ascribed this result to the facile autoxidation of the THNs in the surrounding aqueous medium, to which the hydrophilic THNs will partition to a greater extent.[19] The experiments described here were initially designed and carried out to assess the RTA activity of the same set of THNs in mammalian cell culture to determine if the tremendous reactivity of these compounds – which were designed to be the 'optimal' phenolic-like RTAs – extend from organic solution to cells.

The sidechain substitution of the THNs proves to be even more important in cell culture than in liposomes. The lipophilic THNs were found to be significantly more potent inhibitors of DEM-induced lipid peroxidation in Tf1a erythroblasts than α-TOH, while the hydrophilic THNs were significantly less potent (**Figure 3.2 and 3.3**). For example, THN-C12 and THN-C15 were over 50-fold more potent than α-TOH, with EC_{50} values of ~17 nM compared to 1 μM for α-TOH, while all THNs with sidechains containing fewer than eight carbon atoms were ineffective at concentrations less than 5 μM. Interestingly, the THN-C16 was noticeably less potent (EC_{50} = 78±5 nM) than the THN-C12/C15, as was the THN-C10 (EC_{50} = 27 ±1 nM), suggesting that a balance must be struck between the THN being sufficiently lipophilic to localize in lipid bilayers, but not so lipophilic that rapid cell entry and good dynamics within the bilayer is sacrificed.[27,28]

Interestingly, the relative efficacy of the lipophilic THNs depended on the length of the incubation time in the cell culture medium prior to the lipid peroxidation assay. On increasing the incubation time from 5 to 22 hours, the potency of all of the lipophilic THNs decreased by an average of ~3-fold while the potency of α-TOH increased ~25-fold. The increased potency of α-TOH with incubation time suggests that it is relatively slow to incorporate into the cells (a fact suggested also by other measurements)[29] while the opposite trend with the THNs suggests that they are rapidly incorporated, but either autoxidize or undergo other deleterious reactions, which limit their potency with increasing incubation time. Indeed, we have found that the half-life of a representative THN in buffer is on the order of a few hours. This is explained by its relatively low redox potential ($E°$= 0.4 V) – substantially lower than that of α-TOH ($E°$ = 0.98 V). Results of oxidations of liposomes incubated with RTAs for various times support this hypothesis to some extent. Prolonged incubation time (up to 22 hours) had no substantial effect on the potency of THN-C15 in EggPC liposomes, suggesting fast incorporation of THN-C15 and little or no autoxidation of THN-C15 once incorporated into the lipid bilayers. In contrast, oxidations of liposomes supplemented with α-TOH yielded irreproducible results. In some trials, the efficacy of α-TOH improved slightly with increased incubation time (e.g. increasing from 17 to 38 minutes upon increasing the incubation time from 0 hr to 22 hr) but for other trials, no change was observed. We surmise that batch to batch variability of egg PC liposome composition has considerable effects on the activity of α-TOH relative to the other RTAs we studied, perhaps due to changes in the viscosity or fluidity of the bilayers.[30,31] Decreasing inhibition periods for THN-C4 with longer incubation time suggest that decreased hydrophobicity for THN-C4 could not completely retain their location in lipid. As a result, a bigger fraction of added THN-C4 autoxidizes with longer incubation time leading to decreased inhibition period. Although the differences are not as significant as those observed in cell culture, they are consistent, and imply that α-TOH is slow to incorporate into the lipid bilayers, but stable to autoxidation, whereas the THNs are quick to incorporate into the lipid bilayers, but are relatively more labile to autoxidation. In contrast, PMC did not show time-dependence effect on the incubation time, which suggests that it is

relatively fast incorporated into the liposomes and are stable throughout the experimental period.

α-TOH is often sold and/or administered as the acetate in order to prevent its oxidation, and α-TOH acetate is known to have higher bioavailability compared to equivalent quantities of the free phenol in rat fetal gestation-resorption assay.[32] Therefore, we sought to protect the THNs from autoxidation in the cell culture media before their incorporation into cells by doing the same (see **Experimental Section** for the synthesis of THN acetate). Indeed, the THN-C15 acetate was completely stable in pH 7.4 PBS buffer (**Figure 3.15**) – consistent with the fact that its oxidation potential is 0.69 V higher than that of the free THNs, with $E°$ = 1.09 V *vs* NHE. The THN-C15 acetate was significantly less potent in Tf1a erythroblasts or HEK293 cells compared to the free THN-C15, with a EC_{50} = 0.25 ± 0.007 μM and 0.4 ± 0.04 μM in Tf1a cells and HEK 293 cells, respectively (22 hours incubation time). THN-C15 acetate itself is inactive as an antioxidant and it is hydrolyzed to free phenolic THN-C15 as the authentic RTA. The low potency of THN-C15 acetate compared to THN-C15 is presumably because of the slow hydrolysis of acetate groups in cells within the experimental period or the increased lipophilicity of THN-C15 acetate (log*P* = 8.44) limits its cell incorporation. Different from the free THN-C15, changes in incubation time had no obvious effect on the potency of THN-C15 acetate, with EC_{50} ~ 220 nM and ~250 nM after 5 and 22 hours incubation in Tf1a cells, respectively. Neither THN-C4 acetate nor THN-C4 exhibited obvious activity up to 5 μM due to their poor lipophilicity and facile autoxidation in aqueous media as mentioned above.

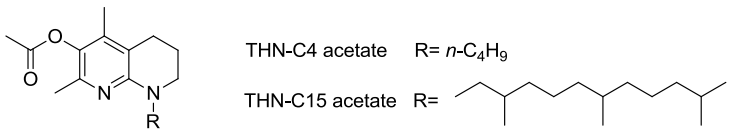

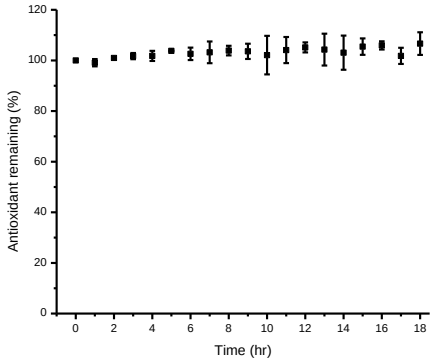

Figure 3.15. Stability of THN-C15 acetate in pH 7.4 PBS buffer (10 μM) determined as its conjugate acid by reverse-phase HPLC with ESI-MS detection in positive ion mode. MS (SIR) $[M+H]^+$ is 431.

The greater potency of the lipophilic THNs compared to α-TOH as inhibitors of lipid peroxidation in cell culture prompted us to consider whether they are inhibitors of ferroptosis – the recently identified form of cell death associated with the iron-dependent accumulation of lipid hydroperoxides. The best inhibitors of ferroptosis identified to date, Fer-1 and Lip-1 (**Chart 3.1**), were identified from extensive screening efforts, and we wondered how the THNs – compounds designed from the ground up to inhibit lipid peroxidation – would compare. Initial experiments carried out in mouse Pf1a fibroblasts revealed that the lipophilic THNs were potent inhibitors of ferroptosis induced by Gpx4 inhibition using RSL3. The most potent THNs were C12 and C15 with EC_{50} values of 13±5 and 50±2 nM, respectively, which compare very favourably with α-TOH (**3**) (**Chart 3.2**), and similarly potent to Lip-1 (**1**) and Fer-1 (**2**) (**Chart 3.1**).

The THNs were also assayed for their ability to prevent glutamate-induced cell death in neuronal cells to model cells involved with neurodegenerative disease. Glutamate inhibits cystine uptake by the cystine/glutamate antiporter (system x_c^-), leading to a precipitous drop in cellular glutathione and iron-dependent, non-apoptotic death believed to contribute to neurodegeneration (e.g. Huntington's disease).[21,33] In this cell model, the lipophilic THNs again perform extremely well, rescuing HT22 mouse hippocampal cells from lethal concentrations of glutamate (5 mM) at nanomolar concentrations. Their activity was similar to that observed for Fer-1 and Lip-1. Again, the more hydrophilic compounds were essentially inactive, with C8 being the minimum sidechain length to give rise to a

significant increase in cell viability. Importantly, each of the THNs (as well as Fer-1 and Lip-1) had no effect on GSH levels, and the cell viability data tracked inhibition of lipid peroxidation as reported by the C11-BODIPY$^{581/591}$ probe.

Stockwell and co-workers have made the completely reasonable suggestion that Fer-1 inhibits ferroptosis by slowing lipid peroxidation.[12] Indeed, Fer-1 is an arylamine, and decades of research have shown that arylamines are good radical-trapping antioxidants.[13,25] However, they are generally only moderately reactive at ambient temperatures. In fact, the most reactive arylamines (alkylated diphenylamines, universally used in petroleum-derived products) react ca. 20-fold more slowly with peroxyl radicals than does α-TOH[17] – and yet Fer-1 is much more effective at preventing lipid peroxidation in cells than α-TOH. We wondered whether there was something special about the arylamine structure of Fer-1 that confers a significant reactivity difference relative to common diarylamine RTAs. Likewise, we wondered about the core structure of Lip-1. Could these molecules represent a new paradigm in RTA development?

Using the same kinetic methods that were used to assess the activity of the THNs in their development as "ideal" RTAs, we sought to evaluate the inherent chemical reactivity of Fer-1 and Lip-1 toward chain-carrying peroxyl radicals. Thus, we carried out inhibited autoxidations of styrene – the venerable method for obtaining both the kinetics and stoichiometry of the reactions of RTAs with peroxyl radicals – and found that both compounds were not very potent. The rate constants for reactions of Lip-1 and Fer-1 with peroxyl radicals are $(3.0\pm0.1)\times10^5$ and $(3.1\pm0.2)\times10^5$ $M^{-1}s^{-1}$, respectively – orders of magnitude lower than that determined for the THNs (2.8×10^8 $M^{-1}s^{-1}$),[16] and even significantly lower than that obtained for α-TOH ($(3.7\pm0.2)\times10^6$ $M^{-1}s^{-1}$ using the same method and 3.2×10^6 $M^{-1}s^{-1}$ obtained previously).[34] Moreover, while α-TOH and the THNs trap two peroxyl radicals each, Lip-1 and Fer-1 were found to trap significantly fewer (1.2 and 0.9, respectively). To understand these results, one must consider the fate of the resultant arylaminyl radicals that form upon initial H-atom donation from Lip-1/Fer-1 to peroxyl radicals (cf. **Scheme 3.4**). Since Fer-1 is a *o*-phenylenediamine, the intermediate radical can be expected to react with another radical to form a *o*-quinonediimide. However,

it is also possible that the intermediate radical also reacts with O_2 to yield a chain-propagating hydroperoxyl radical, as is the case of the analogous semiquinone radicals derived from structurally related catechols and hydroquinones.[35] Likewise for Lip-1 – the intermediate aminyl radical may trap another peroxyl radical, but this must compete with the reaction with O_2.

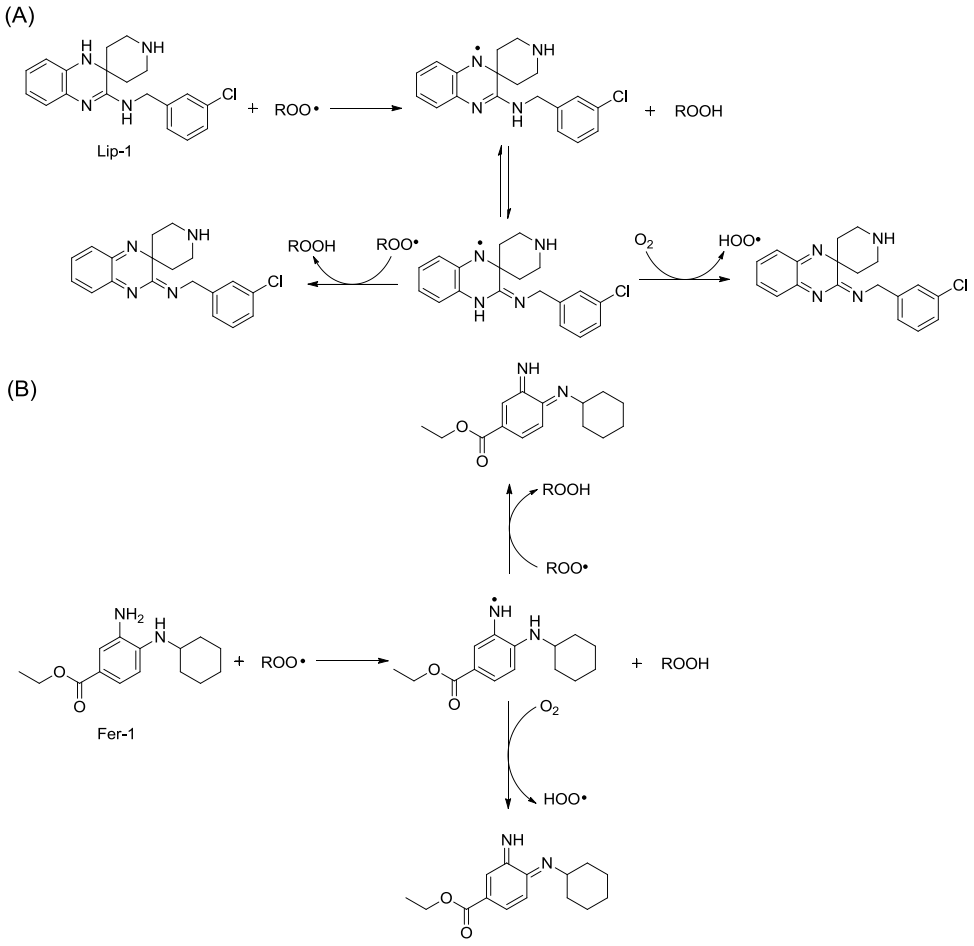

Scheme 3.4. Competing fates of the Lip-1 and Fer-1 derived arylaminyl radicals.

Extending our studies to solutions of EggPC liposomes dispersed in phosphate-buffered saline, we found that Lip-1 and Fer-1 are even less reactive in heterogenous systems. In fact, they reacted with peroxyl radicals so slowly that they could not compete with oxidation of H_2B-PMHC fluorogenic tocopherol-inspired probe even when present in 50-fold excess. This suggests that Lip-1 and Fer-1 are at least 50-fold less reactive than α-TOH and hundreds of times less reactive than the THNs in lipid bilayers.[19] It seems reasonable to suggest that this is, in part, due to the fact that Lip-1 and Fer-1 are

both not very lipophilic, with log*P* = 2.43 and 3.00, respectively (estimated by ChemBioDraw Ultra 12.0), which diminishes their inherent peroxyl radical-trapping antioxidant activity (as evidenced from the inhibited autoxidation studies) further owing to greater phase separation from chain-carrying lipid peroxyl radicals. Increasing incubation time of Fer-1 and Lip-1 in liposomes does not have any effect on their activities, indicating they are either not embedded in the lipid bilayers and/or are too slow to trap peroxyl radicals effectively in liposomes.

Given the modest activity of Lip-1 and Fer-1 as RTAs in homogeneous solution, and poor activity in lipid bilayers, it is likely that their potent anti-ferroptotic activity is based on another mechanism. It has been suggested that Fer-1 inhibits ferroptosis by iron chelation, thereby reducing free iron and precluding ROS formation *via* Fenton chemistry.[5,36] Moreover, the fact that deferoxamine, an excellent iron chelator, is ~10 times less potent than Fer-1,[7] suggests that iron chelation is unlikely to be the mechanism of action. On the other hand, the lower potency of deferoxamine might also be due to lower cell incorporation compared to Fer-1 (log*P*= -0.49 estimated by ChemBioDraw Ultra 12.0), although this has not been addressed. Alternatively, Fer-1 and Lip-1 could possibly inhibit lipoxygenases – the enzymes that catalyze the peroxidation of arachidonic acid.[37] Cornad *et. al.* have shown that loss of arachidonate 15-lipoxygenase gene did not rescue ferroptosis induced by knocking out Gpx4, indicating that inhibition of 15-lipoxygenase is probably not at the root of ferroptosis inhibition.[7] Another possibility is that Fer-1 or Lip-1 is oxidized under physiological conditions to electrophilic species that activate the Nrf-2/KEAP-1 system and induce the expression of protective (antioxidant) enzymes.[38] Indeed, the *o*-quinonediimide species in **Scheme 3.4** are likely to be good electrophiles. Although Fer-1 and Lip-1 don't trap radicals particularly well, they might act as multi-modal "antioxidants" via a combination of the mechanisms mentioned above (**Scheme 3.5**). Research to elucidate the biological mechanism of action of Fer-1 and Lip-1 is currently being explored in the Pratt laboratory.

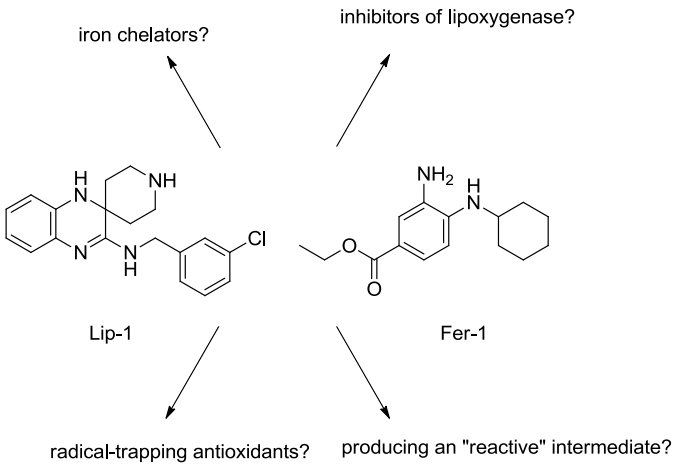

Scheme 3.5. Possible biological mechanism of Lip-1 and Fer-1.

Considerable excitement has arisen for the potential of Lip-1 and Fer-1 as preventive and/or therapeutic agents against ferroptosis involved degenerative disease although the mechanism is not clarified yet. In contrast to Lip-1 and Fer-1, lipophilic THNs are orders of magnitude faster in organic solution, very effective in liposomes to inhibit lipid peroxidation and as potent in cellular models. It is clear that lipophilic THNs inhibit lipid peroxidation and ferroptosis via scavenging lipid peroxyl radicals, a distinct mechanism from Lip-1 and Fer-1. The similar potency of lipophilic THNs to inhibit lipid peroxidation and ferroptosis studied in mammalian cells in this work suggest that the next step should be taken: bioavailability and biological activity in an animal model of degenerative disease in which lipid peroxidation and/or ferroptosis has been involved (e.g. neurodegeneration or cardiovascular disease). At first glance it would appear that the autoxidizability of the THNs may preclude any potential biological activity. However, it must be pointed out that these compounds may be better suited for *in vivo* studies than cell culture. Binding of α-TOH with human tocopherol transport protein (hTTP) protects α-TOH from being metabolized, and assists its transportation in plasma, therefore ensures their bioavailability.[39] THNs can be very good ligands for hTTP, with sidechains of eight or more carbons have affinities for hTTP which are similar to α-TOH, and THN-C15 has a 10-fold higher binding than α-TOH.[19] Binding of THNs to hTTP also precludes their permeating to aqueous phase *in vivo*, which precludes THN from autoxidation. In animal studies, THNs will be first digested in gut, where the acidic environment will preclude their autoxidation

as well.[19] Therefore, autoxidation of THNs will not be a problem *in vivo*, which is more representative than *in vitro* cellular studies. Future application of THNs in animal studies would almost certainly help in shedding definitive light on whether optimal radical-trapping antioxidants play a role in prevention and/or therapeutics of degenerative disease pathogenesis.

3.5 Conclusions

The lipophilic tetrahydronaphthyridinols, designer radical-trapping antioxidants which we have shown to possess 30-fold greater reactivity toward peroxyl radicals than α-TOH in organic solution and lipid bilayers, were found to be up to 50-fold more potent as inhibitors of lipid peroxidation in Tf1a erythroblasts and HEK-293 kidney cells. Moreover, they were far more potent as inhibitors of ferroptosis in cell models of kidney and neurodegenerative disease. The potency of THNs increased as the sidechain was systematically elongated to a dodecyl chain and then decreased slightly upon further elongation. THNs having sidechain substitution of fewer than 8 carbons were ineffective inhibitors of cellular lipid peroxidation and ferroptosis. THN-C12 and THN-C15 were 50% more potent than the recently discovered Fer-1 and Lip-1, which were identified in high-throughput screening efforts directed to uncover ferroptosis inhibitors. Since Fer-1 and Lip-1 were found to be one order of magnitude less reactive in organic solution and more than 50-fold less effective in lipid bilayers than α-TOH, the mechanism behind their biological activity is unlikely to be radical-trapping. THN acetates are more stable than the free phenolic THNs, however, they did not exhibit greater potency in any cell studies we carried out, presumably due to slow hydrolysis to give rise to the reactive THN RTA. Although THNs are more oxidizable compared to α-TOH, their optimized radical-trapping kinetics, greater stability of the THN derived radicals compared to α-TOH derived radical and similar or greater affinity for the human tocopherol transport protein suggest that they are excellent candidates for study in animal models of disease in which ferroptosis and/or accumulation of lipid hydroperoxides have been implicated.

3.6 Experimental Section

Materials.C11-BODIPY$^{581/591}$(4,4-difluoro-5-(4-phenyl-1,3-butadienyl)-4-bora-3a,4a-diazsi ndacene-3-undecanoic acid), RPMI-1640 media with/without phenol red, MEM media with/without phenol red, non-essential amino acid (100×), fetal bovine serum (FBS), penicillin-streptomycin, Dulbecco's phosphate buffered saline (DPBS), MTT (3-(4,5-dimethylthiazol-2-yl)-2,5-diphenyltetrazolium bromide), Hank's balanced salt solution (HBSS) were purchased from commercial sources and used as received. Fer-1, Lip-1 and (*1S, 3R*)-RSL3 were used as obtained.

Synthesis of 2,4-dimethyl-8-(3,7,11-trimethyldodecyl)-5,6,7,8-tetrahydro-1,8-naphthyridin-3-yl acetate (C15 acetate). THN-C15[19] (0.05 mmol) was dissolved in 5 ml dry DMF, triethylamine (0.1 mmol) was added to the reaction mixture followed by acetic anhydride (0.15 mmol). The reaction was stirred under inert atmosphere at 60 °C overnight. Product was then purified by prep-TLC using 5 % EtOAc: 95 % hexane. (0.016 g, 74 %). ^{1}H NMR (400 MHz, $CDCl_3$): δ 3.59-3.54 (m, J = 8 Hz, 2H), 3.25 (t, J = 8 Hz, 2H), 2.58 (t, J = 8 Hz, 2H), 2.28 (s, 3H), 2.15 (s, 3H), 1.92-1.86 (m, 5H), 1.58-1.01 (m, 17H), 0.92-0.82 (m, 12H); ^{13}C NMR (125 MHz, $CDCl_3$): δ 169.78, 152.98, 144.56, 136.45, 135.34, 113.04, 47.12, 46.70, 39.33, 37.39, 37.29, 33.85, 32.77, 30.78, 27.95, 24.80, 24.78, 24.72, 24.33, 22.71, 22.61, 21.64, 20.55, 19.81, 19.66, 19.26, 12.15; HRMS (EI) calcd for $C_{27}H_{46}N_2O_2$ [M] 430.3559, obsd 430.3525

Synthesis of 8-butyl-2,4-dimethyl-5,6,7,8-tetrahydro-1,8-naphthyridin-3-yl acetate (C4 acetate). THN-C4[19] (0.05 mmol) was dissolved in 5 ml dry DMF, triethylamine (0.1 mmol) was added to the reaction mixture followed by acetic anhydride (0.15 mmol). The reaction was stirred under inert atmosphere at 60 °C overnight. Product was then purified by prep-TLC using 10 % EtOAc: 90 % hexane. (0.009 g, 70 %). ^{1}H NMR (400 MHz, $CDCl_3$): δ 3.54 (t, J = 8 Hz, 2H), 3.26 (t, J = 8 Hz, 2H), 2.58 (t, J = 8 Hz, 2H), 2.28 (s, 3H), 2.15 (s, 3H), 1.92-1.86 (m, 5H), 1.56-1.49 (m, 2H), 1.36-1.26 (m, 2H), 0.92 (t, J = 8 Hz, 3H); ^{13}C NMR (100 MHz, $CDCl_3$): δ 169.70, 153.04, 144.54, 136.45, 135.40, 113.00, 48.30, 47.35, 29.35, 24.73, 21.63, 20.52, 20.26, 19.24, 14.00, 12.12; HRMS (EI) calcd for $C_{16}H_{24}N_2O_2$ [M] 276.1838, obsd 276.1843

Cellular Lipid Peroxidation. Tf1a cells were cultured in RPMI-1640 media with 10% FBS and 1% penicillin-streptomycin. HEK 293 cells were cultured in MEM media with 10% FBS, 1% non-essential amino acid, 1 mM sodium pyruvate and 1% penicillin-streptomycin. Cells (5×10^5 cells/mL) were treated with each antioxidant at different concentrations and incubated at 37 °C for 5 hours or 22 hours in phenol red-free RPMI-1640 media with 10% FBS and 1% penicillin-streptomycin for Tf1a cells and phenol red-free MEM media with 10% FBS, 1% non-essential amino acid, 1 mM sodium pyruvate and 1% penicillin-streptomycin for HEK 293 cells in a humidified atmosphere containing 5% CO_2 in air. Cells were then treated with 1 μM C11-BODIPY$^{581/591}$ in media and incubated at 37 °C in dark for 30 minutes after which oxidative stress was induced with diethylmaleate (9 mM) for 2 hours. Cells were then analyzed by flow cytometry at a final concentration of 5×10^5 cells/ml (λ_{ex} = 488 nm; λ_{em} = 525±25 nm). Cells not treated with DEM were used as negative control. Cells not treated with antioxidants were used as positive control.

Inhibition of Ferroptosis Induced by Gpx4. Pfa1 cells were cultured at 37 °C in a 10% CO_2 atmosphere and DMEM containing 10% FBS, 10 mM glutamine, 100 IU/ml penicillin and 100 μg/ml streptomycin. Cells were passaged by dissociation with 0.05% trypsin and 0.2% EDTA every other day. 1000 Pfa1 cells were seeded in 100 μL into 96 well plates in the presence of 1 μM Tamoxifen. Compounds tested were added 24 hour later and viability was assessed using the Aquabluer (aquaplasmid) at the end of 48h in the presence of tamoxifen. Aquabluer assay: at the end of the incubation period, the media was removed and cells were incubated for 5h with a 100x diluted Aquabluer solution, as recommended by the manufacturer. Subsequently viability was assessed by reading the fluorescence ((λ_{ex} = 540 nm, λ_{em} = 590 nm) in a plate reader. Percentage of cell viability was calculated by normalizing the data to the untreated controls.

Inhibition of Ferroptosis Induced by (1S, 3R)-RSL3. 3000 Pfa1 cells were seeded in 100 μL into 96 well plates, after 6h a mixture of linoleic acid (10 μM) and BSA (0.1%) was added overnight to the cells. The next day media was exchanged and washed twice with PBS and tested compound were pre-incubated for 30 minutes before addition of 100 nM

(1S, 3R)-RSL3 in a final volume of 100 µl. Cell viability was assessed 6 hours after (1S, 3R)-RSL3 addition. Viability was assessed using the Aquabluer assay according to manufcturar instructions (aquaplasmid).

Inhibition of Glutamate Toxicity and Cell Death in Mouse Hippocampal Cells. HT22 cells were cultured at 37 °C in a 10% CO_2 atmosphere and DMEM containing 10% FBS, 10 mM glutamine, 100 IU/ml penicillin and 100 μg/ml streptomycin. Cells were passaged by dissociation with 0.05% trypsin and 0.2% EDTA every other day. 3000 HT22 cells were seeded in 100 µL into 96-well plates. To induce cell death, glutamate (5mM) was added 24 h after plating for 10 h and subsequently viability was assessed using Aquabluer. Lipid peroxidation levels were assessed using C11-BODIPY$^{581/591}$. Briefly, C11-BODIPY$^{581/591}$ (1 µM) was added for 30 min at the end of the 10h incubation with glutamate, cells were trypsinized, washed and resuspended in PBS; flow cytometry was performed using 488 nm UV line argon laser for excitation and BODIPY emission was recorded on channels FL1 at 530 nm (green) and FL2 at 585 nm (red). Data were collected from at least 30 000 cells. Total glutathione in the cells was measured by the enzymatic method described previously,[40] which is based on the catalytic action of glutathione reductase system. 100 nM of the different compounds were pre-incubated for 1h before glutamate addition.

MTT cell viability assay. HepG2 cells were cultured in MEM media with 10 % FBS, 1 % non-essential amino acid, 1 mM sodium pyruvate and 1% penicillin-streptomycin. HepG2 cells (1×10^5 cells) were added to 96 well plate and incubate overnight or until confluent. Cells in each well were then treated with each antioxidant in DMSO at different concentrations (final DMSO concentration was to not exceeds 1 % by volume) in 100 µL MEM media with no phenol red, supplemented with 10 % FBS, 1 % non-essential amino acid, 1 mM sodium pyruvate and 1% penicillin-streptomycin. After incubation at 37°C for 22 hours in phenol red-free media in a humidified atmosphere containing 5% CO_2 in air in a 96 well plate, the 96 well plate was centrifuged at 300×g for 5 min and medium was aspirated. 200 µL of fresh MEM media with no phenol red supplemented with 10 % FBS, 1 % non-essential amino acid, 1 mM sodium pyruvate and 1% penicillin-streptomycin and 50 µL of MTT (5mg/mL) in HBSS was added into each well. After 4 hrs incubation, the

treated cells were centrifuged at 300×g for 5 minutes and the medium was aspirated. The resultant purple crystals were dissolved with 200 μL isopropanol solution with 0.1 M HCl and 10 % by volume Triton X-100. After 3 hrs incubation at room temperature to dissolve the resultant purple crystals in the dark, absorbance (λ = 570 nm) was measured by microplate reader. Results are compared to a negative control (1 % DMSO, no antioxidant treated) and a positive control (1 % Triton X-100). In a control experiment, no toxicity was observed for DMSO up to 1 % volume.

Stability of THN (C15, C15 acetate), Fer-1, Lip-1 and α-TOH. The stability of THN (C15, C15 acetate), Fer-1 and Lip-1 were determined in PBS buffer (pH 7.4) at 10 μM in the presence of 2 μM THNC10-OMe[19] as the internal standard at 37°C in triplicate. Each of the compounds were determined as their conjugate acid by reverse-phase HPLC with ESI-MS detection in positive ion mode. THN-C15 and THN-C15 acetate were analyzed using an Acquity UPLC C18 column (1.7 μm, 2.1×50 mm) with mobile phase 28% water and 70% methanol and 2% of water with 2% (volumn) formic acid flowing at 0.2 mL/min. Lip-1 was analyzed using an Acquity UPLC C18 column (1.7 μm, 2.1×50 mm) with mobile phase 75% methanol and 25% water flowing at 0.1 mL/min. Fer-1 was analyzed using an XBridge C8 column (2.5 μm, 4.6×75 mm) with mobile phase 15% water and 85% methanol flowing at 0.4 mL/min. THN-C15 was quantified by MS (SIR) ($[M+H]^+$ = 389, t_R = 17.1 min; C10-OMe: $[M+H]^+$ = 333, t_R = 2.3 min). THN-C15 acetate was quantified by MS (SIR) ($[M+H]^+$ = 431, t_R = 23.1 min; C10-OMe: $[M+H]^+$ = 333, t_R = 2.6 min). Fer-1 was quantified by MS (SIR) ($[M+H]^+$ = 263, t_R = 3.0 min; C10-OMe: $[M+H]^+$ = 333, t_R = 11.2 min). Lip-1 was quantified by MS (SIR) ($[M+H]^+$ = 341, t_R = 2.6 mins; C10-OMe: $[M+H]^+$ = 333, t_R = 6.7 mins). Stability of α-TOH was determined by monitoring the decreasing of absorbance at 300 nm.

Voltammetry. Standard potentials for the oxidation of THN (C15) (in the presence of 1 equivalent triethylamine), THN-C15 acetate, Fer-1, Lip-1 were determined from cyclic voltammagrams measured using a three-electrode cell equipped with a glassy carbon working electrode, a platinum counter electrode, and an $Ag/AgNO_3$ reference electrode. Voltammagrams were obtained in dry acetonitrile using $Bu_4N{\cdot}PF_6$ (0.1 M) as electrolyte at

room temperature. All potentials are reported vs the normal hydrogen electrode (NHE) via reference to the ferrocene/ferrocenium couple.

Inhibited autoxidation of styrene. Styrene was washed 3× with 1 M aqueous NaOH, dried over $MgSO_4$, filtered, distilled under vacuum and purified by percolating through silica, then basic alumina. Synthesis of PBD-BODIPY and determination of the propagation rate constant with styrene peroxyl radicals is reported by Haidasz *et al.*[24] To a cuvette of 1.25 mL styrene and 1.18 mL chlorobenzene at 37°C was added 11 μL of 2 mM PBD-BODIPY in 2,3,5-trichlorobenzene followed by 50 μL of 0.3 M AIBN in chlorobenzene and thoroughly mixed. After 20 min, 10 μL of Lip-1, Fer-1 or α-TOH stock solution in chlorobenzene was added and the loss of absorbance followed at 591 nm. Final concentration of Lip-1, Fer-1 and α-TOH is 2, 3, 4 μM. In the case of THN-C15, 10 μL of 1 mM Et_3N was added followed immediately by 10 μL of 1 mM THN-C15 as an oxalate salt giving final concentration of THN-C15 as 2, 3, 4 μM. The experimental data was fit to a model using COPASI to determine the second order rate constant. k_{inh} was determined with the Parameter Estimation feature of COPASI using a model of styrene autoxidation. Autoxidations were completed in triplicate.

Inhibited oxidations in Liposomes. To individual 21.4 μL aliquots of the 20 mM liposome solution were added increasing amounts (0.75, 1.5, 2.25, 3, and 3.75 μL, respectively) of 857 μM tested compound in DMSO and 5 μL of 12.9 μM H_2B-PMHC in acetonitrile. Each resultant solution was diluted to 400 μL with PBS pH 7.4 buffer and 280 μL was loaded into a well of a 96-well microplate. The plate was equilibrated to 37°C for 5 min, after which 20 μL of 40.5 mM 2,2'-azobis-(2-amidinopropane)monohydrochloride (AAPH) in PBS pH 7.4 buffer or 10.1 mM 2,2'-azobis-(4-methoxy-2,4-dimethylvaleronitrile) (MeO-AMVN) in acetonitrile was added to each well. The fluorescence was then monitored at 50 s time intervals (λ_{ex} = 485 nm; λ_{em} = 520 nm). The final solutions in each well were 1 mM lipids, 0.15 μM H_2B-PMHC, and 2.7 mM AAPH or 0.68 mM MeOAMVN and either 1.5, 3, 4.5, 6 or 7.5 μM antioxidant. Antioxidants were incubated with liposomes for 0 hr, 5 hrs and 22 hrs before adding H_2B-PMHC and initiators when testing the effect of incubation time.

3.7 References

[1] Vitale, G.; Salvioli, S.; Franceschi, C., *Nat. Rev. Endocrinol* **2013,** *9* (4), 228-240.

[2] Jenner, P. *Ann. Neurol.* **2003,** *53 Suppl 3*, S26-36; discussion S36-28.

[3] Fuchs, Y.; Steller, H. *Cell* **2011,** *147* (4), 742-758.

[4] Edinger, A. L.; Thompson, C. B. *Curr. Opin. Cell Biol.* **2004,** *16* (6), 663-669.

[5] Dixon, S. J.; Lemberg, K. M.; Lamprecht, M. R.; Skouta, R.; Zaitsev, E. M.; Gleason, C. E.; Patel, D. N.; Bauer, A. J.; Cantley, A. M.; Yang, W. S.; Morrison, B.; Stockwell, B. R. *Cell* **2012,** *149* (5), 1060-1072.

[6] Yang, W. S.; Stockwell, B. R. Ch*em. Biol.* **2008,** *15* (3), 234-245.

[7] Friedmann Angeli, J. P.; Schneider, M.; Proneth, B.; Tyurina, Y. Y.; Tyurin, V. A.; Hammond, V. J.; Herbach, N.; Aichler, M.; Walch, A.; Eggenhofer, E.; Basavarajappa, D.; Radmark, O.; Kobayashi, S.; Seibt, T.; Beck, H.; Neff, F.; Esposito, I.; Wanke, R.; Forster, H.; Yefremova, O.; Heinrichmeyer, M.; Bornkamm, G. W.; Geissler, E. K.; Thomas, S. B.; Stockwell, B. R.; O'Donnell, V. B.; Kagan, V. E.; Schick, J. A.; Conrad, M. *Nat. Cell. Biol.* **2014,** *16* (12), 1180-1191.

[8] Yang, W. S.; SriRamaratnam, R.; Welsch, M. E.; Shimada, K.; Skouta, R.; Viswanathan, V. S.; Cheah, J. H.; Clemons, P. A.; Shamji, A. F.; Clish, C. B.; Brown, L. M.; Girotti, A. W.; Cornish, V. W.; Schreiber, S. L.; Stockwell, B. R. *Cell* **2014,** *156* (1-2), 317-331.

[9] (a) Circu, M. L.; Aw, T. Y. *Free Radic. Biol. Med.* **2010,** *48* (6), 749-762; (b) Di Paolo, G.; Kim, T. W. *Nat. Rev. Neurosci.* **2011,** *12* (5), 284-296.

[10] Kuhn, H.; Borchert, A. *Free Radic. Biol. Med.* **2002,** *33* (2), 154-172.

[11] Girotti, A. W. *J. Lipid Res.* **1998,** *39* (8), 1529-1542.

[12] Skouta, R.; Dixon, S. J.; Wang, J.; Dunn, D. E.; Orman, M.; Shimada, K.; Rosenberg, P. A.; Lo, D. C.; Weinberg, J. M.; Linkermann, A.; Stockwell, B. R. *J. Am. Chem. Soc.* **2014,** *136* (12), 4551-4556.

[13] Ingold, K. U.; Pratt, D. A. *Chem. Rev.* **2014,** *114* (18), 9022-9046.

[14] Burton , G. W.; Ingold, K. U. *Acc. Chem. Res.* **1986,** *19* (7), 194-201.

[15] Pratt, D. A.; DiLabio, G. A.; Brigati, G.; Pedulli, G. F.; Valgimigli, L. *J. Am. Chem. Soc.* **2001,** *123* (19), 4625-4626.

[16] Wijtmans, M.; Pratt, D. A.; Valgimigli, L.; DiLabio, G. A.; Pedulli, G. F.; Porter, N. A.,

Angew. Chem. Int. Ed. Engl. **2003,** *42* (36), 4370-4373.

[17] Valgimigli, L.; Pratt, D. A. *Acc. Chem. Res.* **2015,** *48* (4), 966-975.

[18] Nam, T. G.; Rector, C. L.; Kim, H. Y.; Sonnen, A. F.; Meyer, R.; Nau, W. M.; Atkinson, J.; Rintoul, J.; Pratt, D. A.; Porter, N. A. *J. Am. Chem. Soc.* **2007,** *129* (33), 10211-10219.

[19] Li, B.; Harjani, J. R.; Cormier, N. S.; Madarati, H.; Atkinson, J.; Cosa, G.; Pratt, D. A., *J. Am. Chem. Soc.* **2013,** *135* (4), 1394-1405.

[20] Drummen, G. P.; van Liebergen, L. C.; Op den Kamp, J. A.; Post, J. A. *Free Radic. Biol. Med.* **2002,** *33* (4), 473-490.

[21] Lewerenz, J.; Hewett, S. J.; Huang, Y.; Lambros, M.; Gout, P. W.; Kalivas, P. W.; Massie, A.; Smolders, I.; Methner, A.; Pergande, M.; Smith, S. B.; Ganapathy, V.; Maher, P. *Antioxid. Redox Signal* **2013,** *18* (5), 522-555.

[22] Mandal, P. K.; Seiler, A.; Perisic, T.; Kolle, P.; Banjac Canak, A.; Forster, H.; Weiss, N.; Kremmer, E.; Lieberman, M. W.; Bannai, S.; Kuhlencordt, P.; Sato, H.; Bornkamm, G. W.; Conrad, M. *J. Biol. Chem.* **2010,** *285* (29), 22244-22253.

[23] Plumb, J. A. *Methods Mol. Med.* **1999,** *28*, 25-30.

[24] Haidasz, E. A.; Kessel, A. V.; Pratt, D. A., *J. Org. Chem.*, **2016**, *81* (3), 737–744.

[25] Ingold, K. U. *Chem. Rev.* **1961,** *61* (6), 563-589.

[26] Krumova, K.; Friedland, S.; Cosa, G. *J. Am. Chem. Soc.* **2012,** *134* (24), 10102-10113.

[27] Laguerre, M.; Lopez Giraldo, L. J.; Lecomte, J.; Figueroa-Espinoza, M. C.; Barea, B.; Weiss, J.; Decker, E. A.; Villeneuve, P. *J. Agric. Food Chem.* **2010,** *58* (5), 2869-2876.

[28] Laguerre, M.; Giraldo, L. J.; Lecomte, J.; Figueroa-Espinoza, M. C.; Barea, B.; Weiss, J.; Decker, E. A.; Villeneuve, P. *J. Agric. Food Chem.* **2009,** *57* (23), 11335-11342.

[29] Saito, Y.; Yoshida, Y.; Nishio, K.; Hayakawa, M.; Niki, E. *Ann. N Y Acad. Sci.* **2004,** *1031*, 368-375.

[30] Niki, E.; Noguchi, N. *Acc. Chem. Res.* **2004,** *37* (1), 45-51.

[31] Barclay, L. R. C.; Ingold, K. U. *J. Am. Chem. Soc.* **1981,** *103* (21), 6478-6485.

[32] (a) Harris, P. L.; Ludwig, M. I. *J. Biol. Chem.* **1949,** *180* (2), 611-614; (b) Burton, G. W.; Traber, M. G. *Annu. Rev. Nutr.* **1990,** *10*, 357-382.

[33] Bridges, R.; Lutgen, V.; Lobner, D.; Baker, D. A. *Pharmacol. Rev.* **2012,** *64* (3), 780-802.

[34] Burton, G. W.; Doba, T.; Gabe, E. J.; Hughes, L.; Lee, F. L.; Prasad, L.; Ingold, K. U. *J. Am. Chem. Soc.* **1985,** *107* (24), 7053-7065.

[35] Valgimigli, L.; Amorati, R.; Fumo, M. G.; DiLabio, G. A.; Pedulli, G. F.; Ingold, K. U.; Pratt, D. A. *J. Org. Chem.* **2008,** *73* (5), 1830-1841.

[36] Kremer, M. L. *Phys. Chem. Chem. Phys.* **1999,** *1*, 3595-3605.

[37] Brash, A. R. *J. Biol. Chem.* **1999,** *274* (34), 23679-23682.

[38] Hong, F.; Sekhar, K. R.; Freeman, M. L.; Liebler, D. C. *J. Biol. Chem.* **2005,** *280* (36), 31768-31775.

[39] Dutta-Roy, A. K.; Gordon, M. J.; Campbell, F. M.; Duthie, G. G.; James, W. P. T, *J. Nutr. Biochem.*, **1994,** *5* (12), 562-570.

[40] Sato, H.; Shiiya, A.; Kimata, M.; Maebara, K.; Tamba, M.; Sakakura, Y.; Makino, N.; Sugiyama, F.; Yagami, K.; Moriguchi, T.; Takahashi, S.; Bannai, S. *J. Biol. Chem.* **2005,** *280* (45), 37423-37429.

Chapter 4:

On the Molecular Mechanisms of the Medicinal Thiosulfinates from Garlic and Petiveria

4.1 Preface

We recently reported the results of our efforts towards understanding the molecular mechanisms of allicin and petivericin, the thiosulfinates widely believed to be responsible for the medicinal properties of garlic and *Petiveria alliacae*, respectively (Li, B.; Zheng, F.; Chauvin, J-P. R.; Pratt, D. A., The medicinal thiosulfinates from garlic and Petiveria are not radical-trapping antioxidants in liposomes and cells, but lipophilic analogs are, *Chem. Sci.*, **2015**, *6*, 6165-6178). Therein, the radical-trapping antioxidant activities of allicin, petivericin and a lipophilic (hexylated) analog of petivericin were assayed in egg phosphatidylcholine lipid bilayers, as well as in human Tf1a erythroblasts and HEK-293 kidney cells. The results indicate that both compounds are surprisingly ineffective, in sharp contrast with previous studies in organic solution which showed that they undergo facile Cope elimination to produce sulfenic acids – potent radical-trapping agents. In an effort to understand the medium dependence of this activity, a more lipophilic (hexylated) analog of petivericin was synthesized and shown to be among the most effective RTAs known, but only in the presence of a hydrophilic thiol (*e.g. N*-acetylcysteine). Additional symmetric and unsymmetric thiosulfinates were synthesized to shed light on the structural features that underlie this reactivity. These studies reveal that amphiphilic thiosulfinates which undergo *S*-thiolation with a hydrophilic thiol to give lipophilic sulfenic acids are required, and that an activated methylene group – key to promote Cope elimination – is not. Interestingly, the added thiol was also found to regenerate the sulfenic acid following its reaction with peroxyl radicals. This activity was diminished at more acidic pH, suggesting that it occurs by electron transfer from the thiolate. Allicin, petivericin and hexylated petivericin were assayed as inhibitors of lipid peroxidation in human TF1a erythroblasts

and HEK-293 kidney cells, revealing similar efficacies in the low μM range – the same range in which allicin and petivericin were found to induce cell death concomitant with, or as a result of, glutathione (GSH) depletion. In contrast, hexylated petivericin was not cytotoxic throughout the concentration range assayed, and had no effect on GSH levels. Taken together, the results in lipid bilayers and in cell culture suggest that the greater lipophilicity of hexylated petivericin enables it to partition to membranous cell compartments where it forms a lipid-soluble sulfenic acid that traps peroxyl radicals, whereas allicin and petivericin partition to the cytosol where they deplete GSH and induce cell death. This chapter is presented largely as it was in the manuscript, but includes supplementary results. The thiosulfinates were synthesized by Dr. Feng Zheng, a former post-doctoral researcher in the Pratt lab. Radical-trapping antioxidant activity measurements in liposomes were carried out in collaboration with Dr. Feng Zheng.

4.2 Introduction

A staggering number of purported antioxidants have been found in Nature.[1] Most of these compounds contain phenolic moieties, such as in curcumin and resveratrol (**Chart 4.1**), the compounds believed to be responsible for the medicinal properties of turmeric and red wine. Garlic (and some other members of the allium genus of plants) has been used medicinially for millennia, and much of its biological activity has recently been ascribed to the antioxidant properties of the organosulfur compounds which are abundant in them.[2] Organosulfur compounds are important components of allium plants, and may comprise up to 5% dry weight of the organism.[2] Of these, allicin (**Chart 4.1**) is widely believed to be the most bioactive compound in garlic.[3] Allicin is formed through an enzymatic process that occurs when crushing garlic cloves. When crushing the cloves, 2-propenesulfenic acid is formed from S-allyl-cysteine-S-oxide (the non-proteinogenic amino acid alliin) by enzymatic cleavage of the C-S bond by alliinase. Two 2-propenesulfenic acid molecules condense to form allicin (**Scheme 4.1**). Allicin has demonstrated biocidal activities against several types of microorganisms including yeast, fungi and bacteria.[4,5] Recent research has focused on its potential chemopreventive properties against cardiovascular disease, neurodegenerative disease and cancer.[6,7] Petivericin is a similar thiosulfinate (**Chart 4.1**)

derived from *Petiveria alliacae*, a plant which used in folk medicines in South and Central America for hundreds of years.[8] The biological activity of *Petiveria* extracts has been ascribed to petivericin's antioxidant properties.[9]

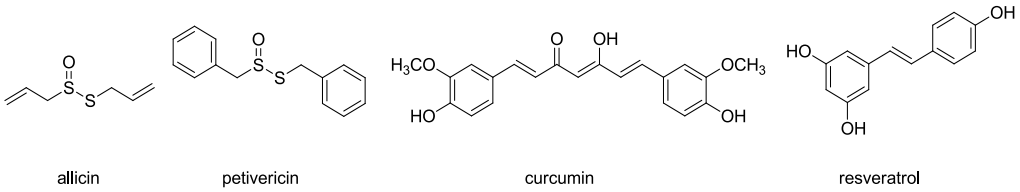

Chart 4.1. Natural health promoting "antioxidants".

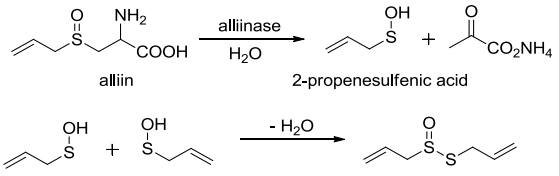

Scheme 4.1. Generation of allicin from garlic.

The medicinal properties of allicin are often ascribed to its controversial "antioxidant" activity.[10,11] The controversy surrounds the fact that while many reports show that allicin traps radicals or induces phase II antioxidant enzymes, a similar number of reports suggest that it is highly cytotoxic. In early work, allicin was shown to inhibit lipid peroxidation in liver homogenates by scavenging hydroxyl radicals in a concentration dependent manner,[12] and a rate constant for its reaction with hydroxyl radicals was estimated to be 2×10^8 $M^{-1}s^{-1}$.[13] However, as others have already correctly noted,[14] essentially all organic molecules react with hydroxyl radicals at or near diffusion controlled rates, making it unlikely that this reactivity underlies allicin's biological activities. The trapping of peroxyl radicals is far more relevant as they react relatively discriminately,[15,16] carrying the chain reaction that peroxidizes lipids to products that have been implicated in degenerative disease onset and progression.[17,18]

A few years ago, it was suggested that allicin behaves as a RTA by trapping chain-carrying peroxyl radicals through the allylic H-atom adjacent to the divalent sulfur atom in the inhibited autoxidation of cumene or methyl linoleate at k_{inh} 2.6×10^3 and 1.6×10^5 $M^{-1}s^{-1}$, respectively (**Scheme 4.2**).[19] Their result suggests that allicin is a moderate

radical-trapping antioxidant, 20-fold less reactive than α-TOH (k_{inh}= 3.2×10^6 M^{-1} s^{-1}),[20] the most potent form of vitamin E and Nature's premier lipophilic RTA.[21] They also suggest that petivericin behaves similar to allicin and it is assumed that petivericin traps peroxyl radical by the benzylic H-atom.[9] However, this suggested mechanism is unlikely for two reasons. First, rate constants for H-atom transfer from carbon to peroxyl radicals are several orders of magnitude lower than the apparent k_{inh} determined from the allicin/petivericin inhibited autoxidation.econd, carbon-centered radicals generally react with O_2 to yield peroxyl radicals at – or near diffusion-controlled rate, which will propagate the autoxidation chain reaction rather than inhibiting the autoxidation reaction.[22] On the other hand, diallyl disulfide is not an effective RTA, made evident by its inability to inhibit the autoxidation of styrene or cumene initiated by azo compounds.[23] The rate constant for transfer of the allylic H-atom transfer to peroxyl radicals was estimated to be only ca. 1.6 M^{-1} s^{-1}.[23] Furthermore, adding an oxygen atom on one of the sulfur atoms in diallyl disulfide – as in allicin – is not expected to change the reactivity of the allylic H-atom (the C-H BDEs calculated using CBS-QB3 are 82.4 and 81.8 kcal/mol, respectively).[24]

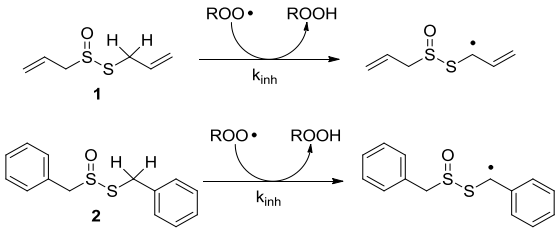

Scheme 4.2. Proposed mechanism by which allicin (**1**) and petivericin (**2**) trap peroxyl radicals.[19]

Intrigued by the reported high reactivity of allicin toward peroxyl radicals despite the fact that it is devoid of any of the structural features common to good RTAs (e.g. an electron-rich phenolic moiety such as in α-TOH),[21,25] our lab investigated the mechanism of peroxyl radical-trapping by allicin. Allicin undergoes a 5-centre Cope elimination to give 2-propenesulfenic acid (**Scheme 4.3**), a reaction that has historically made allicin a difficult molecule to study.[26] Several years ago, our groups demonstrated that in organic solvents, both allicin (**1**) and petivericin (**2**) are not RTAs, as they both undergo facile Cope elimination to produce sulfenic acids-which are potent radical-trapping agents (**Scheme 4.3**).[24,27]

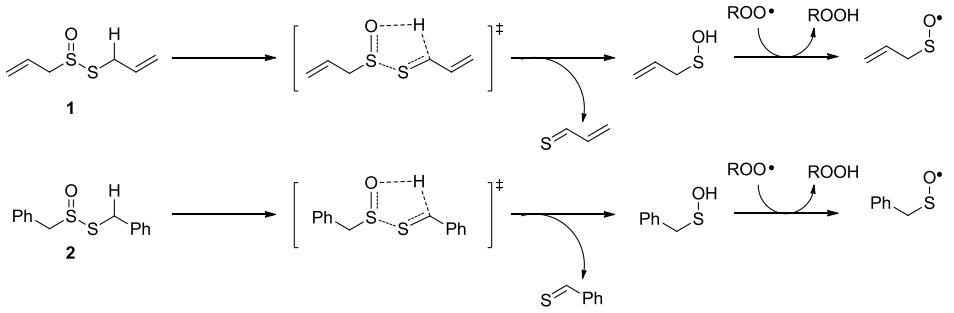

Scheme 4.3. Cope elimination of allicin (**1**) and petivericin (**2**).

In early experiments, the addition of a hydrogen bond donating co-solvent (hexafluoroisopropanol) to allicin inhibited autoxidations of methyl linoleate. It was suggested that the added H-bond donor retarded the decomposition of allicin, precluding sulfenic acid formation (**Scheme 4.4**).[27] This solvent effect would not be observed if the radical-trapping activity of allicin was HAT from the methylene group in allicin. It has been shown that each allicin or petivericin can trap one chain-carrying peroxyl radical in inhibited autoxidations.[24,27]

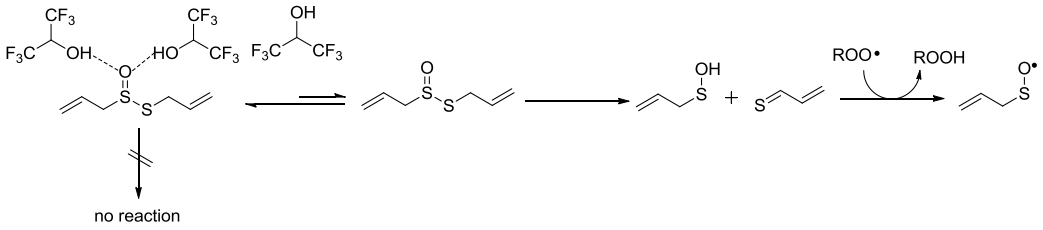

Scheme 4.4. Kinetic solvent effect for Cope elimination of allicin.

Due to the rapid self-condensation reactions of allyl and phenylmethane sulfenic acids,[28] sulfenic acids derived from allicin and petivericin cannot be isolated to study their radical-trapping activities. Theoretical calculation of the O-H BDE in sulfenic acid RSOH was 68.6 kcal/mol for R=$PhCH_2$ and $C_2H_3CH_2$ (roughly the same as in hydroxylamines, such as TEMPO-H),[27] which indicated sulfenic acids derived from petivericin and allicin would be outstanding RTAs. A deuterium kinetic isotope effect (DKIE) was measured to be 4.5 for the Cope elimination of petivericin and overall DKIE of 18.2 for the reaction between petivericin and peroxyl radicals using the radical clock method.[29] To study the kinetics of sulfenic acid in the oxidation of hydrocarbons, our lab synthesized a persistent sulfenic acid, 9-triptycenesulfenic acid (**3** in **Scheme 4.5**). Radical equilibriation

experiments showed that **3** had one of the weakest O-H BDEs known (72 kcal/mol),[30] indicating that the thermodynamics of the formal H-atom transfer to peroxyl radicals was indeed quite favourable. Subsequent inhibited autoxidations of styrene revealed that 9-triptycenesulfenic acid reacted with peroxyl radicals (**Scheme 4.5**) with a second order rate constant of 3×10^6 M^{-1} s^{-1} – indistinguishable from that of Nature's best RTA, α-TOH.

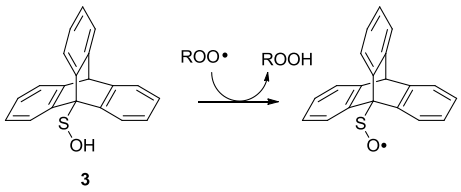

3

Scheme 4.5. 9-triptycenesulfenic acid traps peroxyl radicals.

A rate constant for the reaction of petivericin derived α-toluenesulfenic acid with peroxyl radicals could be estimated to be k_{inh} = 3×10^7 $M^{-1}s^{-1}$ by fitting the data from autoxidations inhibited by petivericin to the standard kinetic scheme for a RTA-inhibited autoxidation modified to include this key Cope elimination pre-equilibrium.[29] This rate constant agreed well with the earlier computations,[27] indicating α-toluenesulfenic acid derived from petivericin had 10-fold greater reactivity toward peroxyl radicals than α-TOH.

The previous results in organic solution prompted us to study whether the above mentioned mechanisms of allicin and petivericin would be relevant in biological systems. We decided to study the activities of allicin and petivericin in egg phosphatidylcholine (EggPC) lipid bilayers as a model for mammalian cells as the next step. The relative reactivities of allicin and petivericin were determined in EggPC liposomes using the H_2B-PMHC probe mentioned in **Chapter 2**, a recently developed analog of α-TOH which undergoes fluorescence enhancement upon reaction with peroxyl radicals (ROO•).[31] The results showed that neither allicin nor petivericin were able to slow the oxidation of the H_2B-PMHC fluorescent probe by trapping peroxyl radicals derived from either water- or lipid-soluble azo initiator, AAPH or MeOAMVN in EggPC liposomes over the concentration range we studied (up to 22.5 μM).[32] This indicates that both of them were far less reactive than α-TOH in liposomes (at least 100 fold).[32] However, oxidation of the H_2B-PMHC probe in the presence of 9-triptycenesulfenic acid (**3**) was dramatically slowed

down, which means that sulfenic acid was a good peroxyl radical trapping agent in liposomes. Kinetic analysis of the data demonstrated that 9-triptycenesulfenic acid (**3**) reacted with peroxyl radicals with a rate constant that is at least 10 fold faster than that of H_2B-PMHC probe. It was concluded that each 9-triptycenesulfenic acid (**3**) trapped one peroxyl radical in liposomes, the same as in organic solution. We hypothesized that the poor radical-trapping activities of allicin or petivericin in liposomes might be explained by their partitioning to the aqueous phase in the lipid bilayer, where Cope elimination to produce the sulfenic acid was slowed dramatically by H-bonding, and the sulfenic acids derived therefrom partitioned to the aqueous phase and underwent other reactions. In an effort to understand the medium-dependence of the reactivities of allicin and petivericin, a more lipophilic analog of petivericin, hexylated petivericin (**4** in **Scheme 4.6**), was synthesized.[32] Results showed that hexylated petivericin (**4**) also failed to effectively inhibit oxidation of the probe, as it was only able to slightly retard the oxidation of probe but did not display a clear inhibited period. However, in the presence of a hydrophilic thiol *N*-acetylcysteine (NAC), hexylated petivericin (**4**) was an excellent RTA, conditions that did not improve the poor reactivity of allicin and petivericin.

To account for these observations, the mechanism shown in **Scheme 4.6** was proposed, where S-thiolation of **4** by NAC produces a lipophilic sulfenic acid which traps lipophilic peroxyl radicals and can be regenerated via reaction with another molecule of NAC at the bilayer interface.[32] Herein, we have in the interim expanded the scope of our investigations to: (1) elucidate the structural factors that contribute to the efficacy of hexylated petivericin as a RTA in lipid bilayers, (2) provide experimental support for our proposed mechanism, and (3) include a comparative study of the antioxidant activity and cytotoxicity of allicin, petivericin and hexylated petivericin in mammalian cell culture. Cytotoxicity studies were carried out in parallel with the lipid peroxidation inhibition studies. Further experiments to support the different activities of allicin, petivericin and the lipophilic thiosulfinate hexylated petivericin are described as well.

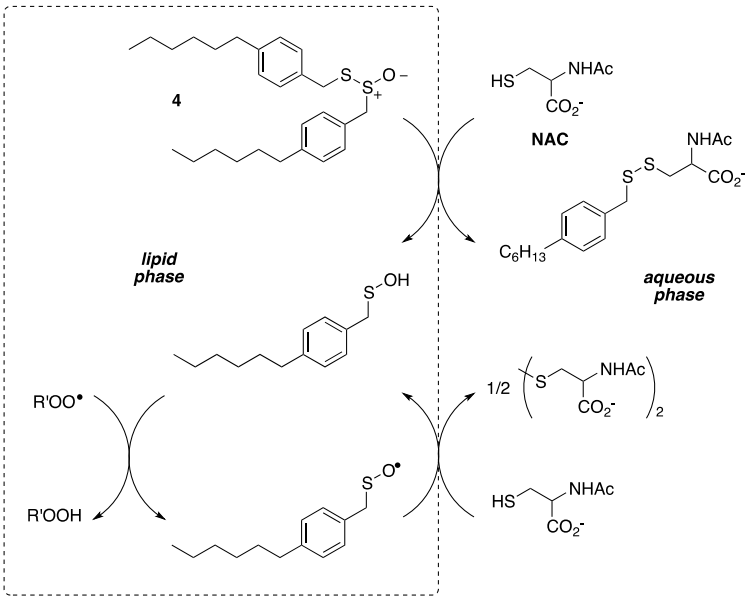

Scheme 4.6. Proposed mechanism for the radical-trapping antioxidant activity of hexylated petivericin (**4**) in the presence of *N*-acetylcysteine (NAC).

4.3 Results

4.3.1 Phosphatidylcholine Liposome Oxidation – Competition with H_2B-PMHC

Allicin (**1**) was synthesized according to the previous report and purified by preparative TLC using 5% EtOAc in hexane immediately before using.[27] Petivericin (**2**),[24] 9-triptycenesulfenic acid (**3**),[30] hexylated petivericin (**4**),[32] symmetrical n-alkylthiosulfinates **5** and **6**, and unsymmetrical thiosulfinates **7-10** were prepared by Feng Zheng to shed light on the structural features that underlie regeneration and inhibition lipid peroxidation in lipid bilayer (**Chart 4.2**).

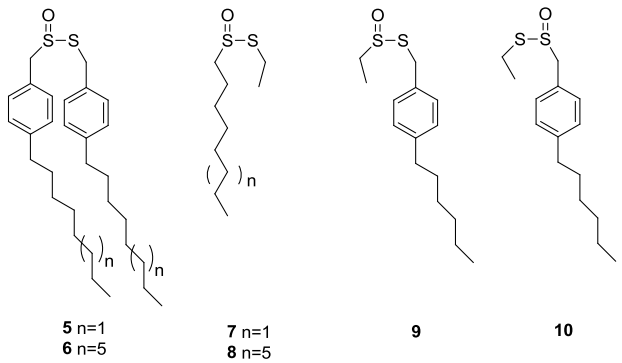

Chart 4.2. Symmetric and unsymmertric thiosulfinates.

The RTA activities of allicin (**1**), petivericin (**2**), 9-triptycenesulfenic acid (**3**) and the synthetic thiosulfinates (**4-10**) were determined in EggPC liposomes using H_2B-PMHC, a fluorogenic lipid oxidation probe as mentioned in **Chapter 2**. Representative results are shown in **Figure 4.1** for oxidations initiated with the lipophilic azo initiator MeOAMVN at 37 °C. The initial rate of fluorescence increase is indicative of the relative rates of reaction of H_2B-PMHC and the added antioxidant with peroxyl radicals. No inhibition of the oxidation of H_2B-PMHC is observed for **1** (**Figure 4.1A**) and **2** (**Figure 4.1B**) over the concentration range examined (4.5-22.5 μM). In contrast, the persistent 9-triptycenesulfenic acid (**3**) was an excellent inhibitor (**Figure 4.1C**). The expression in **Eq. 4.1**, which is derived from a kinetic analysis of the initial rates of H_2B-PMHC oxidation in the presence and absence of added RTA,[31] enables derivation of the relative inhibition rate constants (hereafter referred to as k_{rel}) from a plot of $\ln[(I_\infty - I_t)/(I_\infty - I_0)]$ vs $\ln(1-t/\tau)$:

$$\ln\left(\frac{I_\infty - I_t}{I_\infty - I_0}\right) = \frac{k_{inh}^{H2B-PMHC}}{k_{inh}^{RTA}} \ln\left(1 - \frac{t}{\tau}\right) \qquad \textbf{Eq. 4.1}$$

This analysis indicates that the rate constant for the reaction of **3** with lipophilic peroxyl radicals is a factor of 25±3 greater than that of H_2B-PMHC, which is known to be roughly the same as that of PMC.[33] The time required to reach maximum fluorescence in the first phase of the plots (*ca.* 400 counts), hereafter referred to as the 'inhibited period' (τ in **Eq. 4.1**), reflects the stoichiometry of the reaction between the added antioxidant and the peroxyl radicals. The inhibited periods in **Figure 4.1C** correlate nicely with the concentration of **3** yielding a slope of 12±0.8 min μM^{-1}. Since the dependence of the inhibited period on the concentration of α-TOH under similar conditions is roughly twice that of **3** and α-TOH is known to trap two peroxyl radicals,[33] each molecule of **3** must trap only one MeOAMVN-derived peroxyl radical. This is consistent with our results with **1** and **2** in homogenous organic solution.[24,27] Thiosulfinate **4**, a more lipophilic analog of petivericin (**2**), was able to retard the oxidation of H_2B-PMHC (**Figure 4.1D**), but did not display a clear inhibited period as was observed for the persistent sulfenic acid **3**. Therefore, although **4** is clearly more reactive than **1** or **2**, it is far less reactive than the authentic sulfenic acid **3**.

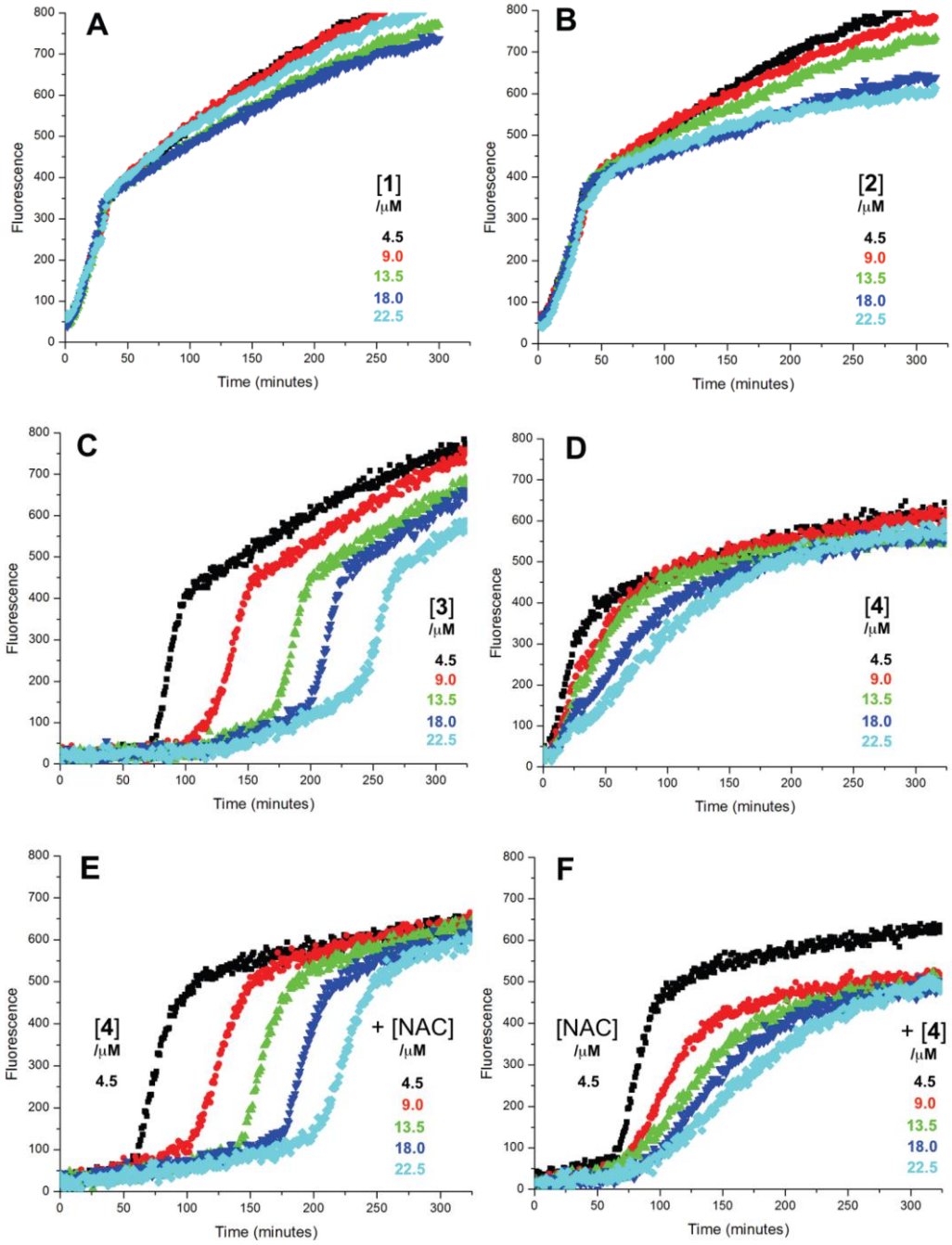

Figure 4.1. Representative fluorescence (at 520 nm) intensity-time profiles from MeOAMVN-mediated (0.2 mM) oxidations of EggPC liposomes (1 mM in PBS, pH 7.4) containing H_2B-PMHC (0.15 μM) and increasing concentrations (4.5, 9.0, 13.5, 18 and 22.5 μM) of allicin (**1**, A), petivericin (**2**, B), 9-triptycenesulfenic acid (**3**, C) and hexylated petivericin (**4**, D) at 37 °C. Also shown are corresponding oxidations inhibited by 4.5 μM of **4** and increasing concentrations of *N*-acetylcysteine (1-5 equivalents) (E) and 4.5 μM *N*-acetylcysteine with increasing concentrations of **4** (1-5 equivalents) (F).

Sulfenic acids are also formed from thiosulfinates by reaction with thiols. Therefore, we investigated the addition of a thiol to the liposome oxidations in the presence of **1**, **2** and

4. We chose the popular glutathione analog NAC as a model thiol for these studies. While the addition of NAC did not impact the rate of oxidation of H_2B-PMHC in the presence of **1** or **2**,[32] it had a marked effect when used in combination with **4** (**Figure 4.1E**). The initial rates indicate an apparent k_{rel} of 9±2 and the inhibited period scales with total antioxidant concentration (i.e. [**4**]+[NAC]) at 7.6±0.2 min μM^{-1}. Interestingly, when increasing concentrations of **4** are used with a constant concentration of NAC (**Figure 4.1F**), the data appears to be the additive result of the first data set in **Figure 4.2E** with the data in **Figure 4.1D**. That is, there is a short inhibited period followed by a retarded phase.

Since each of **1**, **2** and **4** possess a similar pseudo-symmetric core structure with activated methylene groups adjacent the thiosulfinate moiety, the reactivities of six additional synthetic thiosulfinates were determined under the same conditions in an attempt to clarify any structure-reactivity relationships. Although the thiosulfinates **5**-**10** did not display any RTA activity in the absence of NAC (data not shown), significant activity was observed for some of these compounds in the presence of NAC. Representative results are shown in **Figure 4.2**.

The lipophilic bis(*n*-alkyl)thiosulfinates **5** and **6** were ineffective when co-administered with increasing amounts of NAC. However, the unsymmetrical thiosulfinates **7** and **8** (wherein an ethyl group was substituted for one of the two octyl or dodecyl chains in 5 and 6, respectively) were effective (cf. **Figures 4.2C** and **4.2D**). Although their reactivity was noticeably lower than for **4**, with apparent k_{rel} of 3.5±0.9 and 4.5±1.0, respectively, (compared to 9±2 for **4**) the dependence of their inhibited periods on total antioxidant concentration (7.3±0.4 and 6.6±0.5 min μM^{-1}, respectively), was essentially identical to **4** (7.6±0.2 min μM^{-1}). The two additional unsymmetrical thiosulfinates **9** and **10**, which differ only in the sulfur atom to which oxygen is attached, differed markedly in their reactivity. Thiosulfinate **10**, which is expected to react with NAC to yield the same sulfenic acid as that which arises in the *S*-thiolation of **4**, displays similar activity, but with a lower relative apparent rate constants of 3.6±0.8. In sharp contrast, thiosulfinate **9** is devoid of any radical-trapping activity.

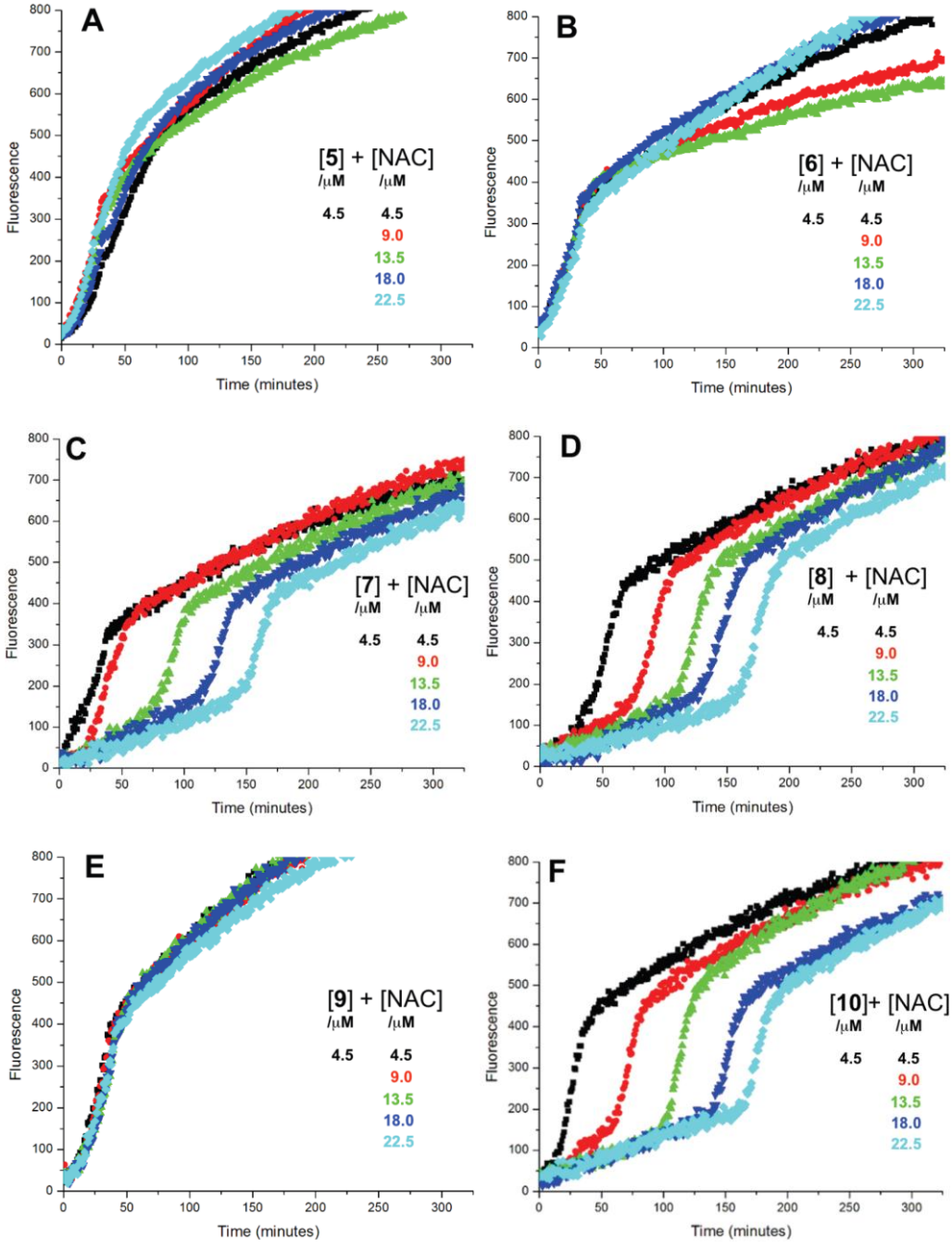

Figure 4.2. Representative fluorescence (at 520 nm) intensity-time profiles from MeOAMVN-mediated (0.2 mM) oxidations of EggPC liposomes (1 mM in PBS, pH 7.4) containing H_2B-PMHC (0.15 μM) with 4.5 μM of either the symmetric n-alkylthiosulfinates 5 (A) and 6 (B), the unsymmetric n-alkylthiosulfinates 7 (C) and 8 (D) and hexylated petivericin hybrids 9 (E) and 10 (F) with increasing concentrations of N-acetylcysteine (1-5 equivalents) at 37 °C.

The putative interaction between NAC and sulfenic acids in EggPC liposomes was probed using the persistent 9-triptycenesulfenic acid as shown in **Figure 4.3A**. In these experiments, NAC extended the inhibited period attributed to the sulfenic acid while maintaining the same radical-trapping kinetics, despite not being able to inhibit the oxidation of H_2B-PMHC on its own (**Figure 4.3B**). Moreover, the dependence of the inhibited period on the total antioxidant concentration (sulfenic acid *and* NAC) of 12±0.6 min μM^{-1} is indistinguishable from that of the sulfenic acid alone (12±0.8 min μM^{-1}, data in **Figure 4.1C**; see comparison in **Figure 4.3C**). Ascorbate was also used in conjunction with the sulfenic acid in place of NAC (**Figure 4.3D**). Similar to NAC, ascorbate also extends the inhibition period attributed to the sulfenic acid. With ascorbate, the dependence of the length of the inhibited period on the total antioxidant concentration (sulfenic acid *and* ascorbate) is slightly larger (15±0.9 min μM^{-1}) than the sulfenic acid alone (12±0.8 min μM^{-1}, data in **Figure 4.1C**; see comparison in **Figure 4.3F**). From control experiments it is clear that ascorbate appears to inhibit oxidation (**Figure 4.3E**), in contrast with NAC (**Figure 4.3B**). However, it is likely that this apparent inhibition is in fact due to the reduction of the phenoxyl radical derived from H_2B-PMHC oxidation,[33] consistent with the known chemistry of ascorbate and PMHC or α-TOH.

The radical-trapping activity of a select number of thiosulfinates was also explored in buffer at acidic pH (5.8). Representative data are presented for thiosulfinates **8** and **10** in **Figure 4.4**. A qualitative comparison of **Figures 4.4A** and **4.2D** suggests that while the k_{rel} of **8** does not change significantly at pH 5.8 relative to 7.4, the inhibited periods are noticeably shorter at lower pH. The same trend is evident on comparing the data for **10** in **Figures 4.4B** and **4.2F**. The inhibited periods are given as a function of added NAC at pH 5.8 and 7.4 for **8** and **10** in **Figures 4.4D** and **4.4E**, respectively. For comparison, analogous data was obtained in the presence of the persistent sulfenic acid 3, and is shown in **Figures 4.4C** and **4.4F**.

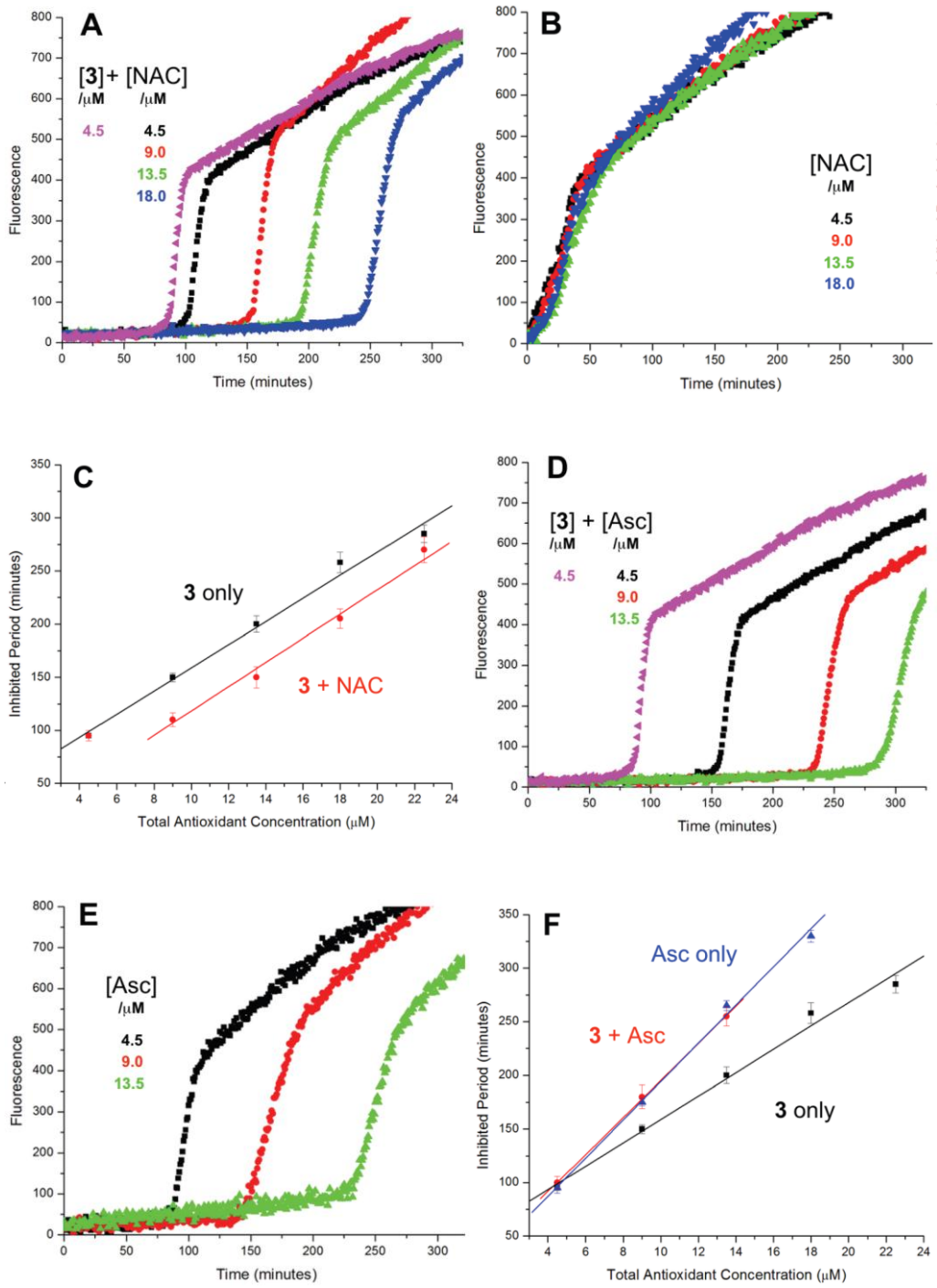

Figure 4.3. Representative fluorescence (at 520 nm) intensity-time profiles from MeOAMVN-mediated (0.2 mM) oxidations of EggPC liposomes (1 mM in PBS, pH 7.4) containing H_2B-PMHC (0.15 μM) and 9-triptycenesulfenic acid (**3**, 4.5 μM) with increasing concentrations (1-5 equivalents) of NAC (A) or ascorbate (Asc, D) at 37 °C. Also shown are corresponding results for NAC (B) or ascorbate used alone (E). The inhibited periods are plotted as a function of total antioxidant concentration in panels C ([3]+[NAC]) and F ([3]+[ascorbate]).

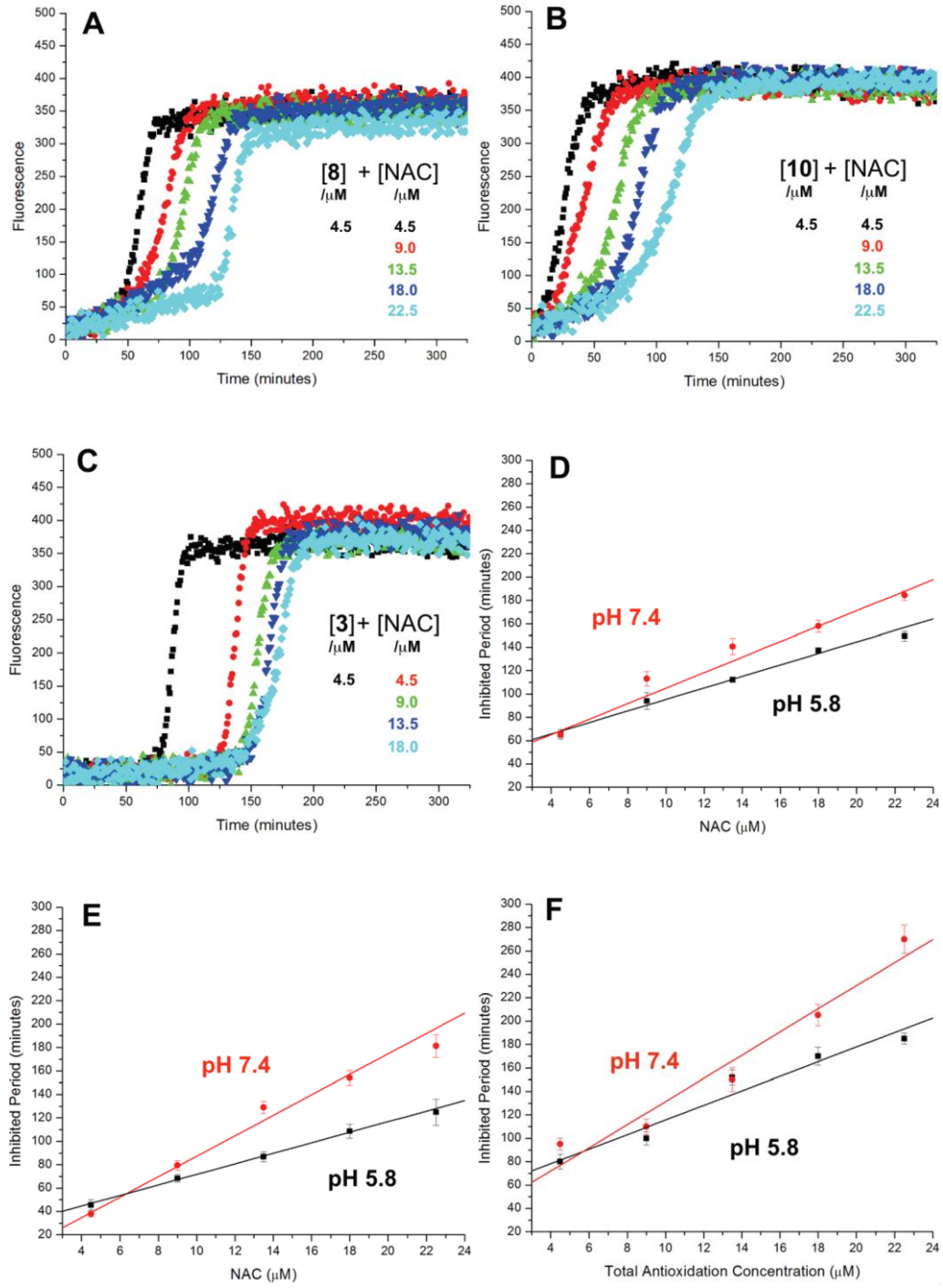

Figure 4.4. Representative fluorescence (at 520 nm) intensity-time profiles from MeOAMVN-mediated (0.2 mM) oxidations of EggPC liposomes (1 mM in PBS, pH 5.8) containing 0.15 μM H_2B-PMHC, 4.5 μM of either **9** (A), **10** (B) or **3** (C) and increasing concentrations of NAC (1-5 equivalents) at 37°C. Panels D, E and F show the dependence of the inhibited periods versus antioxidant concentration at pH 5.8 and 7.4.

4.3.2 PLPC Liposome Oxidation – Determination of Hydroperoxides

Lipid hydroperoxide formation was also monitored directly in a select set of MeOAMVN-mediated oxidations of liposomes (at 37°C) made exclusively from a polyunsaturated phospholipid (1-palmitoyl-2-linoleyl-*sn*-glycero-3-phosphocholine, PLPC) mentioned in **Chapter 2**. The hydroperoxide concentrations were determined using a phosphine-coumarin conjugate as mentioned in **Chapter 2**, which undergoes fluorescence enhancement upon oxidation to the phosphine oxide in the presence of hydroperoxides **Scheme 4.7**. The results are shown in **Figure 4.5**. The uninhibited autoxidation displays a linear growth in [ROOH] with time, as was expected for the initial part of the reaction (<20% conversion). Addition of 25 μM of each of the hexylated petivericin and NAC afforded a clear inhibited period, where ROOH production is effectively suppressed for ca. 96 minutes. When two equivalents of NAC are used with hexylated petivericin, the inhibited period is extended further, to roughly 170 minutes (**Figure 4.5A**). In contrast, hexylated petivericin or NAC alone did not suppress lipid peroxidation (**Figure 4.5B**).

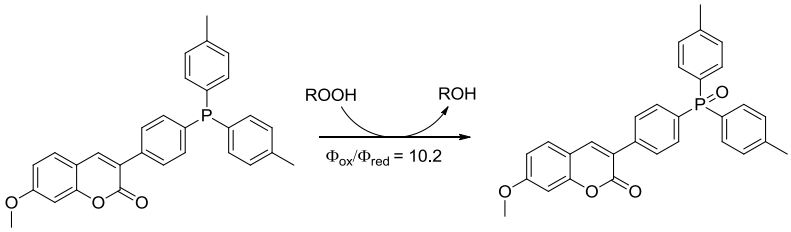

Scheme 4.7. Reaction of coumarin-triarylphosphine probe with hydroperoxide.

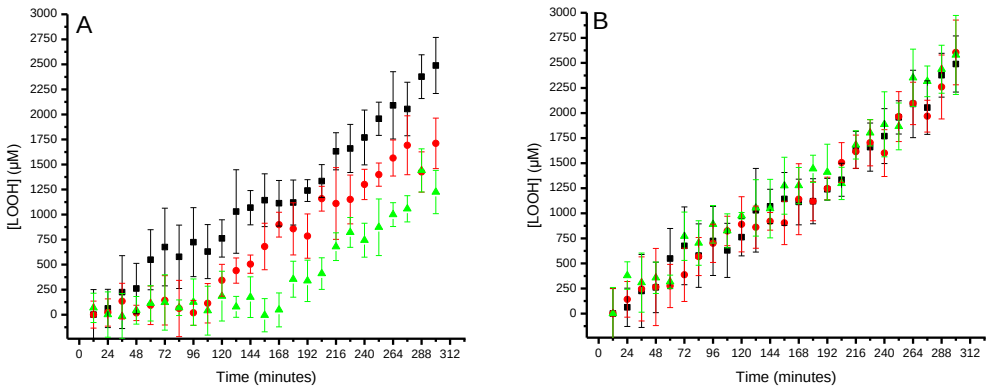

Figure 4.5. Hydroperoxide formation in the autoxidation of PLPC liposomes (13.3 mM in PBS buffer,

pH 7.4) initiated by MeOAMVN (150 μM) at 37°C in the presence of 25 μM of **4** + 25 μM NAC (red), 25 μM of **4** + 50 μM NAC (green) or no additives (black) (A); 25 μM **4** only (red), 25 μM NAC only (green), or no additives (black) (B).

4.3.3 Inhibition of Lipid Peroxidation and Cytotoxicity in Cell Culture

The results with the natural and synthetic thiosulfinates in liposomes prompted us to investigate whether the different activities of allicin, petivericin and the lipophilic thiosulfinate hexylated petivericin translate from the lipid bilayers of phosphatidylcholine liposomes to the lipid bilayers of mammalian cells. To probe the potential biological activity of hexylated petivericin, its efficacy in preventing lipid peroxidation was determined in several cell lines including human Tf1a erythroblasts, HEK-293 embryonic kidney cells and HepG2 hepatocellular carcinoma cells and compared to allicin and petivericin. The lipophilic C11-BODIPY$^{581/591}$ probe was used to monitor membrane lipid oxidation by flow cytometry (λ_{ex} = 488 nm, λ_{em} = 525±25 nm) as mentioned in **Chapter 3**. Lipid peroxidation was initiated either by depleting cells of glutathione with diethylmaleate (DEM), or by inhibition of glutathione peroxidase-4 (Gpx4) with RSL3 mentioned in **Chapter 3** in Tf1a erythroblasts.[34,35] Representative dose-response curves for experiments with Tf1a cells are shown in **Figure 4.6**. Cytotoxicity studies were carried out in parallel using 7-aminoactinomycin (7-AAD), a fluorophore which can pass through the membranes of dead cells, but not live ones, and binds to DNA by flow cytometry (λ_{ex} = 488 nm, λ_{em} = 675±25 nm; 10,000 events).

A clear dose-dependence was observed when each of allicin (**Figure 4.6A**), petivericin (**Figure 4.6B**) and hexylated petivericin (**Figure 4.6C**) were used to inhibit lipid peroxidation after 22 hours incubation time, with EC_{50} values of 20±1, 23±2 and 74±9 μM, respectively, when DEM was used as the initiator. Similar trends were observed in HEK-293 cells and HepG2 cells (see **Figure 4.7** and **Figure 4.8**). Although the EC_{50} values were essentially the same when either allicin or petivericin were used to inhibit lipid peroxidation initiated with RSL3 (EC_{50} = 24±2 and 19±2 μM), a two-fold increase in potency was observed for hexylated petivericin (EC_{50} = 39±3 μM). Allicin and petivericin induced cell death at concentrations similar to those that were effective in inhibiting lipid

peroxidation, i.e. EC_{50} = 39±1 and 56±3 μM, respectively in Tf1a erythroblasts, while hexylated petivericin had no impact on cell viability throughout the concentration range studied (5-200 μM) (similar trends were observed in HEK-293 cells and HepG2 cells, see **Figure 4.7** and **Figure 4.8**).

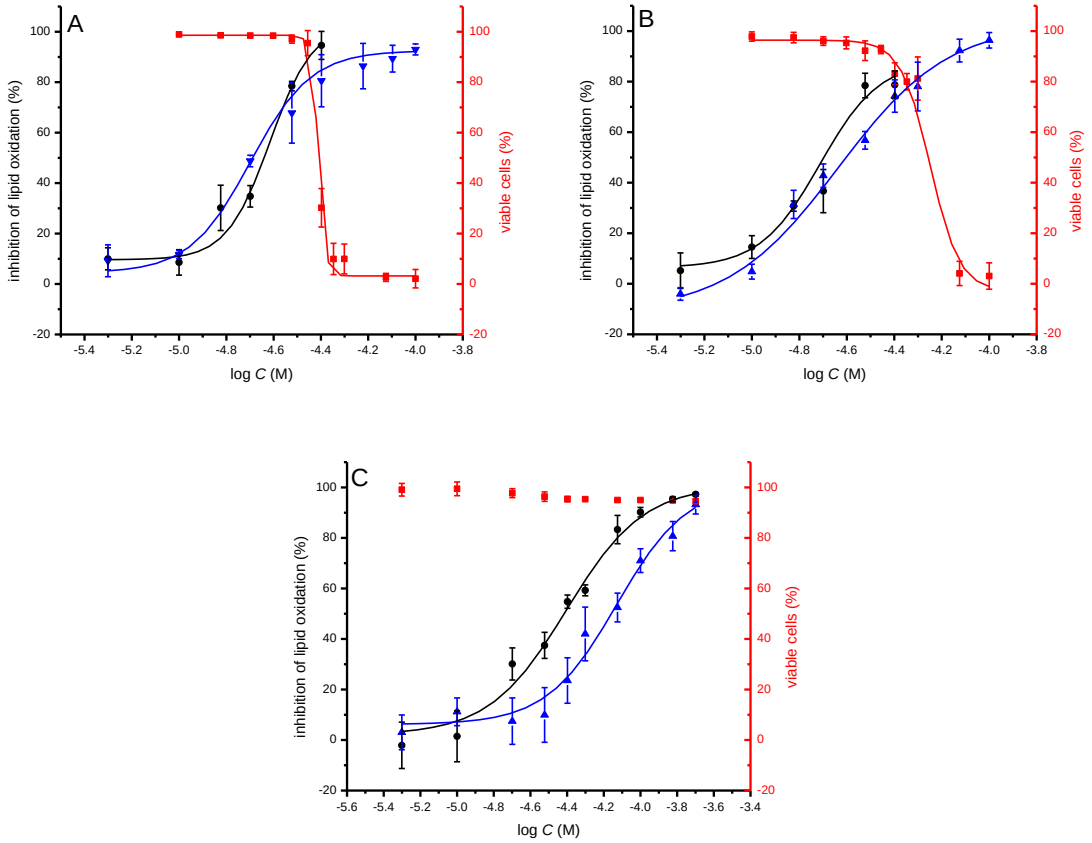

Figure 4.6. Representative dose-response curves obtained from flow cytometry (1×10^6 cells/mL; λ_{ex} = 488 nm, λ_{em} = 525±25 nm; 10,000 events) following induction of oxidative stress by addition of either diethylmaleate (9 mM) or RSL3 (4 μM) in Tf1a cells grown in RPMI media containing either allicin (A), petivericin (B) or hexylated petivericin (C) for 22 hours at 37°C. The lipid peroxidation reporter C11-BODIPY$^{581/591}$ (1 μM) was added to each of the cell cultures for 30 minutes prior to either DEM (blue) or RSL3 (black) treatment. Cell viability (red) was also determined by flow cytometry (5×10^5 cells/mL; λ_{ex} = 488 nm, λ_{em} = 675±25 nm; 10,000 events) following treatment of the cells pre-incubated with allicin (A), petivericin (B) or hexylated petivericin (C) for 22 hours at 37°C with a solution of 7-aminoactinomycin D (5 μL/1×10^5 cells, 10 min).

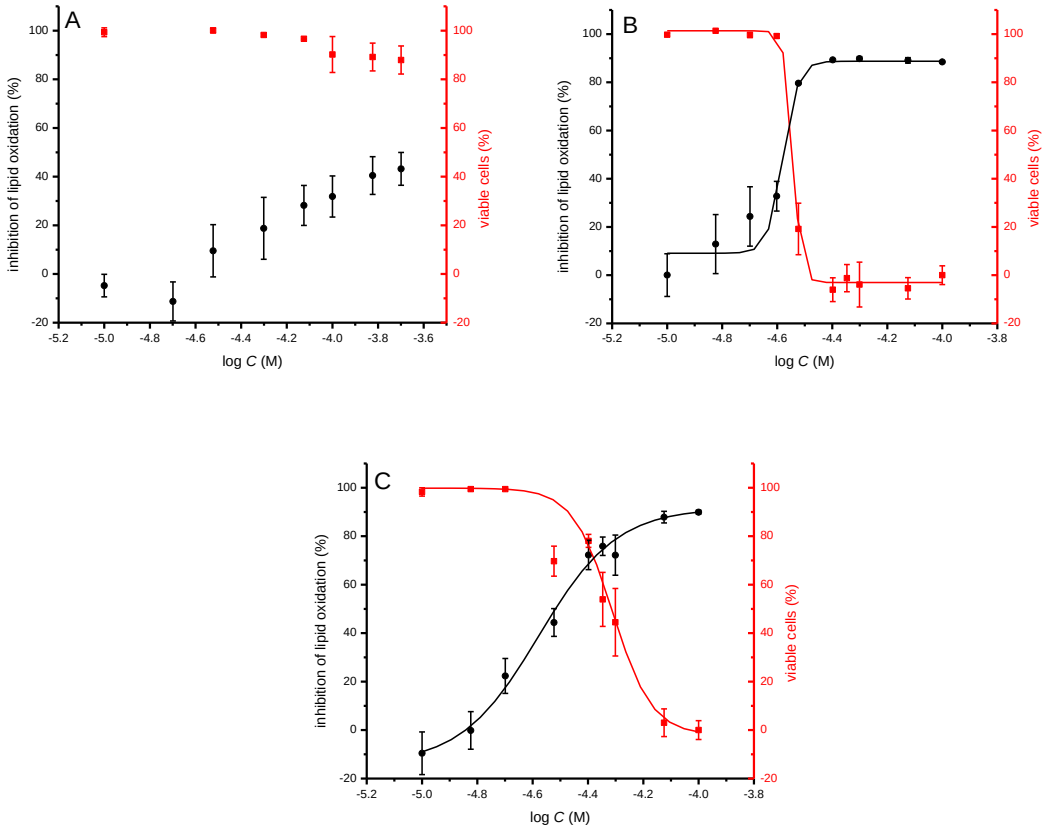

Figure 4.7. Representative dose-response curves obtained from flow cytometry (1×10^6 cells/mL; λ_{ex} = 488 nm, λ_{em} = 525±25 nm; 10,000 events) following induction of oxidative stress with diethylmaleate (DEM, 9 mM) in HEK293 cells grown in MEM media containing either hexylated petivericin (**4**, A), allicin (**1**, B) or petivericin (**2**, C) (5-200 μM) for 22 hours at 37 °C. Cells were incubated with the lipid peroxidation reporter C11-BODIPY$^{581/591}$ (1 μM) for 30 minutes prior to DEM treatment. Cell viability (red) was also determined by flow cytometry (5×10^5 cells/mL; λ_{ex} = 488 nm, λ_{em} = 675±25 nm; 10,000 events) following treatment of the cells pre-incubated with allicin (A), petivericin (B) or hexylated petivericin (C) for 22 hours at 37°C with a solution of 7-aminoactinomycin D (5 μL/1×10^5 cells, 10 min). EC_{50} values for lipid peroxidation inhibition for allicin is 26±1 μM, petivericin is 26±3 μM. TC_{50} values for cell viability for allicin is 29±1 μM, petivericin is 49±2 μM.

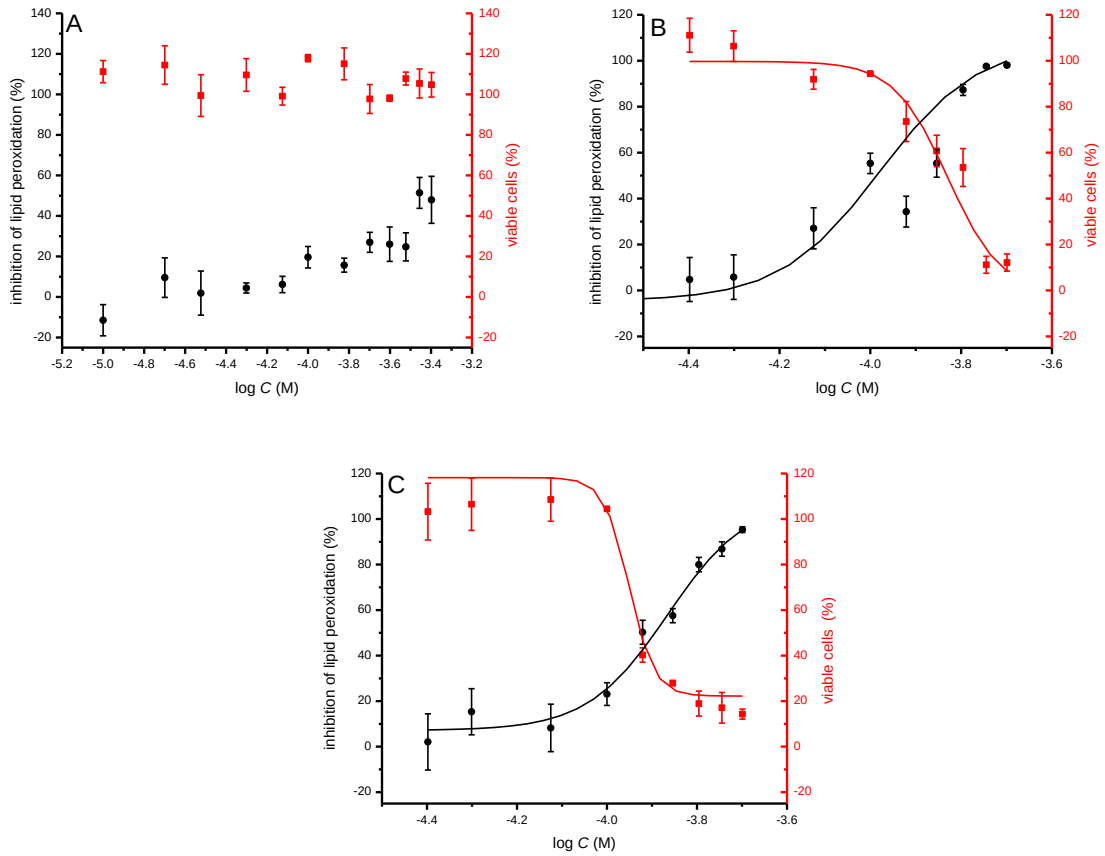

Figure 4.8. Representative dose-response curves obtained from flow cytometry (1×10^6 cells/mL; λ_{ex} = 488 nm, λ_{em} = 525±25 nm; 10,000 events) following induction of oxidative stress with diethylmaleate (DEM, 9 mM) in HepG2 cells grown in MEM media containing either hexylated petivericin (**4**, A), allicin (**1**, B) or petivericin (**2**, C) (5-200 μM) for 22 hours at 37 °C. Cells were incubated with the lipid peroxidation reporter C11-BODIPY$^{581/591}$ (1 μM) for 30 minutes prior to DEM treatment. Cell viability (red) was determined by MTT assay. EC_{50} values for lipid peroxidation inhibition for allicin is 105±4 μM, petivericin is 134±6 μM. TC_{50} values for cell viability for allicin is 148±6 μM, petivericin is 112±2 μM.

4.3.4 Effect of Thiosulfinates on Cellular Thiol Concentration

Given allicin's proclivity to react with glutathione and other cellular thiols,[13] we determined the effect of each of allicin, petivericin and hexylated petivericin on total cellular thiol concentration over the concentration range employed in the foregoing lipid peroxidation/cytotoxicity assays. Following incubation of cells in media supplemented with varying amounts of each thiosulfinate for 22 hours, cells were lysed and the protein

concentration and total thiol concentration were determined using Ellman's reagent. Small increases were observed for allicin at non-lethal concentrations in Tf1a cells (e.g. 10 and 30 μM, *cf.* **Figure 4.9**). The trend persists, but is even less obvious for petivericin, and thiol levels were severely reduced relative to total protein at cytotoxic concentrations of both compounds. However, hexylated petivericin showed essentially no effect on total thiol concentration over the concentration range studied. Interestingly, a different profile was observed for allicin and petivericin in HEK-293 cells, where thiol was progressively depleted. In contrast, and consistent with the results in Tf1a cells, progressive diminution in cellular thiol with increasing concentration of hexylated petivericin was not observed in HEK-293 cells. Surprisingly, another trend was observed for all the three thiosulfinates in HepG2 cells at non-lethal concentrations, in which increasing total thiol concentrations was noticed for allicin and hexylated petivericin, but total thiol concentration was not significantly changed for petivericin.

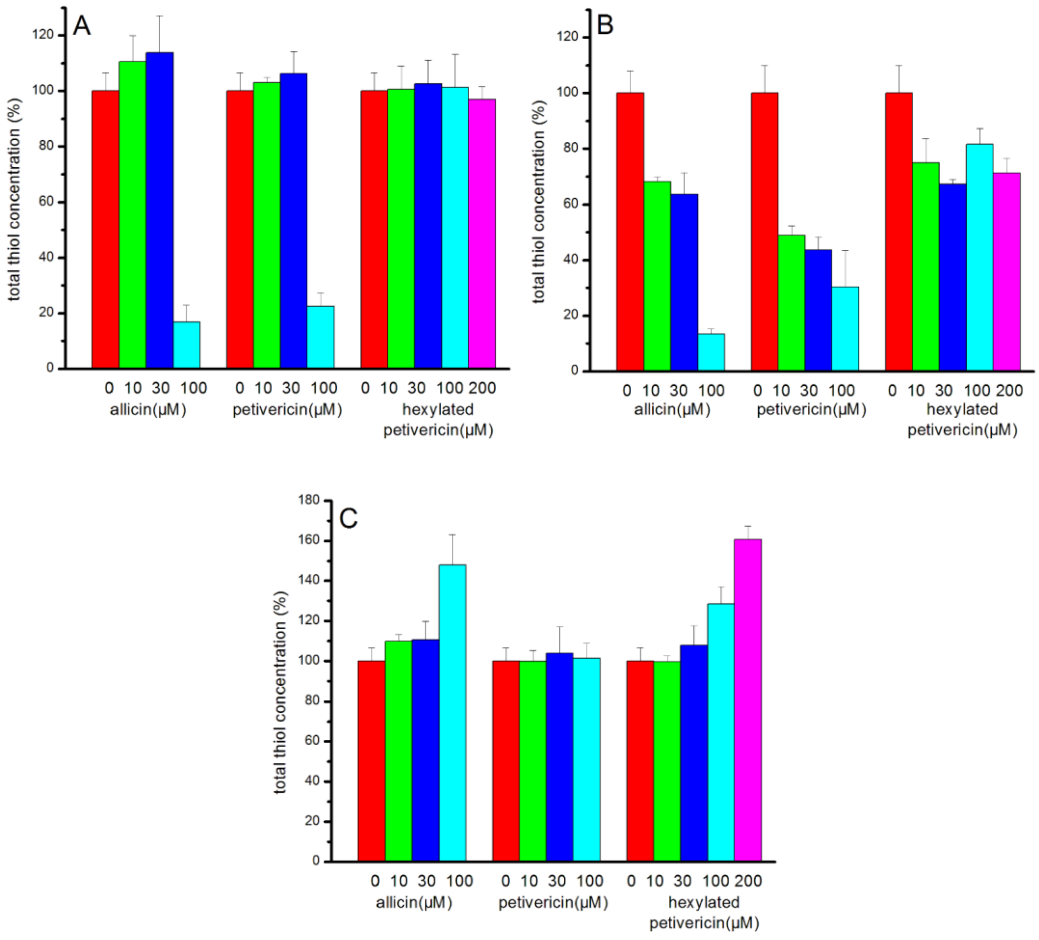

Figure 4.9. Cellular thiol concentration determined as a function of thiosulfinate concentration after 22 hours incubation in Tf1a (A), HEK-293 (B) and HepG2 (C) cells. Total thiol concentrations were determined relative to total protein in a minimum of three trials.

4.3.5 Cytotoxicity Mechanism of Allicin and Petivericin

To shed some light on the cytotoxicity mechanism of allicin and petivericin, Tf1a cells treated with various concentration of allicin and petivericin were assayed by flow cytometry using Annexin-V-Phycoerythrin (PE)/7-AAD probes. Annexin V is a calcium-dependent phospholipid-binding protein that binds phosphatidylserine (PS).[36] PS is predominantly located in the inner leaflet of the plasma membrane under normal physiological conditions, and it is translocated to the extracellular membrane leaflet upon initiation of apoptosis.[37] Therefore, the Annexin-V assay offers the possibility of detecting early apoptosis by fluorescently labeled Annexin-V-PE before the loss of cell membrane integrity in a calcium-dependent manner.[38] 7-AAD is a commonly used cell viability probe as mentioned earlier in this chapter. Time-dependent and concentration-dependent studies were carried out with both allicin and petivericin in Tf1a cell culture. Flow cytometry was carried out on Beckman Coulter Flow Cytometer (10,000 events, λ_{ex} = 488 nm; λ_{em} = 675±25 nm for 7-AAD on FL4; λ_{ex} = 488 nm; λ_{em} = 575±25 nm for Annexin-V-PE on FL2). Flow cytometry profiles were analyzed by Kaluza Analysis 1.3 software. Untreated cells were negative for both Annexin-V-PE and 7-AAD (**Figure 4.10A**). Gating on FL2 for Annexin-V-PE was set up using camptothecin (6 μM) as positive control. After incubation for 22 hours, 59% of the cells localized in the right lower quadrant (positive for Annexin-V-PE on FL2, negative for 7-AAD) (**Figure 4.10B**), consistent with cells that were in early apoptotic stage without disrupting cell membranes. Gating on FL4 for 7-AAD was set up using DMSO (10% v/v) as positive control – again after incubation for 22 hours (positive for Annexin-V-PE on FL2, positive for 7-AAD). When treating the cells with either petivericin or allicin, we were not able to observe cells in early apoptosis (i.e. without inducing cell death) when cells were incubated with 10-100 μM either allicin or petivericin for 4-72 hours (representative results are shown in **Figure 4.10C** and **4.10D)**. Cells were either healthy or in the late stage of cell death.

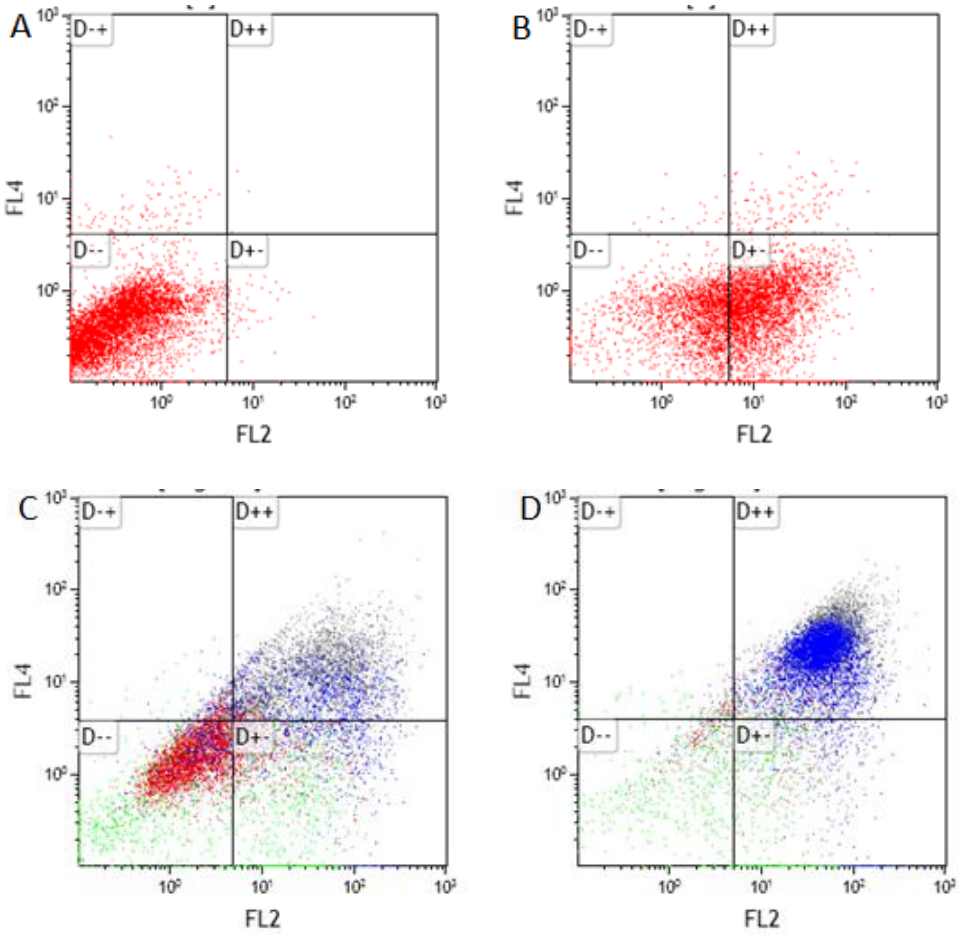

Figure 4.10. Density plots for cell apoptosis assay in Tf1a cells obtained from flow cytometry (1×10^6 cells/mL) for Tf1a cells (A), incubation of 6 μM camptothecin for 22 hours (B), 30 μM allicin for 72 hours (C), 100 μM allicin for 72 hours (D) at 37 °C followed by adding Annexin-V-PE and 7-AAD probes. (10,000 events; λ_{ex} = 488 nm; λ_{em} = 675±25 nm for 7-AAD on FL4; λ_{ex} = 488 nm; λ_{em} = 575±25 nm for Annexin-V-PE on FL2).

4.3.6 Inhibition of Lipid Peroxidation and Cytotoxicity of 9-Triptycenesulfenic Acid in Cell Culture

To compare the lipid peroxidation inhibition activities of an authentic sulfenic acid to that of the thiosulfinates allicin, petivericin and hexylated petivericin, the persistent 9-triptycenesulfenic acid (**3**) was also examined in Tf1a cell culture. Again, cytotoxicity studies were carried out in parallel. A clear dose-dependence was observed, with an EC_{50} value for inhibition of lipid peroxidation of 9.2±1.3 μM. Interestingly, 9-triptycenesulfenic acid **3** induced cell death at concentrations much higher than those that were effective in

inhibiting lipid peroxidation, with TC_{50} = 85.0 ± 9.8 μM (**Figure 4.11)** – making it more similar to hexylated petivericin than to allicin or petiviericin.

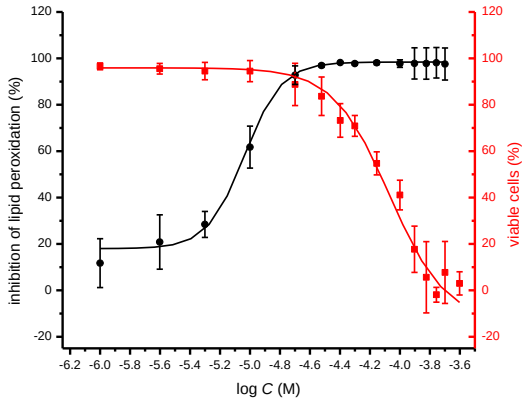

Figure 4.11. Representative dose-response curves obtained from flow cytometry (1×10^6 cells/mL; λ_{ex} = 488 nm, λ_{em} = 525±25 nm; 10,000 events) following induction of oxidative stress with diethylmaleate (DEM, 9 mM) in Tf1a cells grown in 1640 media containing 9-triptycenesulfenic acid (**3**) (5-200 μM) for 22 hours at 37 °C. Cells were incubated with the lipid peroxidation reporter C11-BODIPY$^{581/591}$ (1 μM) for 30 minutes prior to DEM treatment. Cell viability (red) was determined by flow cytometry (λ_{ex} = 488 nm, λ_{em} = 675±25 nm; 10,000 events) with a solution of 7-AAD.

4.4 Discussion

Allicin and petivericin are effective RTAs in homogenous organic solution because they undergo Cope elimination to yield 2-propenesulfenic acid and phenylmethanesulfenic acid, respectively, and these molecules react with peroxyl radicals without an enthalpic barrier.[24,27] The foregoing experiments were undertaken to assess the RTA activity of allicin and petivericin in more biologically relevant contexts: the lipid bilayers of liposomes and mammalian cells. In liposomes, allicin and petivericin were found to be at least 100 times less reactive than α-TOH, while an authentic sulfenic acid, 9-triptycenesulfenic acid, was roughly 25-times more reactive than α-TOH. Reconciling these results requires that either: 1) Cope elimination of 2-propenesulfenic acid and phenylmethanesulfenic acid from allicin and petivericin, respectively, is slowed in the lipid bilayer due to H-bonding at the interface (The Cope elimination of 2-propenesulfenic acid from allicin is known to be slowed in

H-bond donating solvents, such as water.)[39] or 2) the sulfenic acids produced are sufficiently hydrophilic to partition to the aqueous phase where they undergo other reactions (i.e. oxidation, condensation). Although allicin itself is quite lipophilic, which facilitates its ready diffusion across membranes (the K_p of allicin in phosphatidylcholine/H_2O mixtures at 37°C has been reported as ca. 11),[40] 2-propenesulfenic acid can be expected to be significantly less so. The former explanation can be ruled out since the kinetics of allicin and petivericin decomposition (due to Cope elimination) was similar in liposomes to homogenous organic solution.[24,27,41] The latter explanation is supported by the significantly higher reactivity observed for thiosulfinate **4**, an analog of petivericin which includes *n*-hexyl substitution at the 4-position of the phenyl ring. The requirement for Cope elimination of (4-hexylphenyl) methanesulfenic acid to account for the activity of **4** is evident in its diminished kinetics for radical-trapping (k_{rel} = 0.9±0.1) relative to the persistent sulfenic acid **3** (k_{rel} = 25±3); a difference which is fully consistent with that observed in chlorobenzene, where petivericin and **3** have k_{inh} values of 2.0×10^5 and 3.0×10^6 $M^{-1}s^{-1}$, respectively.[24,29]

Sulfenic acids are also formed from thiosulfinates by *S*-thiolation reactions, with either a thiol or another molecule of thiosulfinate as the nucleophile.[2,3, 42] Since thiols are ubiquitous *in vivo*, with some tissues containing mM concentrations of glutathione, it is plausible that such an interaction may contribute to any potential RTA activity of allicin in biological contexts. Interestingly, whilst the addition of *N*-acetylcysteine had no impact on the RTA activity of either allicin or petivericin in liposomes, there was a significant increase in activity of hexylated petivericin. Since allicin (and petivericin) are rapidly consumed in the presence of NAC,[41] this implies that the hydrophilic sulfenic acids that are produced are consumed by reaction with another equivalent of thiol to give a disulfide. *S*-thiolation of hexylated petivericin, however, yields a lipophilic sulfenic acid that can trap lipophilic peroxyl radicals (**Scheme 4.8**).

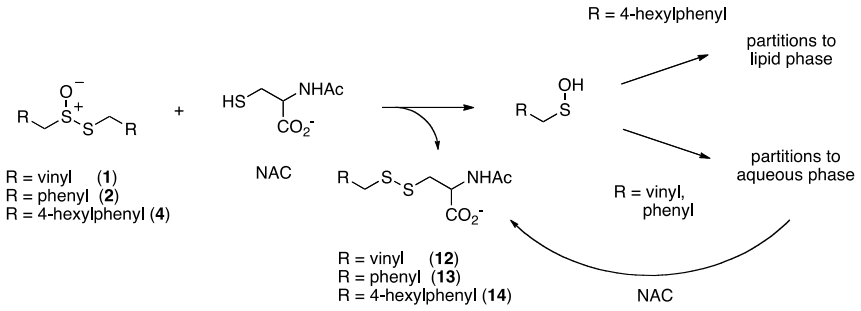

Scheme 4.8. Allicin and petivericin undergo *S*-thiolation by NAC to yield sulfenic acids that partition to the aqueous phase where they can react with NAC, whereas hexylated petivericin undergoes *S*-thiolation to yield a lipophilic sulfenic acid.

Interestingly, LC/MS analysis of aliquots from liposome oxidations inhibited by hexylated petivericin in the presence of NAC showed little (ca. 5%) conversion of the thiosulfinate to the corresponding mixed disulfide **14**.[41] Nevertheless, the inhibited periods observed in **Figure 4.1** for the combination of hexylated petivericin and NAC are consistent with a radical-trapping capacity that exceeds the small amount of the lipophilic sulfenic acid that corresponds to the amount of **14** observed by LC/MS. Indeed, the addition of increasing amounts of NAC beyond one or two equivalents led to a concentration-dependent extension in the inhibited period, while maintaining the same overall kinetics – suggesting that NAC is able to regenerate the lipophilic sulfenic acid derived from **4**.

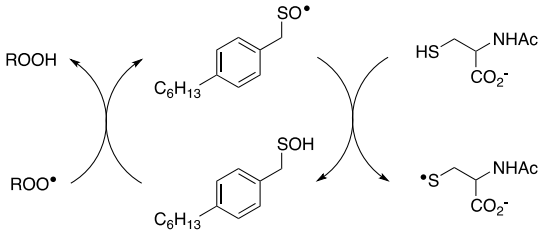

Scheme 4.9. Regeneration of the lipophilic sulfenic acid derived from **4** (see Scheme 4.7) by NAC.

The sequence in **Scheme 4.9** is supported by the results of liposome oxidations carried out in the presence of the persistent 9-triptycenesulfenic acid **3** and varying concentrations of NAC. The addition of increasing amounts of NAC lead to a concentration-dependent extension in the inhibited period, while maintaining the same overall kinetics as when **3**

alone was present. The dependence of the inhibited period on the concentration of NAC was essentially indistinguishable from the dependence of the inhibited period on the concentration of **3** alone, suggesting that the sulfenic acid was fully regenerated by NAC. Ascorbate was also able to regenerate **3**, but this was less obvious from the primary data because ascorbate is also able to reduce the aryloxyl radical derived from H_2B-PMHC.[33] The indication that ascorbate actually regenerates **3** comes from the fact that the initial rate of probe oxidation is the same as for the sulfenic acid alone, as compared to ascorbate alone (cf. **Figure 4.3D** with **Figure 4.3E**). Ascorbate, on the other hand, bolsters the radical-trapping capacity of **3** beyond that of **3** alone. Indeed, it is similar to that of ascorbate alone, and roughly 25% more than the sulfenic acid alone, or the sulfenic acid and NAC combination. This can be explained by the fact that ascorbate can, in principle, provide two reducing equivalents, as it is oxidized to dehydroascorbic acid. While this implies that the combination of sulfenic acid and ascorbate should yield a dependence of the inhibited period on added ascorbate that is double that of the sulfenic acid alone. Ingold,[43] Barclay,[44] and others have found that regeneration of lipophilic antioxidants such as α-TOH proceeds without complete fidelity due to reactions of ascorbate and/or the ascorbyl radical anion with O_2.

The regeneration of a lipid-soluble RTA using a water-soluble reducing agent is well-precedented. The most famous example is the combination of α-TOH and ascorbate.[43,44] Ascorbate reduces the α-tocopheroxyl radical that is formed following the reaction of α-TOH with lipophilic peroxyl radicals, thereby effectively converting a water-soluble reducing equivalent into a lipid-soluble one. While thiols do not regenerate α-TOH from its corresponding α-tocopheroxyl radical,[45,46] NAC is believed to regenerate simple selenophenols from their corresponding selenophenoxyl radicals when NAC is used in great excess.[46,47] Since a direct H-atom transfer is thermodynamically not favored for the reaction of NAC with the selenophenoxyl radicals, it was suggested that the reaction occurs by electron transfer from the thiolate to the selenophenoxyl radical. The electron transfer would be rendered irreversible by protonation of the selenophenoxide and partitioning of the selenophenol to the organic phase, with concomitant formation of the NAC-derived disulfide. It would appear necessary to invoke such a mechanism for the regeneration of a

sulfenic acid with NAC; direct H-atom is highly unfavourable on thermodynamic grounds (the RSO-H BDE is ca. 18 kcal/mol weaker than the RS-H BDE),[27,30,48] but the redox couples for RSO•/RSO^- and RSSR/RS^- are 0.74[30] and –0.20[49] V vs. NHE in acetonitrile and water (pH 7) (The reduction potential for NAC has been reported to be slightly more positive (+63 mV) than that for glutathione),[50] respectively, suggest that the electron transfer is feasible.

Independent evidence that *S*-thiolation (and not Cope elimination) is responsible for the formation of (4-hexylphenyl)methanesulfenic acid from **4** in lipid bilayers comes from studies of thiosulfinates that lack an activated methylene group adjacent to the divalent sulfur atom – necessary for facile Cope elimination.[24] Interestingly, whilst the symmetrical bis(*n*-octyl)thiosulfinate and bis(*n*-dodecyl)thiosulfinate were ineffective, the corresponding unsymmetrical thiosulfinates wherein either the octyl or dodecyl chain adjacent the divalent sulfur was replaced with an ethyl group displayed reactivity similar to the hexylated petivericin. Since the sulfenic acid that results from *S*-thiolation would be identical from thiosulfinates **5** and **7** (or **6** and **8)**, the lack of activity of **5** and **6** suggests that these compounds are too hydrophobic for efficient *S*-thiolation, which presumably takes place at the lipid/aqueous interface.

The importance of the lipophilicity of the sulfenic acid was demonstrated unequivocally by experiments with the unsymmetrical thiosulfinates **9** and **10**. Thiosulfinate **9**, which is expected to undergo *S*-thiolation with NAC to produce ethanesulfenic acid was completely ineffective, whilst thiosulfinate **10** which is expected to undergo *S*-thiolation with NAC to yield (4-hexylphenyl)methanesulfenic acid was similarly effective to hexylated petivericin**.** The disparate behaviour of **9** and **10** is illustrated in **Scheme 4.10**.

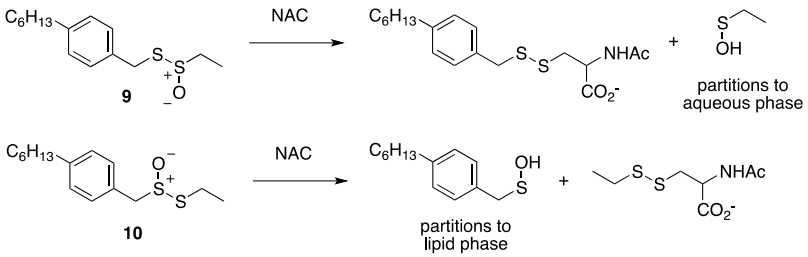

Scheme 4.10. The disparate behaviour of thiosulfinates **9** and **10** is believed to result from the differing lipophilicities of the sulfenic acids formed by *S*-thiolation with NAC.

The dependence of the inhibited periods attributed to the thiosulfinates in the presence of added NAC (given as minutes/μM) suggest that the regeneration of the persistent sulfenic acid **3** (12±0.6) is more efficient than the regeneration of the sulfenic acids derived from the thiosulfinates **4** (7.6±0.2), **7** (7.3±0.4), **8** (6.6±0.5) and **10** (8.4±0.6). This difference reflects the relative persistence of the sulfinyl radicals formed following H-atom transfer from the sulfenic acids to peroxyl radicals. The sulfinyl radical derived from **3** is known to be persistent under the experimental conditions due to steric hindrance,[30] enabling it to be quantitatively reduced by NAC. In contrast, unhindered sulfinyl radicals are expected to be less persistent,[24] and self-reactions as well as reactions with O_2 and/or peroxyl radicals can compete with reduction by NAC. The pH dependence of the radical-trapping activities of the thiosulfinates further reinforces this point. While the apparent rates of radical-trapping do not vary significantly with pH, the dependence of the length of the inhibited period on antioxidant concentration decreased at lower pH. This is consistent with slower regeneration of the sulfenic acid by the lower concentration of the thiolate form of NAC at more acidic pH, allowing more time for deleterious side reactions.

The foregoing results prompted an investigation of whether the disparate reactivity of allicin/petivericin and the amphiphilic thiosulfinates translate from the lipid bilayers of phosphatidylcholine liposomes to cells. The lipid peroxidation inhibition activities for allicin, petivericin and the lipophilic thiosulfinate hexylated petivericin were studied in human erythroblast Tf1a cells, human embryonic kidney HEK-293 cells, and human hepatocellular carcinoma HepG2 cells. Surprisingly, despite the numerous reports of allicin as a RTA (*vide supra*), no reports of cell-based assays of this activity can be found in the

literature. Likewise for petivericin – although this is understandable since it was only relatively recently identified as the primary thiosulfinate in petiveria.[8] Of the synthetic thiosulfinates, hexylated petivericin was chosen for study alongside the natural products. All three compounds were able to prevent oxidation of the lipid peroxidation reporter C11-BODIPY$^{581/591}$ in Tf1a erythroblasts, with EC_{50} values of 20±1, 23±2 and 74±9 μM for allicin, petivericin and hexylated petivericin, respectively after 22 hr incubation of antioxidants prior to inducing lipid peroxidation by DEM. In light of the lack of RTA activity displayed by allicin and petivericin in liposomes, at first glance these data suggest that the antioxidant mechanism of the three compounds cannot be due to radical-trapping.

Given the well-known electrophilic reactivity of thiosulfinates, it has been suggested that allicin's antioxidant activity derives from upregulation of expression of phase II detoxifying enzymes.[51-52] This leads to an increase in the cellular glutathione level, presumably via activation of the transcription factor Nrf2.[51-52] In this connection, allicin and petivericin may be slightly more effective than hexylated petivericin at inhibiting lipid peroxidation in the Tf1a (as well as in HEK-293 and HepG2) cells simply due to their greater accessibility to reactive cysteines on KEAP1, the cytosolic protein which prevents Nrf2 transclocation to the nucleus.[53] Cysteine modification by electrophiles mediates KEAP1/Nrf2 signaling events, and is now believed to underlie the activities of most nutritional antioxidants.[54] However, our own measurements indicate that the effects of the thiosulfinates on the total thiol concentration is highly dependent on the cell line. Allicin and petivericin do not upregulate GSH production to any significant extent in either Tf1a or HEK-293 cells; rather they promote a visible decrease in GSH in HEK-293 cells. Moreover, hexylated petivericin has no significant effect on GSH levels in Tf1a cells, but progressive diminution in cellular thiol with increasing concentration of hexylated petivericin was not observed in HEK-293 cells. In addition, increasing total thiol concentrations was noticed for allicin and hexylated petivericin in HepG2 cells when treating with non-lethal concentration of thiosulfinates, but total thiol concentration was not obviously changed for petivericin. Glutathione is the most abundant unique thiol group in cells; it can be found in millimolar concentrations in most cells and is especially highly concentrated in liver cells (5-10 mM).[55] It plays important role in antioxidant defense, metabolism, and regulation of

cellular processes including cell differentiation, proliferation and apoptosis.[55] HepG2 are cancer cells and are more resistant to glutathione depletion compared to normal cells such as Tf1a erythroblasts or HEK293 embryonic kidney cells due to the elevated GSH levels which generally increase antioxidant capacity and resistance to oxidative stress as compared to normal cells.[56,57] Therefore, the inconsistent effect of thiosulfinates on total thiol concentrations in different cell lines can be ascribed to the various basal levels of glutathione and regulation ability of glutathione synthetase in different cell lines.

Allicin's reactivity as an electrophile is apparently paradoxical; it is also believed to underlie its antimicrobial and anticancer activities. It has been determined to be highly cytotoxic to a wide variety of human cancer cells, including mammary MCF-7, endometrial and HT-29 colon cells,[58] HeLa and SiHa cervical and SW480 colon cells,[59] gastric epithelial cells,[60] and leukemia HL60 and U937 cells[61] with EC_{50} values in the low micromolar range under similar conditions to those employed here. The antiproliferative activity of allicin has been ascribed to activation of the mitochondrial apoptotic pathway by GSH depletion and concomitant changes in the intracellular redox status. While petivericin has been reported to display antimicrobial and antifungal activities,[62] there has been, to the best of our knowledge, no report on its cytotoxicity. Given the structural similarity between allicin and petivericin, it seems reasonable to suggest that it shares the same mechanisms.

Since the concentrations of allicin necessary to prevent lipid peroxidation in the assays above have been reported to be cytotoxic in some human cell lines, we determined the cytotoxicities of allicin, petivericin and hexylated petivericin toward the same human Tf1a, HEK-293 and HepG2 cells in parallel with the lipid peroxidation inhibition assays. Cell viability was assayed using 7-aminoactinomycin D (7-AAD), a DNA binding fluorophore impermeable to intact cellular membranes. Uptake of 7-AAD by cells cultured in media supplemented with allicin and petivericin occurred at concentrations only marginally higher than those necessary to inhibit lipid peroxidation in all the three cell lines (e.g. TC_{50} = 39±1 and 56±3 μM for allicin and petivericin in Tf1a erythroblasts, respectively). These results suggests that the apparent inhibition of lipid peroxidation observed in the presence of allicin and petivericin may result simply from growth arrest and the resultant slowing (or halting) of aerobic metabolism associated with their toxicity (See F**igure 4.6-4.8**). Accordingly, it

would be inappropriate to refer to allicin or petivericin as antioxidants in a biological context.

Allicin and petivericin are electrophiles which can react with GSH or protein nucleophiles having nucleophilic cysteines and therefore modulate several cell signaling pathways, including pro-apoptotic events, kinase/phosphatase activities, and antioxidant responsive nuclear transcription factor function.[63] Reactivity of cysteine group in signaling proteins such as Keap1[53] or pro-apoptotic response element caspase[64] towards electrophiles is much higher in order for it to compete with the much higher concentration of GSH in cells to form conjugates with electrophiles.[65,66] Thus, it seems reasonable to suggest that addition of non-lethal amounts of thiosulfinates initiates antioxidant signaling, including the upregulation of glutathione biosynthesis as what we have observed in HepG2 cells. On the other hand, upon addition of lethal amounts of thiosulfinates such as in Tf1a or HEK293 cells, pro-apoptotic signaling proteins are modified, and apoptotic signal transduction pathways are activated leading to cell death.

Our attempts to investigate whether allicin and petivericin induce apoptosis using Annexin V-PE/7-AAD probes in Tf1a cells seems to show that they do not induce apoptosis. This is inconsistent with literature in which they showed allicin induced apoptosis by activation of caspase in multiple cell lines.[59,61,67] Allicin was also reported to induce apoptosis using a similar assay where Annexin V-FITC was used to detect early apoptosis and propidium iodide (PI) was used to detect late stage cell death in cancer cells.[68] However, in that manuscript, the results seemed to be contradict their conclusion – investigators did not show any early stage apoptosis, where the cells could only be stained by Annexin V-FITC, but not PI.[68] There is no report on the cytotoxicity mechanism of petivericin to date. The concentration of thiosulfinates that were used in this type of study need to be sufficient to cause the early apoptosis in cells, but cannot reach the concentration that induces lethal cell death. Therefore, it is very difficult to find the optimized concentration of thiosulfinates and the proper time-scale to induce early apoptosis without cell death. It is also likely that looking for caspase activation would be a better approach for determining the pro-apoptotic potential of allicin/petivericin compared to Annexin V-PE/7-AAD probes staining assay used here. Both Annexin V and 7-AAD relies on the

damage of cell membranes, therefore it would be difficult to monitor the different stages of cell membrane leakage. We decided not to spend more time to study the toxicity mechanism of allicin and petivericin since our focus is to determine whether they are radical-trapping antioxidants, but not how they induce cell death.

In contrast to allicin and petivericin, hexylated petivericin was not toxic throughout the concentration range examined in the lipid peroxidation assay (5-200 μM in Tf1a cells and HEK293 cells, 5-400 μM in HepG2 cells). As a result of its increased lipophilicity, rather than simply killing cells as does allicin and petivericin, hexylated petivericin appears to be a *bona fide* RTA. This difference is underscored by the results obtained when lipid peroxidation was induced by Gpx4 inhibition with RSL3[35] rather than GSH depletion with DEM; the relative efficacy of hexylated petivericin increased, while no improvement was observed for either allicin or petivericin (**Figure 4.6**). Unlike DEM administration, RSL3 inhibition of Gpx4 does not lead to a precipitous drop in GSH levels, leaving it available to recycle the lipophilic sulfenic acid and increasing the relative potency of hexylated petivericin. This is fully consistent with the observations in the liposome oxidations – wherein addition of thiol (NAC) was able to prolong inhibitory activity due to recycling of the lipophilic sulfenic acid derived from hexylated petivericin, but afforded no improvement on the activity of allicin or petivericin.

The foregoing results prompted an investigation of the persistent 9-triptycenesulfenic acid (**3**) in Tf1a cells for its ability to inhibit lipid peroxidation. Again, a clear dose-dependence was observed for both lipid peroxidation inhibition and cytotoxicity. Although 9-triptycenesulfenic acid induces cytotoxicity at lower concentration compared to hexylated petivericin, it is a more potent RTA which inhibits lipid peroxidation at ~6-fold lower concentration. In contrast with allicin and petivericin, no obvious cytotoxicity is observed within the concentration range where lipid peroxidation was efficiently inhibited. These results indicate that 9-triptycenesulfenic acid is a better RTA than hexylated petivericin and does not simply kill cells as do allicin and petivericin. This is fully consistent with the observations in organic solution and liposome oxidations – wherein 9-triptycenesulfenic acid (**3**) is a better RTA compared to hexylated petivericin, which relies on Cope-elimination to produce the authentic RTA sulfenic acid.

4.5 Conclusions

Several years ago, the Pratt lab found that the radical-trapping activities of the garlic-derived thiosulfinate allicin and the analogous secondary metabolite from the related Allium sp. anamu, petivericin, were due to their Cope-elimination products sulfenic acids in organic solution.[24,27] Herein we extended the studies of allicin and petivericin from organic solution to lipid bilayers and mammalian cells to provide insights on whether this reactivity is relevant to their biological activities.

The results pointed out that both allicin and petivericin were ineffective to inhibit lipid peroxidation in lipid bilayers, in sharp contrast with previous studies in organic solution that demonstrated they underwent facile Cope elimination to produce sulfenic acids as potent radical-trapping agents.[9,27] The sulfenic acids that derive from these thiosulfinates by either Cope elimination or S-thiolation are not sufficiently lipophilic to be retained in the lipid bilayer, precluding their reaction with peroxyl radicals. In contrast, synthetic thiosulfinates which give rise to lipophilic sulfenic acids are highly effective RTAs, provided that the thiosulfinates are sufficiently amphiphilic for S-thiolation to take place at the interface of the lipid and aqueous phases. Thiols serve not only to yield sulfenic acids via S-thiolation, but they are also capable of regenerating the sulfenic acids by reducing the sulfinyl radicals (formed following formal H-atom transfer to peroxyl radicals) by electron transfer from the corresponding thiolate.

Assays in human Tf1a erythroblasts, HEK293 kidney cells and HepG2 liver hepatocellular carcinoma cells revealed that allicin and petivericin appeared to inhibit lipid peroxidation in the low μM range, but they were found to induce cell death concomitant with, or as a result of glutathione depletion within the same concentration range. In contrast, lipophilic hexylated petivericin is able to inhibit lipid peroxidation without inducing cell death or depleting glutathione levels, presumably due to its more favourable partitioning to the lipid bilayer. The greater apparent activity of hexylated petivericin observed when lipid peroxidation is induced by Gpx4 inhibition with RSL3 without depleting GSH suggests that the mechanism that operates in the lipid bilayers of liposomes extends to those that make up, and are found within, cells. This requirement for formation of a lipophilic

sulfenic acid is consistent with results obtained with the authentic 9-triptycenesulfenic acid, which is found to be an excellent RTA in each of transfer from organic phase, liposomes to mammalian cells.

4.6 Experimental Section

Materials. Egg phosphatidylcholine, penicillin-streptomycin, Dulbecco's phosphate buffered saline (DPBS), phosphate buffered saline (PBS), MeOAMVN, N-acetylcysteine, ascorbate, trypan blue, C11-BODIPY$^{581/591}$ (4,4-difluoro-5-(4-phenyl-1,3-butadienyl)-4-bora-3a,4a-diaza-s-indacene-3-undecanoic acid), RPMI-1640 media with/without phenol red, MEM media with/without phenol red, non-essential amino acid (100×), fetal bovine serum (FBS) and 7-aminoactinomycin D (7-AAD) were purchased from commercial sources and used as received. BCA protein assay kit was purchased from Thermo Scientific. Palmitoyl-2-linoleyl-sn-glycero-3-phosphocholine (PLPC) was synthesized according to the literature with purification by column chromatography right before using as mentioned in **Chapter 2**.[69]

Liposome preparation. Egg phosphatidylcholine (EggPC) or PLPC (75 mg) was weighed in a dry vial and dissolved in a minimum volume of chloroform. The solvent was then evaporated under argon to yield a thin film on the vial wall. The film was left under vacuum for 2 hours to remove any remaining solvent. The lipid film was then hydrated with 4.0 mL of a 10 mM phosphate-buffered saline (PBS) solution containing 150 mM NaCl, yielding a 24 mM lipid suspension. The lipid suspension was then subjected to 10 freeze-thaw-sonication cycles, followed by extrusion using a mini-extruder equipped with a 100 nm polycarbonate membrane.

Inhibited autoxidation of unilamellar EggPC liposomes. To individual 45 μL aliquots of the 24 mM liposome solution were added increasing amounts (4.5, 9, 13.5, 18 and 22.5 μL, respectively) of a solution of the test antioxidant in acetonitrile (1.1 mM) and 10 μL of a solution of H_2B-PMHC in acetonitrile (13 μM). Each resultant solution was then diluted to 1 mL with PBS, from which 280 μL of each was loaded into a well of a 96-well microplate. The solution was equilibrated to 37°C for 5 min, after which 20 μL of a

solution of 3 mM in MeOAMVN in acetonitrile was added to each well using the reagent dispenser of a microplate reader. The fluorescence was then monitored for 6 h at 50 s time intervals (λ_{ex} = 485 nm; λ_{em} = 520 nm). The final solutions in each well were 1 mM in lipids, 0.15 μM in H_2B-PMHC, 0.2 mM in MeOAMVN and either 4.5, 9, 13.5, 18, 22.5 μM in testing compounds.

Inhibited autoxidation of unilamellar PLPC liposomes. Stock solutions of the different antioxidants in acetonitrile were added into various amounts of unilamellar PLPC liposomes in pH 7.4 buffer. MeOAMVN (48 μL of a 2.3 mM solution in acetonitrile) was then added to initiate lipid peroxidation. The reaction mixtures were stirred at 37°C in an aluminium heating block. The final concentrations of PLPC and MeOAMVN were 8.75 mM and 0.15 mM, repsectively. Every 12 minutes, 10 μL of the reaction mixture was withdrawn and transferred to a well of a 96-well microplate and 165 μL of MeOH containing butylated hydroxytoluene (45 mM) was added to destroy the liposome and prevent adventitious oxidation. Using the reagent dispenser of the microplate reader, 25 μL of a solution of coumarin-phosphine probe in acetonitrile (160 μM) was added to each well and the initial rate of the reaction was obtained by measuring the fluorescence (λ_{ex} = 340 nm; λ_{em} = 425 nm) for 50 s using a microplate reader. The lipid hydroperoxide concentration was calculated based on the initial rate of the reaction.[70]

Cellular lipid peroxidation. Cells (5×10^5 cells/mL for Tf1a and HEK-293 or 1×10^6 cells/mL for HepG2) were treated with each of the thiosulfinates at final concentrations from 5 μM to 200 μM and incubated at 37 °C for 22 hours in phenol red-free RPMI-1640 media with 10% FBS and 1% penicillin-streptomycin for Tf1a cells and phenol red-free MEM media with 10% FBS, 1% non-essential amino acid, 1 mM sodium pyruvate and 1% penicillin-streptomycin for HEK-293 and HepG2 cells in a humidified atmosphere containing 5% CO_2 in air. Attaching cells were detached by eppendorf pipette thoroughly. Half of the cultured cells were divided for cell viability assay. The other half of cells were then treated with 1 μM C11-BODIPY$^{581/591}$ in media and incubated at 37 °C in the dark for 30 minutes after which lipid peroxidation was initiated with either diethylmaleate (9 mM) for 2 hours or (*1S*,*3R*)-RSL3 (4 μM) for 6 hours. Treated cells were then washed by DPBS, and then resuspended in DPBS and analyzed by flow cytometry at a final concentration of

1×10^6 cells/ml (λ_{ex} = 488 nm; λ_{em} = 525±25 nm). Cells that were not treated with DEM/RSL3 were used as negative control. Cells that were not treated with thiosulfinates were used as positive control.

Cell viability. Cells (5×10^5 cells/mL for Tf1a and HEK-293) were treated with each of the thiosulfinates at final concentrations ranging from 5 μM to 200 μM and incubated at 37 ^oC for 22 hours, respectively. Adherent cells were detached by eppendorf pipette thoroughly. Half of the cultured cells were divided for cell viability assay. Cells were collected into the flow cytometry tubes and then treated with 7-AAD (5 μL of a 50 μg/mL solution/1 × 10^6 cells) for 10 minutes and analyzed by flow cytometry at a final concentration of 5×10^5 cells/mL (10,000 events; λ_{ex} = 488 nm; λ_{em} = 675±25 nm). Cell viability was also determined using hemocytometry with trypan blue for Tf1a cells. After incubation of Tf1a cells (5 × 10^5 cells/mL) with each thiosulfinates for 22 hours, 50 μL of 0.4% trypan blue solution was added into 350 μL of cells. The cells were counted using a hemocytometer under light microscopy. The cells which excluded the probe were considered viable. About 200-250 cells were counted for each sample.

MTT assay was used to assay the toxicity for HepG2 cells because cell clumping resulted in inaccuracy measurements using the 7-AAD probe by flow cytometry. HepG2 cells (1×10^6 cells/mL) were cultured in phenol red-free MEM media with 10 % FBS, 1 % non-essential amino acid, 1 mM sodium pyruvate and 1% penicillin-streptomycin in 96 well plate and treated with each antioxidants in DMSO at different concentrations (final DMSO concentration was to not exceeds 1 % volume) at 37°C for 22 hours in a humidified atmosphere containing 5% CO_2 in air. The 96 well plate was centrifuged at 300×g for 5 min and medium was aspirated. 200 μL of fresh MEM media with no phenol red supplemented with 10 % FBS, 1 % non-essential amino acid, 1 mM sodium pyruvate and 1% penicillin-streptomycin and 50 μL of MTT (5mg/mL) in HBSS was added into each well. After 4 hrs incubation, the treated cells were centrifuged at 300×g for 5 minutes and the medium was aspirated. The resultant purple crystals were dissolved with 200 μL isopropanol solution with 0.1 M HCl and 10 % volumn Triton X-100. After 3 hrs incubation at room temperature to dissolve the resultant purple crystals in dark, absorbance (λ = 570

nm) was measured by microplate reader. Results are compared to a negative control (1 % DMSO, no antioxidant treated) and a positive control (1 % Triton X-100). In a control experiment, no toxicity was observed for DMSO up to 1 % volumn.

Cellular thiol concentration. Tf1a (5×10^5 cells/mL), HEK-293 (5×10^5 cells/mL), HepG2 (1×10^6 cells/ mL) cells were treated with each of the thiosulfinates at final concentrations from 10 μM to 200 μM separately and incubated at 37 ºC for 22 hours in phenol red-free media in a humidified atmosphere containing 5% CO_2 in air. Cells were then lysed with HEPES hypotonic buffer and the cytosolic fraction was collected. Intracellular thiol concentration was determined by absorbance at 412 nm using the glutathione colorimetric assay by titration with Ellman's reagent (5,5'-dithio-bis-2-nitrobenzoic acid) using glutathione as a standard. Intracellular protein concentration was determined using a commercial Bradford assay kit.

Cell Apoptosis. Tf1a cells were cultured in RPMI-1640 phenol red free media with 10% FBS and 1% penicillin-streptomycin. Cells (5×10^5 cells/mL) were treated with each of the thiosulfinates 1, 2 and 4 at final concentrations from 10 μM to 200 μM and incubated at 37°C for 22 hours in a humidified atmosphere containing 5% CO_2 in air. Cells were then collected into the flow cytometry tubes followed by centrifugation at 300×g for 3 minutes. Cells were washed with 0.3 mL AnnexinV-PE binding buffer and centrifuged at 300×g for another 3 minutes. Cells were then resuspended in 0.3 mL AnnexinV-PE binding buffer, treated with Annexin V-PE (5 μL/1×10^6 cells) for 10 min. Another 0.2 mL Annexin V-PE binding buffer was added into each sample and 7-AAD staining solution (5 μL/1×10^6 cells) was added. Cells were analyzed by flow cytometry at a final concentration of 1×10^6 cells/mL (10,000 events; λ_{ex} = 488 nm; λ_{em} = 675±25 nm for 7-AAD; λ_{ex} = 488 nm; λ_{em} = 575±25 nm for Annexin-V-PE). Cells incubated with 6 μM camptothecin for 22 hrs were used as positive control for Annexin-V-PE on FL2. Cells incubated with 10 % dmso for 22 hrs were used as positive control for 7-AAD on FL4.

4.7 References

[1] Tanaka, T. *Oncol. Rep.* **1994,** *1* (6), 1139-1155.

[2] Block, E., Garlic and Other Alliums: the Lore and the Science. *The Royal Society of Chemistry, Cambridge, UK* **2010**.

[3] Cavallito, C. J.; Bailey, J. H.; Buck, J. S. *J. Am. Chem. Soc.* **1945,** *67* (6), 1032-1033.

[4] Ankri, S.; Mirelman, D. *Microbes. Infect.* **1999,** *1* (2), 125-129.

[5] Harris, J. C.; Cottrell, S. L.; Plummer, S.; Lloyd, D. *Appl. Microbiol. Biotechnol.* **2001,** *57* (3), 282-286.

[6] Kris-Etherton, P. M.; Hecker, K. D; Bonanome, A.; Coval, S. M.; Binkoski, A. E.; Hilpert, K. F.; Griel, A. E.; Etherton, T. D. *Am. J. Med. Dec 30; :* **2002,** *113* (Suppl 9B), 71S-88S.

[7] Youdim, K. A.; Joseph, J. A. *Free Radic. Biol. Med.* **2001,** *30* (6), 583-594.

[8] Kubec, R.; Kim, S.; Musah, R. A. *Phytochemistry* **2002,** *61* (6), 675-680.

[9] Okada, Y.; Tanaka, K.; Sato, E.; Okajima, H. *Org. Biomol. Chem.* **2008,** *6* (6), 1097-1102.

[10] Capasso, A. *Molecules* **2013,** *18* (1), 690-700.

[11] Banerjee, S. K.; Mukherjee, P. K.; Maulik, S. K. *Phytother. Res.* **2003,** *17* (2), 97-106.

[12] Prasad, K.; Laxdal, V. A.; Yu, M.; Raney, B. L. *Mol. Cell Biochem.* **1995,** *148* (2), 183-189.

[13] Rabinkov, A.; Miron, T.; Konstantinovski, L.; Wilchek, M.; Mirelman, D.; Weiner, L., *Biochem. Biophys. Acta.* **1998,** *1379* (2), 233-244.

[14] Xiao, H.; Parkin, K. L. *J. Agric. Food Chem.* **2002,** *50* (9), 2488-2493.

[15] Li, B.; Pratt, D. A. *Free Radic. Biol. Med.* **2015,** *82*, 187-202.

[16] Amorati, R.; Valgimigli, L. *Free Radic. Res.* **2015,** *49* (5), 633-649.

[17] Yin, H.; Xu, L.; Porter, N. A. *Chem. Rev.* **2011,** *111* (10), 5944-5972.

[18] Porter, N. A. *Acc. Chem. Res.* **1986,** *19* (9), 262-268.

[19] Okada, Y.; Tanaka, K.; Sato, E.; Okajima, H. *Org. Biomol. Chem.* **2006,** *4* (22), 4113-4117.

[20] Burton, G. W.; Doba, T.; Gabe, E. J.; Hughes, L.; Lee, F. L.; Prasad, L.; Ingold, K. U. , *J. Am. Chem. Soc.* **1985,** *107* (24), 7053-7065.

[21] Burton , G. W. Ingold, K. U. *Acc. Chem. Res.* **1986,** *19* (7), 194-201.

[22] Maillard, B.; Ingold, K. U.; Scaiano, J. C. *J. Am. Chem. Soc.* **1983,** *105* (15),

5095-5099.

[23] Amorati, R.; Pedulli, G. F. *Org. Biomol. Chem.* **2008,** *6* (6), 1103-1107.

[24] Lynett, P. T.; Butts, K.; Vaidya, V.; Garrett, G. E.; Pratt, D. A. *Org. Biomol. Chem.* **2011,** *9* (9), 3320-3330.

[25] Ingold, K. U.; Pratt, D. A. *Chem. Rev.* **2014,** *114* (18), 9022-9046.

[26] Block, E. *Adv. Exp. Med. Biol.* **1996,** *401*, 155-169.

[27] Vaidya, V.; Ingold, K. U.; Pratt, D. A. *Angew. Chem. Int. Ed. Engl.* **2009,** *48* (1), 157-160.

[28] Davis, F. A.; Jenkins, L. A.; Billmers, R. L., *J. Org. Chem.* **1986,** *51* (7), 1033.

[29] Amorati, R.; Lynett, P. T.; Valgimigli, L.; Pratt, D. A. *Chemistry* **2012,** *18* (20), 6370-6379.

[30] McGrath, A. J.; Garrett, G. E.; Valgimigli, L.; Pratt, D. A. *J. Am. Chem. Soc.* **2010,** *132* (47), 16759-16761.

[31] Krumova, K.; Friedland, S.; Cosa, G. *J. Am. Chem. Soc.* **2012,** *134* (24), 10102-10113.

[32] Zheng, F.; Pratt, D. A. *Chem. Commun. (Camb)* **2013,** *49* (74), 8181-8183.

[33] Li, B.; Harjani, J. R.; Cormier, N. S.; Madarati, H.; Atkinson, J.; Cosa, G.; Pratt, D. A. *J. Am. Chem. Soc.* **2013,** *135* (4), 1394-1405.

[34] Yang, W. S.; Stockwell, B. R. *Chem. Biol.* **2008,** *15* (3), 234-245.

[35] Yang, W. S.; SriRamaratnam, R.; Welsch, M. E.; Shimada, K.; Skouta, R.; Viswanathan, V. S.; Cheah, J. H.; Clemons, P. A.; Shamji, A. F.; Clish, C. B.; Brown, L. M.; Girotti, A. W.; Cornish, V. W.; Schreiber, S. L.; Stockwell, B. R. *Cell* **2014,** *156* (1-2), 317-331.

[36] Tait, J. F.; Gibson, D. *Arch. Biochem. Biophys.* **1992,** *298* (1), 187-191.

[37] Elmore, S. *Toxicol. Pathol.* **2007,** *35* (4), 495-516.

[38] Vermes, I.; Haanen, C.; Steffens-Nakken, H.; Reutelingsperger, C. *J. Immunol. Methods* **1995,** *184* (1), 39-51.

[39] Freeman, F.; Kodera, Y. *J. Agric. Food Chem.* **1995,** *43* (9), 2332–2338.

[40] Miron, T. R., A.; Mirelman, D.; Wilchek, M.; Weiner, L. *Biochim. Biophys. Acta.* **2000,** *1463* (1), 20-30.

[41] Li, B.; Zheng, F.; Chauvin, J-P. R.; Pratt, D. A. *Chem. Sci.* **2015,** 6 (11), 6165-6178

[42] Block, E. *Angew. Chem. Int. Ed. Engl.* **1992,** *31* (9), 1135-1178.

[43] Doba, T.; Burton, G. W.; Ingold, K. U. *Biochem. Biophys. Acta.* **1985,** *835* (2), 298-303.

[44] Barclay, L. R. C.; Locke, S. J.; MacNeil, J. M., *Can. J. Chem.* **1983,** *61* (6), 1288-1290.

[45] Barclay, L. R. *J. Biol. Chem.* **1988,** *263* (31), 16138-16142.

[46] Malmstrom, J.; Jonsson, M.; Cotgreave, I. A.; Hammarstrom, L.; Sjodin, M.; Engman, L. *J. Am. Chem. Soc.* **2001,** *123* (15), 3434-3440.

[47] Kumar, S.; Johansson, H.; Engman, L.; Valgimigli, L.; Amorati, R.; Fumo, M. G.; Pedulli, G. F. *J. Org. Chem.* **2007,** *72* (7), 2583-2595.

[48] Zielinski, Z.; Presseau, N.; Amorati, R.; Valgimigli, L.; Pratt, D. A. *J. Am. Chem. Soc.* **2014,** *136* (4), 1570-1578.

[49] Millis, K. K.; Weaver, K. H.; Rabenstein, D. L. *J. Org. Chem.* **1993,** *58* (15), 4144–4146.

[50] Noszal, B.; Visky, D.; Kraszni, M. *J. Med. Chem.* **2000,** *43* (11), 2176-2182.

[51] Horev-Azaria, L.; Eliav, S.; Izigov, N.; Pri-Chen, S.; Mirelman, D.; Miron, T.; Rabinkov, A.; Wilchek, M.; Jacob-Hirsch, J.; Amariglio, N.; Savion, N. *Eur. J. Nutr.* **2009,** *48* (2), 67-74.

[52] Li, X. H.; Li, C. Y.; Xiang, Z. G.; Hu, J. J.; Lu, J. M.; Tian, R. B.; Jia, W. *Cardiovasc. Drugs Ther.* **2012,** *26* (6), 457–465.

[53] Ma, Q. *Annu. Rev. Pharmacol. Toxicol.* **2013,** *53,* 401-426.

[54] Forman, H. J. D., K. J. A.; Ursini, F. *Free Radic. Biol. Med.* **2014,** *66,* 24-35.

[55] Lu, S. C. *Mol. Aspects. Med.* **2009,** *30* (1-2), 42-59.

[56] Balendiran,G.K.; Dabur, R.; Fraser, D.; *Cell Biochem. Funct.* **2004**, *22* (6), 343-352.

[57] Hirsch, K.; Danilenko, M.; Giat, J.; Miron, T.; Rabinkov, A.; Wilchek, M.; Mirelman, D.; Levy, J.; Sharoni, Y. *Nutr. Canc*er **2000**, *38* (2), 245-254.

[58] Hirsch, K.; Danilenko, M.; Giat, J.; Miron, T.; Rabinkov, A.; Wilchek, M.; Mirelman, D.; Levy, J.; Sharoni, Y. *Nutr. Cancer* **2000,** *38* (2), 245-254.

[59] Oommen, S.; Anto, R. J.; Srinivas, G.; Karunagaran, D. *Eur. J. Pharmacol.* **2004,** *485* (1-3), 97-103.

[60] Park, S. Y.; Cho, S. J.; Kwon, H. C.; Lee, K. R.; Rhee, D. K.; Pyo, S. *Cancer Lett.* **2005,** *224* (1), 123-132.

[61] Miron, T.; Wilchek, M.; Sharp, A.; Nakagawa, Y.; Naoi, M.; Nozawa, Y.; Akao, Y. *J. Nutr. Biochem.* **2008,** *19* (8), 524-535.

[62] Kim, S.; Kubec, R.; Musah, R. A. *J. Ethnopharmacol* **2006,** *104* (1-2), 188-192.

[63] Groeger, A. L.; Freeman, B. A. *Mol. Interv* **2010**, *10* (1), 39-50.

[64] Lamkanfi, M.; Festjens, N.; Declercq, W.; Vanden Berghe, T.; Vandenabeele, P. *Cell Death Differ.* **2007**, *14* (1), 44-55.

[65] Forman, H. J.; Ursini, F.; Maiorino, M. *J. Mol. Cell. Cardiol*, **2014**, *73*, 2-9.

[66] Velichkova, M.; Hasson, T. *Cell Motil. Cytoskeleton* **2003**, *56* (2), 109-119.

[67] Wang, Z.; Liu, Z.; Cao, Z.; Li, L. *Nat. Prod. Res.* **2012**, *26* (11), 1033-1037.

[68] Zhang, W.; Ha, M.; Gong, Y.; Xu, Y.; Dong, N.; Yuan, Y. *Oncol. Rep.* **2010,** *24* (6), 1585-1592.

[69] O'Neil, E. J.; DiVittorio, K. M.; Smith, B. D. *Org. Lett.* **2007,** *9* (2), 199-202.

[70] Hanthorn, J. J.; Haidasz, E.; Gebhardt, P.; Pratt, D. A. *Chem. Commun. (Camb)* **2012,** *48* (81), 10141-10143.

Chapter 5:

Towards an Understanding of the Biological Mechanism of Resveratrol and its Dimers

5.1 Preface

Resveratrol has been of tremendous interest to the scientific community over the past three decades due to the so-called "French paradox". It has been suggested that the low occurrence of cardiovascular disease in some regions of France, despite the high fat intake of its population, is due to resveratrol – a polyphenolic 'antioxidant' that is relatively abundant in the skins of red grapes used to make wine.[1] Resveratrol has been broadly studied for its antioxidant, anti-inflammatory, anti-proliferative, and anti-angiogenic effects.[2] Although significant efforts have been made to study the biological activities of resveratrol, its mechanism of action remains the subject of wide-ranging debate. Dimers and higher oligomers of resveratrol are prominent natural products, but systematic study of these compounds has been difficult due to the difficulty in obtaining high purity samples from natural sources, and lengthy total syntheses required for their *de novo* preparation.

A recent collaboration with Prof. Corey Stephenson and his group has led to the development of a novel and highly efficient synthetic pathway to the resveratrol dimers pallidol and quadrangularin A. This has enabled the systematic study of their radical-trapping antioxidant activity in organic solution, lipid bilayers and mammalian cells (Matsuura, B. S.; Keylor, M.; Li, B.; Lin, Y.; Allison, S.; Pratt. D., Stephenson, C., "A Scalable Biomimetic Synthesis of Resveratrol Dimers and Systematic Evaluation of their Antioxidant Activities" *Angew. Chem. Int. Ed.* **2015**, *54*, 3754-3757). In the manuscript, we suggested that the mode of action of resveratrol and its dimers pallidol and quadrangularin A is unlikely to be due to their radical-trapping activities. Their synthetic precursors, however, displayed very high reactivity. This chapter is presented largely as it was in the manuscript that was published, but also includes some subsequent studies aimed at assessing the electrophilic

potential of resveratrol and its dimers – a more likely explanation for the biological activity of these compounds.

Resveratrol, pallidol, quadrangularin A and their synthetic precursors were obtained from our collaborators. The kinetics of their reactions with peroxyl radicals were determined in homogenous organic solution by Shelby Allison, an undergraduate student in the Pratt lab. Some of the studies in liposomes and cell culture, autoxidation of resveratrol were carried out in collaboration with YuXuan Lin, another undergraduate student in the Pratt lab, under my immediate supervision.

5.2 Introduction

Resveratrol (**Chart 5.1**) is a naturally-occuring polyphenol present mainly in the skin of grapes, but also other plants.[2] Several naturally-occurring oligomers of resveratrol have been identified; indeed, they are the largest group of oligomeric stilbenes. Pallidol, quandranqularin A, and ε-viniferin are examples of naturally-occurring resveratrol dimers. α-Viniferin, miyabenol C are examples of naturally-occurring trimers. Vaticanol C, kobophenol A, and hopeaphenol are example of naturally-occurring tetramers.[3]

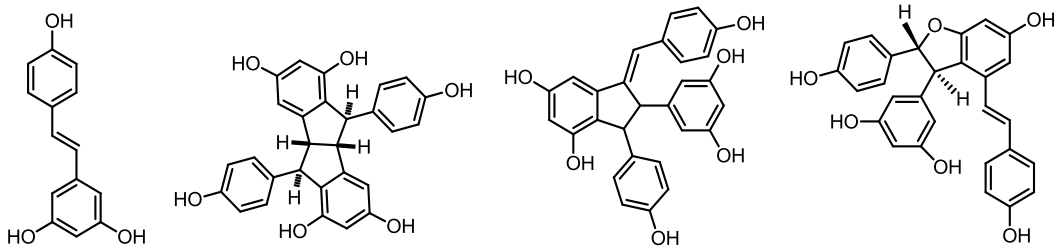

Chart 5.1. Resveratrol and its dimers

Resveratrol and its oligomers have been (perhaps dubiously) linked to the low occurrence of heart disease in some regions of France, despite a high fat diet, due to the popularity of drinking wine; this is referred to as the "French paradox". As such, considerable research effort has been directed toward elucidating the mechanisms of the putative biological activities of these compounds due to their potential health benefits.[4] Particular attention has been paid to a role for resveratrol and its oligomers in the prevention of cancer,

neurodegenerative disease and cardiovascular disease. Moreover, numerous animal studies showed that resveratrol provided protection against diabetes, Alzheimer's, cardiovascular disease and aging.[5-7] Resveratrol dimers pallidol and ε-viniferin have also been demonstrated to inhibit growth of human cancer cells.[8,9] In recent years, several reviews have been published to summarize the biological effects of resveratrol and its oligomers. For example, Sinclair *et. al.* reviewed resveratrol as anti-cancer, anti-diabetic, anti-aging, and anti-inflammatory agents.[4] Shi *et. al.* reviewed the cellular activity of resveratrol and its oligomers as preventive and therapeutic agents for cancers in various cell lines.[3] Stephenson *et. al.* reviewed recent progress to study resveratrol oligomers as anticancer agents, inhibitors of enzymes including cyclooxygenase and hydroperoxidase and their antioxidant activities.[10]

The biological activity of resveratrol and its oligomers has been a highly controversial topic in the past – and much of the controversy has focused on their antioxidant potential. For example, the antioxidant property of resveratrol has been explored previously using traditional assays such as trapping DPPH radical and ABTS.[11] The resveratrol dimer pallidol has been reported to show stronger antioxidant activity than resveratrol using DPPH radical scavenging assay.[12] However, these previous studies on the radical-trapping activities of resveratrol and its oligomers did not focus on their kinetic activities to trap peroxyl radicals; most of them were carried out using assays such as DPPH and ABTS assays in which thermodynamic equilibrium with oxidants in solution was tested. It has also been suggested that resveratrol can prevent lipid peroxidation by the regeneration of α-TOH from α-TO•, akin to the activity of ascorbate, however careful consideration of reliable thermodynamic data clearly indicates that this equilibrium is unfavourable.[13] Therefore, there is no clear scientific evidence to show that resveratrol and its oligomers are RTAs and the structure-activity relationship of resveratrol and related oligomers is unclear at this time.

The synthesis of oligomers of resveratrol has garnered great interest in recent years due to their biologically beneficial properties and their fascinating chemical structures.[14,15] Efforts to synthesize resveratrol oligomers have proven to be challenging; where most of the methods resulted in low yields and tended to lead to complex mixtures of products. Recently, our collaborators at the University of Michigan developed a highly efficient, scalable biomimetic synthetic route to synthesize the resveratrol dimers pallidol and quadrangularin

A using the pathway shown in **Scheme 5.1**.[16] They were able to synthesize natural dimers of resveratrol, pallidol and quadrangularin A using ferrocenium hexafluorophosphate as the oxidant with excellent yield and complete regioselectivity. With these molecules in hand, we set out to systematically determine the radical-trapping activities of resveratrol, its dimers, and their synthetic precursors in organic solution, lipid bilayers and mammalian cells. Moreover, we describe preliminary studies to determine a viable non-RTA mechanism for resveratrol's biological activity.

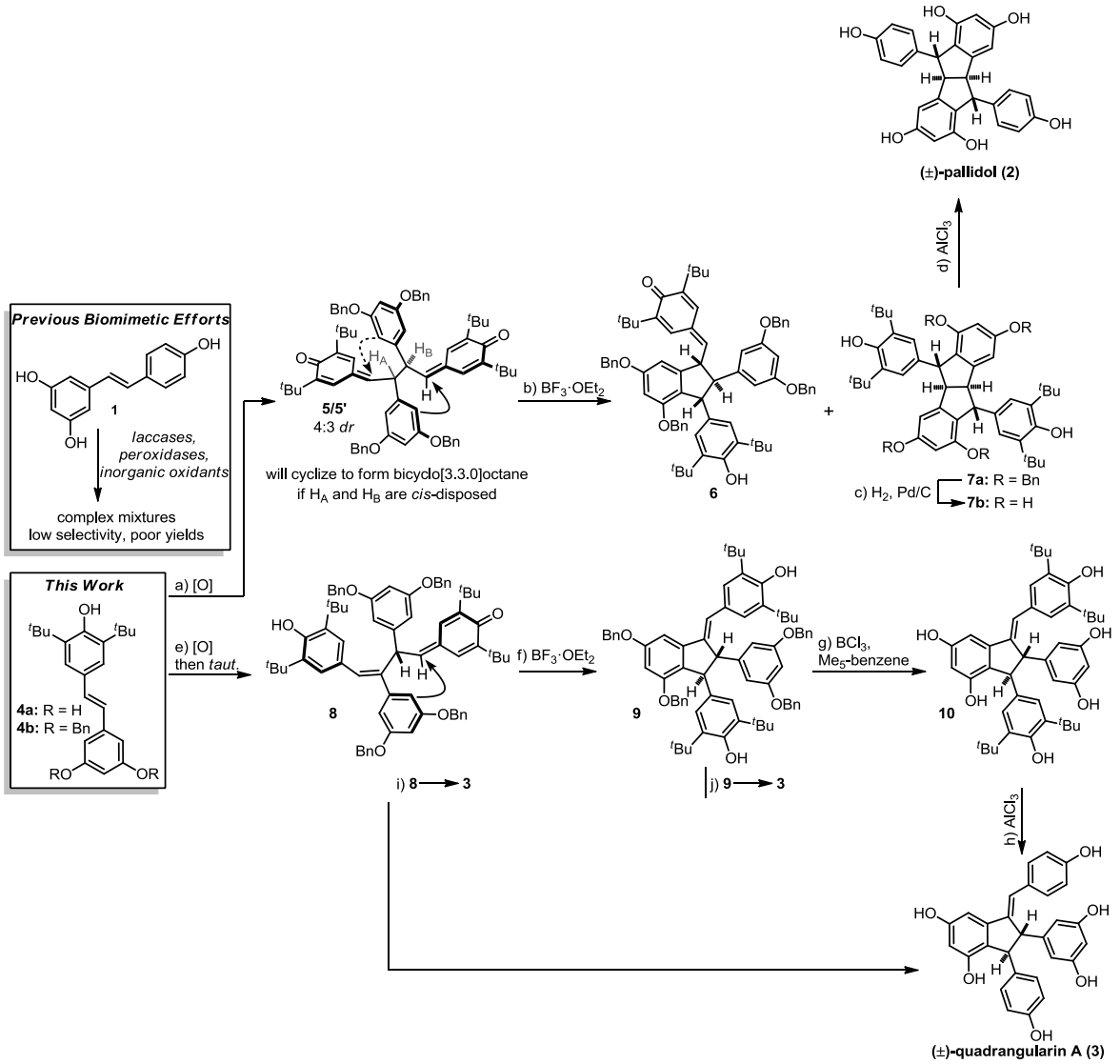

Scheme 5.1. The total synthesis of pallidol (**2**), quadrangularin A (**3**) and their *tert*-butylated derivatives.[16]

5.3 Results

5.3.1 Peroxyl Radical Trapping by Resveratrol, Pallidol, Quadrangularin A and Their Synthetic Precursors in Organic Solution

Recently, Prof. Corey Stephenson *et al.* developed an efficient biomimetic synthetic route to the resveratrol dimers pallidol and quadrangularin A (**Scheme 5.1**).[16] With these compounds in hand, their peroxyl radical-trapping activities in a homogenous organic solution were systematically studied in chlorobenzene using the methyl linoleate peroxyl radical clock method.[17,18] The rate constant for the reaction of a given compound with peroxyl radicals k_{inh} was obtained from the dependence of the oxidation products of methyl linoleate on antioxidant concentration (**Figure 5.1**).[17,18] The benzylated synthetic precursors **4b**, **7a**, **9** were used to determine the rate constants in chlorobenzene because the solubility of the natural products resveratrol **1**, pallidol **2**, and quadrangularin A **3** were poor. Rate constants for the reaction of the natural compounds and their *tert*-butylated synthetic precursors with peroxyl radicals are summarized in **Table 5.1**. The results revealed that *t*Bu$_4$-quadrangularin A **10** (6.2×10^4 $M^{-1}s^{-1}$) was slightly more reactive than *t*Bu$_2$-resveratrol **4a** (5.9×10^4 $M^{-1}s^{-1}$). The k_{inh} of *t*Bu$_4$-pallidol **7b** (2.1×10^4 $M^{-1}s^{-1}$) was less due to the lack of an activating alkene group and a structure similar to that of the common antioxidant BHT (the two-fold statistical advantage of pallidol was considered). The reactivity of the authentic natural products could be estimated from the relative rate constants given above and the known rate constant for resveratrol determined by Valgimigli and coworkers to be 2.0×10^5 $M^{-1}s^{-1}$.[19]

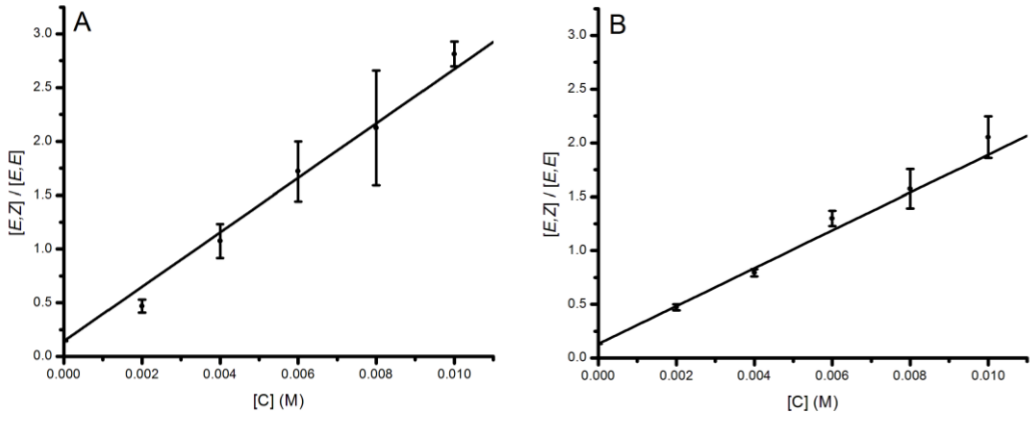

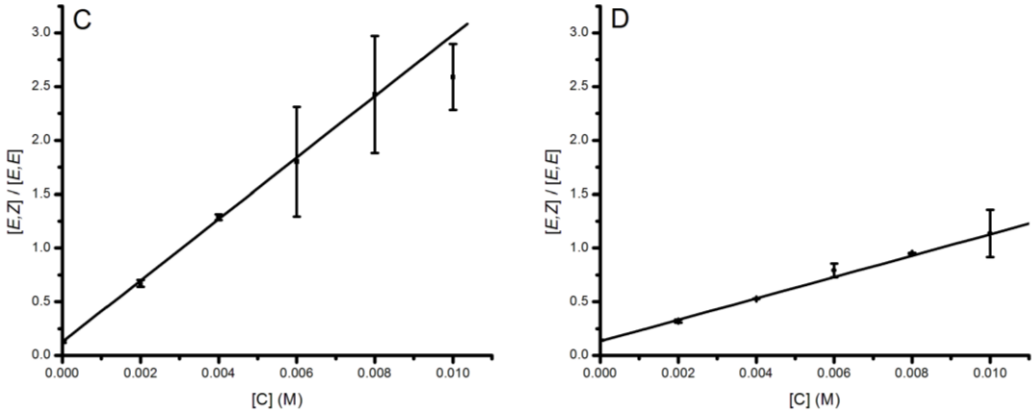

Figure 5.1. Ratio of [*E,Z*]/[*E,E*] products versus concentration of *t*-Bu$_2$-resveratrol (**4a**) (A), *t*-Bu$_2$-pallidol (**7b**) (B), *t*-Bu$_2$-quadrangularin A (**10**) (C), and BHT (D) in the MeOAMVN-initiated (0.01 M) autoxidation of methyl linoleate (0.1 M) in chlorobenzene at 37°C.

Table 5.1. Radical-trapping antioxidant activity of resveratrol, pallidol and quadrangularin A and their synthetic precursors in chlorobenzene.

Antioxidants	Solution	k_{inh}[a] (PhCl) / $M^{-1}s^{-1}$
resveratrol (**1**)		2.0×10^{5} [b]
pallidol **(2)**[c]		8.5×10^{4} [d]
quadrangularin A **(3)**		2.3×10^{5} [d]
α-TOH		3.2×10^{6} [b]
*t*Bu$_2$-resveratrol **(4a)**		$(5.9\pm0.8)\times10^{4}$ [e]
*t*Bu$_4$-pallidol **(7b)** [c]		$(2.1\pm0.3)\times10^{4}$ [e]
*t*Bu$_4$-quadrangularin A **(10)**		$(6.2\pm0.9)\times10^{4}$ [e]
BHT		$(2.2\pm0.1)\times10^{4}$ [e]

[a]Second order rate constant for the reaction with (linoleyl) peroxyl radicals [b]Determined at 30 °C from the inhibited autoxidation of styrene.[19] [c]Since two equivalent units exist on the same molecule, the observed rate constant has been divided by 2. [d]Estimated from the value for resveratrol and the relative reactivity of the corresponding synthetic precursors (*tert*-butylated analogs). [e]Determined at 37°C by the peroxyl radical clock methodology on resorcinol ring-protected (benzyl) compounds.

5.3.2 Peroxyl Radical-Trapping by Resveratrol, Pallidol, Quadrangularin A and Their Synthetic Precursors in Lipid Bilayers-Competition with H_2B-PMHC

The RTA activities of resveratrol **1**, pallidol **2**, quadrangularin A **3** and their synthetic *tert*-butylated and benzylated precursors were determined in EggPC liposomes using the competitive kinetics approach employing H_2B-PMHC a fluorogenic lipid oxidation probe as mentioned in **Chapter 2**. Representative results are shown in **Figure 5.2** and **Figure 5.3** for oxidations initiated with the lipophilic azo initiator MeOAMVN in the presence of various concentrations of added compounds. Natural resveratrol **1**, pallidol **2,** and quadrangularin A **3** were largely ineffective in competing with the fluorogenic H_2B-PMHC for reaction with peroxyl radicals up to 30 μM (**Figure 5.2**). In comparison, their synthetic precursors *t*-Bu_2-resveratrol **4a** and *t*-Bu_4-quadrangularin A **10** were effective in slowing down the oxidation of the fluorogenic H_2B-PMHC under the same conditions with *t*-Bu_2-resveratrol 10-fold and *t*-Bu_4-quadrangularin A 4-fold faster than α-TOH respectively. Six concentrations of each compound were examined from which a clear dose-response relationship was evident. The inhibited periods observed for *t*-Bu_2-resveratrol **4a** and *t*-Bu_4-quadrangularin A **10** were very similar for the inhibited periods obtained with the same concentrations of 2,2,5,7,8-pentamethyl-6-chromanol (PMHC); this allowed for the determination of the stoichiometric number of *t*-Bu_2-resveratrol **4a** and *t*-Bu_4-quadrangularin A **10** (**Table 5.2**). The activity exhibited by *t*-Bu_4-pallidol **7b** and BHT were not as high as that of *t*-Bu_2-resveratrol **4a** and *t*-Bu_4-quadrangularin A **10**, however, the activity of *t*-Bu_4-pallidol **7b** was slightly better than its corresponding natural product pallidol **2** (comparing **Figure 5.3B** and **Figure 5.2B**). None of the benzylated or quinone methide precursors (compounds **4b**, **6**, **7a**, **8**, **9**) could compete with the fluorogenic H_2B-PMHC in lipid bilayers (data not shown).

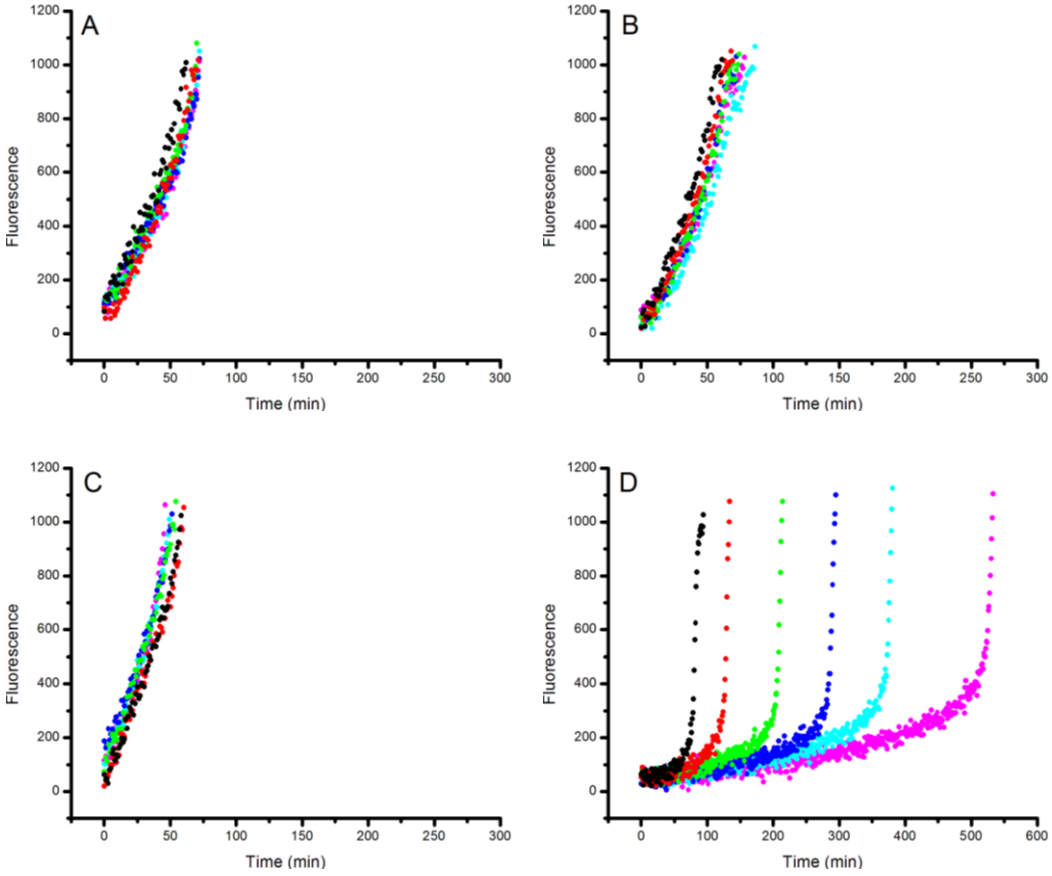

Figure 5.2. Representative fluorescence intensity-time profiles from MeOAMVN-mediated (0.68 mM) oxidations of EggPC liposomes (1 mM in pH 7.4 PBS buffer) containing 0.15 µM H_2B-PMHC probe and increasing concentrations (2.5 µM - black, 5.0 µM - red, 10 µM - green, 15 µM - blue, 20 µM- cyan, 30 µM- pink) of resveratrol (**1**) (A), pallidol (**2**) (B), quadrangularin A (**3**) (C) and PMHC (D). Fluorescence (λ_{ex} = 485 nm, λ_{em} = 520 nM) was recorded every 60 s.

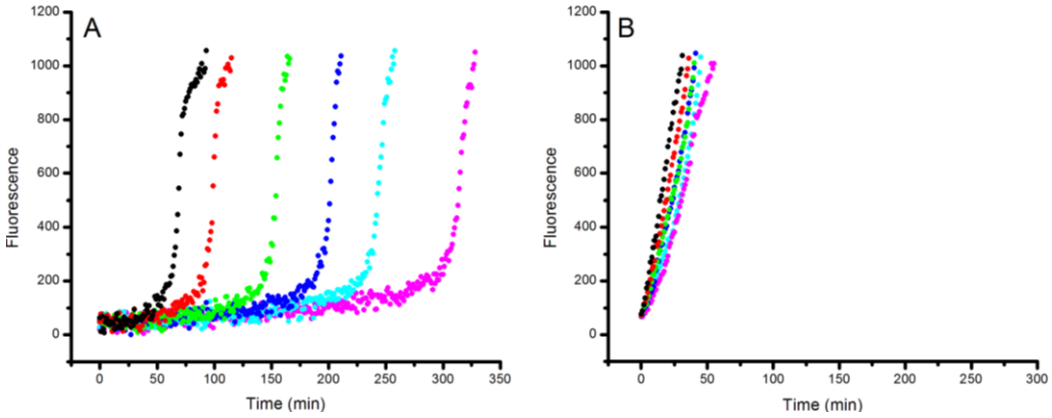

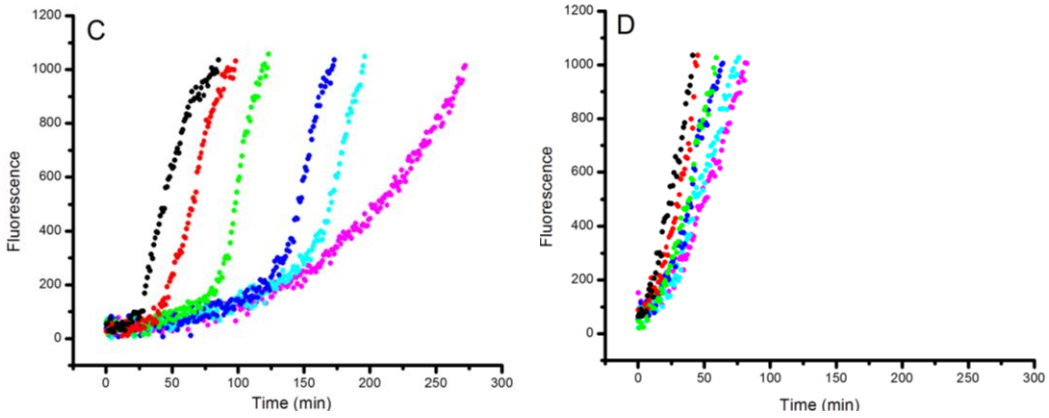

Figure 5.3. Representative fluorescence intensity-time profiles from MeOAMVN-mediated (0.68 mM) oxidations of EggPC liposomes (1 mM in pH7.4 PBS buffer) containing 0.15 μM H_2B-PMHC and increasing concentrations (2.5 μM - black, 5.0 μM - red, 10 μM - green, 15 μM - blue, 20 μM - cyan, 30 μM- pink) of *t*-Bu$_2$-resveratrol (**4a**) (A), *t*-Bu$_4$-pallidol (**7b**) (B), *t*-Bu$_4$-quadrangularin A (**10**) (C) and BHT (D). Fluorescence (λ_{ex} = 485 nm; λ_{em} = 520 nM) was recorded every 60 s.

Similar trends were observed when the oxidation was initiated with the aqueous initiator AAPH, wherein *t*Bu$_2$-resveratrol **4a** exhibited the best activity among the compounds that were evaluated with a 16-fold faster rate than α-TOH (see **Figure 5.4** and **Figure 5.5** for details). In contrast to oxidations that were initiated with MeOAMVN, the oxidation of quadrangularin A **3** and *t*-Bu$_4$-quadrangularin A **10** had similar reactivity, around 10-fold faster than resveratrol **1**, pallidol **2**, and *t*-Bu$_4$-pallidol **7b,** although they were more than orders of magnitude slower than *t*Bu$_2$-resveratrol **4a**.

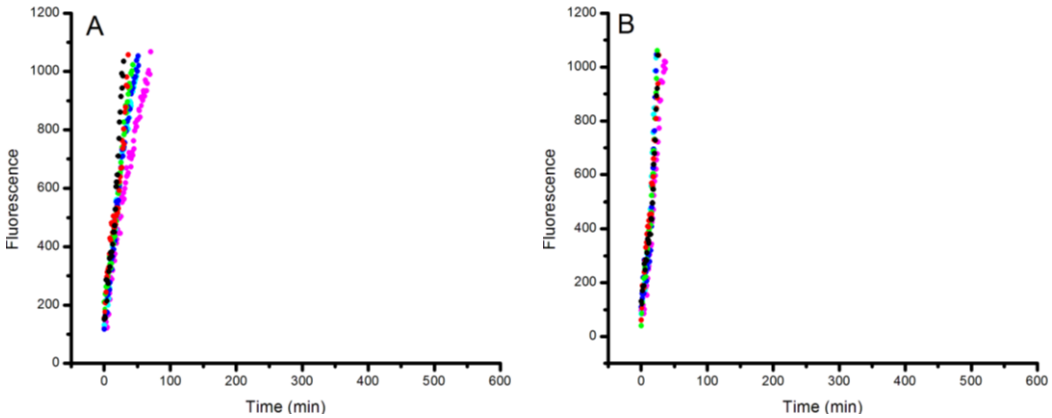

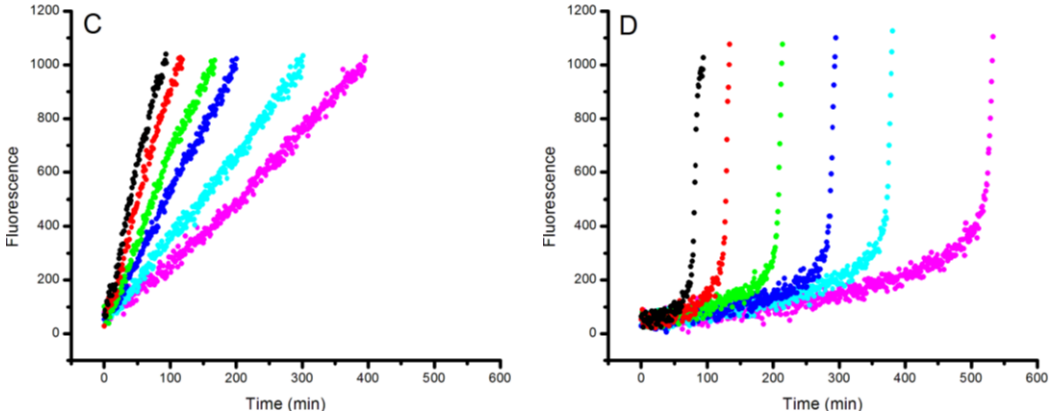

Figure 5.4. Representative fluorescence intensity-time profiles from AAPH-mediated (2.7 mM) oxidations of EggPC liposomes (1 mM in pH 7.4 PBS buffer) containing 0.15 μM H_2B-PMHC and increasing concentrations (2.5 μM - black, 5.0 μM - red, 10 μM - green, 15 μM - blue, 20 μM - cyan, 30 μM- pink) of resveratrol (**1**) (A), pallidol (**2**) (B), quadrangularin A (**3**) (C) and PMHC (D). Fluorescence (λ_{ex} = 485 nm; λ_{em} = 520 nM) was recorded every 60 s.

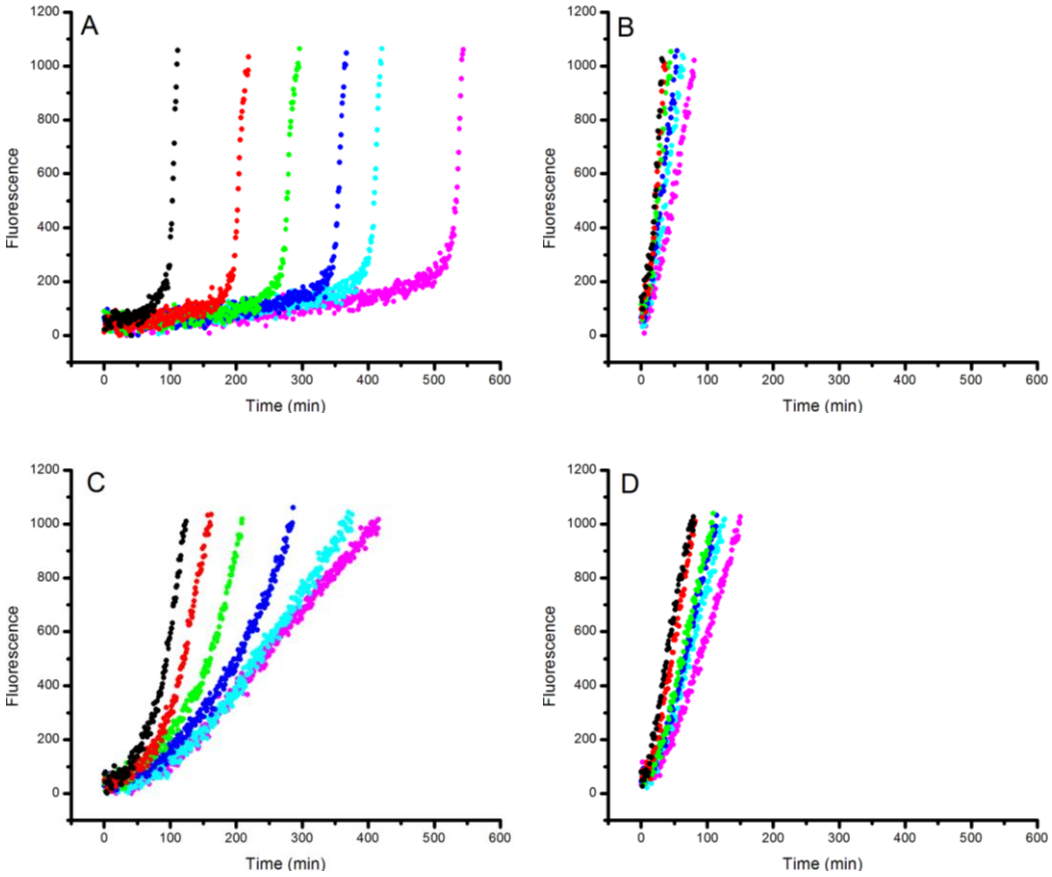

Figure 5.5. Representative fluorescence intensity-time profiles from AAPH-mediated (2.7 mM) oxidations of EggPC liposomes (1 mM in pH 7.4 PBS buffer) containing 0.15 μM H_2B-PMHC and increasing concentrations (2.5 μM - black, 5.0 μM - red, 10 μM - green, 15 μM - blue, 20 μM- cyan, 30 μM- pink) of *t*-Bu_2-resveratrol (4a) (A), *t*-Bu_2-pallidol (7b) (B), *t*-Bu_2-quadrangularin A (10) (C) and BHT (D). Fluorescence (λ_{ex} = 485 nm; λ_{em} = 520 nM) was recorded every 60 s.

Compared to the measurements in homogenous solution, the relative rate constants determined in heterogeneous lipid bilayers using **Eq. 5.1** clearly indicated an inversion in the relative reactivity between the natural products and their *tert*-butylated synthetic precursors (**Table 5.2**).

$$\ln\left(\frac{I_\infty - I_t}{I_\infty - I_0}\right) = \frac{k_{inh}^{H2B-PMHC}}{k_{inh}^{RTA}} \ln\left(1 - 1n\frac{t}{\tau}\right) \qquad \textbf{Eq 5.1}$$

Table 5.2. Radical-trapping antioxidant activity of resveratrol, pallidol and quadrangularin A and their synthetic precursors in EggPC lipid bilayers. Data for benchmark phenolic antioxidants α-TOH and BHT is also provided.

Antioxidants	Lipid Bilayers	
	k_{rel},[a] n[b] (ROO•$_{lipid}$)[c]	k_{rel},[a] n[b] (ROO•$_{aq}$)[c]
resveratrol (**1**)	<0.01	<0.01
pallidol **(2)**[d]	<0.01	<0.01
quadrangularin A **(3)**	<0.01	<0.1
α-TOH	1.8±0.2, 2.0[e]	1.3±0.1, 2.0[e]
tBu_2-resveratrol **(4a)**	17.9±3.3, 1.8±0.1	21.0±6.8, 1.8±0.1
tBu_4-pallidol **(7b)**[d]	<0.01	<0.01
tBu_4-quadrangularin A **(10)**	7.5±0.6, 1.9±0.1	<0.1
BHT	<0.01	<0.01

[a]Second order rate constant for the reaction with peroxyl radicals relative to the fluorescent probe H_2B-PMHC. [b]Number of peroxyl radicals trapped per molecule of test compound. [c]Initiated with MeOAMVN (lipid soluble) and AAPH (water soluble), respectively [d]Since two equivalent units exist on the same molecule, the observed rate constant has been divided by 2 [e]From previous reference.[20]

5.3.3 Inhibition of Lipid Peroxidation and Cytotoxicity in Cell Culture

To probe the potential biological activity of natural products and their synthetic precursors, their efficacy in preventing lipid peroxidation was determined in human Tf1a erythroblasts and was compared to α-TOH and BHT. The lipophilic C11-BODIPY$^{581/591}$ probe mentioned in **Chapter 3** was used to monitor membrane lipid oxidation that was initiated by adding DEM to deplete glutathione using flow cytometry. A clear dose-dependence was observed for each compound (**Figure 5.6, 5.7**), and the half maximal effective concentration (EC_{50}) values to inhibit lipid peroxidation were determined from the dose-response curve (**Table 5.3**).

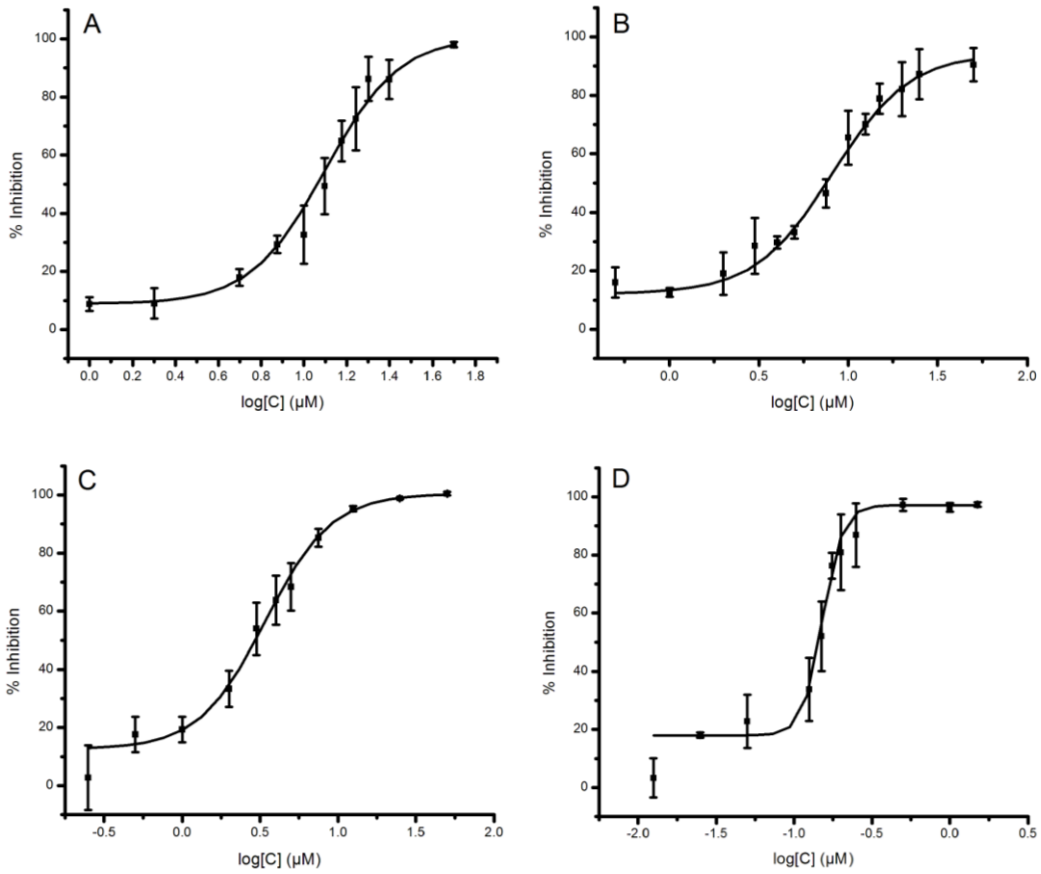

Figure 5.6. Dose-response curves obtained from flow cytometry (5×10^5 cells/ mL; λ_{ex} = 488 nm, λ_{em} = 525±25 nm; 10,000 events) following induction of oxidative stress with diethylmaleate (DEM, 9 mM) in Tf1a cells grown in media containing resveratrol (**1**) (A), pallidol (**2**) (B), quadrangularin A (**3**) (C) and α-TOH (D) (0.015-50 μM) for 22 hours at 37 °C. Cells were incubated with the lipid peroxidation reporter C11-BODIPY$^{581/591}$ (1 μM) for 30 minutes prior to DEM treatment.

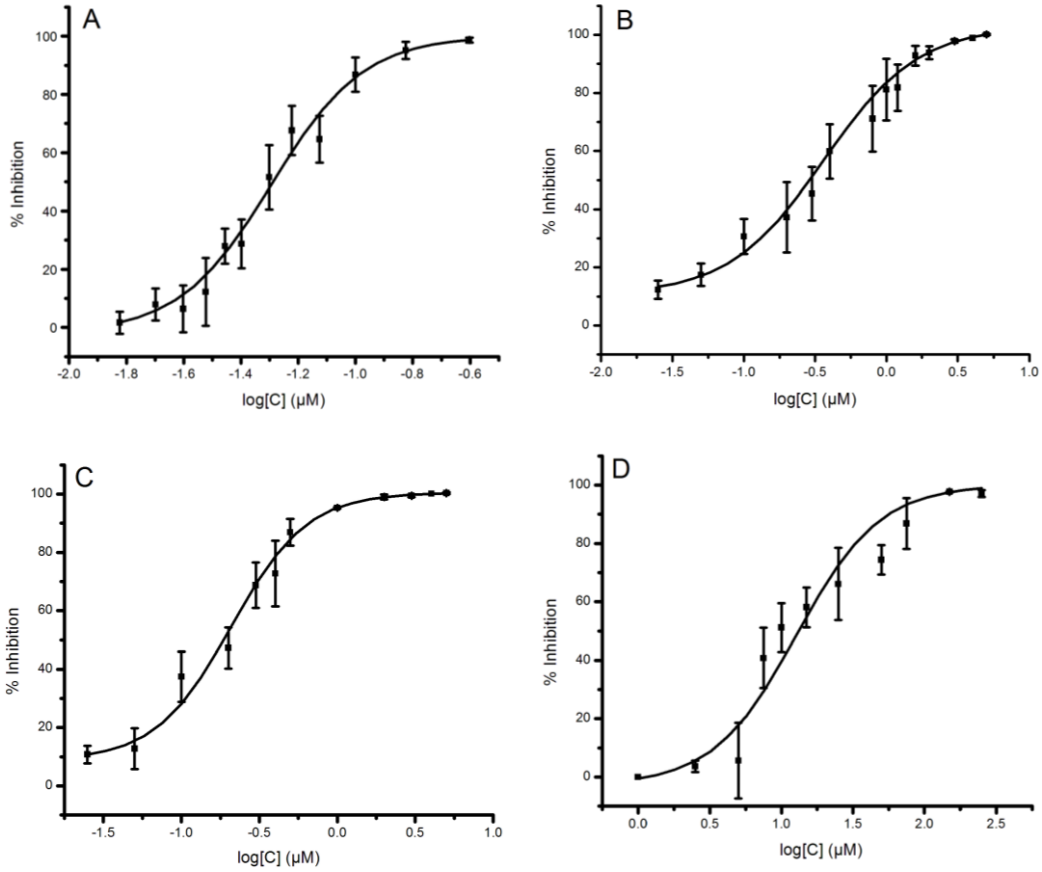

Figure 5.7. Dose-response curves obtained from flow cytometry (5×10^5 cells/ mL; λ_{ex} = 488 nm, λ_{em} = 525±25 nm; 10,000 events) following induction of oxidative stress with diethylmaleate (DEM, 9 mM) in Tf1a cells grown in media containing *t*-Bu_2-resveratrol (**4a**) (A), *t*-Bu_2-pallidol (**7b**) (B), *t*-Bu_2-quadrangularin A (**10**) (C) and BHT (D) (0.015-50 μM) for 22 hours at 37 °C. Cells were incubated with the lipid peroxidation reporter C11-BODIPY$^{581/591}$ (1 μM) for 30 minutes prior to DEM treatment.

Again, the natural products were orders of magnitude less effective at inhibiting lipid peroxidation than their *tert*-butylated analogues. In the case of pallidol **2** and quadrangularin A **3**, roughly 20-fold (8.1 μM and 3.4 μM vs. 0.39 μM and 0.21 μM, respectively) difference was determined in their EC_{50} values, whereas for resveratrol, the difference was almost 250-fold higher (12.6 μM vs. 51 nM). In fact, consistent with its higher reactivity in lipid bilayers, *tert*-butylated resveratrol **4a** was even more effective in cell culture than α-TOH under the same conditions (EC_{50}=0.15 μM). This reinforces the fact that dynamics of RTA must trump inherent reactivity in heterogeneous systems.[21,22] In fact, *tert*-butylated resveratrol **4a** is one of the most reactive RTAs to be studied in cell culture by our group; this is similar to the lipophilic tetrahydronaphthyridinols that are described in **Chapter 3**. Curiously, although the

tert-butylated pallidol **7b** was inefficient at trapping radicals in lipid bilayers initiated by both lipophilic or aqueous initiators, it was surprisingly potent against lipid peroxidation in cellular models; the EC_{50} value obtained was only around 1.5-fold higher than *tert*-butylated quadrangularin A **10**. Both *tert*-butylated pallidol **7b** and *tert*-butylated quadrangularin A **10** were only around 2-fold less effective than α-TOH in Tf1a erythroblasts although their efficacy in lipid bilayers was very poor. These results suggested that they may operate through a different mechanism. In comparison, none of the benzylated and quinone methide precursors (compounds **4b**, **6**, **7a**, **8**, **9**) showed inhibition on lipid peroxidation up to 50 μM where the poor solubility of the compounds in aqueous phase might limit their incorporation into the cell (data not shown).

Table 5.3. Radical-trapping antioxidant activity of resveratrol, pallidol and quadrangularin A and their synthetic precursors in human Tf1a erythroblasts. Data is also provided for benchmark phenolic antioxidants α-TOH and BHT.

Antioxidants	Potency EC_{50} / μM	Cytotoxicity TC_{50} / μM
resveratrol (**1**)	12.6±0.9	118±14
pallidol **(2)**	8.1±0.9	205±11
quadrangularin A **(3)**	3.4±0.4	63.5±3.0
α-TOH	0.15±0.01	>100
tBu_2-resveratrol **(4a)**	0.051±0.004	10.2±0.3
tBu_4-pallidol **(7b)**	0.39±0.07	10.2±0.4
tBu_4-quadrangularin A **(10)**	0.21±0.03	8.7±0.5
BHT	12.7±1.5	49.5±2.0

The cytotoxicity was assayed in human Tf1a erythroblasts using MTT assay (**Figure 5.8 and 5.9**) to confirm that the lipid peroxidation inhibition that we observed was not due to cell death. The concentration ranges where the compounds induced cytotoxicity did not overlap with the concentrations where they inhibited lipid peroxidation. The EC_{50} value of *tert*-butylated resveratrol **4a** for inhibiting lipid peroxidation under the experimental

conditions was 200-fold lower than the corresponding EC_{50} values for inducing cell death; this is a much larger margin than for natural resveratrol **1** (ca. 10-fold). For all other tested compounds, EC_{50} values of cytotoxicity were around 18-42 fold higher than that of lipid peroxidation inhibition. Again, *tert*-butylated pallidol **7b** exhibited similar toxicity compared to *tert*-butylated quadrangularin A **10**, although their activities in lipid bilayers were ~1.5 fold different.

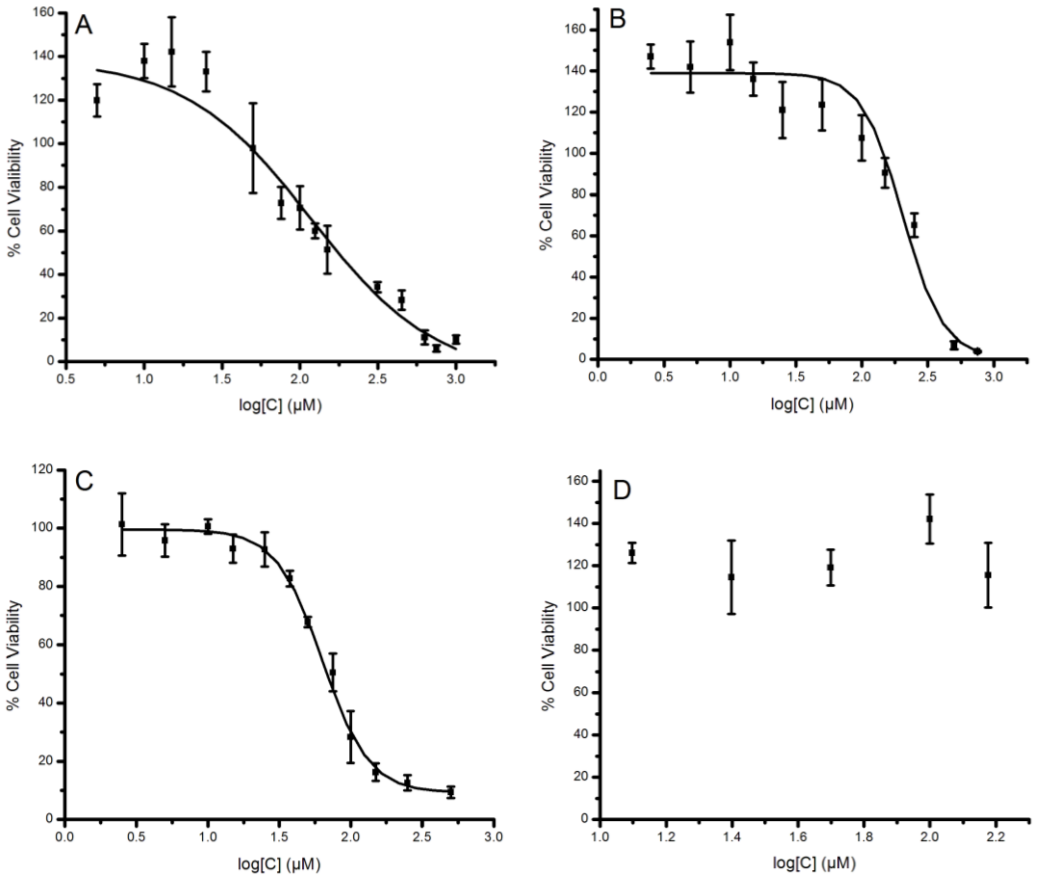

Figure 5.8. Dose-response curves obtained from MTT cell viability studies with Tf1a erythroblasts (0.2×10^6 cells/ mL) containing varying concentrations of resveratrol **1** (A), pallidol (**2**) (B), quadrangularin A (**3**) (C), α-TOH (D) incubated at 37 °C for 22h.

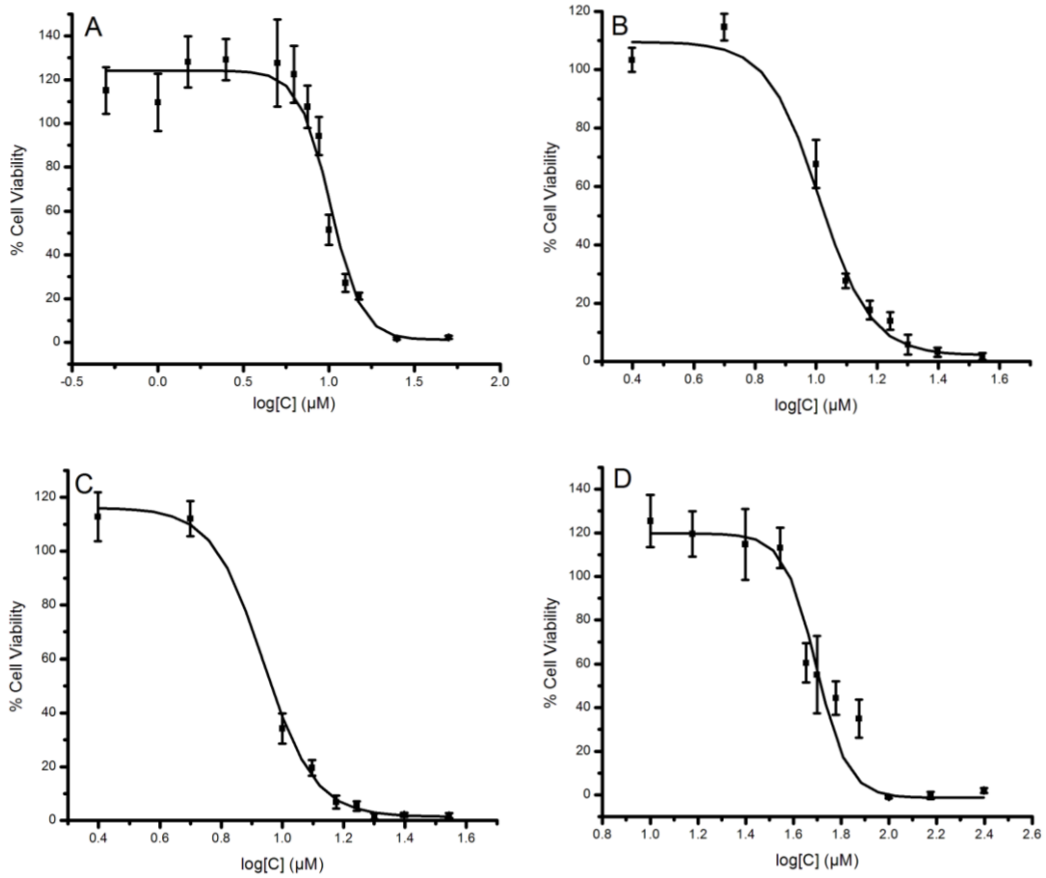

Figure 5.9. Dose-response curves obtained from MTT cell viability studies with Tf1a erythroblasts (0.2×10^6 cells/ mL) containing varying concentrations of *t*-Bu_2-resveratrol (**4a**) (A), *t*-Bu_2-pallidol (**7b**) (B), *t*-Bu_2-quadrangularin A (**10**) (C), BHT (D) incubated at 37 °C for 22h.

5.3.4 Autoxidation of Resveratrol

In the course of the forgoing studies, we observed that resveratrol undergoes autoxidation in aqueous media. To provide a preliminary understanding of the autoxidation kinetics of resveratrol, its degradation was studied. Reaction progress was followed by monitoring the decrease of the maximum absorption of resveratrol at 306 nm.[23] Representative results are shown in **Figure 5.10** for experiments carried out with 10, 50 and 200 μM of resveratrol, and clearly show that the stability of resveratrol is quite poor at 10 μM ($t_{1/2}$ ~ 30 minutes), but improves at higher concentrations.[23] Further experimentation (not shown) indicates that O_2 becomes rate limiting at higher resveratrol concentrations; the solubility of O_2 in aqueous

buffer is approximately 200 μM at 37 °C.[24] We have also demonstrated that the autoxidation rate of resveratrol is pH dependent, with higher observed rate under more basic conditions (**Figure 5.10B**).[23]

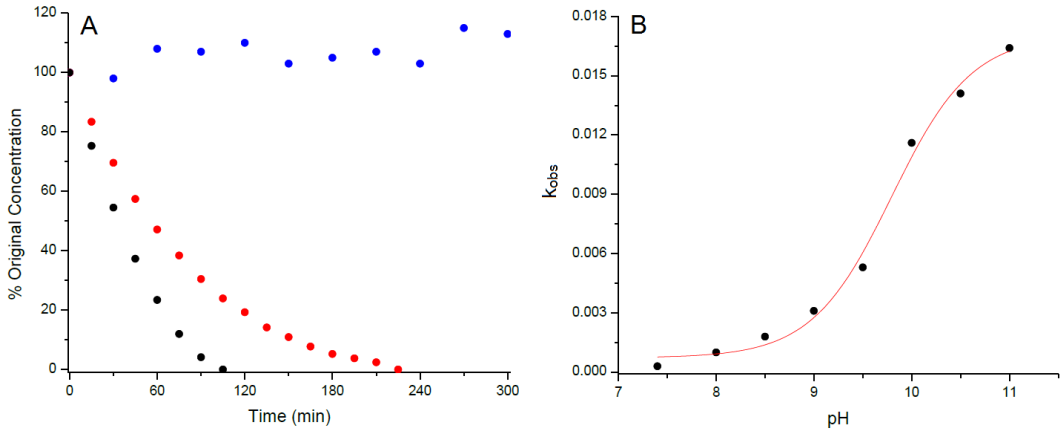

Figure 5.10. (A) Autoxidation of resveratrol with various starting concentrations at 37 °C, 10 μM (black), 50 μM (red), 200 μM (blue) resveratrol sample dissolved in 100 mM pH 7.4 PBS buffer and injections onto LC-MS were made at set time intervals. Signal strength of resveratrol's absorbance peak was detected at 306 nm. (B) pH-dependent first order observed rate constant for autoxidation of 10 μM resveratrol in 100 mM PBS buffer from pH 7.4 to pH 11.0 by monitoring the decreasing resveratrol absorption at 306 nm.[23]

5.3.5 Electrophilic Potential of Oxidation Products of Resveratrol

Given that resveratrol is readily oxidized under physiological pH, it is possible that its biological activity as an apparent 'antioxidant' may instead derive from the reactivity of its oxidation products toward sensitive signaling proteins that control expression of antioxidant genes. Since these signaling proteins invariably possess nucleophilic cysteines as sensors of oxidative/electrophilic stress,[25] we evaluated the electrophilic potential of the resveratrol oxidation products by assessing their potency as inhibitors of papain, the archetype cysteine protease. Papain activity was assessed using a chromogenic substrate *N*α-benzoyl-DL-arginine 4-nitroanilide hydrochloride (BAPNA) by monitoring the rate at 410 nm corresponding to production of 4-nitroaniline.[26]

Resveratrol had no effect on papain activity up to 125 μM (**Figure 5.11B**).[16] However,

when resveratrol was oxidized in PBS buffer (pH 10) overnight with O_2 continuously infused through the media until the absorbance at 306 nm disappeared, the resultant product(s) inhibited papain in a dose-dependent manner with an EC_{50} of 8.6±1.0 μM (**Figure 5.11A**). (The concentration of the oxidation product(s) was assumed to be the same as for the starting resveratrol.) Since we anticipated that one of the resveratrol autoxidation products may be H_2O_2, we also assayed its ability to inhibit papain, and found an EC_{50} of 2.9±0.57 μM (**Figure 5.11C**). In contrast, deactivation of papain was lost (**Figure 5.11D, E**) if either the resveratrol autoxidation product mixture or H_2O_2 was pre-incubated with catalase for 10 minutes prior to the assay.

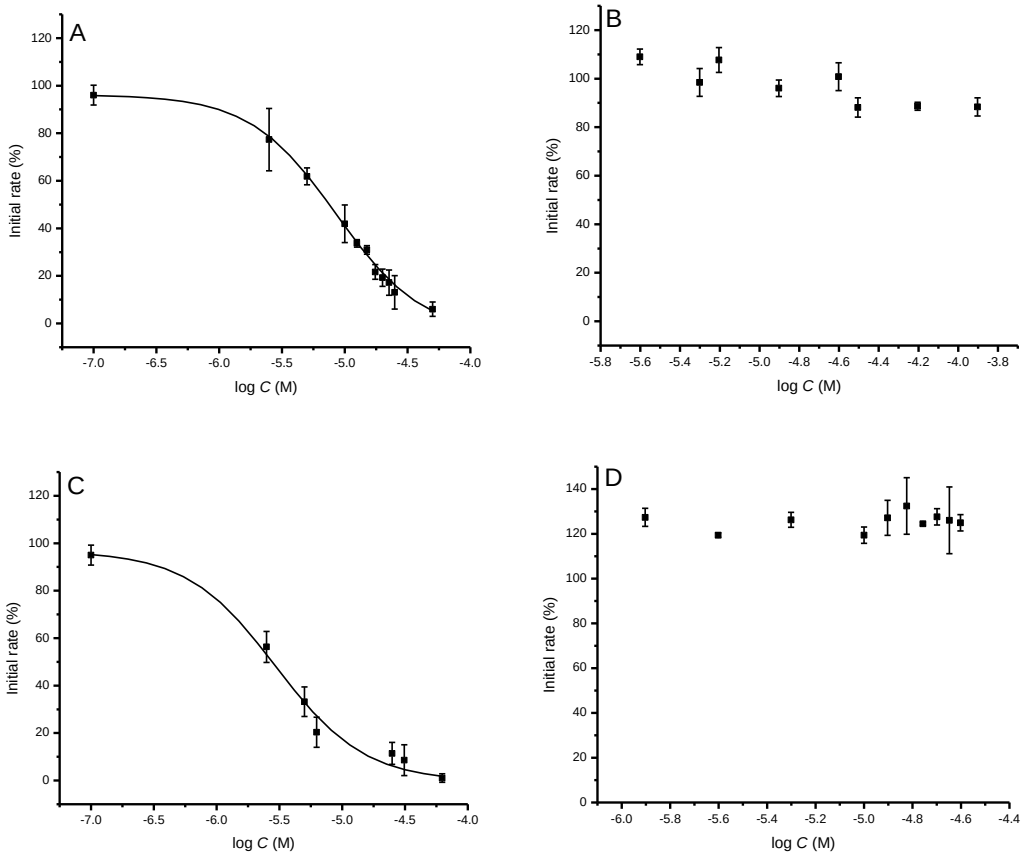

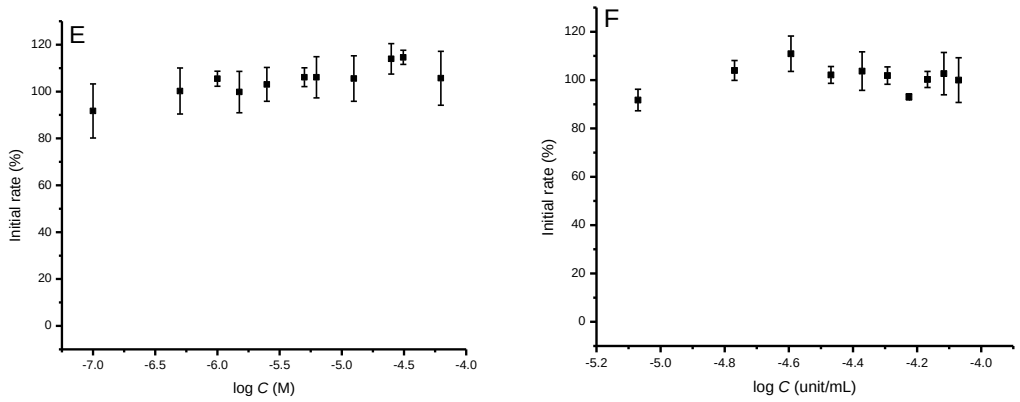

Figure 5.11. Dose-response curves obtained from the papain inactivation assay in EDTA/sodium acetate buffer (pH 6.1) for the oxidation solution of resveratrol (A, EC_{50} = 8.6±1.0 μM), resveratrol (B), H_2O_2 (C, EC_{50} = 2.9±0.57 μM), oxidation solution of resveratrol followed by incubation with catalase for 10 min (D), H_2O_2 incubated with catalase for 10 min (E), catalase (F, one unit will decompose 1 μmole of H_2O_2 per min at pH 7.0 at 25 °C). Papain activity was determined by measuring the rate of increase of absorbance at 410 nm.

5.4 Discussion

The biological activity of resveratrol and its oligomers has been a controversial topic for the past 20 years. However, the mechanism of action of resveratrol remains unclear – and, even less is known about the oligomers that presumably derive from its oxidation. It has been widely speculated that the biological activities of resveratrol and its oligomers were due to their RTA properties; however, experimental evidence to support this hypothesis is insufficient. The experiments described here were designed and carried out to 1) assess the RTA activity of resveratrol, its dimers pallidol and quadrangularin A, and their synthetic precursors from organic solution to more biologically relevant contexts such as the lipid bilayers of liposomes and mammalian cells; 2) provide preliminary experimental results to help clarify the mechanism responsible for resveratrol's biological activity.

Of the three phenolic moieties in resveratrol, it is expected that resveratrol will react with peroxyl radicals by H-atom transfer (HAT) from the 4'-OH group (**Scheme 5.2**) due to its lower BDE compared to that of the hydroxyl groups at the 1 or 3 positions in the A ring.[27]

The phenoxyl radical arising from HAT from the 4'-OH group is significantly better stabilized than HAT from hydroxyl groups at the 1 or 3 positions due to better delocalization of the electrons on the alkene group to 4'-OH, which is also predicted by calculation.[28] However, since the O-H BDE of the 4'OH group in resveratrol has been measured to be 5.5 kcal/mol higher than that of α-TOH,[29] it is unlikely that resveratrol is a particularly good radical-trapping antioxidant.

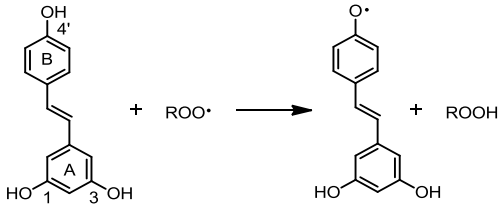

Scheme 5.2. Hydrogen atom transfer from resveratrol to lipid peroxyl radicals.

Among hundreds of studies on resveratrol, to the best of our knowledge there are only two reports on the kinetics of the reaction of resveratrol with peroxyl radicals. Valgimigli *et al.* reported that resveratrol reacted with peroxyl radicals in chlorobenzene at 298 K with a rate constant of k_{inh} = 2.0×10^5 $M^{-1}s^{-1}$; this is ~15-fold slower than α-TOH under the same conditions, and consistent with its stronger O-H bond.[19] The second reported k_{inh} value of resveratrol towards peroxyl radicals is that of resveratrol inhibited peroxidation of linoleic acids with k_{inh} = 1.3×10^4 $M^{-1}s^{-1}$ in a sodium dodecyl sulfate (SDS) micelle system and k_{inh} = 0.7×10^4 $M^{-1}s^{-1}$ in a hexadecyltrimethylammonium bromide (CTAB) micelle system, respectively.[30] To the best of our knowledge, there is no experimental data showing the k_{inh} of resveratrol dimers pallidol and quadrangularin A towards peroxyl radicals.

The rate constant of resveratrol dimers pallidol and quadrangularin A and their synthetic precursors were predicted using methyl linoleate peroxyl radical clock experiments. Since the natural products could not be solubilized in chlorobenzene at sufficiently high concentrations to ensure pseudo-first order conditions, the experiments were carried out on the synthetic precursors to pallidol and quadrangularin A, as well as the analogous resveratrol derivative, which all feature *t*-butyl substitution adjacent the reactive phenolic groups. These rate constants of natural products were predicted to be all one or two orders of magnitude smaller than for α-TOH, (k_{inh}=3.2×10^6 $m^{-1}s^{-1}$),[31] the best lipophilic RTA in nature; this

suggests that natural resveratrol dimers pallidol and quadrangularin A were unlikely to owe their biological activities to RTA activity. Compared to the natural products, *tert*-butylated synthetic precursors of resveratrol, pallidol and quadrangularin A, were predicted to be around four times less effective towards lipid peroxyl radicals due to the steric hindrance caused by *tert*-butyl groups, which decreased the rate of HAT to peroxyl radicals.[32]

In liposomes, the recently developed fluorogenic probe H_2B-PMHC mentioned in **Chapter 2** was used as a competitive oxidation substrate to study the radical-trapping activities in the lipid bilayer. At concentrations of up to 30 μM, none of the natural products were able to alter the rate of oxidation of the probe (0.15 μM); this suggests that they were at least 30 times less effective than α-TOH in lipid bilayers. α-TOH is able to trap MeOAMVN derived peroxyl radicals twice as fast as the probe in EggPC liposomes.[20] These results reflect our predicted k_{inh}; resveratrol and its dimers trap peroxyl radicals orders of magnitude slower than PMHC and α-TOH. A second factor is kinetic solvent effect. Due to the lower pKa of the 4'-OH group in resveratrol (pK_a = 8.8)[33] compared to the hydroxyl group in PMHC and α-TOH (pK_a = 13.1)[34] caused by the electron conjugation from the alkene group, resveratrol forms a stronger H-bond with phosphatidylcholine moieties and/or water at the interface, which will further decrease its ability to transfer an H atom to peroxyl radicals. At first glance, a third possible reason for the poor activities of natural compounds could be the poor lipophilicity of resveratrol (log*P* = 3.06 predicted by ChemBioDraw Ultra 12.0 software), pallidol (predicted log*P* = 5.05) and quadrangularin A (predicted log*P* = 5.09), precluded their localization to lipid bilayers and resulted in decreased lipid peroxyl radical trapping activities. However, since PMHC (predicted log*P* = 3.42) has similar lipophilicity compared to resveratrol and reacts with peroxyl radicals derived from MeOAMVN approximately five times as fast as the H_2B-PMHC probe in EggPC liposomes,[20] this seems an unlikely explanation.

Measurement of resveratrol kinetics towards peroxyl radicals in lipid bilayers is different from what has been reported by Liu *et al.* indicating that the activity of resveratrol in heterogeneous micelles of linoleic acid and either SDS or CTAB detergents was only 3-fold slower than α-TOH.[30] Because absolute rate constants towards peroxyl radicals, localization and accessibility, and fluidity of the system are all important factors contributing

to the activities in heterogeneous solution, it was very difficult to make direct comparison based on reactivity in different systems performed by various researchers.

Interestingly, in contrast to the reactivity measured in organic solution, *t*Bu$_2$-resveratrol and *t*Bu$_4$-quadrangularin A exhibited almost 10-fold and 4-fold greater reactivity than α-TOH in lipid bilayers, respectively. From the inhibition periods at each individual concentration compared to PMHC, we could conclude that each molecule of *t*-Bu$_2$-resveratrol and *t*Bu$_4$-quadrangularin A trapped two peroxyl radicals. As mentioned in the previous chapter, the physical properties of RTAs in lipid bilayers are as important as their inherent reactivities.[21,22] The results presented here underscore this point.

First, the natural products were expected to be less soluble than the *tert*-butylated analogues in the lipid membrane, resulting in less accessibility of the RTAs to lipid peroxyl radicals; therefore, *tert*-butylated analogues exhibited better inhibition activities in liposomes. Second, in general, the reactivity of the key hydroxyl group in a phenolic antioxidant will be lowered to a greater extent in heterogeneous system due to H-bond formation with phosphatidylcholine moieties and/or water at the interface.[35] Introducing the *tert*-butyl groups at the ortho-positions relative to the reactive hydroxyl group precludes this strong H-bond formation; therefore, the activities of O-H *tert*-butylated analogues is greater than α-TOH. Third, although the lipid solubility of *t*-Bu$_2$-resveratrol (log*P* = 6.47 estimated by Chemdraw 12.0) is lower than α-TOH (predicted log*P* = 9.98), the smaller size of the molecule ensures better dynamics and accessibility towards peroxyl radicals in lipid bilayers. All of these factors improve the activity of *t*Bu$_2$-resveratrol and *t*Bu$_4$-quadrangularin A in a heterogeneous system than α-TOH. The symmetric dimer *t*Bu$_4$-pallidol did not show any inhibition activities in lipid bilayers presumably because of its flatter shape compared to *t*Bu$_4$-quadrangularin A; this led to the limited solubility in lipid bilayers. On the other hand, none of the benzylated synthetic precursors (compounds **4b**, **7a** and **9)** or quinone methide precursors (compounds **6** and **8**) exhibited any activities in lipid bilayers; this indicated that the free phenolic groups on the resorcinol ring also had a significant impact on their reactivity.

The hypothesis that resveratrol and its related natural dimers are not sufficiently reactive as RTAs and for this to be their mode of action in a biological context was further supported by the lipid peroxidation inhibition assay carried out in human Tf1a erythroblasts. Again,

their ability to inhibit lipid peroxidation was assayed by flow cytometry using the C11-BODIPY$^{581/591}$ lipid peroxidation reporter following depletion of cellular glutathione with DEM as mentioned in **Chapter 3**. All of the natural compounds (compounds **1**, **2** and **3**) and their *tert*-butylated precursors (compounds **4a**, **7b** and **10**) prevented oxidation of C11-BODIPY$^{581/591}$ within various concentration ranges that also did not overlap with the concentrations where they induced cytotoxicity. None of the benzylated synthetic precursors (compounds **4b**, **7a** and **9)** or quinone methide precursors (compounds **6** and **8**) exhibited any activities up to 50 μM, the concentration at which the insolubility of the compounds in aqueous media was observed. Because the reactivity of resveratrol and its dimers, pallidol and quadrangularin A towards peroxyl radicals were orders of magnitude lower than α-TOH in organic solution, lipid bilayers and mammalian cell models, as well as their poor lipophilicity, it is unlikely that the biological activities of resveratrol and its dimers were due to their lipid peroxyl radical-trapping activities.

At this time, there is no conclusive relationship between resveratrol, its oligomers, and their health benefits.[36] It was argued that the concentration of resveratrol in wine was within low ppm range and this was not enough to produce any beneficial effects.[37] Controversy was also sparked from the instability of resveratrol where 200 μM of resveratrol was completely degraded in the presence of sodium bicarbonate in the cell culture media following 24 hours of incubation time;[38] however, the kinetics of autoxidation of resveratrol have never been extensively studied. Under physiological conditions, autoxidation studies of resveratrol indicated that the stability of resveratrol at physiological pH was poor.[23] The half-life of resveratrol at 100 mM PBS pH 7.4 buffer was around 1 hour at 50 μM at 37 °C.[23] We have also demonstrated that the oxidation rate of resveratrol was pH dependent, with a higher rate under increasingly basic conditions.[23] Therefore, it is tempting to suggest that the biological activity of resveratrol is not likely due to the authentic resveratrol, however, it is more likely because of the autoxidation products of resveratrol produced through proposed mechanism shown in **Scheme 5.3**.

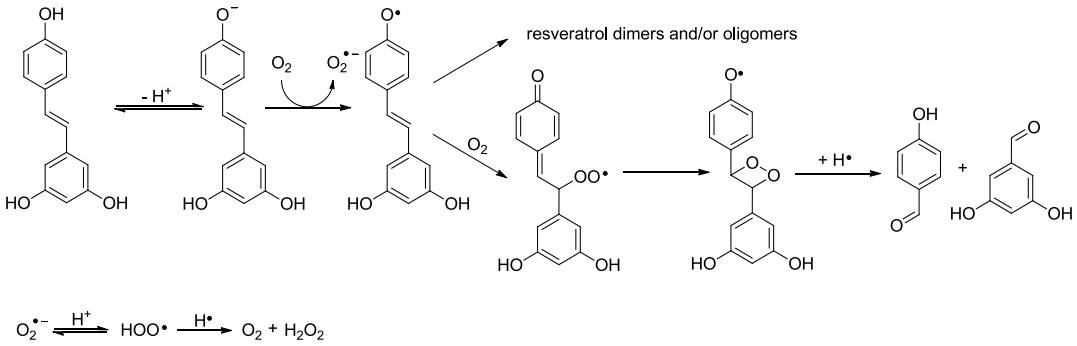

Scheme 5.3. The autoxidation of resveratrol is known to produce dimers/oligomers, *p*-hydroxybenzaldehyde, 5-formylresorcinol and presumably, hydrogen peroxide.

In our proposed oxidation pathway of resveratrol in **Scheme 5.3**, it is clear that H_2O_2 must be a major product; this and other resveratrol derived products have been neglected in the literature, although they have been observed by other groups previously when the oxidation of resveratrol reaction with hydroxyl radicals was initiated by gamma radiolysis,[39] by reaction with singlet oxygen,[40] or by oxidation under strong oxidant $FeCl_3$.[41]

To connect the instability of resveratrol and its biological mode of action, we measured the electrophilicity of the resveratrol oxidation products in solution. The active free thiol group on cysteine in papain could react with the chromogenic substrate BAPNA and produce *p*-nitroaniline, which absorbs light at 410 nm. Therefore, deactivation of the thiol group in papain could be evaluated by monitoring the initial increase of absorbance at 410 nm. Results showed that the oxidation solution of resveratrol deactivated the cysteine thiol group in papain with EC_{50} value at 8.6±1.0 μM, while resveratrol did not show any deactivation ability. These results indicated that oxidation of resveratrol produced compounds which could react with the free thiol group in any signal proteins *in vivo*. Results also confirmed that H_2O_2 deactivated papain at EC_{50} of 2.9±0.57 μM (H_2O_2 is known to deactivate papain by oxidizing the thiol group),[42,43] and the oxidation solution of resveratrol deactivates papain as well. However, no deactivation was observed if the H_2O_2 solution or the oxidation solution of resveratrol was pre-incubated with catalyse, an enzyme that can decompose hydrogen peroxide to water and oxygen.[44] This supports that H_2O_2 is a major autoxidation product of resveratrol and that it may be responsible for resveratrol's biological mechanism of action. H_2O_2 is known to be a signaling molecule through a mechanism in which it oxidizes critical

thiol groups on redox-regulated target proteins,[45] including transcription factors (e.g. Nrf2) which are responsible for regulating the expression of 'phase II' antioxidant genes.[46] In fact, research in other laboratories supported that resveratrol upregulated Nrf2 expression in HepG2 cells[47] and human lung epithelial cells.[48]

Autoxidation of phenolic compounds generally takes place by the well accepted mechanism shown in **Scheme 5.4** – one electron oxidation of the phenolate anion derived from deprotonation of the phenol reacts with molecular oxygen giving rise to superoxide and a phenoxyl radical.[49]

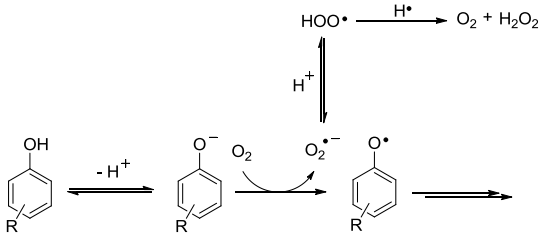

Scheme 5.4. Mechanism of autoxidation of phenols.

Given this mechanism, the oxidation of phenolic compounds is pH dependent,[50] which is consistent to what we have observed for resveratrol – the rate of autoxidation increases with the pH. Due to the lower pKa of the 4'-OH group in resveratrol (pKa=8.8)[33] compared to the hydroxyl group in phenol (pKa=10)[34] caused by the central unsaturation, resveratrol is relatively easily autoxidized compared to many biologically-relevant phenols. Preliminary results from our own group, as well as some literature reports, suggest an almost intractable mixture of oxidation products. However, it now seems likely from the preliminary results presented above that these are not important; instead, that the often ignored *other* product – hydrogen peroxide – may be responsible.[51] Future research will be carried out in Pratt laboratory to further examine this hypothesis.

5.5 Conclusions

The peroxyl radical-trapping activities of resveratrol, its natural dimers pallidol, quandranqularin A, and their synthetic precursors *t*Bu$_2$-resveratrol, *t*Bu$_4$-pallidol and *t*Bu$_4$-quandranqularin A were determined in organic solution, lipid bilayers and mammalian cell

culture. Results indicate the radical-trapping activities of resveratrol and its dimers, pallidol and quadrangularin A, are one or two orders of magnitude lower than α-TOH, Nature's best lipid-soluble radical-trapping antioxidant, in organic solution. Their activity in lipid bilayers and mammalian Tf1a erythroblasts are also poor. From these results, we suggested that the mode of action of natural products resveratrol and its dimers, pallidol and quadrangularin A, is unlikely due to their radical-trapping activities. In contrast, the synthetic precursors to the natural products were effective in lipid bilayers and cells. In fact, *t*Bu$_2$-resveratrol is ~10 times more potent in lipid bilayers and exhibited ~3-fold lower EC_{50} values than α-TOH in Tf1a erythroblasts. This may be an interesting lead compound as anti-ferroptotic agent, or where prevention of lipid peroxidation may serve a preventive role against degenerative disease.

Preliminary results indicated that resveratrol was not stable under physiological conditions, and that one (or more) of its oxidative degradation products could inhibit papain, the archetype cysteine protease, which we employed as a model nucleophilic protein thiol. We showed that H_2O_2 could also deactivate papain, and that no deactivation was observed if H_2O_2 was pre-incubated with catalase. Since the papain inhibitory activity of the mixture of resveratrol oxidation products disappeared upon pre-incubation with catalase, we believe that H_2O_2 is responsible. Therefore, it is our hypothesis that resveratrol's apparent antioxidant activity *in vivo* arises due to induction of expression of genes under control of the antioxidant response element (ARE), by interacting with nucleophilic cysteines on oxidant/electrophile sensitive signaling proteins such as the KEAP1/Nrf2 system.

5.6 Experimental Section

Materials. Methyl linoleate, EggPC, Triton^{TM} X-100 and penicillin-streptomycin were purchased from Sigma-Aldrich. C11-BODIPY$^{581/591}$ (4,4-difluoro-5-(4-phenyl-1,3-butadienyl)-4-bora-3a,4a-diaza-s-indacene-3-undecano-ic acid), MTT (3-(4,5-dimethylthiazol-2-yl)-2,5-diphenyltetrazolium bromide), RPMI-1640 media with/without phenol red, fetal bovine serum (FBS), Hank's balanced salt solution (HBSS) were purchased from Invitrogen (life technologies). Phosphate buffered saline (PBS), 2, 2'- azobis(4-methoxy-2,4-dimethylvaleronitrile) (MeOAMVN), 2,2'-azobis-(2-amidinopropane)

monohydrochloride (AAPH) and all other chemicals were used as received.

Radical Clock Experiments. Methyl linoleate (MeLn) was chromatographed on silica gel (5% EtOAc/ hexanes) prior to use. Stock solutions (0.02 M) of the tested compounds and methyl linoleate (1.0 M) were prepared in chlorobenzene separately. A stock solution of MeOAMVN (0.05 M) was prepared in benzene. Samples were prepared in 1.0 mL auto-sampler vials with a total reaction volume of 100 μL. The solutions were added in the following order to avoid premature oxidation: inhibitor (final concentration is 0.002-0.01M), amount of chlorobenzene required to dilute samples to 100 μL, methyl linoleate (0.1 M), and MeOAMVN (0.01 M). The sealed samples were then incubated at 37 °C for 90 minutes. Stock solutions of BHT (1.0 M in hexanes) and PPh_3 (1.0 M in chlorobenzene) were prepared separately. Following the oxidation, the BHT solution (0.05 M) and then PPh_3 solution (0.05 M), were added to the samples and then diluted to 1 mL with HPLC grade hexanes, and analyzed by HPLC (0.5 % iPrOH/hexanes, 1.1 mL/min for 30 min, Sun-Fire Silica 5 mm 4.6×250 mm column, detection at 234 nm). The ratio of products (*E*,*Z*/*E*,*E*) was plotted versus the concentration of the tested compound to determine k_{inh} according to the reported procedure.[17]

Liposome Preparation and Oxidation. Liposome preparation and oxidations were done following the procedure in one of our recent manuscripts.[20] To individual 21.4 μL aliquots of the 20 mM liposome solution were added increasing amounts (1.25, 2.5, 5, 7.5, 10 and 15 μL, respectively) of a solution of the test antioxidant in DMSO (857.5 μM) and 2.5 μL of a solution of H_2B-PMHC in acetonitrile (25.8 μM). Each resultant solution was then diluted to 400 μL with 10 mM phosphate buffered-saline (PBS) solution containing 150 mM NaCl (pH 7.4), from which 280 μL of each was loaded into a well of a 96-well microplate. The solution was equilibrated to 37 °C for 5 min, after which 20 μL of a solution of azo compound (40.5 mM in AAPH, in PBS or 10.1 mM in MeOAMVN, in acetonitrile was added to each well. The fluorescence was then monitored for 10 h at 60 s time intervals (λ_{ex} = 485 nm; λ_{em} = 520 nm). The final solutions in each well were 1 mM in lipids, 0.15 μM in H_2B-PMHC, 2.7 mM in AAPH or 0.68 mM in MeOAMVN and either 2.5 μM, 5.0 μM, 10 μM, 15 μM, 20 μM, 30 μM in antioxidant. The rates of peroxyl radical trapping by the test compounds relative to the probe H_2B-PMHC were determined by re-plotting the data as $\ln\{(I_\infty - I_t)/(I_\infty - I_0)\}$ versus

ln(1-t/τ) and determining the slope from the initial portion of the graph, which corresponds to $k_{inh}^{H2B\text{-}PMHC}/k_{inh}^{unknown}$ as described in references.[20,50]

Cellular Lipid Peroxidation. Tf1a cells were cultured in RPMI-1640 media (with phenol red) with 10 % FBS and 1 % penicillin-streptomycin. The cells (5×10^5 cells in 1 mL media) were treated with each antioxidant at final concentrations from 1.5 μM to 50 μM and incubated at 37 °C for 22 hours in phenol red-free RPMI-1640 media with 10 % FBS in humidified 5 % CO_2 atmosphere in 12-well plates. Cells were then treated with 1 μM C11-BODIPY$^{581/591}$ and incubated at 37 °C in the dark for 30 minutes after which oxidative stress was induced with diethylmaleate (9 mM) for 2 hours. Treated cells were then collected by centrifugation at 250×g for 4 minutes and washed with PBS. Cells were resuspended in PBS and analyzed by flow cytometry at a final concentration of 5×10^5 cells/ml (λ_{ex} = 488 nm; λ_{em} = 525±25 nm). Cells not treated with DEM were used as negative control. Cells not treated with antioxidants were used as positive control.

Cell Viability. Tf1a cells (5×10^4 cells in 250 μL media) were treated with each antioxidant in DMSO at final concentrations ranging from 0.5 μM to 750 μM (final DMSO concentration was to not exceed 1% v/v) and incubated at 37°C for 22 hours in phenol red-free RPMI-1640 media with 10% FBS in a humidified 5 % CO_2 atmosphere on a 96-well plate. Each well was then treated with 50 μL of MTT (12.1 μM in HBSS) for 4h. The treated cells were collected by centrifugation at 250×g for 5 minutes and the solution was aspirated. The resultant purple crystals were dissolved with a 250 μL 1:4 water:DMSO (v/v) solution followed by 30 minutes incubation at room temperature. Absorbance (λ=570 nm) was measured using the microplate reader. Results were compared to a negative control (1 % DMSO) and a positive control (1 % Triton™ X-100).

Oxidation of Resveratrol. Resveratrol was dissolved in a minimum amount of DMSO and was diluted to 500 μM with 10 mM PBS buffer (pH 10). The solution was stirred with constant infusion of O_2 gas into the media overnight. Complete oxidation was confirmed by the disappearance of resveratrol absorbance intensity at 306 nm.

Deactivation of H_2O_2 and oxidation solution of resveratrol. H_2O_2 solution (30 %) was diluted with 10 mM PBS buffer (pH 7.4) to 0.001%. Resveratrol (500 μM) was oxidized by constant infusion of O_2 gas into the media overnight until the disappearance of resveratrol

absorbance intensity was observed at 306 nm. The oxidized solution of resveratrol or diluted H_2O_2 solution was pre-incubated with catalase for 15 min and was then immeadiately used in the papain deactivation assay.

Papain Deactivation Assay.[26] Papain (125 μM) was incubated with dithiothreitol (DTT) (1 mM) for 30 minutes at 0 °C in pH 6.1 buffer (2 mM EDTA, 50 mM sodium acetate). The small molecules were then removed by filtration through a 10 kDa Amicon Filter. Stock solutions of resveratrol in 10 mM PBS buffer (pH 10) were prepared directly before use. The chromogenic substrate *N*α-benzoyl-DL-arginine 4-nitroanilide hydrochloride (BAPNA) was first dissolved in a minimal amount of DMSO and diluted in buffer to a final concentration of 10 mM. The wells of a 96 well microplate were loaded with 151 μL buffer, 25 μL of 125 μM papain solution (final 15.625 μM,) and 10 μL of resveratrol solution, oxidation solution of resveratrol in 10 mM PBS buffer (pH 10), oxidation solution of resveratrol in 10 mM PBS buffer (pH 10) after incubating with catalase for 10 min, H_2O_2 solution, H_2O_2 solution after incubating with catalase for 10 min, or catalase solution to a final volume of 186 μL. The microplate was then incubated at room temperature for 1 hour. BAPNA (14 μL) was added by the reagent dispenser of the microplate reader and the activity of papain was measured at 37 °C by monitoring the production of p-nitroaniline by absorbance at 410 nm every 2 seconds for 2 minutes. Final concentration of resveratrol and H_2O_2 were 0.1-125 μM. Initial rate measured in the absence of resveratrol or oxidation solution of resveratrol was used as a control to calculate the percentage of initial rates.

5.7 References

[1] Vidavalur, R.; Otani, H.; Singal, P. K.; Maulik, N. *Exp. Clin. Cardiol.* **2006,** *11* (3), 217-225.

[2] Catalgol, B.; Batirel, S.; Taga, Y.; Ozer, N. K. *Front Pharmacol.* **2012,** *3*, 141.

[3] Xue, Y. Q.; Di, J. M.; Luo, Y.; Cheng, K. J.; Wei, X.; Shi, Z. *Oxid. Med. Cell. Longev.* **2014,** *2014*, 765832.

[4] Baur, J. A.; Sinclair, D. A. *Nat. Rev. Drug. Discov.* **2006,** *5* (6), 493-506.

[5] Harikumar, K. B.; Aggarwal, B. B. *Cell Cycle* **2008,** *7* (8), 1020-1035.

[6] Kovacic, P.; Somanathan, R. *Oxid. Med. Cell Longev.* **2010,** *3* (2), 86-100.

[7] Venturini, C. D.; Merlo, S.; Souto, A. A.; Fernandes, M. C.; Gomez, R.; Rhoden, C. R. *Oxid. Med. Cell. Longev.* **2010,** *3* (6), 434-441.

[8] Gonzalez-Sarrias, A.; Gromek, S.; Niesen, D.; Seeram, N. P.; Henry, G. E. *J. Agric. Food Chem.* **2011,** *59* (16), 8632-8638.

[9] Kim, H. J.; Chang, E. J.; Bae, S. J.; Shim, S. M.; Park, H. D.; Rhee, C. H.; Park, J. H.; Choi, S. W. *Arch. Pharm. Res.* **2002,** *25* (3), 293-299.

[10] Keylor, M. H.; Matsuura, B. S.; Stephenson, C. R. *Chem. Rev.* **2015,** *115* (17), 8976-9027.

[11] Gülçin, İ. *Innov. Food Sci. Emerg. Technol.* **2010,** *11* (1), 210-218.

[12] Kim, H. J.; Saleem, M.; Seo, S. H.; Jin, C.; Lee, Y. S. *Planta. Med.* **2005,** *71* (10), 973-976.

[13] Amorati, R.; Ferroni, F.; Lucarini, M.; Pedulli, G. F.; Valgimigli, L. *J. Org. Chem.* **2002,** *67* (26), 9295-9303.

[14] Snyder, S. A.; ElSohly, A. M.; Kontes, F. *Nat. Prod. Rep.* **2011,** *28* (5), 897-924.

[15] Velu, S. S.; Thomas, N. F.; Weber, J.-F. F. *Curr. Org. Chem.* **2012,** *16* (5), 605 -662.

[16] Matsuura, B. S.; Keylor, M. H.; Li, B.; Lin, Y.; Allison, S.; Pratt, D. A.; Stephenson, C. R. *Angew. Chem. Int. Ed. Engl.* **2015,** *54* (12), 3754-3757.

[17] Roschek, B., Jr.; Tallman, K. A.; Rector, C. L.; Gillmore, J. G.; Pratt, D. A.; Punta, C.; Porter, N. A. *J. Org. Chem.* **2006,** *71* (9), 3527-3532.

[18] Pratt, D. A.; Tallman, K. A.; Porter, N. A. *Acc. Chem. Res.* **2011,** *44* (6), 458-467.

[19] Amorati, R.; Ferroni, F.; Pedulli, G. F.; Valgimigli, L. *J. Org. Chem.* **2003,** *68* (25), 9654-9658.

[20] Li, B.; Harjani, J. R.; Cormier, N. S.; Madarati, H.; Atkinson, J.; Cosa, G.; Pratt, D. A. *J. Am. Chem. Soc.* **2013,** *135* (4), 1394-1405.

[21] Barclay, L. R. C. *Can. J. Chem.* **1993,** *71* (1), 1-16.

[22] Niki, E.; Noguchi, N. *Acc. Chem. Res.* **2004,** *37* (1), 45-51.

[23] Lin, Y., Autoxidation conditions, intermediates, and products of phenolic antioxidant resveratrol. *Honour's thesis, Biomedical Science Program in the University of Ottawa* **2015**.

[24] Battino, R.; Rettich, T. R.; Tominaga, T. *J. Phys. Chem. Ref.* **1983,** *12* (2), 163-178.

[25] Ray, P. D.; Huang, B. W.; Tsuji, Y. *Cell Signal* **2012,** *24* (5), 981-990.

[26] Rabinkov, A.; Miron, T.; Konstantinovski, L.; Wilchek, M.; Mirelman, D.; Weiner, L., *Biochim. Biophys. Acta*. **1998,** *1379* (2), 233-244.

[27] Latte, K. P.; Kolodziej, H. *J. Agric. Food Chem.* **2004,** *52* (15), 4899-4902.

[28] Cao, H.; Pan, X.; Li, C.; Zhou, C.; Deng, F.; Li, T. *Bioorg. Med. Chem. Lett.* **2003,** *13* (11), 1869-1871.

[29] Amorati, R.; Ferroni, F.; Pedulli, G. F.; Valgimigli, L. *J. Org. Chem.* **2003,** *68* (25), 9654-9658.

[30] Fang, J. G.; Lu, M.; Chen, Z. H.; Zhu, H. H.; Li, Y.; Yang, L.; Wu, L. M.; Liu, Z. L. *Chemistry* **2002,** *8* (18), 4191-4198.

[31] Burton , G. W.; Ingold, K. U. *Acc. Chem. Res.* **1986,** *19* (7), 194-201.

[32] Burton, G. W.; Doba, T.; Gabe, E. J.; Hughes, L.; Lee, F. L.; Prasad, L.; Ingold, K. U. *J. Am. Chem. Soc.* **1985,** *107* (24), 7053-7065.

[33] Lopez-Nicolas, J. M.; Garcia-Carmona, F. *J. Agric. Food Chem.* **2008,** *56* (17), 7600-7605.

[34] Mukai, K.; Tokunaga, A.; Itoh, S.; Kanesaki, Y.; Ohara, K.; Nagaoka, S.; Abe, K. *J. Phys. Chem. B* **2007,** *111* (3), 652-662.

[35] Litwinienko, G.; Ingold, K. U. *Acc. Chem. Res.* **2007,** *40* (3), 222-230.

[36] Vang, O. A., N.; Baile, C. A.; Baur, J. A.; Brown, K.; Csiszar, A. *PLOS One* **2011,** *6* (6).

[37] Celotti, E. F., R.; Zironi, R.; Conte, L. S. *J. Chromatogr. A.* **1996,** *730* (1-2), 47-52.

[38] Yang, N. C.; Lee, C. H.; Song, T. Y. *Biosci. Biotechnol. Biochem.* **2010,** *74* (1), 63-68.

[39] Camont, L.; Collin, F.; Couturier, M.; Therond, P.; Jore, D.; Gardes-Albert, M.; Bonnefont-Rousselot, D. *Biochimie.* **2012,** *94* (3), 741-747.

[40] Celaje, J. A.; Zhang, D.; Guerrero, A. M.; Selke, M. *Org. Lett.* **2011,** *13* (18), 4846-4849.

[41] Shingai, Y.; Fujimoto, A.; Nakamura, M.; Masuda, T. *J. Agric. Food Chem.* **2011,** *59* (15), 8180-8186.

[42] Lin, W. S.; Armstrong, D. A. *Radiat. Res.* **1977,** *69* (3), 434-441.

[43] Glazer, A. N.; Smith, E. L. *J. Biol. Chem.* **1965,** *240*, 201-208.

[44] Chelikani, P.; Fita, I.; Loewen, P. C. *Cell Mol. Life Sci.* **2004,** *61* (2), 192-208.

[45] D'Autréaux, B.; Toledano, M. B. *Nat. Rev. Mol. Cell Biol.* **2007,** *8* (10), 813-824.

[46] Itoh, K.; Chiba, T.; Takahashi, S.; Ishii, T.; Igarashi, K.; Katoh, Y.; Oyake, T.; Hayashi,

N.; Satoh, K.; Hatayama, I.; Yamamoto, M.; Nabeshima, Y. *Biochem. Biophys. Res. Commun.* **1997,** *236* (2), 313-322.

[47] Cheng, A. S.; Cheng, Y. H.; Chiou, C. H.; Chang, T. L. *J. Agric. Food Chem.* **2012,** *60* (36), 9180-9187.

[48] Kode, A.; Rajendrasozhan, S.; Caito, S.; Yang, S. R.; Megson, I. L.; Rahman, I. *Am. J. Physiol. Lung Cell Mol. Physiol.* **2008,** *294* (3), L478-488.

[49] Costentin, C.; Louault, C.; Robert, M.; Saveant, J-M. *PNAS*, **2007**, *106* (43), 18143-18148..

[50] Enache, T. A.; Oliveira-Brett, A. M. *J. Electroanal. Chem.* **2011,** *655* (1), 9-16.

[51] Rhile, I. J.; Markle, T. F.; Nagao, H.; DiPasquale, A. D.; Lam, O. P.; Lockwood, M. A.; Rotter, K.; Mayer, J. M. *J. Am. Chem. Soc.* **2006**, *128* (18), 6075-6088.

[52] Krumova, K.; Friedland, S.; Cosa, G. *J. Am. Chem. Soc.* **2012,** *134* (24), 10102-10113.

Chapter 6: Perspective

6.1 Perspective

Lipid peroxidation is widely believed to contribute to aging, the onset and progression of many degenerative diseases and cancer.[1-3] For example, the accumulation of oxidized low-density lipoprotein (LDL) – particles responsible for the transport of cholesterol-esterified fatty acids in serum – is observed as atherosclerosis progresses and its level correlates with risk of heart attack and/or stroke.[4,5] The oxidized low-density lipoprotein co-localizes in the arterial vessel wall with white blood cells, which are recruited to clear the oxidized LDL with the assistance of high-density lipoprotein (HDL). When HDL levels are low, or the flux of oxidized LDL is too high, the fat-laden white blood cells (called foam cells) accumulate to form the characteristic fatty streaks or arterial plaque associated with athersclerosis.[6] Thus, the prevention of oxidation of LDL lipids has long been thought of as a potential means to prevent cardiovascular disease.[7,8]

The foregoing view has been reinforced by animal studies wherein α-TOH has been shown to play a preventive role. For example, in ApoE-knockout mice, vitamin E deficiency caused by disruption of the tocopherol transfer protein gene increased the severity of atherosclerotic lesions,[9] and feeding the mice a vitamin E-deficient diet seriously damaged the heart.[10] Vitamin E was able to inhibit atherosclerosis when introduced at an early stage of disease development in ApoE-knockout mice, but not at later stages – suggesting a preventive role, but not a therapeutic one.[11] However, to date, the results of mouse experiments (and those in other animals)[12,13] have not been reproduced in humans, where Vitamin E has failed to prevent coronary events in patients with established atherosclerosis in clinical trials.[14,15] However, it must be noted that clinical trials carried out in humans generally involve middle-aged adults in which the disease has already taken significant root – even if they appear asymptomatic.[16,17] Given that the putative role of α-TOH in this context is to inhibit the oxidation LDL lipids, it is doubtful that α-TOH, or any other compounds capable of doing the same, can serve any therapeutic

role. This point is reinforced by results of animal studies, such as those mentioned above. To clarify the role of lipid peroxidation and its inhibition by Vitamin E in humans, it would be ideal to carry out clinical trials starting from very young ages prior to the onset or significant progression of atherosclerosis, but regulatory approvals for such studies are presumably difficult to obtain, as well as funding for the necessarily lengthy duration of the trial required to determine the outcome of preventive administration of Vitamin E.

However, it must be pointed out that supplementation of a normal diet with Vitamin E does not provide any obvious benefit to mice – from prevention of degenerative disease and/or overall longevity.[18] Thus the question remains: Can an antioxidant additive prevent disease onset and progression? The first objective of this thesis was to lay the foundation to address the question of whether RTAs can play a significant preventive role on progression of degenerative disease by developing the ultimate RTA chemistry. In an attempt to do so, we have extended early studies on the radical-trapping activity of the THNs in organic solution to lipid bilayers and mammalian cell culture. An overall account of the results to date is as follows:

(1) THNs are ~28 fold more reactive than α-TOH at trapping peroxyl radicals in organic solution, enabling them to better inhibit lipid peroxidation,

(2) the THN derived aryloxyl radical is 2 kcal/mol more stable than the α-TOH derived aryloxyl radical, which should minimize chain transfer via reaction with lipids (i.e. tocopherol mediated peroxidation),

(3) the increased reactivity of THNs towards peroxyl radicals translates from organic solution to lipid bilayers, where they react >30 times faster than α-TOH,

(4) the lipophilic THNs are up to ~58 times more potent than α-TOH as inhibitors of lipid peroxidation in Tf1a erythroblasts and ferroptosis in Pfa-1 mouse fibroblasts and HT-22 mouse hippocampal cells,

(5) THN-derived aryloxyl radicals appear to be as regenerable as those derived from α-TOH by phase-separated reductants such as ascorbate, *N*-acetyl cysteine (a model of glutathione) and urate, ensuring their regeneration *in vivo*.

(6) the lipophilic THN-C12/C15/C16 have similar or higher binding affinity to the human tocopherol transport protein (hTTP) ensuring their bioavailability *in vivo*.

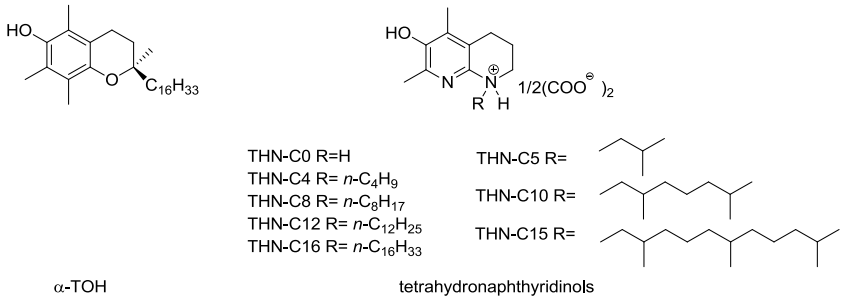

α-TOH tetrahydronaphthyridinols

Preliminary bioavailability experiments with a lipophilic THN (THN-C15) have been disappointing. Chow supplemented with 5 mg THN-C15/kg was fed to a group of 9 C57BL/6J mice for 8 weeks. The blood plasma was analyzed for THN-C15 once per week and compared to a control group of 9 mice supplemented with standard mouse chow. Unfortunately, no THN-C15 was detected by LC-MS in these samples. It may be that the serum concentration was below the detection limit of the LC-MS assay (1 μM, determined as its conjugate acid by reverse-phase HPLC with ESI-MS detection in positive ion mode) at this dosage. Interestingly, the mice fed with THN-C15-supplemented chow consumed 32% more food compared to the mice fed with the regular diet over the 8 week period. Dosages of 25 and 100 mg THN-C15/kg mouse chow were subsequently planned, but have not yet been carried out. In the interim, we have considered whether others means of introducing the test compounds would be more appropriate. The THN-C15-supplemented mouse chow that was used in the foregoing experiments was prepared by blending the THN-C15 with other ingredients and water, formed into pellets and then heated to dry. The THN-C15 might be degraded during this process, since we showed that it is unstable in aqueous solution (**Chapter 3**). Thus, future experiments will be carried out at higher THN-C15 dosage and wherein the THN-C15 will be administered in corn oil by gavage.

Following the bioavailability studies, the efficacy of lipophilic THNs to slow the progression of select degenerative diseases will be assessed in transgenic mouse models. A common animal model for atherosclerosis is the apoE-knockout mouse. ApoE is the protein associated with HDL particles, and the lack of ApoE leads to HDL deficiency and corresponding impairment of means to clear oxidized LDL. These mice develop atherosclerosis in a relatively short period of time – in particular when fed a high fat diet.[19] In collaboration with Professor Marc Ruel at the University of Ottawa Heart Institute, we will monitor whether atherosclerotic lesions are smaller in mice treated with lipophilic

THNs (e.g. THN-C15) compared to mice fed a normal diet, or one supplemented with α-TOH. THNs will also be evaluated in a Parkin-knockout mouse model of Parkinson's disease by Prof. Michael Schlossmacher's laboratory at the Brain and Mind Institute of the University of Ottawa Hospital Research Institute. Parkin, a protein which has 35 cysteine residues,[20] is believed to be an antioxidant enzyme and mutations in Parkin gene causes recessive parkinsonism, a heritable form of Parkinson's disease.[21,22] Thus, we aim to determine if antioxidant supplementation can inhibit the onset and progression of Parkinson's in these Parkin-knockout mice. In addition, the THNs will also be studied in a mouse model of acute kidney failure in which siRNA-knockdown of Gpx4 is induced upon treatment with tamoxifen[23] in collaboration with Prof. Marcus Conrad's laboratory at the Institute of Developmental Genetics of the German Research Centre for Environmental Health in Munich, Germany. Conrad's laboratory has established that a functioning Gpx4 is essential for proper kidney development,[23,24] and since Gpx4's role is to reduce lipid hydroperoxides, lipid peroxidation is likely to play a role in the onset and development of kidney disease.[25]

In recent years, the development of redox sensitive probes designed to enable whole animal imaging of oxidative stress in real time using combination of fluorescence and chemiluminescence,[26] positron emission tomography[27] or magnetic resonance imaging[28] in animals has been a very active area of research. However, to the best of our knowledge, these technologies have yet to be applied to assess the impact of RTAs. We anticipate that these new imaging capabilities will greatly enable the assessment of the impact of the THN RTAs on the onset and progression of diseases associated with oxidative stress and/or damage. The ability to monitor stress levels in real time in specific locations (i.e. organs), in a non-invasive, continuous manner, combined with more traditional end-point analyses, will provide an unprecedented view of the link between oxidative stress and disease etiology and the impact of RTAs thereupon.

α-TOH is generally found as α-tocopheryl acetate in nutritional supplements and multi-vitamins because acetylation of the reactive phenolic moiety slows its autoxidation, giving it a longer shelf-life and greater apparent bioavailability. Tocopheryl acetate itself is inactive as an antioxidant and not bioavailable. It is hydrolyzed to α-TOH in the gut before

absorption can occur.[29] Bioavailability studies in literature show that the bioactivity of α-tocopheryl acetate is twice as much compared to equivalent quantities of the free phenol in rat fetal gestation-resorption assay.[29,30] In cellular models mentioned in **Chapter 3**, THN-C15 acetate did not exhibit better efficacy in mammalian cells than free THN-C15, possibly due to the slow hydrolysis process in cells. But applying THN-C15 acetate in future animal models of degenerative disease is a necessary experiment to provide direct comparison with free phenolic THN-C12, THN-C15, α-TOH, and α-TOH acetate. This will help to confirm whether protection of THN from oxidation by acetylation will be a benefit and whether better activities of THNs compared to α-TOH translate to animal studies.

It is well accepted that mitochondria is the major source of lipid peroxidation-initiating ROS in the cell. Accordingly, mitochondrially-targeted antioxidants have been developed as preventive and/or therapeutic agents against several degenerative diseases, including Parkinson's and Hepatitis C.[31] The first mitochondrially-targeted RTA was MitoE_2 (**Chart 6.1**),[32] a compound comprising an α-tocopherol main moiety linked to a triphenylphosphonium cation via two methylene groups. Substitution with the triphenylphosphonium cation facilitates cell entry[33] and leads to accumulation in mitochondria because of the large mitochondrial membrane potential.[34,35] Although MitoE_2 inhibited oxidative stress in bovine aortic endothelial cells,[36] application of MitoE_2 *in vivo* failed to show clear protection against loss of neurons following acute perinatal ischemia-reperfusion injury in rats.[37] This is not surprising due to the expected low binding affinity of MitoE_2 to hTTP.[38] Murphy *et al.* devised MitoQ_{10} (**Chart 6.1**), a coenzyme Q_{10} derivative targeted to mitochondria by attachment of a triphenylphosphonium cation to the lipophilic carbon sidechain. They showed that this compound was able to inhibit apoptosis induced by H_2O_2 in human osteosarcoma 143B cells.[39] MitoQ_{10} had no effect on the normal lifespan in wild flies, but it offers protection from oxidative stress induced by paraquat in SOD-deficient flies depending on the stage of oxidative stress development from which MitoQ_{10} was given and the dosage of MitoQ_{10}.[40] MitoQ_{10} also has a major drawback since it is not an authentic RTA. Instead it relies on NADPH-dependent quinone reductase, to reduce it to the hydroquinone form.[41,42] Moreover, the reduced coenzyme Q10 is roughly 10-fold less reactive as an RTA than α-TOH.[43]

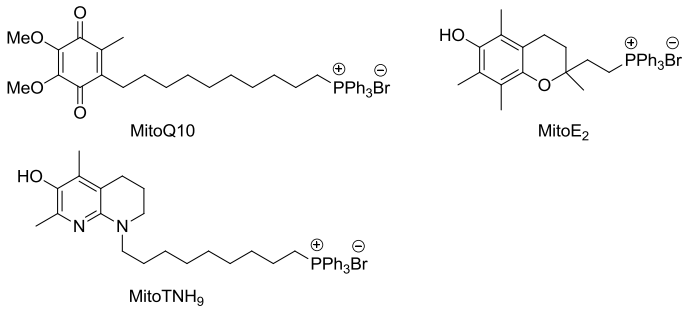

Chart 6.1. Mitochondrially-targeted RTAs.

The THN RTAs described in this thesis can presumably be mitochondrially-targeted (e.g. MitoTNH$_9$, **Chart 6.1**) using the same strategy as for Vitamin E and coenzyme Q. Moreover, the ability to easily vary the sidechain length separating the THN headgroup and the triphenylphosphonium substituent may enable the discovery of mitochondrially-targeted compounds that retain the binding affinity to hTTP, thereby ensuring the bioavailability of the antioxidant *in vivo*.[38,44,45] A combination of optimal inherent peroxyl radical trapping activity as well as good bioavailability could help investigate the contribution of mitochondrial oxidative damage to progression of degenerative disease in future.

Liproxstatin-1 (Lip-1) and ferrostatin-1 (Fer-1) are the most effective compounds to inhibit ferroptosis discovered to date through screening thousands of compounds. In this thesis, we confirmed that they are roughly as potent as THNs to inhibit lipid peroxidation in Tf1a erythroblasts and ferroptosis in Pfa-1 mouse fibroblasts and mouse hippocampal cells. Moreover, we have shown that Fer-1 and Lip-1 react with peroxyl radicals about two orders of magnitude more slowly than THNs in organic solution and they failed to inhibit lipid peroxidation to any significant extent in lipid bilayers. These results imply that their biological mechanisms must be distinct from the THNs (and α-TOH). As mentioned in **Chapter 3**, future work will be carried out to investigate their possible mechanism of action.

The second objective of this thesis was to establish a rigorous, systematic approach for interrogating the reactivity of naturally-occurring purported 'antioxidants' as RTAs. Many natural compounds have been described as "antioxidants" – and their biological activities

ascribed to this reactivity – simply because they are able to reduce persistent radicals, such as dpph•, Fe^{3+} complexes, or 2,2'-azino-di-(3-ethylbenzthiazoline sulphonate), in simple colourimetric assays. These widely used assays generally report only on the position of the redox equilibrium after incubating the tested compounds with the oxidizing reagent for a set amount of time, but not on the kinetics of the reaction of the 'antioxidant' with a peroxyl radical.[46,47] Therefore, it is not appropriate to conclude that compounds that are able to reduce the oxidizing reagents in those assays are radical trapping antioxidants. The garlic and petiveria-derived thiosulfinates allicin and petivericin as well as the grape-derived resveratrol and its oligomers are examples of natural products that have long been described as "antioxidants" without adequate characterization of this reactivity in relevant contexts.

Consideration of results in organic solution, lipid bilayers and mammalian cells shown in previous work and **Chapter 4** in this thesis strongly argue against any role for their radical-trapping antioxidant activities *in vivo*. Instead, they induce cell death as a result of, or concomitant with, glutathione depletion. In contrast, the greater lipophilicity of hexylated petivericin enabled it to partition to lipid membranous cell compartments where it formed a lipid-soluble sulfenic acid that trapped peroxyl radicals. In addition, lipophilic 9-triptycenesulfenic acid is a good RTA in Tf1a erythroblasts, suggesting that their potency as RTA translate from organic solution to liposomes and further to mammalian cells.

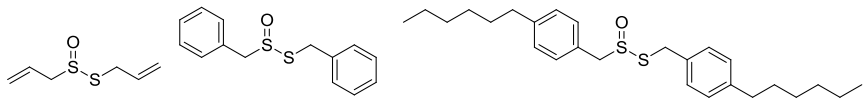

allicin petivericin hexylated petivericin

Likewise, through systematic evaluation of the radical-trapping activities of natural resveratrol, quadrangularin A, pallidol and their synthetic precursors, we suggest that resveratrol, quadrangularin A and pallidol examined in this study are not kinetically competent as RTAs under biologically relevant conditions. Accordingly, another mechanism must be operative. Expression of many of the genes encoding enzymatic antioxidants, such as the phase II enzymes heme oxygenase-1,[48] NAD(P)H:quinone oxidoreductase,[49] and γ-glutamyl-cysteine ligase,[50] are under transcriptional control of the antioxidant response element (ARE),[51] which can be effected by Nrf2 among other

transcription factors.[52] Although it has long been appreciated that cytotoxic electrophiles, such as the lipid peroxidation end-products malondialdehyde and HNE, can induce expression of ARE-controlled genes, the mechanisms by which RTAs could do so is less well appreciated. While some RTAs also contain electrophilic moieties, such as the two α,β-unsaturations in curcumin, and others are readily oxidized to electrophiles by well characterized mechanisms, such as hydroquinones to quinones (**Scheme 6.1**), others are less obvious.

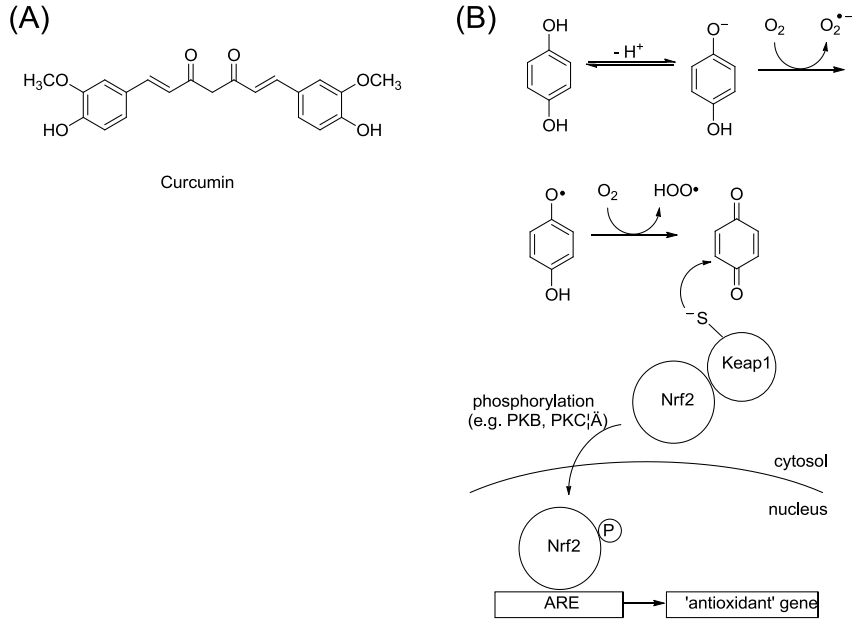

Scheme 6.1. (A) Curcumin; (B) Electrophilic activation of antioxidant gene expression via Nrf2 translocation to the nucleus exemplified by products of hydroquinone autoxidation.

Preliminary results indicate that it is the H_2O_2 produced from resveratrol autoxidation that is responsible for modulating the reactivity of a cysteine protease, and therefore, it may be expected that it is also the molecule that interacts with nucleophilic cysteines in the signal transduction pathway (s) relevant to ARE-controlled gene expression. Resveratrol is but one of many natural products containing phenols. Those with low pKa's and oxidation potentials are therefore expected to undergo autoxidation in aqueous solution by the well accepted autoxidation mechanism shown in **Scheme 5.4** in **Chapter 5**.[53,54] Although it is often assumed that the oxidation products derived from the phenol are the electrophiles that induce an antioxidant response, the other autoxidation product is H_2O_2. H_2O_2 is a well-known hormetic[55] agent. At low concentration, it is not sufficient to negatively impact

the cell apoptotic machinery, but just enough to upregulate expression of many of the genes encoding enzymatic antioxidants.[56] Since H_2O_2 will be the common autoxidation product of phenolic natural products, it may be responsible for the biological activity of many so-called 'natural antioxidants'.

One main shortcoming in "antioxidant" research is the lack of rigorous, widely-employed approaches for quantifying antioxidant properties, which poses difficulties when seeking to compare results between different procedures and researchers. Popular titration assays to evaluate antioxidant activities such as reducing dpph• or Fe^{3+} are suggested to be discarded when seeking kinetic information to compare radical-trapping antioxidant activities in organic solutions. The recently developed analytical methods applied in this thesis provide a thorough uniform process for determining whether compounds do indeed have significant RTA activity, which may assist in explaining their potential biological mechanism of action.

Another important point that needs to be emphasized is that the interpretation of cell-based data with respect to the mechanism of action of compounds must also be carefully considered. The activities of "antioxidants" in cellular assays must be interpreted with caution – and not just based on the potential localization and/or phase separation of the fluorescent probes that are used to monitor peroxidation. The concentrations of antioxidant reported in cell studies are almost always based upon the amount added to the cell culture media, and not the actual intracellular concentration of the compounds. Indeed, the ability of different antioxidants to traverse the cell membrane is generally ignored. The competition between cell penetration and degradation of antioxidants in the cell culture media is also generally not considered – despite the fact that many RTAs are electron-rich phenolics that undergo spontaneous reactions with O_2 at competitive rates.[57]

The expectation that a given compound is an RTA *in vivo* simply because it acts as an RTA in a given solution-phase assay and that it apparently prevents oxidation in cell culture is one that is drawn by many investigators, but is over-reaching to say the least. Antioxidant activities evaluated in each of solution, liposomes and cell culture need to be considered complementarily to provide the best possible mechanism insight (**Table 6.1**). First, if a compound is a potent inhibitor of lipid peroxidation in each of organic solution, liposomes

and cells, but does not induce significant cytotoxicity, it is likely they inhibit lipid peroxidation *via* a radical-trapping mechanism *in vivo*, such as α-TOH and the THNs. However, if a compound is potent in cells without inducing toxicity, but not so in organic solution and liposomes, it is likely to inhibit lipid peroxidation by another mechanism than lipid peroxyl radical-trapping, such as Lip-1 and Fer-1. Importantly, if a compound appears to inhibit lipid peroxidation in cell studies, but is cytotoxic in the same concentration range, it is likely that the apparent antioxidant activity arises simply from growth arrest and the resultant lowering (or halting) of aerobic metabolism associated with their toxicity, such as is the case for allicin and petivericin. If a compound just performs moderately in cells without inducing toxicity but poor in solution and liposomes, it is unlikely that this compound is an RTA even if it appears to inhibit lipid peroxidation in cells, such as resveratrol, quadrangularin A and pallidol.

Table 6.1. Summary of radical-trapping antioxidants activities of different compounds measured in organic solution, EggPC liposomes and Tf1a erythroblasts (EC_{50}) and their toxicity (TC_{50}) mentioned in the thesis.

Compound	*Solution*	*Liposomes*	*Cells*	*Cells*
	$M^{-1}s^{-1}$	k_{rel}[a]	EC_{50} / μM	TC_{50} / μM
α-TOH	3.2×10^{6} [58]	1.8	0.042	>100
THN-C15	8.8×10^{7} [59]	30	0.017	85.3
Lip-1	2.6×10^{5}	<0.01	0.021	41.4
Fer-1	3.4×10^{5}	<0.01	0.031	212.7
resveratrol	2.0×10^{5} [60]	<0.01	12.6	118
pallidol	8.5×10^{4}	<0.01	8.1	205
quadrangularin A	2.3×10^{5}	<0.01	3.4	63.5
allicin	1.6×10^{5} [61]	<0.01	20	39
petivericin	2.0×10^{5} [62]	<0.01	23	56

[a] k_{rel} is the reactivity of compounds to trap peroxyl radicals compared to H_2B-PMHC probe

Research on antioxidants continues to be one of the hottest topics in science. In fact,

publications related to work in this field appear with startling frequency (e.g. **Figure 6.1**).

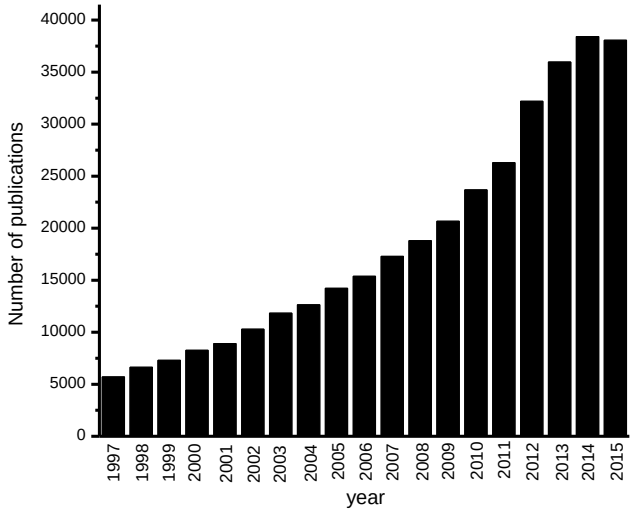

Figure 6.1. Numbers of publications in SciFinder database on antioxidants in recent years.

Despite this extensive body of work, the role of antioxidants in human health remains highly controversial – particularly due to the lack of clear evidence for a preventive role for antioxidants in clinical trials as discussed above. That issue notwithstanding, there are other significant issues in this field. One of the most important is the lack of a standard protocol to determine the activities of antioxidants – either natural or synthetic – in order to produce consistent, reliable and comparable results across different investigators and different classes of antioxidants, as mentioned above and detailed in **Chapter 1**. Perhaps the most relevant issue is that the stability of the compounds under physiologically-relevant conditions is often ignored. We have presented one such an example in **Chapter 5** (resveratrol), but the oxidative ability of plant-derived phenolics that are widely believed to be radical-trapping antioxidants, is likely to be widespread. As a result, part of the uncertainty with respect to the efficacies and mechanisms of these types of compounds may derive simply from the fact that the 'natural products' are not themselves biologically active, but instead it is the oxidation products derived therefrom that are. A striking example is curcumin, the yellow-orange phenolic pigment found in turmeric and the subject of an enormous amount of research interest as an antioxidant, anti-inflammatory and anti-cancer agent.[63-,65] There are 126 ongoing/completed clinical trials on curcumin to

date.[66] The Pratt group and its collaborators have shown that curcumin is very unstable and decomposes within minutes in aerated buffer at 37°C to yield a variety of products, but primarily the bicyclopentadione shown in **Scheme 6.2**.[57] Therefore, it seems highly likely that this product, or another of curcumin's autoxidation products, is actually responsible for its biological activity rather than curcumin itself. Other natural purported radical-trapping antioxidants have also been reported to undergo autoxidative degradation under physiological relevant conditions. For example, quercetin and luteolin have invoked lots of research due to their antioxidant activities,[67] but their degradation were reported to be within one hour in aqueous buffer at pH 7 and pH 8.[68,69] A common characteristic of these natural compounds is that they all process an acidic phenolic moiety which gives rise to an electron-rich phenoxide anion that readily transfer an electron to O_2 (**Scheme 5.4**). Understanding the stability and the fate of the natural molecules will provide fully understanding of their biological mechanisms as well as their potential application possibilities. Answers to these questions are likely to clarify some of the controversial and sometimes contradictory assertions about natural product radical-trapping antioxidants that have plagued this field for some time.

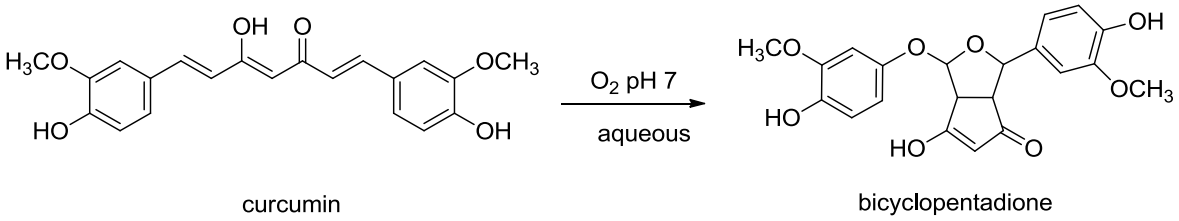

Scheme 6.2. Autoxidation of curcumin in pH 7 aqueous buffer made from 200 mM Na_2HPO_4 and 100 mM citric acid buffer.[57]

6.2 References

[1] Witztum, J. L.; Steinberg, D. **1991,** *88* (6), 1785-1792.

[2] Ames, B. N.; Shigenaga, M. K.; Hagen, T. M. *Proc. Natl. Acad. Sci. U S A* **1993,** *90* (17), 7915-7922.

[3] Reed, T. T. *Free Radic. Biol. Med.* **2011,** *51* (7), 1302-1319.

[4] Holvoet, P.; Stassen, J. M.; Van Cleemput, J.; Collen, D.; Vanhaecke, J. *Arterioscler. Thromb. Vasc. Biol.* **1998,** *18* (1), 100-107.

[5] Parthasarathy, S.; Raghavamenon, A.; Garelnabi, M. O. *Methods Mol. Biol.* **2010,** *610*, 403-417.

[6] Carpenter, K. L.; Wilkins, G. M.; Fussell, B.; Ballantine, J. A.; Taylor, S. E.; Mitchinson, M. J.; Leake, D. S. *Biochem. J.* **1994,** *304 (Pt 2)*, 625-633.

[7] Bandeali, S.; Farmer, J. *Curr. Atheroscler. Rep.* **2012,** *14* (2), 101-107.

[8] Tribble, D. L. *Circulation* **1999,** *99* (4), 591-595.

[9] Terasawa, Y.; Ladha, Z.; Leonard, S. W.; Morrow, J. D.; Newland, D.; Sanan, D.; Packer, L.; Traber, M. G.; Farese, R. V. *Proc. Natl. Acad. Sci. U S A* **2000,** *97* (25), 13830-13834.

[10] Beck, M. A.; Kolbeck, P. C.; Rohr, L. H.; Shi, Q.; Morris, V. C.; Levander, O. A. *J. Nutr.* **1994,** *124* (3), 345-358.

[11] Tang, F.; Lu, M.; Zhang, S.; Mei, M.; Wang, T.; Liu, P.; Wang, H. *Lipids* **2014,** *49* (12), 1215-1223.

[12] Schwenke, D. C.; Behr, S. R. *Circ. Res.* **1998,** *83* (4), 366-377.

[13] Hamre, K.; Waagbo, R.; Berge, R. K.; Lie, O. *Free Radic. Biol. Med.* **1997,** *22* (1-2), 137-149.

[14] Dietary supplementation with n-3 polyunsaturated fatty acids and vitamin E after myocardial infarction: results of the GISSI-Prevenzione trial. Gruppo Italiano per lo Studio della Sopravvivenza nell'Infarto miocardico. *Lancet* **1999,** *354* (9177), 447-455.

[15] Yusuf, S.; Dagenais, G.; Pogue, J.; Bosch, J.; Sleight, P. *N. Engl. J. Med.* **2000,** *342* (3), 154-160.

[16] Greenland, P.; Smith, S. C., Jr.; Grundy, S. M. *Circulation* **2001,** *104* (15), 1863-1867.

[17] Chimowitz, M. I.; Mancini, G. B. *Stroke* **1992,** *23* (3), 433-436.

[18] Sumien, N.; Forster, M. J.; Sohal, R. S. *Exp. Gerontol.* **2003,** *38* (6), 699-704.

[19] Kolovou, G.; Anagnostopoulou, K.; Mikhailidis, D. P.; Cokkinos, D. V. *Curr. Pharm. Des.* **2008,** *14* (4), 338-351.

[20] Wong, E. S.; Tan, J. M.; Wang, C.; Zhang, Z.; Tay, S. P.; Zaiden, N.; Ko, H. S.; Dawson, V. L.; Dawson, T. M.; Lim, K. L. *J. Biol. Chem.* **2007,** *282* (16), 12310-12318.

[21] Kitada, T.; Asakawa, S.; Hattori, N.; Matsumine, H.; Yamamura, Y.; Minoshima, S.; Yokochi, M.; Mizuno, Y.; Shimizu, N. *Nature* **1998,** *392* (6676), 605-608.

[22] Periquet, M.; Corti, O.; Jacquier, S.; Brice, A. *J. Neurochem.* **2005,** *95* (5), 1259-1276.

[23] Friedmann Angeli, J. P.; Schneider, M.; Proneth, B.; Tyurina, Y. Y.; Tyurin, V. A.; Hammond, V. J.; Herbach, N.; Aichler, M.; Walch, A.; Eggenhofer, E.; Basavarajappa, D.; Radmark, O.; Kobayashi, S.; Seibt, T.; Beck, H.; Neff, F.; Esposito, I.; Wanke, R.; Forster, H.; Yefremova, O.; Heinrichmeyer, M.; Bornkamm, G. W.; Geissler, E. K.; Thomas, S. B.; Stockwell, B. R.; O'Donnell, V. B.; Kagan, V. E.; Schick, J. A.; Conrad, M. *Nat. Cell Biol.* **2014,** *16* (12), 1180-1191.

[24] Cong, W. N.; Cai, H.; Wang, R.; Daimon, C. M.; Maudsley, S.; Raber, K.; Canneva, F.; von Horsten, S.; Martin, B. *PLoS One* **2012,** *7* (10), e47240.

[25] Brigelius-Flohe, R.; Maiorino, M. *Biochim. Biophys. Acta.* **2013,** *1830* (5), 3289-3303.

[26] Shuhendler, A. J.; Pu, K.; Cui, L.; Uetrecht, J. P.; Rao, J. *Nat. Biotechnol.* **2014,** *32* (4), 373-380.

[27] Okazawa, H.; Ikawa, M.; Tsujikawa, T.; Kiyono, Y.; Yoneda, M. *Q. J. Nucl. Med. Mol. Imaging* **2014,** *58* (4), 387-397.

[28] Elas, M.; Ichikawa, K.; Halpern, H. J. *Radiat. Res.* **2012,** *177* (4), 514-523.

[29] Burton, G. W.; Traber, M. G. *Annu. Rev. Nutr.* **1990,** *10*, 357-382.

[30] Harris, P. L.; Ludwig, M. I. *J. Biol. Chem.* **1949,** *180* (2), 611-614.

[31] Smith, R. A.; Murphy, M. P. *Discov. Med.* **2011,** *11* (57), 106-114.

[32] Smith, R. A.; Porteous, C. M.; Coulter, C. V. *Eur. J. Biochem.* **1999,** *263* (3), 709-716.

[33] Flewelling, R. F.; Hubbell, W. L. *Biophys. J.* **1986,** *49* (2), 531-540.

[34] (a) Murphy, M. P.; Smith, R. A. *Adv. Drug Deliv. Rev.* **2000,** *41* (2), 235-250; (b) Murphy, M. P.; Smith, R. A. *Annu. Rev. Pharmacol. Toxicol.* **2007,** *47*, 629-656.

[35] Murphy, M. P. *Biochim. Biophys. Acta.* **2008,** *1777* (7-8), 1028-1031.

[36] Dhanasekaran, A.; Kotamraju, S.; Kalivendi, S. V.; Matsunaga, T.; Shang, T.; Keszler, A.; Joseph, J.; Kalyanaraman, B. *J. Biol. Chem.* **2004,** *279* (36), 37575-37587.

[37] Covey, M. V.; Murphy, M. P.; Hobbs, C. E.; Smith, R. A.; Oorschot, D. E. *Exp. Neurol.* **2006,** *199* (2), 513-519.

[38] Meier, R.; Tomizaki, T.; Schulze-Briese, C.; Baumann, U.; Stocker, A. *J. Mol. Biol.* **2003,** *331* (3), 725-734.

[39] Kelso, G. F.; Porteous, C. M.; Coulter, C. V.; Hughes, G.; Porteous, W. K.;

Ledgerwood, E. C.; Smith, R. A.; Murphy, M. P. *J. Biol. Chem.* **2001,** *276* (7), 4588-4596.

[40] Magwere, T.; West, M.; Riyahi, K.; Murphy, M. P.; Smith, R. A.; Partridge, L. *Mech. Ageing Dev.* **2006,** *127* (4), 356-370.

[41] Li, R.; Bianchet, M. A.; Talalay, P.; Amzel, L. M. *Proc. Natl. Acad. Sci. U S A* **1995,** *92* (19), 8846-8850.

[42] Benson, A. M.; Hunkeler, M. J.; Talalay, P. *Proc. Natl. Acad. Sci. U S A* **1980,** *77* (9), 5216-5220.

[43] Ingold, K. U.; Pratt, D. A. *Chem. Rev.* **2014,** *114* (18), 9022-9046.

[44] Panagabko, C.; Morley, S.; Hernandez, M.; Cassolato, P.; Gordon, H.; Parsons, R.; Manor, D. *Biochemistry* **2003,** *42* (21), 6467-6474.

[45] Min, K. C.; Kovall, R. A.; Hendrickson, W. A. *Proc. Natl. Acad. Sci. U S A* **2003,** *100* (25), 14713-14718.

[46] Schlesier, K.; Harwat, M.; Böhm, V. *Free Radical. Res.* **2002,** *36* (2), 177-187.

[47] Li, B.; Pratt, D. A. *Free Radic. Biol. Med.* **2015,** *82*, 187-202.

[48] Alam, J.; Stewart, D.; Touchard, C.; Boinapally, S.; Choi, A. M.; Cook, J. L. *J. Biol. Chem.* **1999,** *274* (37), 26071-26078.

[49] Venugopal, R.; Jaiswal, A. K. *Proc. Natl. Acad. Sci. U S A* **1996,** *93* (25), 14960-14965.

[50] Botta, D.; White, C. C.; Vliet-Gregg, P.; Mohar, I.; Shi, S.; McGrath, M. B.; McConnachie, L. A.; Kavanagh, T. J. *Drug Metab. Rev.* **2008,** *40* (3), 465–477.

[51] Itoh, K.; Chiba, T.; Takahashi, S.; Ishii, T.; Igarashi, K.; Katoh, Y.; Oyake, T.; Hayashi, N.; Satoh, K.; Hatayama, I.; Yamamoto, M.; Nabeshima, Y. *Biochem. Biophys. Res. Commun.* **1997,** *236* (2), 313-322.

[52] Hong, F.; Sekhar, K. R.; Freeman, M. L.; Liebler, D. C. *J. Biol. Chem.* **2005,** *280* (36), 31768-31775.

[53] Costentin, C.; Louault, C.; Robert, M.; Saveant, J. M. *Proc. Natl. Acad. Sci. U S A* **2009,** *106* (43), 18143-18148.

[54] Enache, T. A.; Oliveira-Brett, A. M. *J. Electroanal. Chem.* **2011,** *655* ((1)), 9-16.

[55] Forman, H. J.; Davies, K. J. A.; Ursini, F. *Free Radic. Biol. Med.* **2014,** *66*, 24-35.

[56] Ludovico, P.; Burhans, W. C. *FEMS Yeast Res.* **2014,** *14* (1), 33-39.

[57] Griesser, M.; Pistis, V.; Suzuki, T.; Tejera, N.; Pratt, D. A. *J. Biol. Chem.* **2011,** *286* (2),

1114-1124.

[58] Burton , G. W.; Ingold, K. U. *Acc. Chem. Res.* **1986,** *19* (7), 194-201.

[59] Wijtmans, M.; Pratt, D. A.; Valgimigli, L.; DiLabio, G. A.; Pedulli, G. F.; Porter, N. A. *Angew. Chem. Int. Ed. Engl.* **2003,** *42* (36), 4370-4373.

[60] Amorati, R.; Ferroni, F.; Pedulli, G. F.; Valgimigli, L. *J. Org. Chem.* **2003,** *68* (25), 9654-9658.

[61] Okada, Y.; Tanaka, K.; Sato, E.; Okajima, H. *Org. Biomol. Chem.* **2006,** *4* (22), 4113-4117.

[62] Vaidya, V.; Ingold, K. U.; Pratt, D. A. *Angew. Chem. Int. Ed. Engl.* **2009,** *48* (1), 157-160.

[63] Motterlini, R.; Foresti, R.; Bassi, R.; Green, C. J. *Free Radic. Biol. Med.* **2000,** *28* (8), 1303-1312.

[64] Menon, V. P.; Sudheer, A. R. *Adv. Exp. Med. Biol.* **2007,** *595*, 105-125.

[65] Aggarwal, B. B.; Kumar, A.; Bharti, A. C. *Anticancer Res.* **2003,** *23* (1A), 363-398.

[66] The number was obtained from www.clinicaltrials.gov.

[67] Pietta, P. G. *J. Nat. Prod.* **2000,** *63* (7), 1035-1042.

[68] Hu, J. Chen, L.; Lei, F.; Tian, Y.; Xing, D-M.; Chai, Y-S.; Zhao, S.; Ding, Y; Du, L-J *Afr. J. Pharm. Pharacol.* **2012,** *6* (14), 1069-1076.

[69] Ramesova, S.; Sokolova, R.; Degano, I.; Bulickova, J.; Zabka, J.; Gal, M. *Anal. Bioanal. Chem.* **2012,** *402* (2), 975-982.